PERISOMATIC EXCITATORY INNERVATION ON PARVALBUMIN BASKET CELLS IN THE DENTATE GYRUS. ROLE OF SEMILUNAR GRANULE CELLS IN THE DENTATE GYRUS CIRCUITRY AND INVOLVEMENT IN EPILEPSY

LAURA ROVIRA ESTEBAN

Tesis Doctoral, 2015

VNIVERSITAT DE VALÈNCIA

VNIVERSITAT DE VALÈNCIA

Facultad de Ciencias Biológicas

Departamento de Biología Celular y Parasitología

PERISOMATIC EXCITATORY INNERVATION ON PARVALBUMIN BASKET CELLS IN THE DENTATE GYRUS. ROLE OF SEMILUNAR GRANULE CELLS IN THE DENTATE GYRUS CIRCUITRY AND INVOLVEMENT IN EPILEPSY

LAURA ROVIRA ESTEBAN

Tesis Doctoral, 2015

Director: José Miguel Blasco Ibáñez

Programa de Doctorado: Neurociencias Básicas y Aplicadas,
RD 778/98

El Dr. José Miguel Blasco Ibáñez, Profesor Titular del Departamento de Biología Celular y Parasitología de la Universidad de Valencia,

CERTIFICA:

Que Dña. Laura Rovira Esteban ha realizado en el Departamento de Biología Celular y Parasitología de la Universidad de Valencia, bajo su dirección, el presente trabajo de investigación correspondiente a la Tesis Doctoral titulada: "Perisomatic excitatory innervation on parvalbumin basket cells in the dentate gyrus. Role of semilunar granule cells in the dentate gyrus circuitry and involvement in epilepsy".

Revisado dicho trabajo, estima que puede ser presentado al Tribunal que ha de juzgarlo para optar al grado de Doctor.

Y para que conste, en cumplimiento de la legislación vigente, firma el presente certificado en Valencia, a 21 de Septiembre de 2015.

Fdo. Dr. José Miguel Blasco Ibáñez

Director de la tesis doctoral

Fdo. Laura Rovira Esteban

Durante la realización de esta tesis, Laura Rovira Esteban fue beneficiaria de una ayuda predoctoral dentro del Programa de Formación de Profesorado Universitario (FPU), concedida por el Ministerio de Educación según la resolución del 1 de Octubre de 2010, de la Secretaría General de Universidades. Referencia de la ayuda: AP2009-1080.

A mi familia.

A Samuel.

“If the brain were so simple we could understand it, we would be so simple we couldn’t.”

Lyall Watson

I sometimes feel, in reviewing the evidence on the localization of the memory trace, that the necessary conclusion is that learning just is not possible. It is difficult to conceive of a mechanism which can satisfy the conditions set for it. Nevertheless, in spite of such evidence against it, learning does sometimes occur.

Karl Spencer Lashley

AGRADECIMIENTOS

Quisiera agradecer a todas aquellas personas que, de un modo u otro, han hecho posible este trabajo.

En primer lugar, quisiera dar las gracias al Ministerio de Educación por haberme concedido una beca predoctoral para realizar este proyecto.

Muchas gracias a José Miguel por su confianza, sus consejos y su ayuda durante la realización de los experimentos. Por sus conversaciones de ciencia y no ciencia, y por su paciencia en las correcciones. Gracias por todo lo que me has enseñado. También a Paco Pepe, por darme la oportunidad de entrar en el laboratorio y haberme ayudado a dar los primeros pasos.

A Carlos, Juan y Emilio, también por su ayuda y sus consejos en el laboratorio. Gracias por haber hecho siempre lo posible para facilitarme las cosas. Gracias también a los miembros del departamento, en especial a Carlos López, Chonchi, Xavi y Mª Carmen.

I would also like to thank to Dr. Norbert Hájos the opportunity he gave me to join his lab for my short stay, and the confidence he has shown me. And also to Judit, Orsi and Zsolt, who not only taught me a lot but also made my stay very easy and comfortable. I am also grateful to the other people in the lab: Évi, Zoli, Erzsi, Vicky and Bógi for their help when needed. Y a Ana, fuera del laboratorio, por los buenos momentos descubriendo Budapest.

Gracias a mis compañeros de laboratorio y amigos, que han compartido conmigo no solo inquietudes científicas sino nuestro día a día. En especial, quisiera agradecer a Marta, Teresa y Ramón por vuestra amistad y ánimos en todo momento, por las largas conversaciones que tanto he disfrutado, por prestarme vuestros oídos y vuestros hombros, y por darme el empujoncito que he necesitado dentro y fuera del laboratorio. Por todas las tardes y noches que hemos pasado juntos tomándonos unas cervezas o unos vinos. Muchas gracias a Esther, María y Clara, por ser unas excelentes compañeras y amigas. Me llevo conmigo infinidad de buenos recuerdos.

Gracias también a todas aquellas personas que han pasado por el laboratorio y que sin duda han dejado huella: María y Amparo, que tanto me ayudaron al principio. Samuel, Sandra, David y Ulises, que hacían que los tiempos de incubación pareciesen más cortos. A Vicent y Pau, por no permitir que las comidas en cafetería fuesen monótonas y aburridas. También a Mª Ángeles, Lidia, Ana, Raúl, Simona, Javi, Héctor, Rosa, Clara, y Yasmina. Gracias a todos.

Muchísimas gracias a mis amigos, en especial a Gloria y Choni por haberme acompañando y apoyado desde siempre, por todo lo que hemos vivido juntas, y por lo que nos queda por vivir. Y a Julia, Joni, Robe y Marta, por todas las experiencias, conciertos y buenos momentos.

A Marta, al Sr. Blandito y al Sr. Durito. A mi hermano, por la música, por los ánimos, por todo lo que hemos compartido desde que tengo memoria, por todo.

A mis padres, porque sin su apoyo y cariño incondicional nunca hubiera sido capaz de llevar a cabo este proyecto, ni ningún otro. Gracias por haberme preparado un camino de rosas.

A Samuel, por todo su apoyo. Pero sobre todo por hacer mucho mejor cada día, por ser capaz de arrancarme siempre una sonrisa y darme ánimo para seguir adelante. Todo es más fácil cuando estoy contigo, incluso esta tesis.

CONTENTS

ABBREVIATIONS

ABC	Avidin biotin-peroxidase complex
ACSF	Artificial cerebrospinal fluid
CA1	Region 1 from "*Cornu Ammonis*"
CA3	Region 3 from "*Cornu Ammonis*"
CAMKII	Ca^{2+}/calmodulin-dependent protein kinase II
CART	Cocaine- and amphetamine-regulated transcript
CB	Calbindin
CB1R	Cannabionid receptor type 1
CCK	Cholecystokinin
CR	Calretinin
DAB	Diaminobenzidine
DAB-Ni	Nickel-conjugated diaminobenzidine
DEDTC	N,N-diethyldithiocarbamate
DβH	Dopamine β-hydroxylase
GA	Glutaraldehyde
HICAP	Hilar commisural-associational pathway-related cells
HIPP	Hilar perforant path-associated cells
IS interneurons	Interneuron selective interneurons
MOPP	Molecular layer perforant path neurons
MSDB	Medial Septum – Diagonal Band of Broca
PB	Phosphate buffer 0.1 M
PB-Tx	Phosphate buffer with 0.2% Triton X-100

PBS	Phosphate buffer saline
PBS-Tx	Phosphate saline buffer with 0.2% Triton X-100
PFA	Paraformaldehyde
PSD95	Post-synaptic density protein 95 KDa
PV	Parvalbumin
SOM	Somatostatin
SuM	Supramammillary nuclei
Syn	Synaptophysin
TH	Tyrosine Hydroxylase
Tx	Triton X-100
VIP	Vasointestinal peptide
5-HT	5-hydroxytryptamine or serotonin

INTRODUCTION

1. THE HIPPOCAMPUS

The hippocampus is one of the most important areas of the vertebrate brain. It belongs to the limbic system, and plays many important functions such as short-term and long-term memory consolidation and spatial navigation (Morris et al., 1982; Eichenbaum, 2004).

The hippocampus has been widely studied from anatomical, physiological and pathological points of view. It has been shown to be especially sensitive to ischemia (Schmidt-Kastner and Freund, 1991), and it is affected in several pathologies such as medial temporal lobe epilepsy, Alzheimer's disease, stress and schizophrenia. For a review, see chapters 15 and 16 in "The hippocampus book" (Anderson et al., 2007).

1.1. GENERAL STRUCTURE

The hippocampal region includes two different structures: the hippocampal formation and the parahippocampal region. The hippocampal formation comprises the hippocampus proper or "*Cornu Ammonis*" (CA region, which is in turn subdivided into CA3, CA2 and CA1 regions), the dentate gyrus and the subiculum, whereas the parahippocampal region is formed by the presubiculum, parasubiculum and entorhinal cortex (Ramón y Cajal, 1911; Lorente De Nó, 1934; for a review, see Witter and Amaral, 2004). The term "hippocampus" is commonly used to indicate the structure formed by the *Cornu Ammonis* and the dentate gyrus, and in this way is going to be used in this thesis.

The hippocampus is a three-layered structure (**Figure 1**), and is therefore considered as archicortex. It derives from the cortical lamina, whose end turns and becomes the hippocampus. It presents a highly organized laminar and input distribution, with only one principal cell layer, making it one of the most studied structures of the brain.

1.1.1. DENTATE GYRUS

The dentate gyrus presents a simple U-shaped structure in rodents that is deeply indented in humans, hence the "dentate". It comprises three layers: granule cell layer, molecular layer and hilus.

The granule cell layer contains the soma and dendritic trunk of the principal cells of the dentate gyrus, the granule cells. It is made up of a densely packed layer that is four to eight granule cell thick.

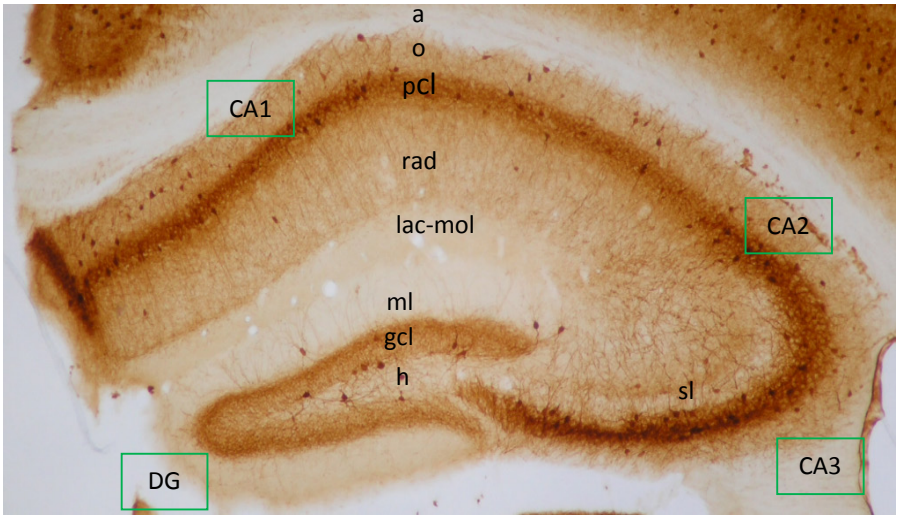

Figure 1 - Parvalbumin immunostainig of a coronal section of the dorsal hippocampus. Each region and layer of the hippocampus is identified. Note the continuity of CA3 to CA1 region.
a, alveus; CA1, *Cornu Ammonis* region 1; CA2, *Cornu Ammonis* region 2; CA3, *Cornu Ammonis* region 3; DG, dentate gyrus; gcl, granule cell layer; h, hilus; lac-mol, stratum lacunosum-moleculare; ml, molecular layer; o, stratum o*riens*; pcl, stratum pyramidale; rad, stratum radiatum; sl, stratum lucidum

The U-shaped granule cell layer limits the hilus, which is penetrated in the open side by the CA3 pyramidal cell layer. Generally, the portion of granule cell layer located between the hilus-CA3 layer and the CA1 region is known as “suprapyramidal granule cell layer”, whereas the portion of granule cell layer below the hilus that faces the thalamus is known as “infrapyramidal granule cell layer”. In coronal sections, the extreme portion of the U-shape granule cell layer is commonly known as the dentate apex.

The packing level of granule cells in the granule cell layer is modified along the septotemporal axis, the granule being cells more tightly packed in the rostral hippocampus than in the caudal hippocampus (Gaarskjaer, 1978). Some GABAergic interneurons can also be found in this layer, usually in the border with the hilus or the inner molecular layer. These interneurons may express calcium binding proteins like parvalbumin (PV), calbindin (CB) or calretinin (CR); or neuropeptides such as cholecystokinin (CCK) or neuropeptide Y. For a review, see (Houser, 2007).

The molecular layer is a relatively cell-free layer, located between the hippocampal fissure and the granule cell layer. It contains the apical dendrites of granule cells, the cell bodies of certain interneurons and of ectopic or misplaced granule cells, and the remaining Cajal-Retzius cells (Liu et al., 1996). It also contains the afferent fibers to the dentate gyrus, located within a precise layered distribution according to their origin.

The molecular layer is conventionally divided into three regions that roughly correspond to its equitable division into three parts. The closest third to the granule cell layer is known as the inner molecular layer (iml), and here we find the axons of the mossy cells in the ipsi and contralateral hemisphere (Buckmaster et al., 1996; Blasco-Ibáñez and Freund, 1997), commissural-associational fibers and afferent fibers from the supramammilary nucleus. The outer two-thirds of the molecular layer are generally included into the term "outer molecular layer" (oml). In this region we find the fibers that come from the entorhinal cortex (for a review, see Witter, 2007). For some particular situations, a finer distinction can be made between the middle third of the molecular layer and the outer third of the molecular layer, but in this thesis only inner molecular layer and outer molecular layer will be used.

In the molecular layer we can also find, though not in as organized manner, GABAergic and cholinergic fibers coming from the medial septum and scarce serotonergic fibers coming from the raphe nuclei.

Finally, the hilus, or polymorphic layer, is enclosed by the granule cell layer and contains both excitatory and inhibitory neurons of different types, spread in a non-laminar fashion. The principal cell population in this layer are the mossy cells. In this region, granule cell axons – the mossy fibers - ramify in their way to the CA3 and their collaterals establish synaptic contacts with both excitatory and GABAergic hilar neurons (Amaral, 1978; Acsády et al., 1998).

1.1.2. CORNU AMMONIS

As this thesis is focused in the dentate gyrus, we will give only a brief description of this region, to be able to understand the functional role of the dentate circuitry and its remodeling.

The Cornu Ammonis (CA) is divided into three regions: CA3, CA2 and CA1, according to their structure and function. The CA3 is located next to the dentate hilus, with a fraction of the principal cell layer placed between both layers of granule cells. CA3 pyramidal cells present thorny excrescences in their proximal dendrites, where they receive input from mossy fibers. This layer is followed by the CA2 region, whose main characteristic is the absence of spines in the most proximal part of pyramidal cell dendrites. Finally, between the CA2 and the subiculum we find the CA1, which is characterized by presenting more tightly packed and smaller pyramidal cells in comparison with the other two regions.

Each of these regions is subdivided in the following layers, presented here from the deepest to the most superficial layer:

- *Alveus*: contains commissural myelinated fibers of hippocampal and subiculum pyramidal cells. It finally merges with the fimbria.
- *Stratum Oriens*: contains different types of interneurons and the basal dendrites of pyramidal neurons. In this region we can find some CA3 to CA3 associational fibers and CA3 to CA1 Schaffer collaterals.
- *Stratum Pyramidale*: contains the soma of pyramidal neurons, which are the principal cells of the *Cornu Ammonis*. In CA1 the pyramidal cell layer is tightly packed, while in CA2 and CA3 are more loosely packed.
- *Stratum Lucidum*: it is present only in the CA3 region, but not in CA2 or CA1. Here, we find the mossy fibers from granule cells that form characteristic giant boutons that synapse onto the complex spines of CA3 proximal dendrites (Claiborne et al., 1986).
- *Stratum Radiatum*: located superficial to the *stratum lucidum* in CA3, and above the pyramidal cell layer in CA2 and CA1. Here, pyramidal cell apical dendrites start to ramify. We also find CA3 to CA3 associational connections and the Schaffer collaterals in the CA3 to CA1 pathway.
- *Stratum Lacunosum-Moleculare*: in this region we find the dendritic arbor of the apical dendrites of pyramidal cells that continue to ramify from the branches in the *stratum radiatum* and reach the hippocampal fissure. Fibers from the entorhinal cortex via the perforant pathway are found here and synapse on distal apical dendrites of pyramidal cells.

For an extensive review of the hippocampal cytoarchitecture, see: (Witter and Amaral, 2004; Anderson et al., 2007)

1.2. CIRCUITRY OF THE HIPPOCAMPUS

One of the most important characteristics of the hippocampal circuitry, compared to other cortical structures, is that its connections are mainly unidirectional (Ramón y Cajal, 1893). The most important hippocampal excitatory circuitry is called “tri-synaptic circuit” (**Figure 2**), and consists of a flow of information from the entorhinal cortex to the dentate gyrus and

hippocampus, and back to the entorhinal cortex. For a review, see chapter 3 in "The hippocampus book" (Anderson et al., 2007).

Layer II principal cells of the entorhinal cortex give rise to axons that project to the dentate gyrus and in a lesser extent to the CA3 region. The entorhinal projection to the dentate gyrus carries sensory information and is called the Perforant Path. The dentate gyrus granule cells receive entorhinal cortex afferents in the outer molecular layer, and give rise to the mossy fibers that travel through the hilus and contact the apical dendrites of the CA3 pyramidal cells in the *stratum lucidum*. The pyramidal cells of CA3 are, in turn, the source of the major input to the CA1 field (the Schaffer collateral axons). Pyramidal cells in the CA1 field project to the deep layers of the entorhinal cortex and to the subiculum, providing its major excitatory input. Principal cells in the subiculum also project to the entorhinal cortex layer V.

Layer III principal cells of the entorhinal cortex also innervate principal cells in the CA1 and subiculum fields, via the perforant and alvear pathways.

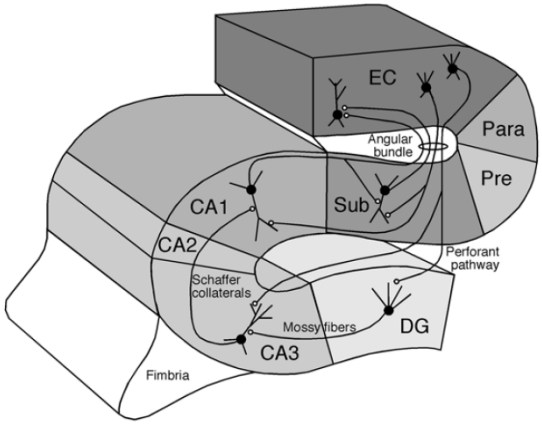

Figure 2 - Tri-synaptic hippocampal circuit. Representation of the three major pathways and the principal cells in charge of the information flow from the entorhinal cortex (EC) to the dentate gyrus (DG), CA3, CA1 and back to the EC. Modified from Anderson et al. (2007). The hippocampus Book

2. THE DENTATE GYRUS

2.1. CELL POPULATIONS IN THE DENTATE GYRUS

The main goal in this thesis is to deepen our knowledge of the dentate gyrus function. To better understand the scenario of the dentate gyrus circuitry, a detailed explanation of the cell populations present in this structure will be given in this chapter.

2.1.1. GRANULE CELLS

Granule cells are the principal excitatory cell type of the dentate gyrus. These cells are densely packed in the granular cell layer, with few glial processes between them. However, the packing density of dentate granule cells decreases along the dorso-ventral axis (Gaarskjaer, 1978). They have a small, ovoid cell body with a single, more or less conical dendritic tree. Their somata are about 10 µm in diameter and about 18 µm in length (Claiborne et al., 1990), with their long axis oriented perpendicularly to the granule cell layer.

Their spiny dendrites extend into the molecular layer and terminate near the hippocampal fissure. Dendritic morphology varies according to several facts: (1) location of the granule cell in the granule cell layer, with a wider dendritic extent in those cells closer to the molecular layer; (2) position in the dentate gyrus, with a higher spine density, more dendritic segments and greater transverse spread in the suprapyramidal blade than in the infrapyramidal blade (Desmond and Levy, 1985; Claiborne et al., 1990).

Granule cells present an unmyelinated axon that emerges from the soma and project directly towards the hilus, where it ramifies before reaching the CA3. Three different types of synaptic terminals have been described for mossy fibers. The first and better known is the large mossy terminals, first described by Ramón y Cajal (1911), that synapse onto the dendritic excrescences of mossy cells and CA3 proximal dendrites (Claiborne et al., 1986). Amaral showed in 1978 a second type of terminal, consisting on filopodial extensions that protrude from the large mossy terminals and that contact hilar interneurons (Amaral, 1978; Acsády et al., 1998). Finally, a third type of terminal consists of small round *en passant* varicosities (Claiborne et al., 1986).

Large mossy terminals target and surround the thorny excrescences of mossy cells and CA3 pyramidal cells, establishing several asymmetric synaptic contacts. These terminals contain small vesicles with the neurotransmitter glutamate that are zincergic, and dense-core vesicles with neuropeptides such as dynorphin (Khachaturian et al., 1982; Conner-Kerr et al., 1993). Filopodial extensions and *en passant* varicosities innervate only interneurons, forming single, often perforated asymmetrical synapses on their cell bodies, dendrites and spines. These terminals outnumber the large mossy terminals (Acsády et al., 1998).

Regarding their afferent connectivity, granule cells receive synaptic input from different sources. They are the first rely of the trisynaptic circuit, with the entorhinal fibers innervating granule cell dendrites in the outer molecular layer. The medial third of the molecular layer receives afferents from the medial entorhinal cortex, and the distal third of the molecular layer

receives input from the lateral entorhinal cortex (van Groen et al., 2003). The overwhelming majority of the fibers coming from the entorhinal cortex are glutamatergic. In the medial molecular layer some of these excitatory fibers are also cholecystokinin-positive, while in the outer molecular layer they also co-express enkephalin (Gall et al., 1981; Witter and Amaral, 2004).

In the inner third of the molecular layer, granule cell dendrites receive excitatory innervation from associational and commissural fibers from hilar neurons (Laurberg and Sørensen, 1981; Buckmaster et al., 1992, 1996; Deller et al., 1996b).

Finally, granule cells are also innervated by GABAergic fibers from dendrite-targeting hilar interneurons on their dendrites located in the molecular layer, and by perisomatic-innervating basket and axo-axonic interneurons on their somata (Freund and Buzsáki, 1996; Witter and Amaral, 2004).

2.1.2. SEMILUNAR GRANULE CELLS

Though semilunar granule cells were first described by Ramon y Cajal, and had also been reported in several classical golgi anatomical studies (Ramón y Cajal, 1911; Martí-Subirana et al., 1986), very little information is available about them. In fact, a clear identification of the different subtypes is missing in the literature, which leads to confusion on the proper term to be used when referring to these cells.

Only recently, one subpopulation of these ectopic cells, located in the inner molecular layer, has been studied more in depth, by Strowbridge's group and Santhakumar's group (Williams et al., 2007; Larimer and Strowbridge, 2010; Gupta et al., 2012). These groups focused on ectopic granule cells located in the inner molecular layer, and they named them as "Semilunar Granule Cells" after Ramon y Cajal's work.

The term "semilunar granule cell" makes reference to their morphology, but in their work they have added valuable information on their physiological features. As they make no distinction between ectopic granule cells and semilunar granule cells in the inner molecular layer, in this thesis all ectopic granule cells located in the inner molecular layer will be considered "Semilunar Granule Cells", and will be assumed to present all the physiological features they described.

On the other hand, as they ignore the ectopic granule cell population in the outer molecular layer, in this thesis we will make no assumption that they belong to the same cell population, and will be further considered as “outer molecular layer ectopic granule cells”.

Despite the fact that semilunar granule cells have many common morphological features with granule cells, they also present some important characteristics. Firstly, they have different-shaped somata (more triangular or "semilunar") located in the inner molecular layer, from which at least two primary dendrites arise. Secondly, they extend their dendritic arbor in a wider extension of the molecular layer than granule cells. Thirdly, the axonal branch in the inner molecular layer is initially oriented parallel to the granule cell layer and can also generate secondary collaterals that enter the granule cell layer (Martí-Subirana et al., 1986; Williams et al., 2007).

Their particular location and morphological characteristics probably allow them to receive and establish synaptic contacts with other different cell populations than common granule cells. Therefore, they may play a different functional role than typical granule cells in the dentate local circuitry.

Functionally, it is reported that semilunar granule cells have different electrophysiological properties than granule cells (Williams et al., 2007; Larimer and Strowbridge, 2010; Gupta et al., 2012). Among these differences, these autors highlight the fact that semilunar granule cells can fire action potentials throughout long-duration depolarizing steps (2s), they present a lower input resistance, and are more strongly activated by hilar stimulation than granule cells.

Considering their connectivity, they establish glutamatergic synapses with distal dendritic segments of mossy cells, and probably receive a strong input from hilar mossy cells (Williams et al., 2007).

The strong glutamatergic input that semilunar granule cells receive make them suitable to trigger plateau potentials. These plateau potentials are maintained by NMDA receptors, T-type and L-type voltage-gated Ca^{+2} channels, and are not a direct result of a reverberation due to the continuous excitatory input from mossy cells. In fact, more than one semilunar granule cell is needed to engage a subset of hilar cells into the hilar up-states (Larimer and Strowbridge, 2010).

In agreement to previous neurochemical studies, semilunar granule cells present nuclear expression of the homeodomain transcription factor Prox1 (Gupta et al., 2012). This protein

has been widely used to identify granule cells both in the granule cell layer and in ectopic locations (Galeeva et al., 2007; Lavado and Oliver, 2007; Lavado et al., 2010; Szabadics et al., 2010). This indicates a shared lineage with granule cells.

2.1.3. MOSSY CELLS

Mossy cells are the hilar principal cells and are glutamatergic, and therefore excitatory (Scharfman, 1994, 1995; Soriano and Frotscher, 1994). They have a large pyramidal soma, of about 20-30 µm of diameter, and three to four primary dendrites. One of the characteristics of mossy cells is the presence of complex thorny excrescences on proximal dendrites and conventional spines on distal dendrites (Ribak et al., 1985).

In the mouse and rat dentate gyrus, mossy cell dendrites remain mostly in the hilus (Ribak et al., 1985) , while their axon innervates mainly the inner third of the molecular layer, but they have been also found to form synapses in the hilus and the granule cell layer (Buckmaster et al., 1996). In the hilus, they establish synaptic contacts with the dendritic shaft of hilar interneurons, and with GABA-negative dendritic spines (Blasco-Ibáñez and Freund, 1997; Freund et al., 1997; Wenzel et al., 1997). An important feature of the mossy cell axons is that they project ipsi and contralaterally, and that they spread extensively through the dorso-temporal axis of the hippocampus.

They receive direct excitatory input from the granule cell mossy fibers (which contact the thorny excrescences), and from CA3 pyramidal cells that backproject to the hilus (Frotscher et al., 1991; Scharfman, 1994, 2007). They also receive inhibitory input, probably from dentate basket cells, hilar interneurons (ipsi and contralaterally), and putatively GABAergic fibers from the medial septum (Lübke et al., 1997).

2.1.4. INHIBITORY PERISOMATIC-TARGETING CELLS

There are two distinct types of perisomatic-targeting interneurons: axo-axonic cells and basket cells (Nunzi et al., 1985; Kosaka et al., 1987; Sloviter and Nilaver, 1987; for a review, see Howard et al., 2005; Freund and Katona, 2007). These interneurons are implied in both “feed-back” and “feed-forward” inhibition, and play a main role in the timing and synchronization of the firing of granule cells.

Axo-axonic cells are characterized by establishing synaptic contacts with the axon initial segment of their target cell. Due to the peculiar axon ending of axo-axonic cells, which presents rows of boutons in the principal cell layer, they are also called chandelier cells. Basket cells, in turn, are characterized by establishing inhibitory synaptic contacts around the soma and dendritic trunk of their targeted cells.

Neurochemically, axo-axonic and a subpopulation of basket cells express the Ca^{+2} binding protein parvalbumin. Parvalbumin-positive interneurons are non-adapting fast-spiking cells and therefore regulate the local generation of Na^{+}-dependent action potentials in the granule cell population in a very effective manner. As there is no marker expressed only by one of these populations, and they are morphologically very similar (even their axonal arbors are very similar), the only way to distinguish between them is checking their postsynaptic targets. On the other hand, they seem to receive similar afferents and fulfil a similar role. The other subpopulation of basket cells are regular spiking interneurons, that coexpress CCK and the vasointenstinal peptide (VIP) (Hájos et al., 1996).

Morphologically, parvalbumin basket cells have aspiny dendrites (or with very few filiform processes) located in all layers of the dentate gyrus. According to the morphology of their somata and dendritic tree, there are 5 different types of basket cells in the dentate gyrus (Ribak and Seress, 1983): pyramidal basket cells, molecular layer basket cells, fusiform basket cells, inverted fusiform basket cells and horizontal basket cells (**Figure 3**).

- Pyramidal basket cells have a triangular-shaped soma located in the hilar border of the granule cell layer. A main thick apical dendrite ascends through the granule cell layer and into the molecular layer, where it branches. Their axon arise from the apical dendrite, or the apical portion of the soma, while their basal dendrites arise from both sides of the soma base and ramify in the hilus.
- Molecular layer basket cells have a multipolar soma located in the molecular layer close to the granule cell layer, and extend their dendrites in the molecular layer and also some of them entering the granule cell layer.
- Fusiform basket cells are similar to pyramidal basket cells, with the exception of their soma and basal dendrites. Fusiform basket cells somata get thinner in their basal pole, and their basal dendrite arise opposite to the apical.

- Inverted fusiform basket cells have their somata in the border of the granule cell layer and the molecular layer. Their apical dendrites descend to the hilus, whereas basal dendrites ramify in the molecular layer. The axons arise from the dendrites in the molecular layer.
- Finally, horizontal basket cells present a non-pyramidal soma, located in the hilar border and oriented obliquely to the granule cell layer. They have only one basal dendrite located in the hilus, and their apical dendrite travels through the granule cell layer to the molecular layer, where it branches. Their axon arise from the apical dendrite.

However, it seems that there is no difference in their function and target cells, as they all extend their axons mainly in the granule cell layer (and proximal molecular layer) and establish multiple basket-like contacts with granule cells (Struble et al., 1978; Sik et al., 1997).

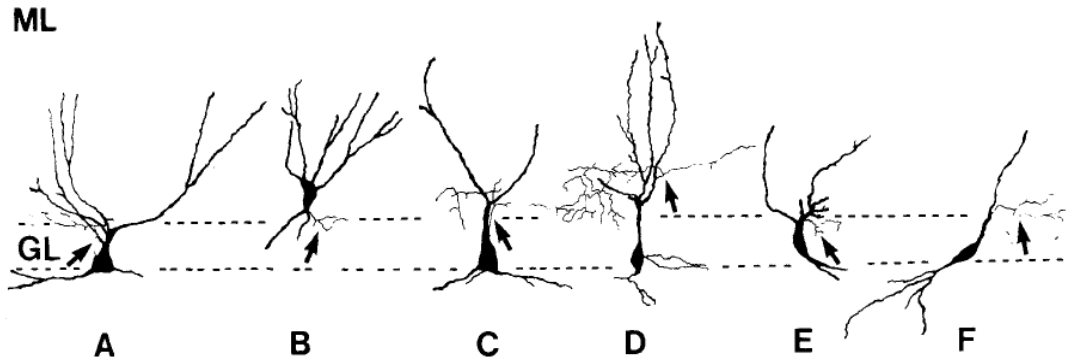

Figure 3. Representation of the different morphologies found on parvalbumin interneurons sitting in the granule cell layer. A and C: pyramidal basket cell; B: molecular layer basket cell; D: fusiform basket cell; E: inverted fusiform basket cell; F: horizontal basket cell. Modified from Ribak and Seress (1993).

Regarding their ultrastructural features, they present infolded nuclei with intranuclear rods and sheets, little amount of heterochromatin, and one large nucleolus. Their cytoplasm presents many RER cisternae and Nissl bodies, as well as well-developed cisternae and vesicles of the Golgi complex, numerous mitochondria, free ribosomes and lysosomes. This suggests a high level of physiological activity. In addition, basket cells terminals present numerous mitochondria near the active site, contain flat vesicles and form symmetric synapses.

2.1.5. OTHER INTERNEURONS

In addition to axo-axonic cells and basket cells, there are different types of dendrite-targeting interneurons (**Figure 4**). The latter play a different role than perisomatic-targeting interneurons. They cannot affect much to the somatic action potential generation, but they

may influence dendritic integration, shunt excitatory inputs on their way to the soma, or regulate dendritic spike initiation and/or propagation (Miles et al., 1996).

The main types of interneurons innervating principal cell dendrites in the dentate gyrus are: Hilar Perforant Path-associated cells (HIPP cells), Hilar Commissural-Associational Pathway-related cells (HICAP cells) and Molecular layer Perforant Path neurons (MOPP cells).

- HIPP cells present a fusiform cell body and all their dendritic tree confined in the hilus. Their dendrites are covered with long thin spines and run mainly parallel to the granule cell layer, avoiding any possible innervation from the perforant or commissural-associational pathways. Their axon originates from the soma, cross the granule cell layer and ramify in the outer two-thirds of the molecular layer (Freund and Buzsáki, 1996; Sik et al., 1997). This interneuron population expresses the neuropeptide somatostatin (SOM) (Morrison et al., 1982; Bakst et al., 1986).
- HICAP cells present a triangular cell body located in the hilus or in the hilar border with the granule cell layer. Their dendrites may be smooth or sparsely spinous and branch in the hilus and molecular layer. Their axon emerge from the soma, travels through the granule cell layer and ramify mainly in the inner molecular layer (Han et al., 1993; Freund and Buzsáki, 1996).
- MOPP cells present a round soma located in the inner molecular layer. Their dendrites are smooth with varicose swellings, and they extend only in the middle and outer molecular layer. Their axon emerge from the cell body and ramify exclusively in the outer molecular layer where they innervate the spines of the granule cells distal dendrites. Due to their position, MOPP cells may play an important role in feed-forward inhibition of dentate granule cells (Han et al., 1993; Freund and Buzsáki, 1996).

There may be also another two different types of interneurons specialized to innervate other interneurons in the dentate gyrus (IS interneurons): IS-1 and IS-3 neurons.

IS-1 are immunoreactive for calretinin and present their cell body in the hilus or granule cell layer. Their smooth dendrites ramify in all layers of the dentate gyrus and form long dendrodendritric gap junctions with each other. Their axons form multiple symmetrical synapses with the dendrites and somata of other interneurons (calbindin, calretinin, VIP, but not parvalbumin- cells). They are thought to control the synchrony of the principal cell

dendrites inhibition. IS-3, on the other hand, are immunoreactive for VIP and present a fusiform cell body located in the molecular or granule cell layer, and ramify their axon in the hilus. They are driven by entorhinal afferents and contact hilar HIPP cells (Freund and Buzsáki, 1996).

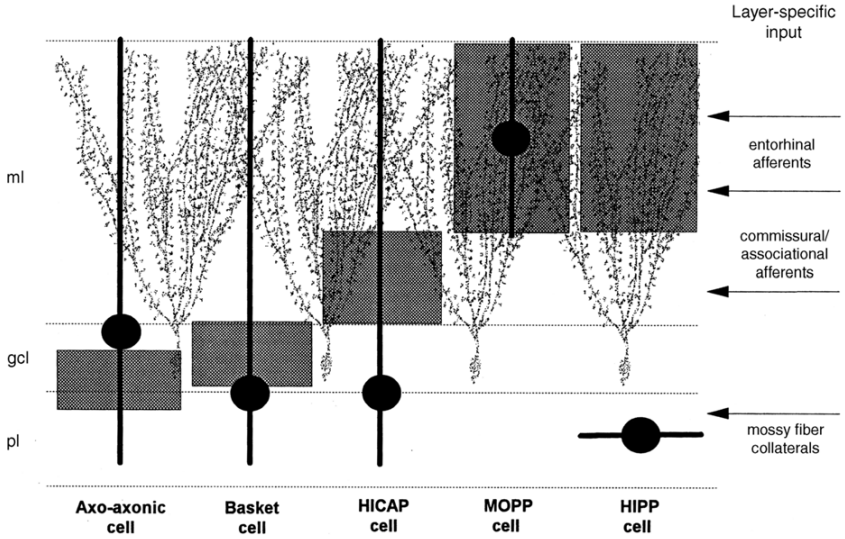

Figure 4 - Scheme showing the different interneuron populations in the dentate gyrus. Modified from Freund and Buzsáki (1996).

2.2. SUBCORTICAL MODULATION OF THE DENTATE GYRUS

The main projection to the dentate gyrus comes from the entorhinal cortex via the perforant pathway. However, the dentate gyrus also receives several modulatory inputs from subcortical regions of the brain, including: (1) excitatory fibers from the supramammilary region of the hypothalamus, that in rat express both substance P and calretinin; (2) afferents from raphe nuclei that contains serotonin (5-HT); (3) norepinephrine containing fibers from the locus coeruleus; (4) dopamine containing fibers coming from the ventral tegmental area and (5) both cholinergic and GABAergic fibers from the medial and lateral septum.

2.2.1. INNERVATION FROM THE SUPRAMAMMILLARY NUCLEI

There are many anatomical and electrophysiological data showing the presence of an innervation from the supramammilary nuclei to the dentate gyrus (for a review, see Leranth and Hajszan, 2007). The supramammilary nuclei play a critical role in the regulation of the information flow into the dentate gyrus. They enhance perforant-path elicited population spike in the dentate gyrus during theta activity (Mizumori et al., 1989; Carre and Harley, 1991), and facilitate synchronization (Vertes, 1981).

Several anatomical studies demonstrate the presence of an innervation from the supramammilary nuclei to the dentate gyrus in the rat (Segal and Landis, 1974; Segal, 1979) and in the monkey hippocampus (Amaral and Cowan, 1980). In the dentate gyrus, supramammillary fibers are mainly located in the border between the inner molecular layer and the granule cell layer, with a more intense labelling in the suprapyramidal blade than in the infrapiramidal blade. However, some fibers can be seen in the granule cell layer, the hilus and in the outer two-thirds of the molecular layer.

The cells projecting from the supramammillary nuclei to the dentate gyrus are calretinin-positive and substance P-positive cells, but are GABA-negative, and therefore, excitatory cells (Nitsch and Leranth, 1993). In addition to calretinin and substance P, another useful marker of supramammilary nuclei afferent boutons is the vesicular glutamate transporter-2 (VGluT2). This protein is expressed in diencephalic neurons (Fremeau et al., 2001), and it has been shown that it is expressed by neurons located in the lateral and medial supramammilary nuclei (Soussi et al., 2010). In fact, projecting neurons from the lateral supramammilary nucleus present in their synaptic terminals vesicular GABA transporter (VGAT) and VGluT2, and spread their fibers in the supragranular region of both dorsal and ventral hippocampus. On the other hand, projecting neurons from the medial supramammilary nuclei express only VGluT2 and locate their fibers in the inner molecular layer of the ventral hippocampus (Soussi et al., 2010).

Supramammillary afferents form asymmetric synapses, usually in a basket-like manner, and target both principal cells (Maglóczky et al., 1994) and interneurons (Leranth and Nitsch, 1994). The interneuron populations in the dentate gyrus innervated are: (1) some parvalbumin-positive basket cells and (2) calbindin-positive neurons located in the hilus and granule cell layer.

Therefore this hypothalamic-hippocampal pathway can exert an excitatory control of the function of the dentate gyrus by two means: straight excitation of granule cells; and excitation of some of the interneurons innervating different subsets of granule cells.

2.2.2. MONOAMINERGIC INPUTS

Though we will not address the monoaminergic input systems to the dentate gyrus in this thesis, a quick overview could be interesting to better understand other regulatory pathways that could influence in the dentate function (**Figure 5**).

The serotonergic raphe-hippocampal pathway, as well as the innervation pattern of 5-HT positive fibers in the dentate gyrus, were first described by Moore and Halaris (1975). The median raphe nucleus seems to be the main source of serotonergic fibers in the dentate gyrus (Vertes et al., 1999). Once in the dentate gyrus, they remain mostly in the hilus, close to the granule cell layer, but some serotonergic fibers can also be seen in the molecular layer.

In 1990 the GABAergic nature of the cells innervated by serotonergic fibers coming from the raphe was confirmed (Freund et al., 1990). However, only calbindin-immunoreactive interneurons were found to receive symmetrical contacts from serotonergic boutons, both in the cell body and in the dendrites. No contacts were found on parvalbumin-containing interneurons, which implies that serotonergic control of the hippocampus is addressed mainly to dendritic-targeting interneurons.

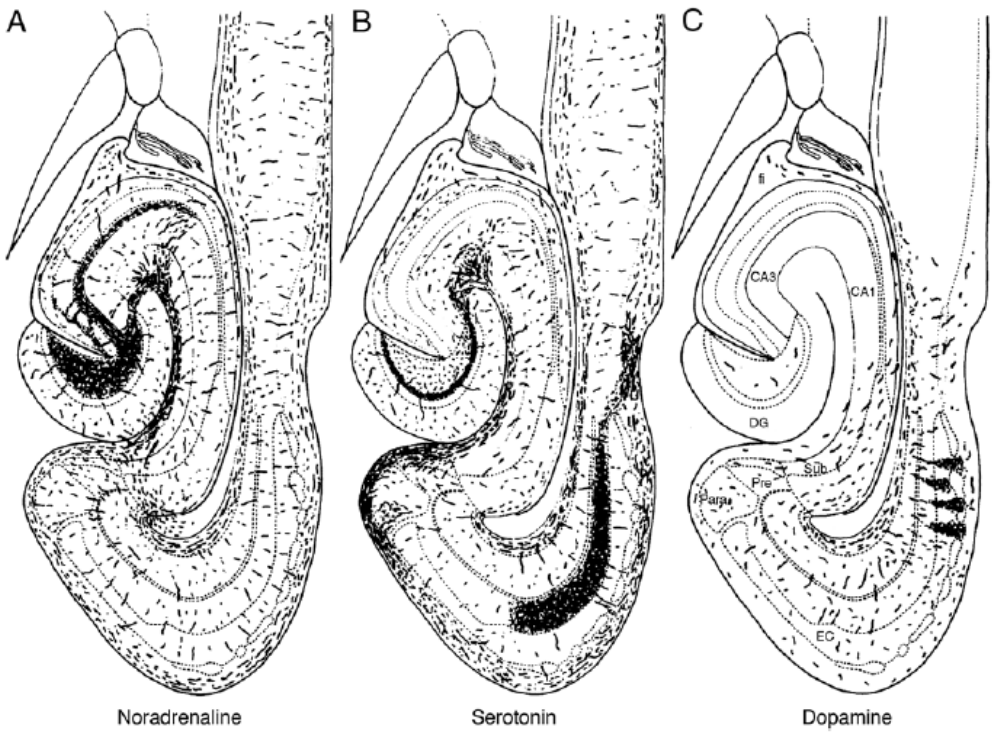

Figure 5 - Drawings of horizontal sections representing the fiber distribution of the three main monoaminergic systems in the hippocampus. Noradrenergic fibers are very abundant in the dentate gyrus, densely populating the hilar region. Serotonergic fibers are also found in the hilus, but they are more restricted to the area close to the granule cell layer. Dopamine fibers are scarce in the dentate gyrus. Adapted from Swanson et al, 1978. Source: The Hippocampus Book.

Dopamine is a catecholamine-type neurotransmitter that is widely found in the central nervous system. It is synthetized by the Tyrosine Hydroxylase (TH) enzyme from the amino acid tyrosine, and is converted in turn into norepinephrine by the Dopamine β-hydroxylase (DβH) enzyme.

These two enzymes are present in both dopaminergic and noradrenergic fibers respectively, and are widely used as their markers.

Dopamine innervation to the dentate gyrus arises from the Ventral Tegmental Area (Swanson, 1982), but it is scarce and unevenly distributed. Though dopamine has been proved to participate in memory consolidation, little information is known about its mechanisms, and generally related to dopamine receptors (Manahan-Vaughan, 2003).

Finally, the main source of noradrenergic fibers is the locus coeruleus, region implicated in the physiological response to stress and panic. There is a dense innervation of noradrenergic fibers in the hilus of the dentate gyrus and in the stratum lucidum of CA3 (Moudy et al., 1993), while in the other layers only testimonial fibers can be found. Usually, these fibers present varicosities in which the neurotransmitter is released in a non-synaptic manner. However, some of the varicosities present in noradrenergic fibers may form inhibitory symmetric synaptic contacts with dendritic shafts and cell bodies of interneurons (Frotscher and Leranth, 1988).

2.2.3. SEPTO-HIPPOCAMPAL CONNECTIONS

The medial septum-diagonal band of Broca (MSDB) represents one of the most important extrahippocampal inputs to the dentate gyrus (Rose and Schubert, 1977). Septohippocampal fibers enter the dentate gyrus via the fimbria, and can be divided into two types of fibers: Type 1, which are GABAergic fibers from parvalbumin interneurons (Freund et al., 1990); and Type 2, which are GABA-negative and correspond to cholinergic fibers (Frotscher and Léránth, 1986; Freund and Antal, 1988).

2.2.3.1. CHOLINERGIC INNERVATION

The cholinergic system in the hippocampus plays a very important role in the cognitive function (Steckler and Sahgal, 1995). Anatomical studies have demonstrated that the dentate gyrus presents a massive cholinergic innervation (Frotscher and Léránth, 1985), with the densest band occurring between the granule cell layer and the molecular layer, and some fibers in the granule cell layer and hilar region.

In the dentate gyrus, cholinergic boutons form asymmetric synaptic contacts with the dendrites and spines of granule cells, and symmetric contacts with non-spiny dendritic shafts belonging

to interneurons (Frotscher and Leranth, 1986). Mossy cells are also perisomatically innervated by cholinergic afferents (Deller et al, 1999).

2.2.3.2. GABAERGIC INNERVATION

It has been described that the discharge of granule cells is facilitated by septohippocampal input (Alvarez-Leefmans and Gardner-Medwin, 1975; Fantie and Goddard, 1982), and that this facilitation is mediated through an inhibitory connection from the MSDB onto inhibitory interneurons in the dentate gyrus (Bilkey and Goodard, 1985). This idea is confirmed anatomically, as several studies have shown that septohippocampal GABAergic terminals establish synaptic contacts with GABAergic interneurons (Freud and Antal, 1988; Gulyas et al, 1990).

In addition, all subpopulations of hippocampal interneurons, including parvalbumin-positive interneurons, receive input from GABAergic septohippocampal afferents in the soma and/or both proximal and distal dendrites (Freund and Antal, 1988; Gulyas et al, 1990; Miettinen and Freund, 1992; Acsady et al, 1993).

3. EXPERIMENTAL EPILEPSY MODELS

Since the cells that we intend to study are located in a key position in the dentate gyrus circuitry and may be affected differently in epilepsy, we will analyze their behavior in some common epilepsy models.

Epilepsy is a common neurological disorder that, according to the World Health Organization, affects around 1% of the world population. It is characterized by a misbalance between excitation and inhibition in the brain, which results in recurrent seizures. The hippocampus is one of the cerebral areas most affected by temporal lobe epilepsy (TLE). Due to the social and economic impact that hippocampal lesions produce, an important effort has been made to design experimental models that mimic the neurological changes and lesions produced by temporal lobe epilepsy disorder.

Different approaches have been used to create experimental models that accurately reflect the most important clinical and neuropathological characteristics of temporal lobe epilepsy in humans, including straight electrical stimulation and chemical over-excitation. In addition, three different types of models can be achieved: acute seizures, chronic seizures and a post-

epileptic state with spontaneous recurrent seizures. For a review, see (Löscher, 2002, 2011; McIntyre et al., 2002; Morimoto et al., 2004).

Experimental epilepsy models include three different stages: (1) induction, in which a convulsive agent is applied and an acute seizure is achieved; (2) a silent period variable in length, which can last from 3 to 42 days and in which a neuronal and circuit reorganization takes place; and (3) a chronic phase, characterized by the appearance of spontaneous recurrent seizures (Morimoto et al., 2004).

Among the most common reagents inducing chemical overexcitation in experimental epilepsy, we find pilocarpine, kainic acid and pentylenetetrazole (Löscher, 2011).

Systemic or local administration of a convulsive dose of pilocarpine (Turski et al., 1983) or kainic acid (Ben-Ari et al., 1980; Ben-Ari, 1985) is generally used to generate an acute epileptic state in rodents that can derive in chronic spontaneous seizures (Nadler et al., 1981; Turski et al., 1984, 1989; Ben-Ari, 1985; Leite et al., 1990; Cavalheiro et al., 1991; Buckmaster and Dudek, 1997).

Both pilocarpine and kainic acid enhance excitation, since they act respectively as a non-selective muscarinic receptor agonist and a specific agonist for the kainate receptor. Pentylenetetrazole, however, is a non-competitive GABA antagonist that binds to the picrotoxin site of GABAA receptor, and therefore acts by diminishing inhibition. Periodical administration of a sub-convulsive dose of pentylenetetrazole is used in rodents to generate a chemical kindling model of status epilepticus (Corda et al., 1991).

Generally, in experimental models of epilepsy several neuropathological changes are observed. First, we find neuronal loss in several regions of the hippocampus. Hilar mossy cells are quite vulnerable to status epilepticus, and it is one of the first neuronal populations to be damaged in temporal lobe epilepsy (Nadler et al., 1980; Babb et al., 1984; Cavazos and Sutula, 1990; Cavazos et al., 1991).

Second, an increase in the dentate gyrus adult neurogenesis has been observed in different models of epilepsy (Parent et al., 1997; Gray and Sundstrom, 1998; Scott et al., 1998; Nakagawa et al., 2000). As a result, an increase in the cellular proliferation and in the number of immature granule cells is observed in the subgranular zone. Many of the newly generated cells mature and integrate in the dentate circuitry.

Finally, granule cells also play an important role in the pathogenesis of temporal lobe epilepsy, as they undergo through several changes: aberrant sprouting of mossy fibers in the inner molecular layer (Tauck and Nadler, 1985), basal dendrites formation and presence of ectopic granular cells in the hilus and in the molecular layer. The above-mentioned sprouting is probably activated by the denervation of the inner molecular layer after mossy cells death (Cavazos and Sutula, 1990; Houser et al., 1990).

This sprouting implies the formation of new asymmetric synaptic contacts between sprouted mossy fiber terminals and granule cells dendrites, and also between inhibitory interneurons in the granule cell layer and inner molecular layer. The innervation of granule cells by sprouted mossy fibers arising from granule cells creates an excitatory loop that increases network excitability and allows the propagation of seizures (Tauck and Nadler, 1985; Lothman et al., 1992). However, other studies find that sprouting granule cell axons function to enhance recurrent inhibition by increasing the excitatory drive to inhibitory interneurons (Sloviter, 1992).

4. STUDY HYPOTHESIS AND OBJECTIVES

According to previous data, it is assumed that parvalbumin basket cells in the granule cell layer are innervated by mossy fibers (Ribak and Peterson, 1991; Blasco-Ibáñez et al., 2000; Seress et al., 2001; Frotscher et al., 2006). However, the number and disposition of granule cells may imply that only a subpopulation of these cells establishes this innervation. Recently, new studies describing a new granule cell subpopulation in the dentate gyrus have appeared (Williams et al., 2007; Larimer and Strowbridge, 2010; Gupta et al., 2012). The semilunar granule cells present some characteristic features, such as an axon traveling in the inner molecular layer and generating collaterals in the granule cell layer, that make them good candidates as the origin of this innervation.

Under this scenario, we hypothesize that semilunar granule cells will be in charge of the excitatory perisomatic control of parvalbumin interneurons in the dentate gyrus. Therefore, our main goals in this work are: first, to study the excitatory afferences on parvalbumin basket cell somata and to confirm the origin of the innervation from the semilunar granule cells; second, to integrate semilunar granule cells in the dentate local circuitry from an anatomical point of view; and third, study the possible implications that this connection may have in epilepsy.

The partial aims of this study are:

1. Study of the perisomatic excitatory input on parvalbumin interneurons in the dentate gyrus. Quantitative analysis of the number of excitatory and inhibitory postsynaptic specializations on the perisomatic region of parvalbumin interneurons under confocal scanning microscopy.
2. Study of the perisomatic excitatory input from mossy cells on parvalbumin interneurons in the dentate gyrus. Quantitative analysis of the number of mossy cell boutons in apposition to parvalbumin interneurons under confocal microscopy. Analysis of this innervation under electron microscopy.
3. Study of the perisomatic excitatory input from granule cells and semilunar granule cells onto parvalbumin interneurons in the dentate gyrus. Analysis of the Timm-positive mossy fiber boutons on morphologically distinct parvalbumin interneurons. Analysis of intracellularly filled typical granule cells and semilunar granule cells at the optical and electron microscopy level.
4. Characterization of the semilunar and ectopic granule cells populations in the dentate gyrus. Quantification of the number of semilunar granule cells and ectopic granule cells in the molecular layer of adult and aged mouse. Qualitative study of the presence of semilunar granule cells in postnatal development.
5. Morphological study of semilunar granule cells. Qualitative study of anatomical features such as dendritic arborization, axonal structure and somatic spines in intracellularly filled semilunar granule cells.
6. Neurochemical characterization of semilunar granule cells and outer molecular layer ectopic granule cells. Quantification in Thy1-transgenic line of the coexpression of principal cell markers, calcium binding proteins and cell activity markers with YFP-positive principal cells in the molecular layer.
7. Study of the perisomatic synaptic input on semilunar granule cells. Qualitative study of the perisomatic inhibitory innervation onto semilunar granule cells and outer molecular layer ectopic granule cells by parvalbumin and cholecystokinin-positive boutons under optical and electron microscopy. Qualitative study of the perisomatic innervation on semilunar granule cells by supramammillary afferents.

8. Study of the role of semilunar granule cells and parvalbumin interneurons in different models of epilepsy: pentylenetetrazole-induced kindling, kainic acid mild overexcitation, DEDTC-driven mild overexcitation and pilocarpine-induced status epilepticus.

MATERIAL AND METHODS

1. ANIMAL EXPERIMENTATION

All animals used in this thesis were housed in groups of three to six under controlled temperature, humidity and on a 12h light/darkness cycle, with access to food and water *ad libitum*. They were allowed to habituate to our facilities at least two days prior to the experiments. An effort was made to avoid unnecessary stress in the animals due to handling.

All animal experimentation was conducted in accordance with the Directive 2010/63/EU of the European Parliament and of the Council of 22 September 2010 on the protection of animals used for scientific purposes.

All adult animals included in this study are comprised between the ages of 2 months and 5 months, and therefore considered adults. Postnatal animals were used for intracellular injection via whole-cell patch clamp, in a range comprised between postnatal days 15 and 23. This range was chosen because it allowed a high survival of cells when slicing for patch clamp, with a relatively well formed dentate gyrus.

For the study of the appearance of semilunar granule cells during development, pups of postnatal days 1, 7, 10 and 14 were used.

No differentiation was generally made between males and females, except in the epilepsy experiments, as there is no evidence of anatomical differences between them in the expression of any of the studied cell markers, or in the studied projections.

We used two different mouse strains in this thesis:

- CD-1 ICR mice (Harlan)
- Thy1 transgenic mice with C57BL/6J background (003709, The Jackson Laboratory). Strain name B6 Cg-Tg (Thy1-YFP) 16 Jrs/J.

Thy1 transgenic mice expresses the YFP protein under the Thy1 promoter, resulting in a selective staining of principal neurons (Feng et al., 2000; Porrero et al., 2010).

We also used adult Wistar rats in several partial objectives of this thesis.

2. STEREOTAXIC INJECTIONS

2.1. TRACER INJECTION

Adult mice (approximately 3-4 months old) were anesthetized with an intraperitoneal injection of chloride hydrate 4% in saline (1 ml/100 g body weight), and put in a stereotaxic apparatus (Kopf Instruments). Skin and connective tissue on the skull were removed, and the skull trepanned to access the desired nuclei. Coordinates for the trepanation were calculated with the Paxinos' Atlas (Paxinos and Franklin, 2001), taking bregma as the reference point. Selected coordinates for the injection site were:

- Medial Septum (MS) → bregma + 0.86 mm, lateral 0 mm, deep 3.8 mm
- Supramammilary nuclei (SuM) → bregma -2.80 mm, lateral 0 mm, deep 4.3 mm

Once the skull was trepanned, the tracer was injected with a glass borosilicate capillary with 2 mm OD and 1.12 ID, pulled with a vertical puller (Model P-30, Sutter Instruments) until the desired length and thickness.

The tracer used was the anterograde tracer biotin dextran amine BDA 10 KDa (Invitrogen), introduced in the capillary by suction at a final concentration of 10% in phosphate buffer 0,1M (PB).

Once the tracer was in the glass capillary, this was injected in the brain at the corresponding coordinates, via 7 second on/off 5-10 µA current pulses during 15 min. The skin was closed with histological glue and the animal was introduced in a warm cage until it woke up.

After 5-7 days of survival, animals were intracardially perfused as described in **Section 5** of this chapter, and the brains resectioned in subseries.

2.2. COLCHICINE TREATMENT

The axonal transport blocker colchicine (Sigma) was injected into the lateral ventricle of three adult mice to better visualize the CART peptide in the cell somata. Each lateral ventricle received 2 µl of a 20 mg/mL solution in physiological saline. The stereotaxic procedure was performed as described in the above section, using the following coordinates:

- Lateral Ventricle → bregma + 0.75 mm, lateral 0.5 mm, deep 2 mm

Two days after the injection, animals were intracardially perfused, as described in **Section 5** of this chapter.

3. WHOLE-CELL PATCH CLAMP

Postnatal CD-1 mice between P15 and P23 were used for this experiment. Briefly, they were deeply anaesthetized with isoflurane (IsoFlo 1385 ESP, Esteve Veterinaria) and decapitated. The skull was immediately immersed into ice-cold solution and the brain quickly removed from it. This ice-cold solution contained (in mM): KCl 2.5; $MgCl_2$ 5; $CaCl_2$ 0.5; NaH_2PO4 1.25; glucose 10; $NaHCO_3$ 26; sucrose 252; bubbled with carbogen gas (95% O_2 / 5% CO_2).

Horizontal hippocampal slices of 300 µm thickness were cut using a vibratome (VT 1000S, Leica) and placed into an interface-type holding chamber containing ACSF (artificial cerebrospinal fluid) at room temperature.

ACSF contained (in mM): KCl 2.5; $MgCl_2$ 2; $CaCl_2$ 2; NaH_2PO4 1.25; glucose 10; $NaHCO_3$ 26; NaCl 126; bubbled with carbogen gas.

After at least one hour incubation, slices were ready for use and transferred individually into a submerged type recording chamber.

Patch pipettes were pulled from borosilicate glass capillaries with 1.5 mm O.D. and 0.84 mm I.D. (World Precision Instruments) using a horizontal puller (Model P-97, Sutter Instruments). They were filled with a solution that contained (in mM): NaCl 4; KGluconate 110; KCl 20; HEPES 10; $MgCl_2$ 2. Biocytin (Sigma) was included in the pipette to procure the intracellular filling of the cell. Pipette resistance was checked in the bath regularly, varying from 3 to 6 MOhm.

Whole-cell patch-clamp was performed under visual guidance using an Olympus Microscope (BX51WI, Olympus) with differential interference contrast optics, visualized by a NIR CCD camera (C7500-51 Hamamatsu). The amplifier used was an AM2400 (AM Systems), connected to a CED Micro 1401 AD converter (Cambridge Electronic Design Limited). The electrophysiological response of the cell was observed with the help of an oscilloscope HAMEG 1507-3 (HAMEG Instruments).

Patched cells were kept 5 minutes in Vclamp with a holding voltage of -75 mV, as it has been described that the these cells present a hyperpolarized resting membrane potential (Spruston and Johnston, 1992; Staley et al., 1992; Penttonen et al., 1997; Williams et al., 2007) . After that, we tested in Iclamp the voltage responses to a series of depolarizing square current pulses of 2 seconds length, as it had been described that semilunar granule cells and typical granule cell showed different responses under this experimental condition (Williams et al., 2007). The amplitudes of the current steps varied from 10 pA increments until 100 pA, and then at 50 pA

increments until 400 pA. No further information was obtained from this recording, but we got the patched cell to fire action potentials to the effect of improving the axonal filling. The response to the cell to the depolarizing current protocol was recorded using the free software WinWCP V4.3.4 (Strathclyde Electrophysiology Software).

After 20 minutes, the slices were fixed by immersion in a fixative solution containing 4% PFA and 0.5% GA.

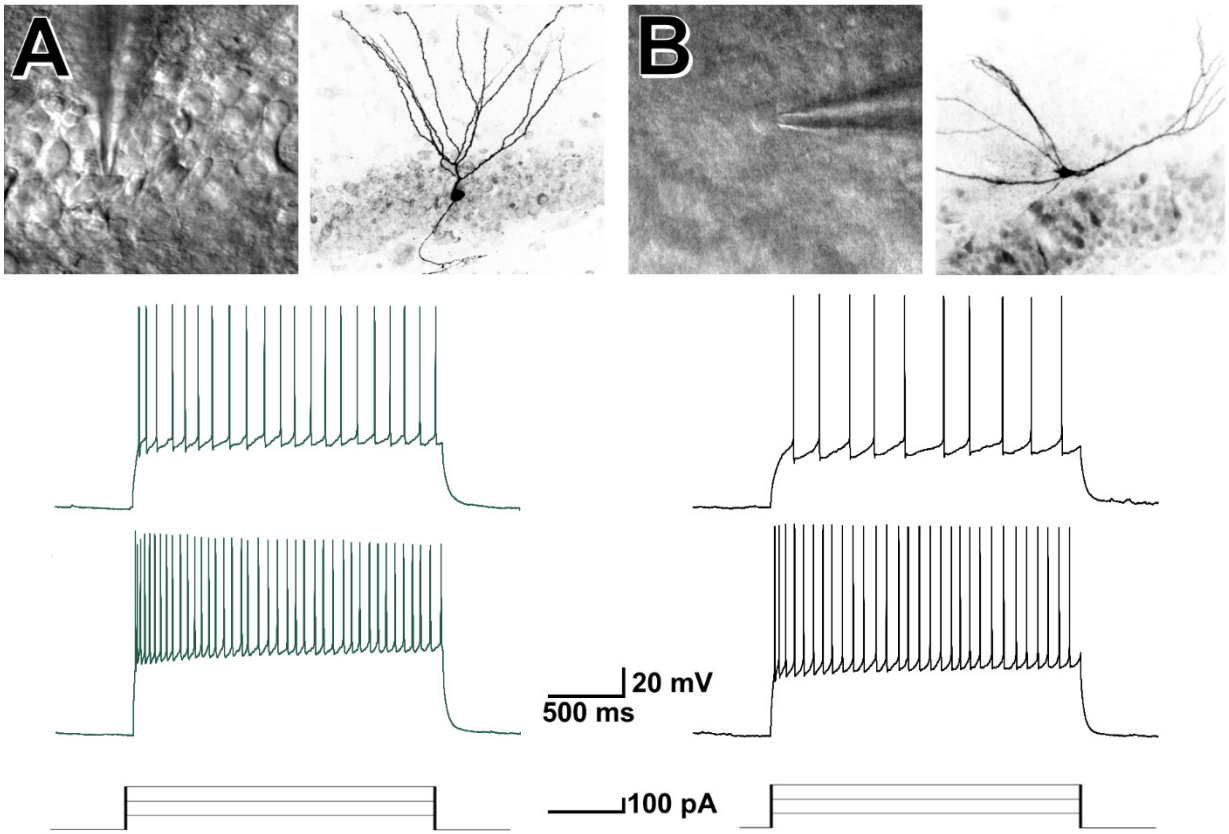

Example of two intracellularly filled typical granule cell (A) and semilunar granule cell (B). Cells were selected due to their morphology and location in the dentate gyrus in a DIC image. Once patched, the firing pattern of the cell was recorded (lower panels), to check whether it may be a granule cell. Due to the experimental conditions, the step protocol obtained for both cell types varied with the one observed by (Williams et al., 2007). However, an anatomical identification of the cell was always performed to confirm that they were granule cells.

4. EXPERIMENTAL MODELS OF EPILEPSY

4.1. PENTYLENETETRAZOLE TREATMENT

A total of 35 two-month old CD-1 mice were used for this experiment. Only males were used in the pentylenetetrazole model of epilepsy, as previous studies have shown a relation between gonadal steroid hormones and seizure susceptibility (Bauer, 2001).

Animals were treated with a subconvulsive dose of pentylenetetrazole [40 mg/Kg in physiological saline, intraperitoneal (Sigma)] every second day, until they reached the "kindled status". Animals were closely observed for 20-30 minutes after the drug was injected, to check their response to the drug and the evolution of the kindling procedure.

The "kindled status" was considered to be achieved when animals reached stage 5 in Racine's scale for four consecutive injections.

CD-1 mice were chosen instead of C57BL/6, as they showed a slower response to the same dose of pentylenetetrazole. As we wanted to study the evolution of the kindling procedure, a slower response suited better our purpose. This dose was previously tested in a pilot experiment, to make sure that it was not convulsive but produced kindling after repeated administrations.

Two different experiments were performed to better assess the initiation and evolution of the kindled status and its neurochemical consequences in the mouse hippocampus:

- Fully kindled: subconvulsive dose of pentylenetetrazole every second day until they reached stage 5 in Racine scale in four consecutive injections. This group was used to study the plastic differences in various cell populations and in the circuitry that occur in the mouse dentate gyrus, once they have reached the kindling status and are hyperexcitable.
- Fully kindled + 1 month of survival: once the kindled status was achieved, mice were kept one month without receiving any injection. The purpose of this experimental group was to study the maintenance and/or evolution of the differences observed in the first group.

One additional control group was added per experimental group. Control groups received the same handling, but were injected with physiological saline. Animals were in all cases intracardially perfused two days after the end of the procedure, to avoid any acute effect of the drug.

4.2. EPILEPSY STUDIES DIFFERENT THAN PENTYLENETETRAZOLE-INDUCED MODEL OF KINDLING

For the last chapter of this thesis, sections from experiments previously performed in our laboratory were analyzed, focusing on the cell populations of interest. The following models were used:

- Pilocarpine-induced status epilepticus in mouse (Marqués-Marí et al., 2007)
- Zinc chelator DEDTC combined with Kainic Acid in mouse (Domínguez et al., 2003a; b, 2006)

4.2.1. DEDTC AND KAINIC ACID MODEL OF EPILEPSY

The zinc chelator diethyldithiocarbamate (DEDTC, Sigma) and the kainate receptor agonist kainic acid (Sigma) were used to induce status epilepticus in adult mice. Animals in this experiment were divided into four groups:

- Control: this group received two injections of distilled water
- Kainic acid treatment: this group received an injection of kainic acid at a subconvulsive dose (15 mg/Kgbw) followed by an injection of distilled water after 15 min.
- DEDTC treatment: this group received an injection of distilled water 15 min before an injection of DEDTC (150 mg/Kgbw).
- Kainic acid + DEDTC treatment: this group received an injection of kainic acid at a subconvulsive dose (15 mg/Kgbw), followed by an injection of DEDTC (150 mg/Kgbw) after 15 minutes.

All drugs were injected intraperitoneally, and solutions were adjusted for the same volume (0.5 ml) for each injection.

4.2.2. PILOCARPINE MODEL OF EPILEPSY

Adult mice were used for this experiment. The experimental group received an intraperitoneal injection of scopolamine methyl-nitrate in physiological saline (1mg/Kgbw, Sigma) to reduce peripheral cholinergic effects. After 30 min, they received an intraperitoneal injection of the muscarinic receptor agonist pilocarpine hydrochloride (360 mg/Kgbw, Sigma).

After the injections, animals were monitored until one and a half hour after the onset of status epilepticus. The seizures were terminated by an intraperitoneal injection of diazepam in physiological saline (10 mg/Kgbw).

The control group received both scopolamine and diazepam injections, but were injected with saline instead of pilocarpine.

5. TISSUE FIXATION

Animals were deeply anesthetized with an intraperitoneal injection of chlorate hydrate 4% in saline (0.9% NaCl), with a dose of 1 ml/100 g weight. Before proceeding with the perfusion, all animals were checked for reflex movements, and higher doses were used until the animal was completely anesthetized.

Animals were perfused intracardially first with 10 ml saline followed by 30 min with the corresponding fixative, at a flow rate of 4 ml/min procured by a perfusion bomb.

Four different fixative solutions were used, depending on the experiment:

- 4% paraformaldehyde (PFA) with 15% of a saturated solution of picric acid was used for conventional optical and confocal studies.
- 0.5% glutaraldehyde (GA), 4% PFA and 15% of a saturated solution of picric acid was used for electron microscopy studies.
- 20 ml of 3.8% acrolein in 2% PFA followed by 100 ml 2% PFA were used for optical microscopy and electron microscopy studies.
- For Timm staining, animals were initially perfused with 20 ml of 0.05% Na_2S, followed by 100 ml of 4% PFA in PB.

Due to the quality of the ultrastructure, and that one of the most used antibodies in this study gave several technical problems with GA, we decided to use acrolein as the main fixative for electron microscopy.

Acrolein reacts with macromolecules in a similar fashion as formaldehyde, but produces more cross-links. An additional characteristic is that it can react with fatty acids through a double bond present in its molecular structure. However, as it is not widely used, and to avoid the analysis of unspecific staining, we tested all the antibodies in 4% PFA, 0.5% GA and in acrolein in both rat and mouse, to check that the labeling obtained of the desired marker corresponded to that described in previous studies.

In all cases since both 0.5% GA and acrolein presented a similar staining, acrolein was chosen due to its better antigenicity and to procure as much homogeneity of the tissue used for the experiments as possible.

Once the animals were perfused, they were decapitated and the heads containing the brains were kept in the fridge for 30 min for post-fixation. After this, the brains were removed from the skull and kept in PB with 0.05% sodium azide at 4°C until they were sliced.

Those animals that were perfused for Timm staining were not postfixed, their brain were immediately removed and fast sliced. This protocol was needed to ensure that the zinc labeling was optimal, as Timm staining critically diminishes with time.

6. MICROTOMY

As a standard procedure, once the brain was fixed, both hemispheres were separated by the middle line and cut in 60 µm-thick coronal sections with a vibratome (VT1000S, Leica), from the rostral to the caudal side, in 6 subseries. All the tissue was kept in PB with 0.05% sodium azide at 4°C, in either glass vials or 1.5 mL tubes.

For further work with 300 µm-thick patched slices, they were flat included in a 4% agar solution (Bacteriologic Agar, Cultimed) and cut into 60 µm-thick sections.

7. IMMUNOHISTOCHEMISTRY

7.1. IMMUNOSTAINING FOR OPTICAL MICROSCOPY

Immunostaining for optical microscopy was performed in free-floating sections, according to the avidin-biotin-peroxidase method. During the whole protocol, sections were in mild agitation and at room temperature (unless specified otherwise).

Briefly, sections were washed three times in PB to completely remove the remaining fixative present in the tissue.

Only if the tissue had been fixed with GA or acrolein, a 20 min incubation with Sodium Borohydride (BH_4Na, Panreac) in PB was performed. Before proceeding with the immunostaining, at least four washes in PB were done.

For blocking the endogenous peroxidase activity, sections were incubated in a solution containing Hydrogen Peroxide 1% (Panreac) in PB for 15 min. Sections were then washed three times in PB.

Following this, a blocking of the non-specific binding of the antibody to the tissue was performed. This was made by incubating the sections in a solution that contained 10% serum of the host species of the secondary antibody. For permeabilization of the tissue, the detergent Triton X-100 (Tx) was added in this solution for a final concentration of 0.2%. In those cases where this procedure was not enough to avoid the background staining, a solution containing the amino acids Lys and Gly was added to the 10% serum solution (amino acids considered as the main target of fixative agents), so they could react with the remaining reactive sites of the fixative and the tissue.

Normal serums used in this study were: normal goat serum (Millipore); normal donkey serum (Jackson ImmunoResearch Laboratories) and horse serum (Sigma).

Sections were then briefly washed in PB, and then incubated either overnight at room temperature, or 48 hours at 4°C, in a solution containing the primary antibody at the working dilution, the normal serum of the host species of the secondary antibody at 1% concentration and sodium azide 0.05% in PB. Triton X-100 was also added in this step for tissue permeabilization at a final concentration of 0.2% (PB-Tx). The working dilution and reference for all primary antibodies are detailed in **Table 1**.

After three washes in PB, sections were incubated in a solution containing the secondary biotinilated antibody in working dilution in PB-Tx. The working dilution and reference for all secondary antibodies used in this study are detailed in **Table 2**.

After three washes in PB, sections were incubated in Avidin Biotin-peroxidase complex (ABC) 1:300 in PB-Tx.

Finally, after three washes in PB, sections were pre-incubated in a solution containing diaminobenzidine DAB (Sigma) at a final concentration of 0.03%, to allow its full penetration in the tissue. Soon after, hydrogen peroxide was added to a final concentration of 0.01% to start the reaction. The brown precipitate formed by the oxidized-DAB indicated the presence of the desired antigen.

7.2. DOUBLE IMMUNOSTAINING FOR OPTICAL MICROSCOPY

The avidin-biotin-peroxidase method was also used for the staining of two different antigens in the same section. The different colors were achieved by doing two consecutive immunostainings and using in the first one DAB conjugated with nickel (DAB-Ni), and the

second one with DAB as chromogens. DAB-Ni produces a bluish black precipitate whereas the precipitate of the DAB is reddish brown.

Briefly, the DAB-Ni solution contained: 0.04% NH_4Cl, approximately 0.1% NH_4NiSO_4 and 0.03% DAB in PB. A pre-incubation of the sections with DAB-Ni was always done to ensure that enough Ni was present and to avoid possible loss of Ni in the second immunostaining and therefore a turn from dark-bluish into brownish of the precipitate. Once pre-incubated, the solution was changed for fresh DAB-Ni solution and then developed.

After the development of DAB-Ni, a second immunostaining was done and a standard DAB development performed.

7.3. IMMUNOSTAINING FOR CONFOCAL MICROSCOPY

The immunostaining for confocal microscopy was always done in free floating sections and consisted in the following steps:

The first step was an incubation with BH_4Na for 20 minutes, only in those animals in which a GA or acrolein based fixative was used. Otherwise, this step was skipped.

Next, the blocking of the non-specific binding of the antibody was performed by incubating the tissue with a 10% normal donkey serum in phosphate buffer saline with 0,2% Triton X-100 (PBS-Tx) for 1 hour at room temperature.

After briefly washing the blocking solution, an incubation with the primary antibodies was performed overnight at room temperature, or 48 hours at 4°C. The working dilution and reference for all primary antibodies are detailed in **Table 1**.

After three washes in PBS-Tx an incubation with the secondary antibodies (always generated in donkey) was performed. From this step on, a special effort was made to keep the tissue in the darkness as much as possible. The working dilution and reference for all secondary antibodies are detailed in **Table 2**.

Dako Mounting Medium was used when mounting the sections in slides, as it acts as an anti-fading agent and prevents the fluorophores from quickly extinguishing their fluorescence.

Slides were kept always at 4°C except when being analyzed under the confocal microscope.

7.4. IMMUNOSTAINING FOR ELECTRON MICROSCOPY

This immunostaining was performed like a normal staining for optical microscopy, with the exception of the following steps:

- No Triton X-100 or detergent of any kind was used in this sections, to avoid the degradation of the lipidic membranes. For permeabilization of the tissue and enhancing the penetration of the antisera, the "Freeze-Thawing" technique was used. Briefly, sections were incubated from 30 min to one hour at room temperature in a solution containing: sucrose 25% and glycerol 10% in PB 0.05 M. Once the sections were cryoprotected, three cycles of freezing and thawing were performed in an aluminium-foil boat over liquid nitrogen.
- Special attention was paid in keeping the PB buffer cold during the incubations.
- All primary antibody incubations were performed for 48 hours at 4°C.

Once the immunostaining was finished, the sections were post-fixed, embedded in epoxy resin and mounted. After the development of diaminobenzidine, the protocol went as follows: sections were incubated in a solution containing 1% OsO_4 (Electron Microscopy Sciences) and 7% glucose in PB for 45 minutes at room temperature. Then, sections were rinsed first three times with PB and then two times of 15 minutes with maleate buffer (pH 5.2;0.93% maleic acid and 0.35% NaOH in distilled water), incubated 90 minutes in a "staining solution" containing 0.61% maleic acid, 0.35% NaOH and 2% uranyl acetate (Panreac) , and rinsed again three times for 10 minutes in maleate buffer. Then, the sections were dehydrated in graded series of cold ethanol (30°, 50°, 70°, 90°, 2 x 96°, 2 x 100°, 100° + $CuSO_4$) and cleared two times in propylene oxide (Sigma). Finally, sections were embedded overnight in epoxy resin (Durcupan, Sigma) and flat mounted on microscope slides. Coverslips used were covered by a commercial liquid release agent (Electron Microscopy Sciences) that facilitates their removal.

Specimens were studied under the optical microscope, and the area of interest to be further studied under electron microscopy was isolated and re-included in an epoxy resin block.

1 to 1.5 µm thick semithin sections, or 50 to 70 nm thick ultrathin sections were obtained using an ultramicrotome (Leica EM UC6). Semithin sections were mounted in microscope slides, and stained with borax-based toluidine blue and covered with durcupan. Ultrathin sections were collected on formvar-coated grids and counterstained with lead citrate for 12 minutes.

7.5. PROCESSING OF HISTOLOGICAL SECTIONS FROM INTRACRANIAL INJECTION

The first subseries was always developed with the DAB-Ni method, and a Toluidine Blue counterstaining was performed after mounting the sections to better study the location of the injection and the presence/absence, amount and distribution of fibers projecting to the dentate gyrus. Only those injections that had relatively small sites of injection, that presented an adequate number and distribution of fibers, and that presumably had a good quality-tissue were used for the study.

Further treatment of these sections was always done with a double immunostaining of the fibers and any other desired marker, developed with DAB-Ni and DAB respectively.

7.6. PROCESSING OF SLICES FROM WHOLE-CELL PATCH CLAMP

Once the cell of interest was patched and presumably filled with biocytin, the slice was fixed by immersion in a PB solution containing 4% PFA and 0.5% GA.

For morphological evaluation of the filled cell, the slices were processed with BH_4Na 1% in PB (to remove any possible auto-fluorescence in the tissue) and incubated in a PB-Tx solution containing A488-conjugated avidin. Then, slices were mounted in DAKO-mounting medium and visualized under confocal microscopy.

To study the synaptic connectivity of semilunar granule cells, 300 µm-thick fixed slices were further processed as follows: first, they were flat included in a 4% agar solution (Bacteriologic Agar, Cultimed) and cut into 60 µm-thick sections. Then, the biocytin-filled cells were developed with DAB-Ni (as described above). Only those cells that showed axonal staining in the granule cell layer, and the level of background staining did not mask the actual axon staining, were further processed for a parvalbumin immunostaining with the DAB method for optical microscopy. Once we found enough examples of the innervation, the same procedure was performed for electron microscopy.

7.7. PROCESSING OF SECTIONS FOR TIMM STAINING

Once the brain was removed from the skull and quickly sliced into 60 µm-thick slices, they were washed in three times of 20-30 min in PB and then incubated in a solution containing: 14% acacia gum, 1.7% hydroquinone, 0.08% silver nitrate, 2.4% citric acid and 2.3% trisodium

citrate. The incubation was held at room temperature and protected from light, as both factors highly influence the speed and background of the reaction. The incubation lasted no less than 20 minutes and no more than one hour, but was continuously checked to reach the optimal signal to background level, and the solution was renewed whenever turbidity was observed. Autometallography was stopped by directly adding 5% sodium thiosulfate in PB, and then an extra incubation of 5 min in the same solution. Sections were then washed three times in PB and mounted.

When additional stainings had to be done on these sections, special attention was taken to perform them in as short a period of time as possible to avoid a possible weakening of the autometallography.

7.8. PROCESSING OF SECTIONS FROM POSTNATAL MICE

For the study of the appearance of semilunar granule cells during postnatal development, pups were intracardially perfused and the brain resectioned in 300 µm-thick slices. These slices were post-fixed as described in **section 7.4**, and included in Durcupan epoxy resin blocks.

Serial ultrathin sections (1 µm-thick) were obtained from these blocks and mounted in parallel consecutive series in gelatin-covered slides with the help of a heating plate. Once fixed in the slide, the following protocol was performed on the semithin sections mounted on the slides:

The first slide of the section was stained with toluidine blue in 1% borax at 75 °C for 2 min. The other two were processed for calretinin and calbindin immunochemistry as follows:

Semithin sections were treated with a solution containing 50% sodium ethoxide, 30% acetone and 20% toluene for 12 minutes, to erode the epoxy resin. Next, they were rehydrated in consecutive ethanol solutions of decreasing concentration, washed in distilled water and finally kept in PB. To remove the osmium, slides were treated with a solution of hydrogen peroxide 3% and then washed three times in PB. After this, the process continued using droplets of the solutions in a humid chamber. The immunostaining was performed according to the avidin-biotin-peroxidase method described in **section 7.1**. Once finished, semithin sections were dehydrated again in consecutive ethanol solutions of increasing concentration, cleared in xylol and mounted with Eukitt.

7.9. TABLE OF ANTIBODIES USED IN THIS THESIS

Primary antibodies

	Host	Dilution	Company	References
5-HT	rabbit	1:2000	Enzo	Cat. No. SZ1021
CAMKII	mouse	1:500	abcam	Cat. No. ab22609
CART	rabbit	1:500	Phoenix Pharmaceuticals	Cat. No. H-003-61
Calbindin D-28k	rabbit	1:1000	Swant	Cat. No. CB-38a
CB1R	rabbit	1:2000	Synaptic Systems	Cat. No. 258 003
CCK8	rabbit	1:1000	Sigma	Cat. No. C2581
c-Fos	rabbit	1:8000	Synaptic Systems	Cat. No. 226 003
Calretinin	rabbit	1:2000	Swant	Cat. No. 7699/3H
Calretinin	mouse	1:5000	Swant	Cat. No. 6B3
DβH	rabbit	1:800	Enzo	Cat. No. DZ1020
Gephyrin	mouse	1.1000	Synaptic Systems	Cat. No. 147 011
HSP72	mouse	1:300	Oncogene Research	Not available
pan-Fos (c-Fos K-25)	rabbit	1:1000	Santa Cruz Biotechnology	Cat. No. sc-253
Parvalbumin	guinea pig	1:2000	Synaptic Systems	Cat. No. 195 004
Parvalbumin	rabbit	1:5000	Swant	Cat. No. PV-28
Prox1	mouse	1:1000	Millipore	Cat. No. MAB5654
PSD95	goat	1:1000	abcam	Cat. No. ab12093
Synaptophysin	mouse	1:1000	Sigma	Cat. No. S5768
Somatostatin	rabbit	1:500	Millipore	Cat. No. AB5494
TH	mouse	1:1000	Millipore	Cat. No. AB152
VAChT	goat	1:3000	Diasorin	Cat. No. 24286
VGluT2	Guinea pig	1:1000	Millipore	Cat. No. AB2251

TABLE 1 – List of primary antibodies used in this thesis. The dilution indicated was generally used for both ABC-DAB immunostaining and immunofluorescence. When the nature of the fixation required it, the dilutions were slightly modified.

Secondary antibodies

	Host	Label	Dilution	Company
Anti-Rabbit IgG	Donkey	Alexa Fluor 488	1:400	Molecular Probes
Anti-Rabbit IgG	Donkey	Alexa Fluor A555	1:400	Molecular Probes
Anti-Rabbit IgG	Donkey	Alexa Fluor 647	1:400	Molecular Probes
Anti-Rabbit IgG	Goat	Biotin	1:300	Thermo Scientific
Anti-Mouse IgG	Goat	Biotin	1:300	Vector
Anti-Mouse IgG	Donkey	Biotin-SP	1:400	Jackson ImmunoResearch
Anti-Mouse IgG	Donkey	DyLight 649	1:400	Jackson ImmunoResearch
Anti-Mouse IgG	Donkey	DyLight 549	1:400	Jackson ImmunoResearch
Anti-Mouse IgG	Donkey	Biotin	1:400	Jackson ImmunoResearch
Anti-Mouse IgG	Donkey	Alexa Fluor 488	1:400	Jackson ImmunoResearch
Anti-Guinea Pig IgG	Donkey	DyLight 549	1:400	Jackson ImmunoResearch
Anti-Guinea Pig IgG	Donkey	DyLight 649	1:400	Jackson ImmunoResearch
Anti-Guinea Pig IgG	Goat	Alexa Fluor 488	1:400	Invitrogen
Avidin		A488	1:400	Molecular Probes

TABLE 2 – List of secondary antibodies used in this thesis.

8. MICROSCOPY AND IMAGE ACQUISITION

An Olympus CX41 optical microscope was used when observing and analyzing the slides processed for optical or electron microscopy. Images were acquired with an Olympus C-5060 wide zoom camera, using Cam2com software. Images were always acquired setting manually the exposure time that best suited the staining.

Electron microscopy analyses were performed using a JEOL JEM-1010 transmission electron microscope, with the voltage set at 60 kV. Images were acquired using either MegaView I digital camera, or AMT RX80 digital camera.

For confocal microscopy analyses, two different confocal microscopes were used:

- Leica TCS SPE confocal microscope
- Olympus Fluoview F10i confocal microscope

Special attention was paid to use the same confocal microscope with the same settings for each experiment.

9. IMAGE PROCESSING AND DATA ANALYSIS

For image processing and analysis, FIJI (ImageJ 1.49j10) and Gimp 2.8 were used.

9.1. QUANTIFICATION OF PERISOMATIC INNERVATION

Quantification of the perisomatic innervation of parvalbumin cells was done under confocal microscopy. Briefly, Z-series of focal planes were taken from the surface of the section to the maximal Z that penetration of the antibody allowed, with a Z-step of 0.5 µm. In all cases, a 63x objective was used, with an optical zoom at 3x.

For the analysis, either the LSM 5 Image Browser software, or ImageJ were used. As our aim was not to compare the quantification between two experimental groups, the color curves in the images were fitted individually to ensure that all the positive profiles were visible and to remove as much background as possible. Only those puncta that were "touching" the edge of the parvalbumin profile with no apparent space between both profiles, were considered as positive.

9.2. CELL NUMBER ESTIMATION

In all cases, both hemispheres of the brain were separated and cut into 60 µm-thick slices independently. Two different methods to estimate the cell number were used:

1. Total number of cells per dentate gyrus. In this case, when the cell marker used was not very abundant in the dentate gyrus, the total number of positive-cells were counted in all sections from one subseries. The total number of cells per subseries was translated into total number of cells by multiplying by 6 subseries.
   As this data is not given in relation to the total dentate volume, the Cavalieri's principle was not applied.
2. When all the cells in a subseries could not be counted, the estimation was given as cell density as number of cells per mm^2, and the sections analyzed were all from the same bregma approximately. In this case, a picture was taken from each section using the same optical parameters, in which the area of interest was included. These pictures were then scaled and the area of the dentate gyrus was calculated using the Image J software. The number of cells was counted and the result was given as number of cells per mm^2.

9.3. SHOLL ANALYSIS

This analysis was performed using the plugin "Simple Neurite Tracer" of the ImageJ software (Longair et al., 2011). In some cases, several stacks of the same cell were joined using the "stitching" plugin in ImageJ, to ensure both the quality of the final image and the presence of all dendritic segments of the analyzed cell (Preibisch et al., 2009).

Concentric spheres centered in the cell soma were drawn with increasing radius and the number of dendrites crossing these spheres were counted. As the assumption of normality could not be accepted in all cases of this analysis, we used a Mann-Whitney test for the statistical analysis.

9.4. STATISTICS

Statistical analysis was performed using SPSS v.19, and data representation was performed with the output values of SPSS in Microsoft Excel.

Although in biological samples the population is always assumed to present a normal distribution, a Shapiro-Wilk test was performed to make sure that our sample also followed a normal distribution.

Shapiro-Wilk test was preferred to Kolmogorov-Smirnov, as this test is preferred when no previous assumption on the population mean and SD is made, and the "n" sampled is low (as in our case).

Levene's test was performed to check whether the population variances were equal, and if a t-test could be performed. When there was no homoscedasticity, a t-test with no assumption of equal variances or a Mann-Whitney non-parametric test was used.

Data is shown as mean ± SD, unless stated otherwise.

RESULTS

RESULTS I:
PERISOMATIC INNERVATION ON PARVALBUMIN BASKET CELLS IN THE MOUSE DENTATE GYRUS

1. PERISOMATIC EXCITATORY INNERVATION ON PARVALBUMIN BASKET CELLS IN THE GRANULE CELL LAYER

As a first approach, we decided to analyze the importance of the perisomatic excitatory innervation within the whole of the innervation that parvalbumin basket cells receive in the perisomatic region. For that purpose, we combined parvalbumin with the following post-synaptic markers:

- Post-Synaptic density protein 95 KDa (PSD95), which is located in the post-synaptic density in asymmetric synapses and functions as an anchoring element for AMPA and NMDA receptors among other synaptic proteins (Lin et al., 2004; Jackson and Nicoll, 2011). Therefore, it labels specifically the postsynaptic specialization of glutamatergic synapses, and can be used as a marker of excitatory synaptic contacts.
- Gephyrin (Geph), which labels specifically the postsynaptic specialization of inhibitory synapses (Fritschy et al., 2008), and can therefore be used as a marker of inhibitory synaptic contacts.

To estimate the relative importance of excitatory and inhibitory innervation onto parvalbumin basket cells, a triple immunostaining was performed using parvalbumin, PSD95 and Gephyrin. In this experiment, a total of 16 molecular layer parvalbumin interneurons (**Figure I.1 A**) and 16 parvalbumin interneurons sitting in the granule cell layer (**Figure I.1 B**) were analyzed in the dentate gyrus of 3 different animals. The cell depth analyzed in each parvalbumin cell was the same for both postsynaptic density markers (an average of 9 µm depth of the cell, taking into account that the penetration of both PSD95 and Gephyrin antibodies should be acceptable). An average of 200 positive elements were quantified per cell, in the soma and in the proximal portion of the dendrites, that has been considered functionally equivalent to the soma (Megías et al., 2001; Papp et al., 2001).

Since the penetration of the postsynaptic markers often did not allow for analysis of the whole depth of the cell, data are shown as percentages of PSD95 or Gephyrin in relation to the total number of postsynaptic densities. The total number of postsynaptic densities is calculated as

the sum of PSD95-positive elements and Gephyrin-positive elements in close apposition of the cell membrane surface by its inner side (**Figure I.1 C-D**).

Our results show that parvalbumin cells presented more PSD95-positive elements in apposition than Gephyrin-positive ones. Therefore, the perisomatic excitatory input in parvalbumin basket cells is at least as important as the inhibitory input, suggesting the relevance of excitatory input on the perisomatic region of these cells. A summary of these results is shown in **Graph I.1**.

For the whole number of parvalbumin cells the percentage of PSD95-positive postsynaptic elements is similar, even higher, than the percentage of Gephyrin-positive postsynaptic elements (56.38 ± 1.62% and 43.62 ± 1.62% respectively; n=32).

When we considered the different location of the parvalbumin cells somata, granule cell layer basket cells showed more PSD95-positive postsynaptic densities than molecular layer basket cells (58.72 ± 2.12% and 54.03 ± 2.39% respectively; n=16 and 16). However, there was no statistical difference between both groups (p=0.153).

Similarly, Gephyrin-positive postsynaptic densities were more abundant in molecular layer parvalbumin interneurons than granule cell layer parvalbumin interneurons (45.97 ± 2.40% and 41.28 ± 2.12% respectively; n=16 and 16). This difference was not statistically significant since the p-value in the statistical analysis is necessarily the same as the one obtained in the comparison of PSD95-positive elements due to the nature of the data.

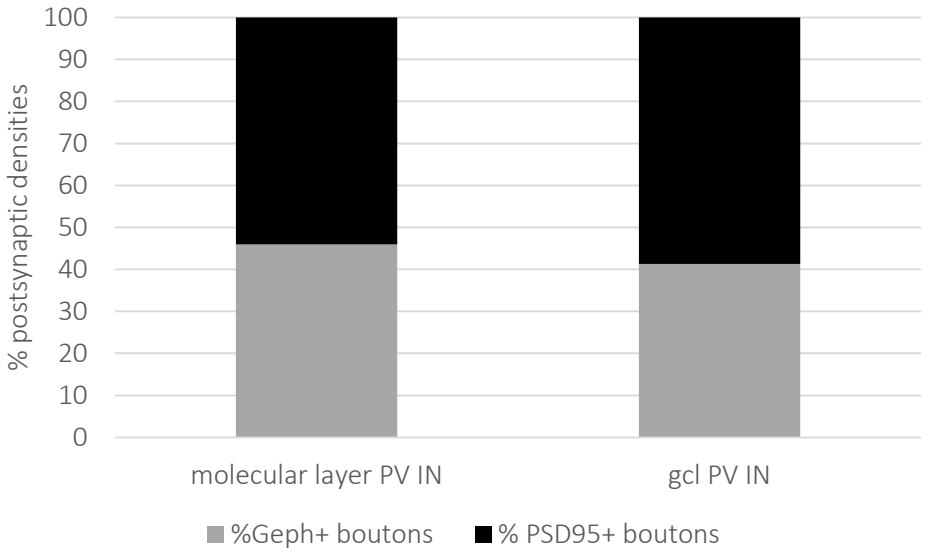

Graph I.1 – Similar excitatory and inhibitory innervation on different subtypes of parvalbumin interneurons
Molecular layer and granule cell layer (gcl) parvalbumin interneurons (IN) receive similar percentages of gephyrin (Geph) and PSD95 puncta in the perisomatic area.

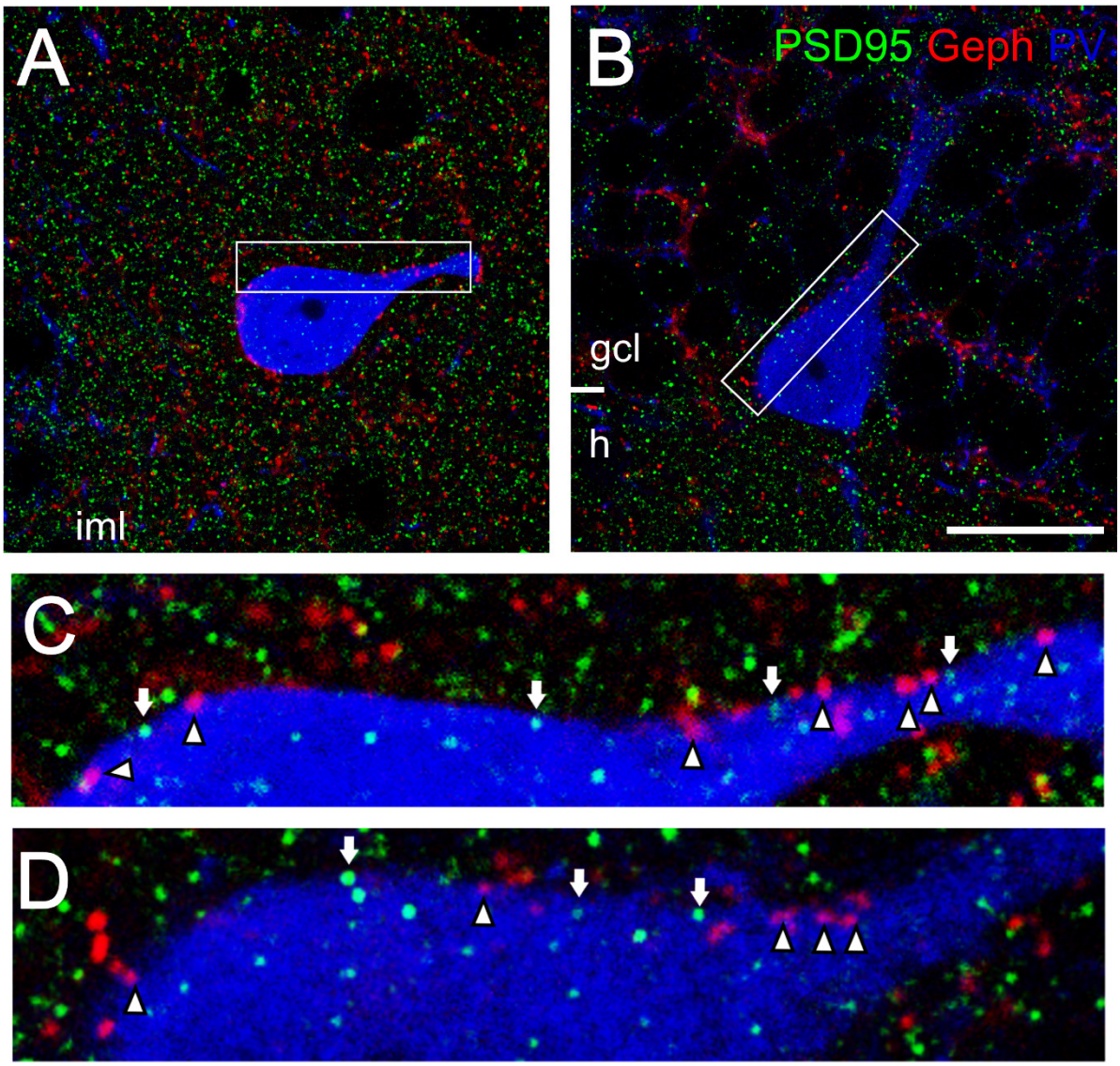

Figure I.1 – Excitatory and inhibitory perisomatic innervation on parvalbumin interneurons in the mouse dentate gyrus

Triple immunostaining for parvalbumin (blue), Gephyrin (red) and PSD95 (green), postsynaptic markers for inhibitory and excitatory synapses respectively. Only those puncta in close apposition to the inner side of the border of the parvalbumin interneuron were considered for the analysis. In the case of PSD95, puncta was also found in the middle of the dendrites and cell body. These puncta were considered as a recently synthetized protein, or a mature form that was being transported to its final destination, and were not considered in the analysis in any case.

A) Confocal plane showing the soma and a principal dendrite of a parvalbumin interneuron located in the inner molecular layer. Note the high density of PSD95 puncta in this area.

B) Confocal plane showing the soma and dendritic trunk of a pyramidal basket parvalbumin interneuron, with the cell body sitting in the border between the granule cell layer and the hilus, and the dendritic trunk traveling to the molecular layer. As expected, the labeling of PSD95 was scarce in the granule cell layer and abundant in the hilus.

C) Higher magnification of the inset shown in (**A**), from a molecular layer parvalbumin interneuron. The number of Gephyrin (arrowheads) and PSD95 puncta (arrows) was approximately the same in all the cells analyzed.

D) Higher magnification of the inset shown in (**B**), from a parvalbumin pyramidal basket interneuron. The number of Gephyrin (arrowheads) and PSD95 puncta (arrows) was approximately the same in all the cells analyzed.

gcl, granule cell layer; Geph, Gephyrin; h, hilus; iml, inner molecular layer; PSD95, postsynaptic density protein 95 KDa; PV, parvalbumin. Scale bar: 20 µm

2. PERISOMATIC EXCITATORY INNERVATION FROM MOSSY CELLS ON PARVALBUMIN INTERNEURONS IN THE GRANULE CELL LAYER

Synaptic contacts from the hilar mossy cells axons in their way into the inner molecular layer have been described among the possible sources of excitatory perisomatic connections on parvalbumin basket cells (Seress and Ribak, 1984). Therefore, we aimed to assess their share in the excitatory innervation on these interneurons. For that purpose, we analyzed the perisomatic innervation on parvalbumin basket cells in the granule cell layer using cellular and synaptic markers and studying their colocalization at the confocal microscopy level.

To specifically stain the mossy cell population we used calretinin, as it has been proved to label mossy cells in the mouse and reliably stains mossy cell fibers and synaptic boutons (Blasco-Ibáñez and Freund, 1997), whereas parvalbumin was used as a marker for fast-spiking basket cells. They were combined with the synaptic markers PSD95, present in the postsynaptic density, and synaptophysin (Syn), present in the membrane of the synaptic vesicles and considered therefore as a marker of the presynaptic element.

A total of 6 parvalbumin cells from 3 different animals, selected by their morphology and dendritic distribution, were analyzed to quantify the presence of calretinin-positive synaptic boutons in close apposition to parvalbumin-positive interneurons (**Figure I.2 A**). For this partial objective, we only considered those parvalbumin interneurons located in the granule cell layer and not those ones located in the molecular layer. The latter were not included as, considering the resolution of confocal microscopy, the high density of calretinin puncta in the inner molecular layer would have introduced a big number of false-positive elements in our analysis.

As a first approach we made a triple immunohistochemistry with parvalbumin, calretinin and synaptophysin (**Figure I.2 D-F**). Synaptophysin allowed for estimation of the totality of boutons on parvalbumin basket cells whereas its colocalization with calretinin set a maximum possible number for calretinin-positive boutons from mossy cells on them. However, this approach had the limitation that it did not allow us to distinguish between GABAergic calretinin-positive boutons and glutamatergic calretinin-positive boutons.

Our results at this level showed that mossy cells may perisomatically innervate parvalbumin basket interneurons, though less than it was expected from literature. We analyzed 294 synaptophysin-positive puncta, from which 43 were located on the soma, 85 were located on

the granule cell layer dendritic shafts, 135 on the dendrites located in the inner molecular layer, and 31 boutons on proximal dendrites located in the hilus.

The data reflected that the presence of putative synaptic boutons in apposition with parvalbumin cells is more evident in the inner molecular layer, were mossy cells send their axon terminals (27 ± 6% of synaptophysin-positive elements in apposition with parvalbumin dendrites contain calretinin). On the soma and the beginning of the main dendritic shaft they are less abundant, although we also found some presynaptic calretinin-positive terminals (16 ± 3%). On the parvalbumin-positive dendrites located in the granule cell layer we only found some calretinin-positive presynaptic element (7 ± 2%). Finally, in the dendrites located in the subgranular region of the dentate gyrus we rarely found some calretinin-positive presynaptic elements (2 ± 4%).

Since the previous data could include GABAergic calretinin-positive boutons, to confirm if the results obtained with synaptophysin could be greatly affected by GABAergic boutons, we made a triple immunohistochemistry with PSD95, calretinin and parvalbumin and analyzed how many calretinin-positive boutons were adjacent to postsynaptic elements in parvalbumin cells (**Figure I.2 A-C**). With this objective we analyzed 6 cells and quantified a total of 281 PSD95 puncta located in the inner side of the cell surface. From these puncta, 104 were located in the soma, 18 in the dendrites of the granule cell layer, 125 in the dendrites of the inner molecular layer and 34 in the hilus.

The data showed that although part of the calretinin-positive boutons can be excitatory boutons presumably from mossy cells, an important part could correspond to GABAergic calretinin boutons or to calretinin-positive varicosities that do not contain an excitatory postsynaptic element. We found PSD95 puncta in close apposition to calretinin elements in the inner molecular layer (13 ± 3%) and in the soma (8 ± 3%). On the dendrites located in the granule cell layer we found some calretinin boutons in apposition to PSD95 puncta, but only testimonial and not representative (3 ± 5%). A summary of these results is shown in table **I.1**.

	soma	iml dendrites	gcl dendrites	hilar dendrites
Syn^+CR^+ puncta compared to Syn^+ puncta	16 ± 3%	27 ± 6%	7 ± 2%	2 ± 4%
$PSD95^+CR^+$ puncta compared to $PSD95^+$ puncta	8 ± 3%	13 ± 3%	3 ± 5%	0%

Table I.1 - Percentage of Synaptophysin (Syn) and PSD95 associated to calretinin (CR) positive elements in the different cellular compartments of dentate gyrus parvalbumin-positive interneurons. Iml, inner molecular layer; gcl, granule cell layer.

Given the packing of the somata in the granule cell layer and the fact that almost all of the excitatory boutons in the inner molecular layer are immunoreactive for calretinin (Blasco-Ibáñez and Freund, 1997), the possibilities of finding boutons that correspond to false-positives were considerably high. Therefore we studied this innervation at an ultrastructural level under electron microscopy.

For this purpose, we performed a double immunohistochemistry with calretinin and parvalbumin. Color development was achieved by DAB-Ni and DAB staining respectively. This methodology allowed us to distinguish both staining patterns at the optical level and then to establish a correlation between optical and electron microscopy.

A total number of 8 cells were analyzed at the electron microscopy level, among which at least one example of each morphology for parvalbumin interneuron -based on Ribak and Seress' classification –was present, to discard the possibility that different morphologies could be correlated with different innervation and therefore different physiological function (**Figure I.3-6**). Only parvalbumin interneurons that presented calretinin-positive elements in putative apposition were used in this study.

Serial ultrathin sections were collected until the penetration of the calretinin antibody diminished. All the perisomatic surface of the selected parvalbumin interneurons was analyzed in all the consecutive ultrathin sections, to verify the identity of calretinin profiles.

As a general rule, perisomatic calretinin-positive synaptic contacts were rarely found on parvalbumin interneurons whose somata were located in the granule cell layer (**Figure I.3-5**). In molecular layer interneurons, however, the frequency of calretinin-positive boutons in apposition was higher (**Figure I.6**), though not as much as expected by confocal microscopy

analysis. In all cases, the majority of calretinin-positive excitatory synapses were observed on the proximal dendrites in the inner molecular layer.

On the other hand, there were numerous unlabeled boutons establishing asymmetric synaptic contacts on these cells (**Figure I.4 E**). The morphology of unlabeled excitatory contacts resembled of *en passant* boutons from mossy fibers: they were filled with round vesicles, though sometimes a dense-core vesicle could be observed, and established more than one synaptic contact on the postsynaptic parvalbumin profile.

We observed thin calretinin-positive profiles, probably mossy cell fibers, running along parvalbumin interneurons in the granule cell layer (**Figure I.3 and I.5**). The proximity of these fibers made us suppose that the probability of presenting synaptic contacts in the soma and apical dendrite was rather high. However, no clear excitatory postsynaptic specialization was usually observed. We sometimes found a submembranous density under a climbing calretinin-positive fiber that could suggest a synaptic contact, but no other features of a synaptic boutons appeared, such as a nearby mitochondria, synaptic vesicles or an enlargement of the fiber. Electron-density in the DAB-Ni labeled calretinin element prevented us to discard them as puncta adherentia.

Finally, calretinin boutons establishing synaptic contacts were also observed in a near vicinity of parvalbumin-positive cells, but not in close apposition. These calretinin profiles could have been considered as false-positives at the optical level and even at the confocal microscope level (**Figure I.4 C**).

In conclusion, although a total of 9 calretinin boutons were found to establish synaptic asymmetric contacts in the perisomatic region of parvalbumin cells, this innervation was indeed scarce. In addition, under our analysis conditions, no clear differences were observed among all types of parvalbumin-positive interneurons except for one type: the molecular layer parvalbumin-positive interneuron, in which perisomatic calretinin boutons establishing a synaptic contact were found more frequently. Therefore the presence of calretinin boutons establishing asymmetrical contacts on parvalbumin elements depended mainly on the location of the somata and dendrites. They were present in the inner molecular layer but could be only rarely found in the granule cell layer. These data point to a layer specificity rather than to a cell morphology distribution.

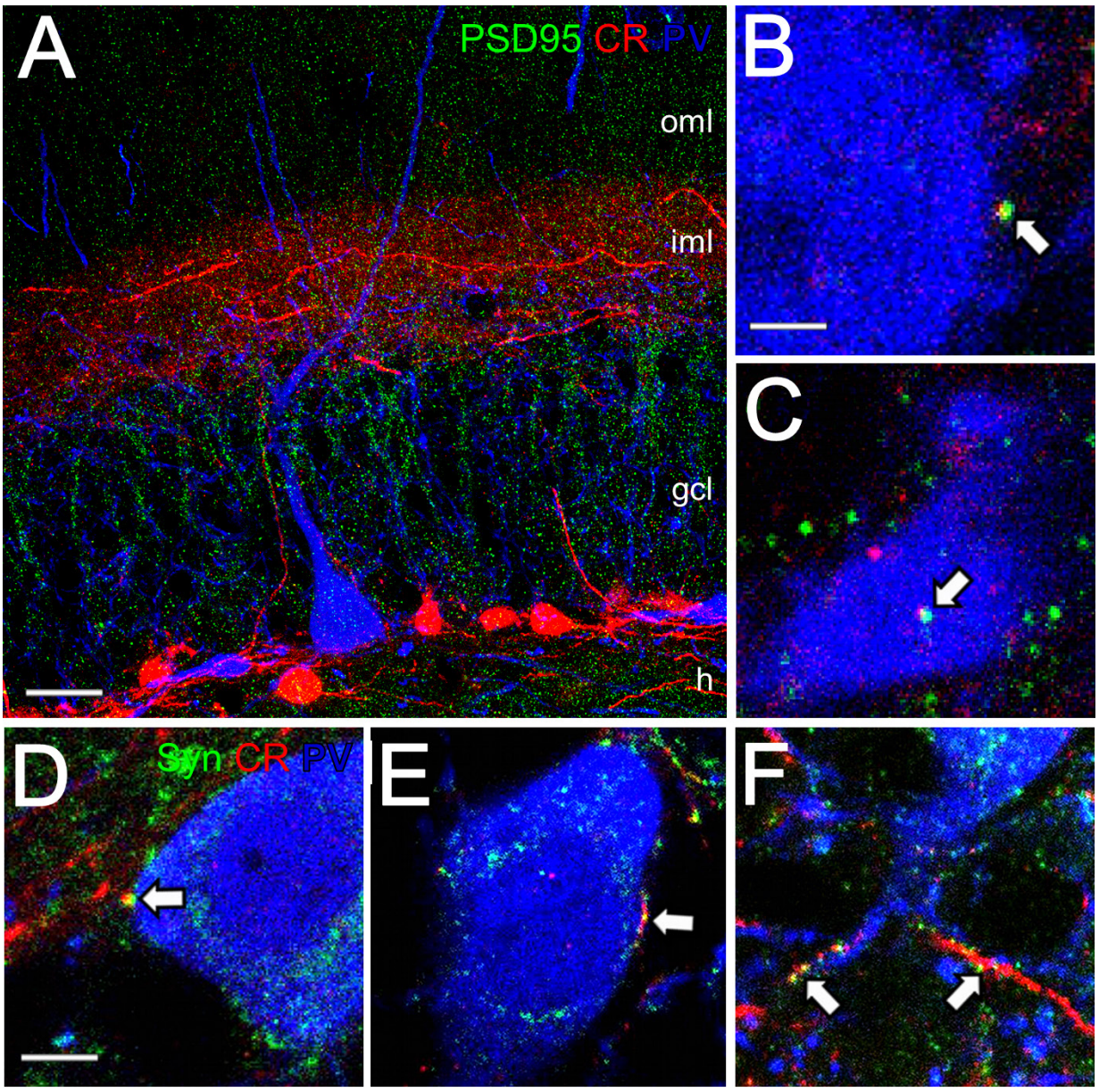

Figure I.2 – Mossy cells innervation on parvalbumin basket cells in the granule cell layer of the mouse dentate gyrus

Confocal analysis of the calretinin-positive elements found in apposition to parvalbumin interneurons and their co-expression of synaptic markers. **A-C)** Confocal plane showing a triple immunohistochemistry for PSD95 (green), calretinin (red) and parvalbumin (blue). **D-F)** Confocal planes of a triple immunohistochemistry for synaptophysin (green), calretinin (red) and parvalbumin (blue).

A) Example of a parvalbumin interneuron selected for analysis because of location, morphology and dendrite disposition. Calretinin mossy cell axonal fibers run through the granule cell layer and sprout densely in the inner molecular layer.

B, C) Colocalization of PSD95 and calretinin puncta in close apposition to the soma and proximal dendritic trunk of a parvalbumin-positive interneuron, respectively. They presented possible perisomatic excitatory synaptic contacts originating from the mossy cells onto parvalbumin basket cells (arrows). This suggests the presence of calretinin-positive boutons associated to postsynaptic densities typical from excitatory synapses.

D, E, F) Colocalization of Syn and calretinin elements in close apposition to a soma (arrows), beginning of the dendritic shaft and inner molecular layer dendrites of different parvalbumin cells. This suggests the presence of presynaptic vesicles in calretinin-positive fibers coming from the mossy cells, and therefore a high probability of synaptic contacts.

CR, calretinin; gcl, granule cell layer; h, hilus; iml, inner molecular layer; oml, outer molecular layer; PSD95, Postsynaptic Density Protein 95 kDa; PV, parvalbumin. Scale bar: A, 20 µm; B-F, 5 µm.

Figure I.3 – Study of the perisomatic innervation from mossy cells on horizontal parvalbumin-positive basket interneurons in the dentate granule cell layer

A) Optical plane of the perisomatic region of a horizontal parvalbumin interneuron (asterisk) analyzed at the electron microscope

B and C) Panoramic view of the proximal dendritic segment (**B**) and cell soma (**C**) of the parvalbumin interneuron (asterisk) shown in (**A**) at low magnification. Note the calretinin-positive elements that are found in apposition to the cell body and dendrite (boxed areas). Calretinin-positive boutons (arrows) are found in close apposition to the cell body and main apical dendrite.

D) Higher magnification of a calretinin-positive bouton shown in (**B**). Though analyzed in consecutive sections, no vesicles and no clear thick postsynaptic density (arrow) was observed.

E) Higher magnification of a calretinin-positive fiber that runs along the parvalbumin-positive dendrite. No signs of synapses can be observed.

F) Higher magnification of two calretinin-positive boutons shown in (**C**)**.** Again, no vesicles were found in this bouton at different levels, but the synaptic cleft and a visible postsynaptic density (arrow) was observed, which means that this bouton most likely established an asymmetric contact. Note that just next to it, another calretinin-positive bouton is establishing an asymmetric synaptic contact (arrowhead) on an immunonegative profile. This element would certainly constitute a false positive in a confocal microscopy analysis.

Scale bar: B-C 2µm; D-F, 400 nm.

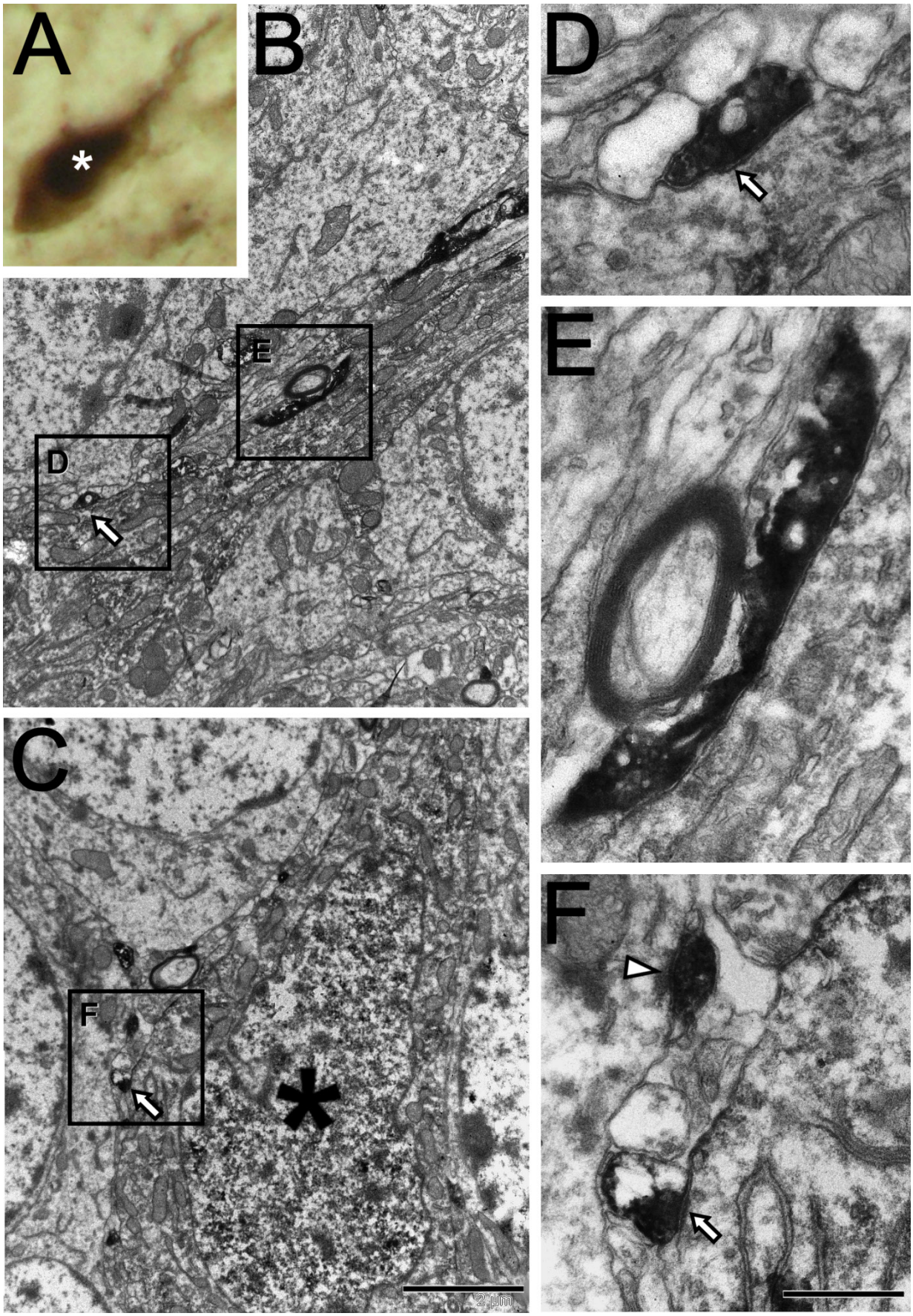
A
B
C
D
E
F
2 µm

Figure I.4 – Study of the perisomatic innervation by mossy cells on a fusiform and a pyramidal parvalbumin-positive basket interneurons in the dentate granule cell layer

A) Immunostainig for calretinin (DAB-Ni) and parvalbumin (DAB) for electron microscopy. Upper panel: optical plane of the perisomatic region of an inverted fusiform parvalbumin interneuron (white asterisk). Lower panel: correlation at the electron microscope.

B) Calretinin-positive bouton establishing a synaptic contact (arrow) on the perisomatic region of the parvalbumin interneuron shown in (**A**). Note the synaptic cleft and the postsynaptic density.

C) Calretinin-positive element in close apposition to the cell shown in (**A**), but with the synaptic release place (arrowhead) oriented towards a negative element.

D) Example of a calretinin-negative bouton establishing a symmetric synapse (arrow). The bouton is filled with flattened oval vesicles and dense-core vesicles.

E) Higher magnification of two calretinin-negative boutons establishing an asymmetric synaptic contact (arrows) with the cell shown in (**A**), and resembling a bouton from a mossy fiber.

F) Optical-electron microscope correlation of the perisomatic region of a pyramidal parvalbumin interneuron (asterisk).

G) Proximal dendrite from the pyramidal parvalbumin shown in (**A,** boxed area), located in the hilus. Three different unlabeled boutons likely from mossy fibers establish asymmetric synapses (arrowheads) with the parvalbumin-positive dendrite.

H) Example of an inhibitory symmetric contact (arrowhead) from a calretinin-negative bouton, with flattened vesicles and a single large mitochondria.

I, J) Calretinin-negative excitatory asymmetric contacts (arrows) received by the pyramidal basket cell shown in (**F**).

Scale bar: A, 5 µm; B-E 500 nm; F, 5 µm; G-J, 500 nm.

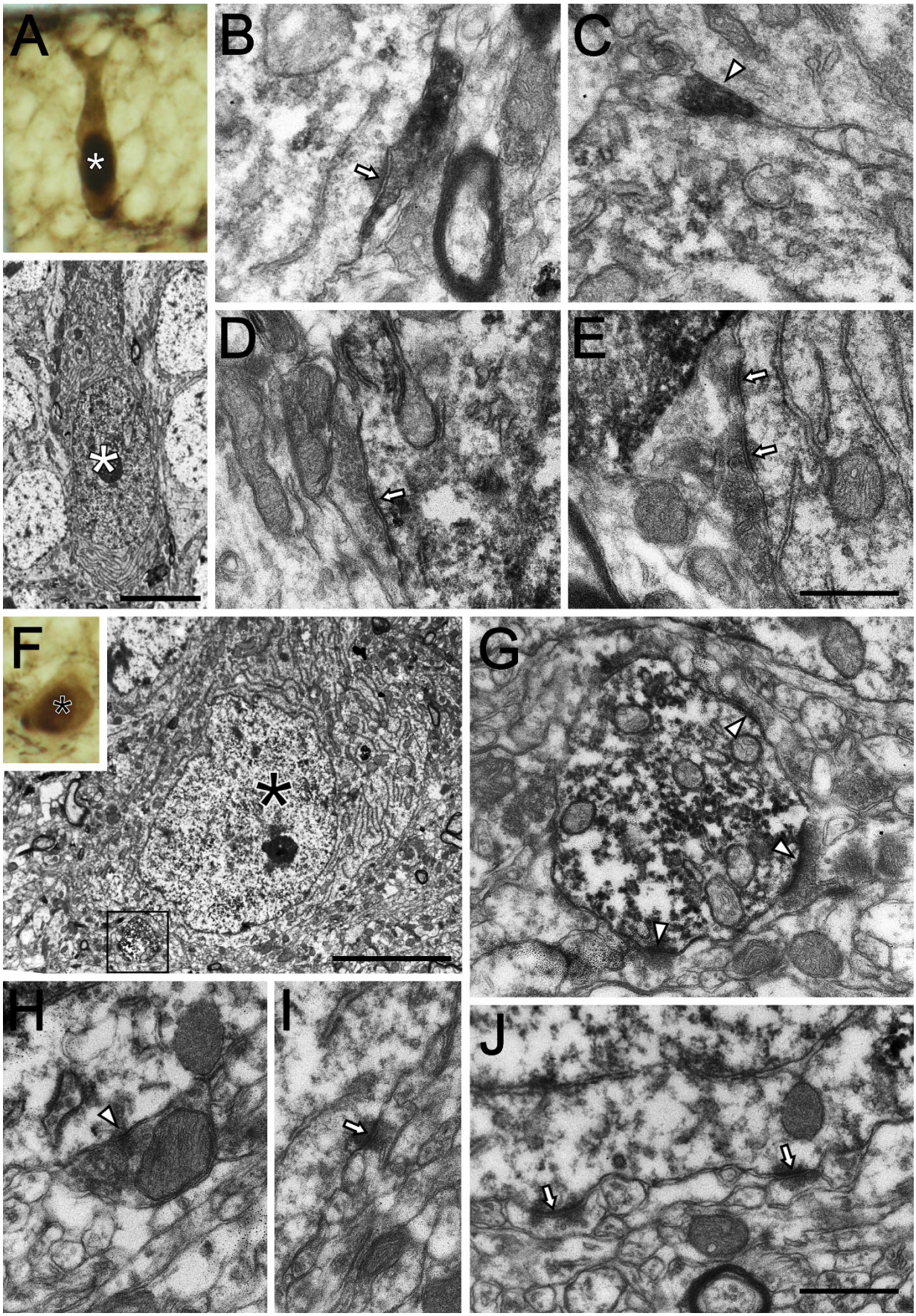
A
B
C
D
E
F
G
H
I
J

Figure I.5 – Study of the perisomatic innervation of a horizontal parvalbumin-positive basket interneuron by mossy cells in the dentate granule cell layer
A) Optical plane of the perisomatic region of a horizontal parvalbumin interneuron (asterisk), and correlation at the electron microscope.
B) Higher magnification of a fiber running along the horizontal parvalbumin interneuron shown in (**A**).
C, D) Higher magnification of two calretinin-positive fibers in close apposition to the horizontal interneuron (black arrows). No synaptic connections were found for these elements in consecutive sections.
E, F) Calretinin-negative boutons establishing an asymmetric synaptic contact (arrowheads) with the cell soma of the horizontal interneuron shown in (**A**). The morphology of the bouton and the synapse resembles the boutons from mossy fibers.
G1, G2) Calretinin-positive boutons from two consecutive ultrathin sections, showing asymmetric synaptic contacts (arrows) with the proximal hilar basal dendrite of the horizontal interneuron shown in (**A,** boxed area).
Scale bar: A, 5 µm; B, 1 µm; C-G, 500 nm.

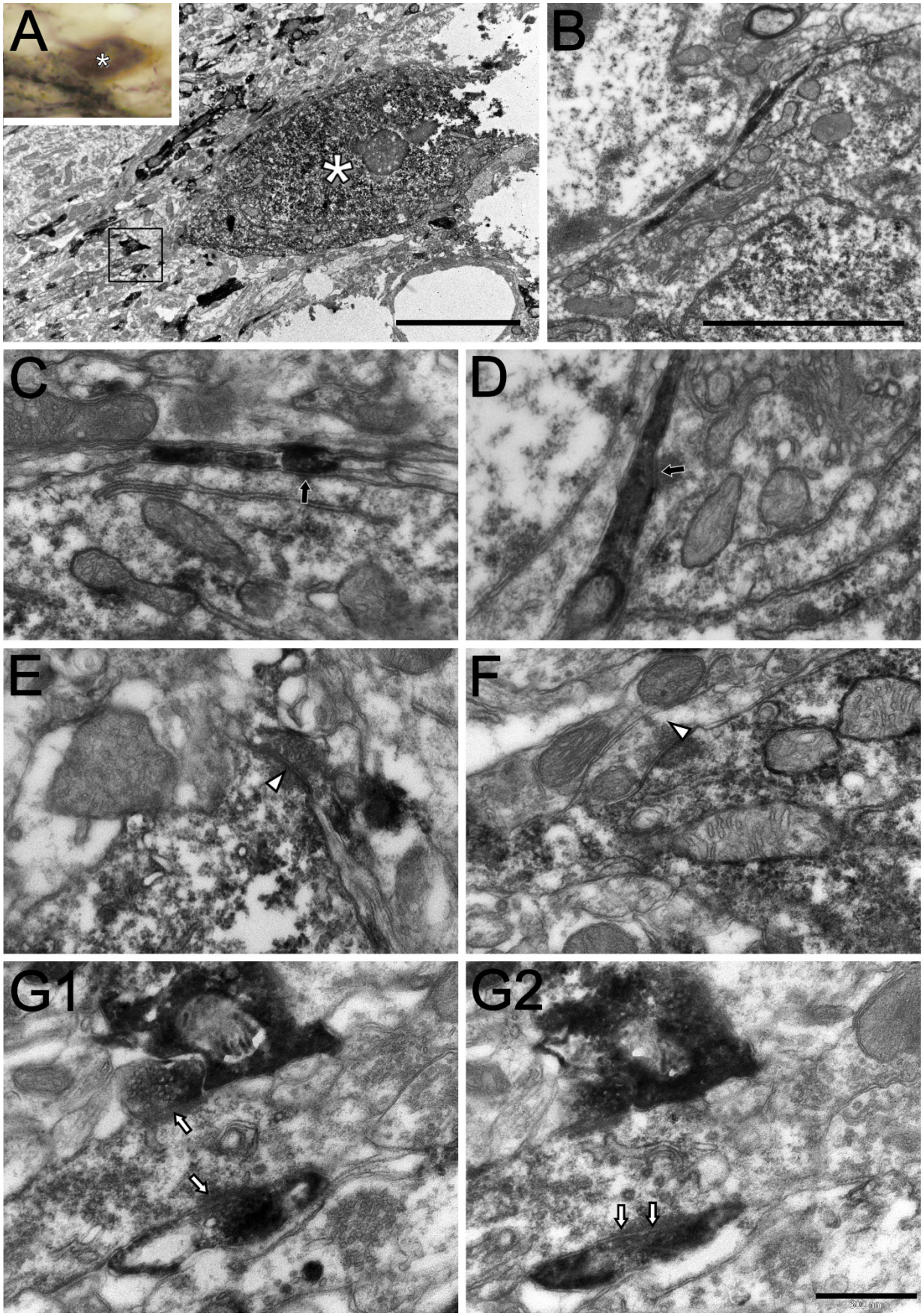
A
B
C
D
E
F
G1
G2

Figure I.6 – Perisomatic innervation of molecular layer parvalbumin-positive basket interneuron by mossy cells in the dentate granule cell layer

A) Optical focal plane of a molecular layer parvalbumin interneuron (asterisk) with the cell soma standing in the border of the granule cell layer and the inner molecular layer. Correlation with electron microscopy.

B) Example of a calretinin-negative bouton establishing multiple symmetric contacts (white arrowheads) in the perisomatic region of the cell in (**A**).

C - E) Three examples of calretinin-negative boutons establishing asymmetric synapses (black arrows) with the cell soma of the molecular layer parvalbumin interneuron shown in (**A**). Note in (**D**) and (**E**) the presence of a calretinin-positive element that could easily lead to a false positive in a confocal study.

F-I) Calretinin-positive boutons establishing asymmetric synapses (white arrows) on the cell soma (**F, G** and **I**), and on the proximal dendrite (**H**) of the molecular layer parvalbumin interneuron shown in (**A**). Note the common features of mossy cells boutons: small boutons filled with round vesicles that establish asymmetric synapses as shown by the thick postsynaptic density.

Scale bar: A, 5 µm; B-I, 500 nm.

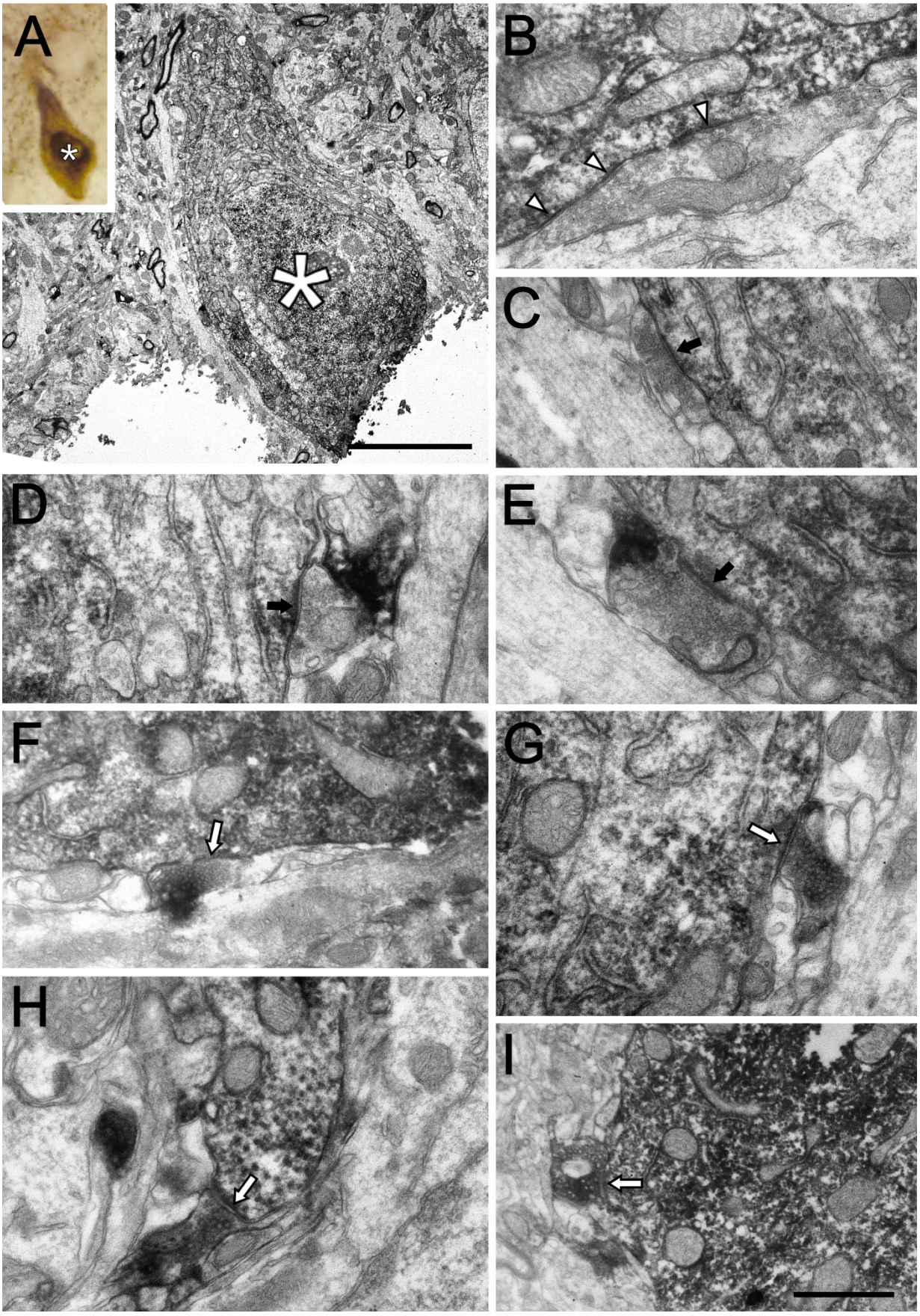
A
B
C
D
E
F
G
H
I

3. PERISOMATIC EXCITATORY INNERVATION FROM GRANULE CELLS ON PARVALBUMIN BASKET CELLS IN THE GRANULE CELL LAYER

In addition to the mossy cells, granule cells provide another source of perisomatic innervation onto parvalbumin interneurons (Ribak and Peterson, 1991; Kneisler and Dingledine, 1995; Blasco-Ibáñez et al., 2000). In some of these studies, Timm staining was used as an evidence of this innervation originating from granule cells, as mossy fibers have vesicular Zn^{+2} in their synaptic boutons. Timm-positive boutons formed basket-like arrangements surrounding the parvalbumin-positive interneurons in the granule cell layer, and following closely the shape of the dendrites present in this area. These boutons were confirmed to make asymmetric synaptic contacts on the parvalbumin cells: they were smaller than the mossy terminals characteristic of the mossy fibers, had round vesicles and presented dense core vesicles (Blasco-Ibáñez et al., 2000).

Although mossy fibers have Zn^{+2} in their synaptic boutons, and therefore are positive for this staining, there is no other evidence that the Timm-positive fibers on parvalbumin basket cells come from granule cells. Timm staining cannot be found on the granule cell somata, or in the axonal segments connecting the boutons, so the axon cannot be followed to the cell from which it originates. On the one hand, the number of fibers necessary to justify the innervation is small when compared with the total population of granule cells. Therefore, although Timm-positive fibers likely originate from granule cells, only a small sub-population of granule cells must participate. On the other hand, only with this staining it cannot be strictly ruled out that these fibers originate from another population of hippocampal or extra-hippocampal excitatory cells.

The studies that demonstrated that Timm-positive fibers innervated parvalbumin interneurons were performed in rats. Since we would work mainly in the mouse, we analyzed if this connectivity was also present in this species. We found Timm-positive fibers establishing putative contacts onto parvalbumin-positive basket cells (**Figure I.7**), as well as fibers travelling through the granule cell layer that did not come close to any parvalbumin interneuron (**Figure I.7 and I.8**). We also found Timm-positive fibers emerging from the outer molecular layer and the inner molecular layer, indicating that these fibers did not represent a mossy fiber collateral ascending from the hilus (**Figure I.8 C**).

In the dorsal dentate gyrus, though present, there were not many Timm-positive fibers in the inner molecular layer or outer molecular layer (**Figure I.8 A**). Timm-positive fibers appeared in

the granule cell layer as individual fibers that spread in the vicinity of the subgranular zone and then reached the hilus, where they could not be followed due to the high density of Timm-positive fibers. In the ventral hippocampus, however, although their morphology was similar, many more Timm-positive fibers were present in the inner molecular layer and granule cell layer (**Figure I.8 B**).

Not all the parvalbumin interneurons were innervated with the same intensity. A different innervation pattern was found regarding the morphology of the distinct parvalbumin interneurons:

1. In molecular layer parvalbumin interneurons, two situations were observed: (a) parvalbumin-positive somata completely located in the molecular layer were generally not contacted by Timm-positive boutons. (b) When the parvalbumin-positive somata were located in the inner molecular layer border with the granule cell layer, only few perisomatic Timm-positive bouton were seen (**Figure I.7 D-F**).
2. Inverted fusiform parvalbumin interneurons were also generally avoided by Timm-positive boutons in their somata, but not in the proximal dendrites, which had generally several Timm-positive boutons in apposition (**Figure I.7 I**).
3. Horizontal parvalbumin interneurons somata were densely surrounded by Timm-positive boutons, as well as their apical dendrites. As the basal dendrites entered the hilus, the dense staining present there precluded further observations (**Figure I.7 G**).
4. Pyramidal parvalbumin interneurons were also surrounded by Timm-positive boutons, though in a lesser extent than the horizontal type, and they generally presented a higher density in their basal pole. Their dendritic trunk also had Timm-positive boutons in apposition, though not as many, generally up to the first branching point of the dendrite. Due to the nature of the staining, pyramidal and fusiform parvalbumin interneurons were difficult to distinguish, as the base of the soma was usually masked by the high density of Timm-positive elements present in the hilus (**Figure I.7 A-C**)**.**

Therefore, although some Timm-positive fibers could go unreported due to low intensity or penetration problems, there is a differential innervation from Timm-positive mossy fibers to parvalbumin interneurons according to their morphological classification. Former studies in rat have not discussed this aspect of the innervation, but it is clear from their images that in this model the different cell types are innervated differently.

On the other hand, there were fibers and even basket arrangements that were not attached to a parvalbumin cell. This fact has also been reported in rat (Blasco-Ibáñez et al., 2000). The nature of the target cells is difficult to identify but their morphology suggest that other unlabeled basket cells are also innervated.

3.1. PERISOMATIC INNERVATION FROM TYPICAL GRANULE CELLS

To undoubtedly identify the source of the Timm-positive innervation on the parvalbumin basket cells we proceeded to reconstruct the morphology of individual granule cells using intracellular injection of biocytin on acute slices. This procedure allows for complete reconstruction of the dendritic and axonal arbor present in the slice and additionally confirms the granule cell nature by observing its firing pattern.

Granule cells located in the granule cell layer were intracellularly filled with biocytin via whole-cell patch clamp in P15-P23 mice, and a total of 19 cells were evaluated for this partial objective. Generally, during the patch-clamp intracellular injection, cells located in the subgranular zone were avoided, to reduce the possibilities of getting immature cells. In addition, once filled, all cells presenting features from immature granule cells, such as an undeveloped dendritic tree or filopodia-like spines, were discarded.

In those granule cells whose axon was well-filled and present in the slice, no collaterals were generated in the granule cell layer, and no varicosities were observed until the axon reached the hilus. This suggests that the vast majority of granule cells do not innervate the perisomatic region of parvalbumin interneurons when they are located in the granule cell layer. In addition, we found no mossy fiber collaterals emerging in the hilus and entering in the granule cell layer in any of the analyzed cells. Only one exception was found, in which we observed an axon collateral initiating in the hilus and entering a very small fraction in the granule cell layer, in a ventral slice. When the parvalbumin immunostaining was performed, no biocytin-filled fibers could be found in apposition to parvalbumin interneurons located in the granule cell layer.

3.2. PERISOMATIC INNERVATION FROM SEMILUNAR GRANULE CELLS

A first batch of filled semilunar granule cells was kindly supplied by Dr. Norbert Hájos, from the Institute of Experimental Medicine in Budapest, Hungary. A preliminary study on these cells suggested that the perisomatic innervation from semilunar granule cells to parvalbumin

interneurons exists, although not all of semilunar granule cells contributed for it. In fact, it seemed that cells located in the inner molecular layer but close to the granule cell layer were better candidates to establish this innervation.

To complete the study, more semilunar granule cells were intracellularly filled with biocytin in our laboratory via whole-cell patch clamp in P15-P23 mice. This age was chosen to ensure that the possible postsynaptic parvalbumin interneurons would remain as healthy as possible and were not degenerating in the slice.

As previously described (Ramón y Cajal, 1911; Williams et al., 2007), semilunar granule cells presented a wider dendritic arbor than typical granule cells and a semilunar-shaped cell body. Their axon used to travel in the inner molecular layer parallel to the granule cell layer, where sometimes ramified and formed one or two axon collaterals. These axons travelled through the granule cell layer to the hilus, where they ramified like the axons of typical granule cells. A more detailed description of semilunar granule cell morphology will be done in the next chapter of this thesis, but the injections confirmed their granular nature, with spiny dendrites extending up to the hippocampal fissure and the presence of typical giant mossy terminals in the hilus.

First, an additional set of 41 semilunar granule cells were filled with biocytin, resectioned and developed with DAB-Ni. Those cells that presented promising characteristics were used for the parvalbumin immunostaining. From those cells, only 4 formed putative contacts on parvalbumin interneurons (**Figures I.9 and I.10**).

These results suggest that the Timm-positive innervation that has been described on parvalbumin basket cells comes from semilunar granule cells. Still, it is clear that the frequency in which we could find these contacts was low. This fact may indicate that not all semilunar granule cells participate in the innervation of parvalbumin basket cells, and that there are a functionally distinct subpopulation of semilunar granule cells. However, this frequency could have been easily underestimated: first, we do not have the complete axonal arbor and could have lost collaterals; second, parvalbumin labelling can be lost from many basket pyramidal interneurons in the acute slices. They could either be dead because of the preparation or simply they could have not expressed parvalbumin. Third, if we consider that the term “semilunar granule cell” may include different subpopulation of granule cells, one of which is involved in the innervation to the parvalbumin basket cells, we could have been not aiming always to the pertinent semilunar granule cell subpopulation when patching the cells.

To confirm that semilunar granule cells do innervate granule cell layer interneurons, we searched for the synaptic contacts at the electron microscopy level. Semilunar granule cells were intracellularly filled and processed for electron microscopy. From a total of 57 filled cells for the electron microscopy study, 30 were further processed for the parvalbumin immunostaining. Under these conditions there were limitations relating the penetration of antibodies and the quality of the ultrastructure. From the most promising examples, the best ultrastructure corresponded to a semilunar granule cell located on the limit between the granule cell layer and the inner molecular layer (**Figure I.11**). Among the collaterals of the semilunar granule cell axon one of them seemed to establish dendritic and perisomatic contacts on a typical pyramidal parvalbumin basket cell.

Under optical and electron microscopy, the identity of the injected cell was confirmed by its morphology and ultrastructure. The dendrites were covered by spines (**Figure I.11 D**), which received small boutons making asymmetric contacts, as it has been described for granule cells. The large varicosities of the axon in the hilus corresponded to typical mossy terminals that made multiple asymmetric contacts on mossy cell complex spines (**Figure I.11 E**). The reconstruction of the axonal collateral in apposition to the parvalbumin cell confirmed that the fiber made asymmetric synaptic contacts on the inner molecular layer proximal dendrites of the target parvalbumin interneuron (**Figure I.12**), and on the dendritic trunk of the same parvalbumin interneuron (**Figure I.13**). The boutons were small and filled with round vesicles. Their morphology was similar to the one described for the Timm-positive boutons on parvalbumin basket cells in rat under electron microscopy (Blasco-Ibáñez et al., 2000). In the juxtagranular hilus the axon also made synaptic contacts on parvalbumin dendrites whose origin could not be determined (**Figure I.13**) and on unlabeled postsynaptic elements corresponding to degenerating dendrites.

In conclusion, our results confirm that the origin of the Timm-positive perisomatic innervation observed on the parvalbumin basket cells comes from granule cells, more concretely from semilunar granule cells, or at least, by a subpopulation of these cells. However, although we found no normal granule cell likely contacting parvalbumin interneurons in the granule cell layer, their presence cannot be completely ruled out.

Altogether, the lack of relevance of the excitatory innervation from mossy cells on parvalbumin basket cells in our study, and the confirmation of the origin of the Timm-positive innervation

on them allows us to establish the semilunar granule cells as the principal source of excitatory perisomatic drive on parvalbumin basket cells.

Figure I.7 – Timm-positive boutons are found in close apposition with different subtypes of parvalbumin-positive interneurons in the rodent dentate gyrus
Focal planes of different subtypes of parvalbumin-positive interneurons (DAB) after Timm staining (black).
A-C) Parvalbumin pyramidal (**B**) and fusiform (**A, C**) basket cells present many Timm-positive boutons (arrows) in their perisomatic region and apical and basal dendrites.
D-F) Molecular layer parvalbumin interneurons present few if any Timm-positive boutons in the soma. In (**F**), a molecular layer parvalbumin interneuron sitting in the outer molecular layer presents no Timm-positive boutons in apposition. The cell somata of the parvalbumin interneurons in (**D**) and (**E**) present none and one Timm positive bouton (arrow). However, their dendrites entering the granule cell layer are highly innervated (arrows).
G-H) Horizontal basket cells present a high density of Timm-positive boutons in the soma (arrows), as well as in the apical dendrite. In (**G**), though out of focus in this focal plane, a parvalbumin interneuron sitting in the inner molecular layer showed no Timm-positive boutons in apposition to the cell soma.
I) Inverted fusiform parvalbumin interneurons present scarce Timm-positive innervation in the soma, but very dense in the dendrites, particularly, in the basal dendrites entering the hilus (arrows).
gcl, granule cell layer; h, hilus; iml, inner molecular layer; oml, outer molecular layer.
Scale bar for all pictures: 20 µm.

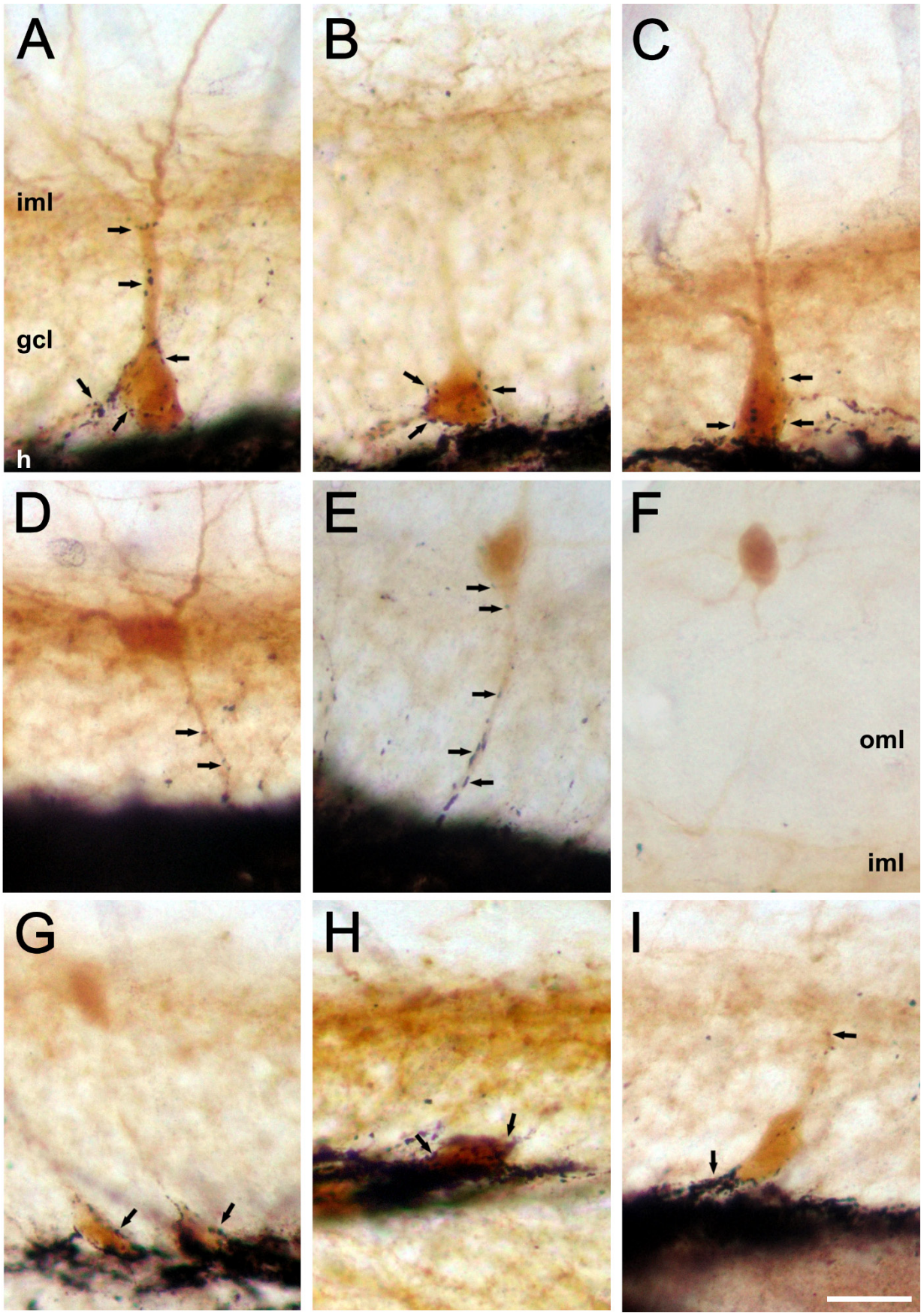
A
iml
gcl
h
B
C
D
E
F
oml
iml
G
H
I

Figure I.8 – Timm-positive boutons distribution in the rodent dentate gyrus
Focal planes of different sections stained for parvalbumin (DAB) after Timm staining (silver enhanced, black).
A) Dorsal level of the dentate gyrus. In this level, Timm-positive fibers in the granule cell layer and inner molecular layer, though present, are scarce and generally observed closer to the hilus.
B) Example of one Timm-positive fiber originating in the inner molecular layer and entering the granule cell layer (black arrows). Most likely, an axon collateral that emerges from the axon can be observed (white arrows). In this section, corresponding to the early ventral or intermediate dentate gyrus, some fibers lacking putative postsynaptic parvalbumin partner are observed.
C) Ventral level of the dentate gyrus. In this level Timm-positive boutons are highly present in the inner molecular layer and in the granule cell layer.
gcl, granule cell layer; iml, inner molecular layer; oml, outer molecular layer.
Scale bar for all pictures: 40 μm.

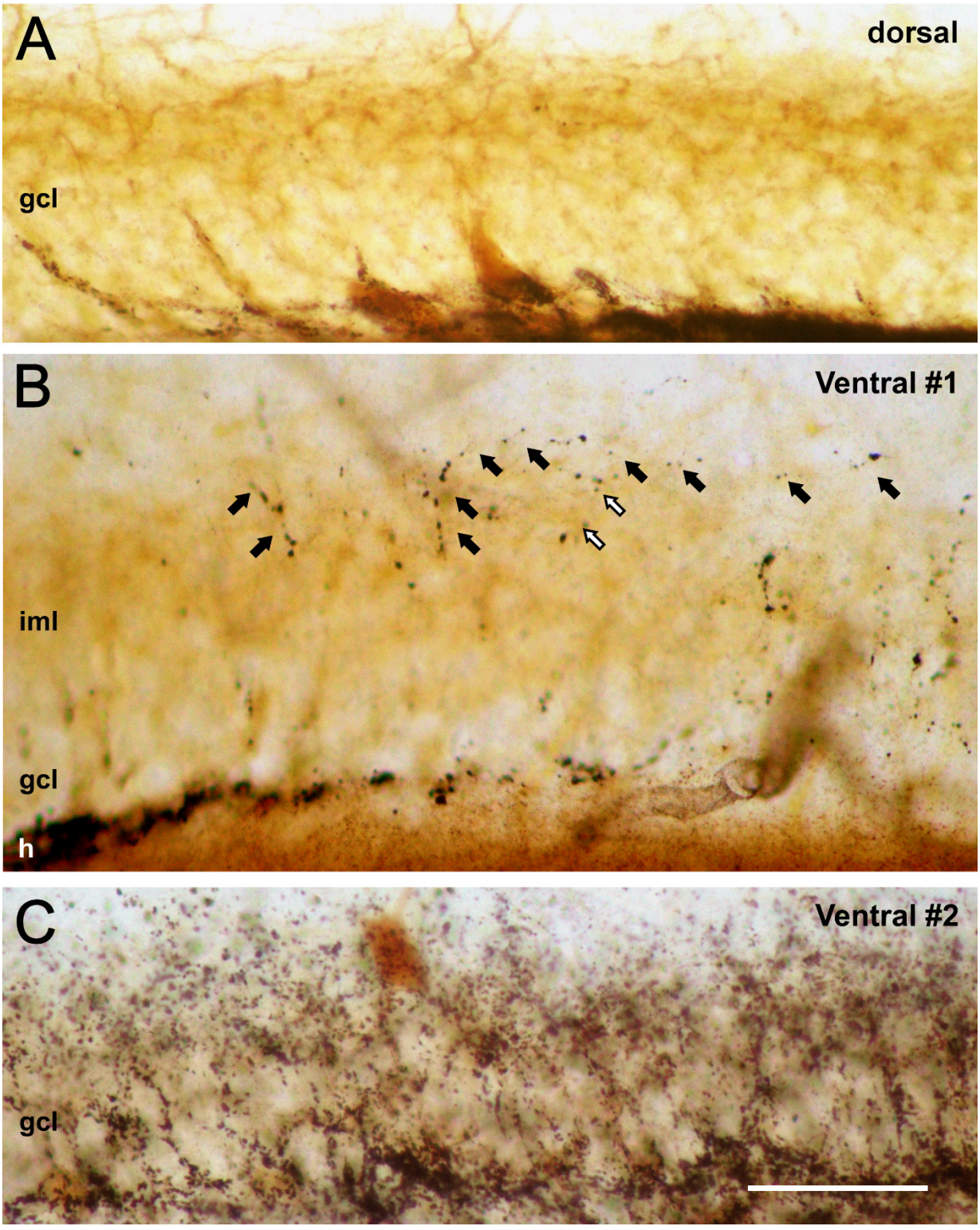
A
dorsal
gcl
B
Ventral #1
iml
gcl
h
C
Ventral #2
gcl

Figure I.9 – Boutons from intracellularly filled semilunar granule cells are found in close apposition to parvalbumin interneurons (I)

A) Panoramic Z-stack projection of the axon of an intracellularly filled semilunar granule cell (DAB-Ni) and parvalbumin immunostaining (DAB). The semilunar granule cell soma is located in the inner molecular layer in other section (not shown). The axon travels along the inner molecular layer and passes through the granule cell layer until it reaches the hilus, where it starts to ramify (black arrows). Boutons from this axon (white arrows) are found in apposition to the cell body and proximal dendrite of a parvalbumin interneuron (asterisk).

B and C) Single plane of the putative synaptic boutons shown in (**A**), in the cell soma and dendrite respectively.

D) Panoramic Z-stack projection of an intracellularly filled semilunar granule cell (DAB-Ni) and parvalbumin immunostaining (DAB). The cell body is located in the border between the granule cell layer and inner molecular layer, with its major axis oriented perpendicular to the granule cell layer, and both the axon (arrows) and a dendrite (white arrowheads) entering the granule cell layer.

E) Stitching of single planes showing synaptic boutons (white arrows) formed by the axon of the cell in (**D**) on parvalbumin interneurons located in the granule cell layer and in the hilar border (asterisks). The main axonal branch is depicted by black arrows, and one ramification is depicted by black arrowheads.

F and G) Single planes of putative synaptic boutons (white arrows) established by the axon of the cell in (**D**) on parvalbumin interneurons located in the hilus (asterisks). The axonal branch is depicted by black arrows. Note the presence of big mossy terminals.

Scale bar: A and D, 100 µm; B-C and E-G, 25 µm.

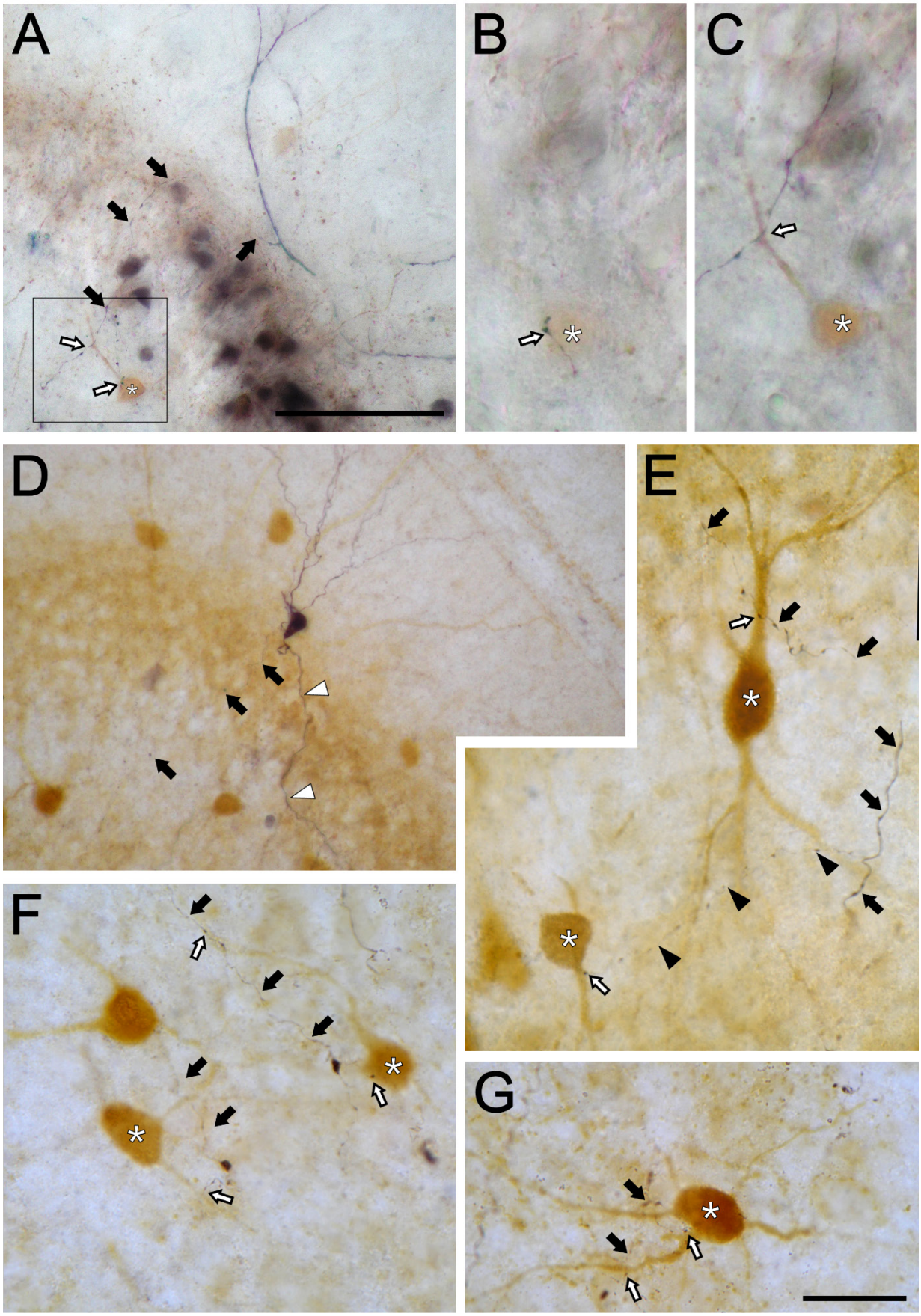
A
B
C
D
E
F
G

Figure I.10 – Boutons from intracellularly filled semilunar granule cells are found in close apposition to parvalbumin basket cells (II)
A) Panoramic Z-stack reconstruction from several focal planes of the axon of an intracellularly filled semilunar granule cell (DAB-Ni) and parvalbumin immunostaining (DAB). The axon travels along the inner molecular layer and establishes several collaterals in the granule cell layer (arrows). Once in the hilus, the axon forms mossy boutons (black arrowheads) and travels to the CA3 area. One of the collaterals forms boutons in close apposition to the cell body and proximal dendrite (white arrows) of a parvalbumin interneuron (asterisk).
B) Detail of the spiny dendrite of the filled semilunar granule cell.
C) Detail of the cell body of the filled semilunar granule cell. The axon can be easily distinguished and followed while it enters the inner molecular layer (arrows).
D) Reconstruction from several focal planes of the targeted parvalbumin interneuron (asterisk) in (**A**), in higher magnification. The putative contacts are shown by white arrows.
E) Panoramic view of a different filled semilunar granule cell, with its axon going straight to the apical dendrite of a parvalbumin interneuron.
F) Reconstruction from several focal planes of the semilunar granule cell and parvalbumin interneuron (asterisk) in (**E**). The axon of the semilunar granule cell follows the dendrite of the parvalbumin interneuron, and forms several boutons (white arrows) in apposition to the cell.
Scale bar: A, C and E, 40 µm; B and D, 10 µm; F, 20 µm.

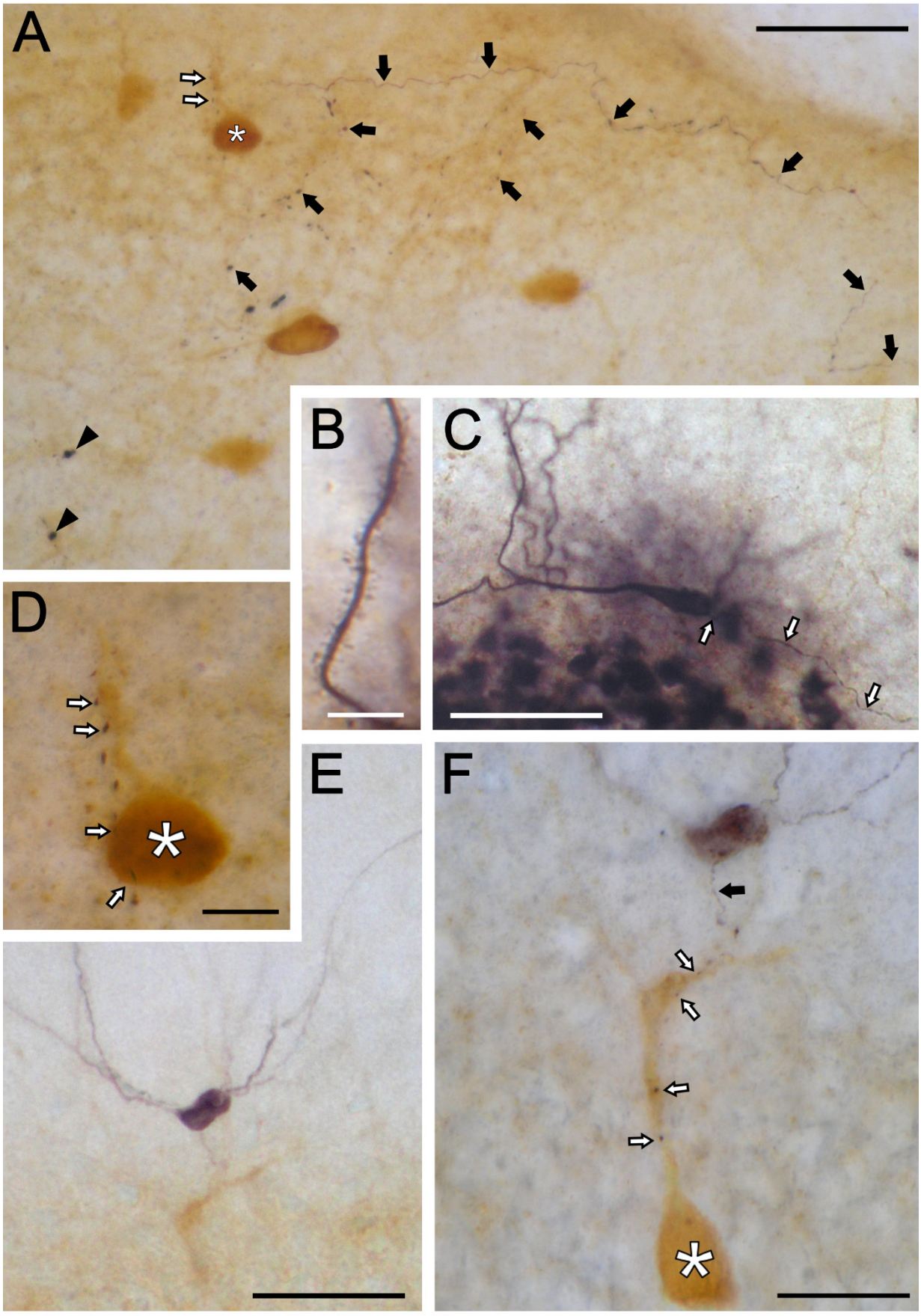
A
B
C
D
E
F

Figure I.11 – Morphological description of a semilunar granule cell establishing synaptic perisomatic contacts with a parvalbumin interneuron

Double immunostaining of an intracellularly filled semilunar granule cell, visualized with DAB-Ni, and parvalbumin (DAB).

A) Panoramic view of the dendritic arbor of the intracellularly filled semilunar granule cell. The axon is observed running along the inner molecular layer (arrows), entering the granule cell layer and reaching the hilus, where it starts to produce collaterals and varicosities.

B) Higher magnification of the axon shown in (**A**). On its way through the granule cell layer, the axon approaches to the perisomatic region of a parvalbumin interneuron. The axon at this level presents varicosities, further characterized as synaptic boutons. Arrows show the varicosities that were studied under the electron microscope.

C) Cell soma of the cell shown in (**A**). The cell body is sitting in the border between the inner molecular layer and granule cell layer. We observe the axon protruding from a proximal dendrite (arrow) and running along the inner molecular layer, where it can be followed in the section represented in (**A**).

D) Higher magnification of the dendrites of the intracellularly filled semilunar granule cell shown in (**A**). Spine morphology is similar to the one observed for typical granule cells.

E) Serial sections under the electron microscope of a hilar mossy bouton from the semilunar granule cell shown in (**A**)**.** The mossy bouton contacts the complex spines forming the thorny excrescences of hilar mossy cells.

gcl, granule cell layer; h, hilus; iml, inner molecular layer.

Scale bars: A, 50 µm; B, 10 µm; C, 25 µm; D, 20 µm; E, 1 µm.

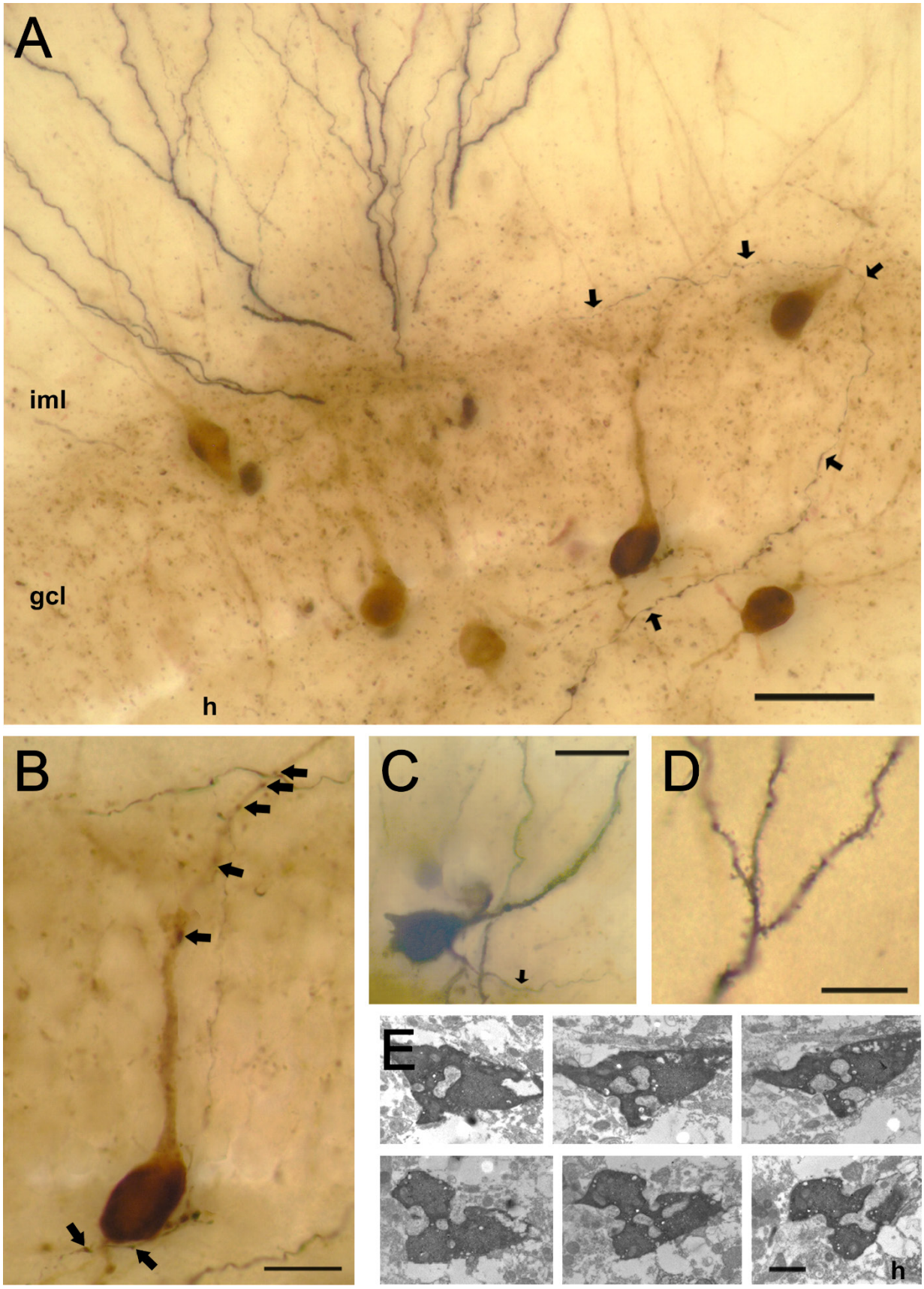
A
iml
gcl
h
B
C
D
E
h

Figure I.12 – Axon collaterals from semilunar granule cells establish asymmetric synaptic contacts on parvalbumin dendrites in the border between the inner molecular layer and granule cell layer.
Same cells as in **Figure I.11**. The axon collateral of the semilunar granule cell is visualized with DAB-Ni, while the parvalbumin interneuron in visualized with DAB.
A) The dendritic trunk of the parvalbumin interneuron presents a DAB-Ni positive fiber in close apposition. Black arrows point to the boutons that were further studied at the electron microscopy level.
B) Electron microscopy panoramic view of the dendritic segment of the parvalbumin interneuron, in which a bouton (boxed area) is observed in close apposition.
C) Consecutive ultrathin sections of the bouton shown in (**B**). The bouton displays the morphology of an *en passant* bouton, filled with round vesicles and establishing a synaptic contact (arrows) with the dendritic profile (**d**) of the parvalbumin basket cell.
D) Electron microscopy panoramic view of the dendritic segment of the parvalbumin interneuron, in which a bouton (boxed area) is observed in close apposition.
E) Two consecutive ultrathin sections of the bouton shown in (**D**)**.** In this example, the ultrastructure allows to distinguish the synaptic cleft and postsynaptic density (arrow), which indicates that the boutons in this collateral establish asymmetric synapses on the parvalbumin dendrite.
F) Electron microscopy panoramic view of the dendritic segment of the parvalbumin interneuron at another level, in which a bouton (boxed area) is observed in close apposition. Note that this bouton was already starting to appear in (**D**, arrowhead).
G) Two consecutive ultrathin sections of the bouton shown in (**F**)**.** The morphology of this bouton, though bigger, is similar as the previous ones, filled with round vesicles and establishing an asymmetric synapse (arrow) with the dendrite of the parvalbumin interneuron.
d, dendrite from the target parvalbumin interneuron.
Scale bars: B, D and F, 2 µm; C, E and G, 500 nm.

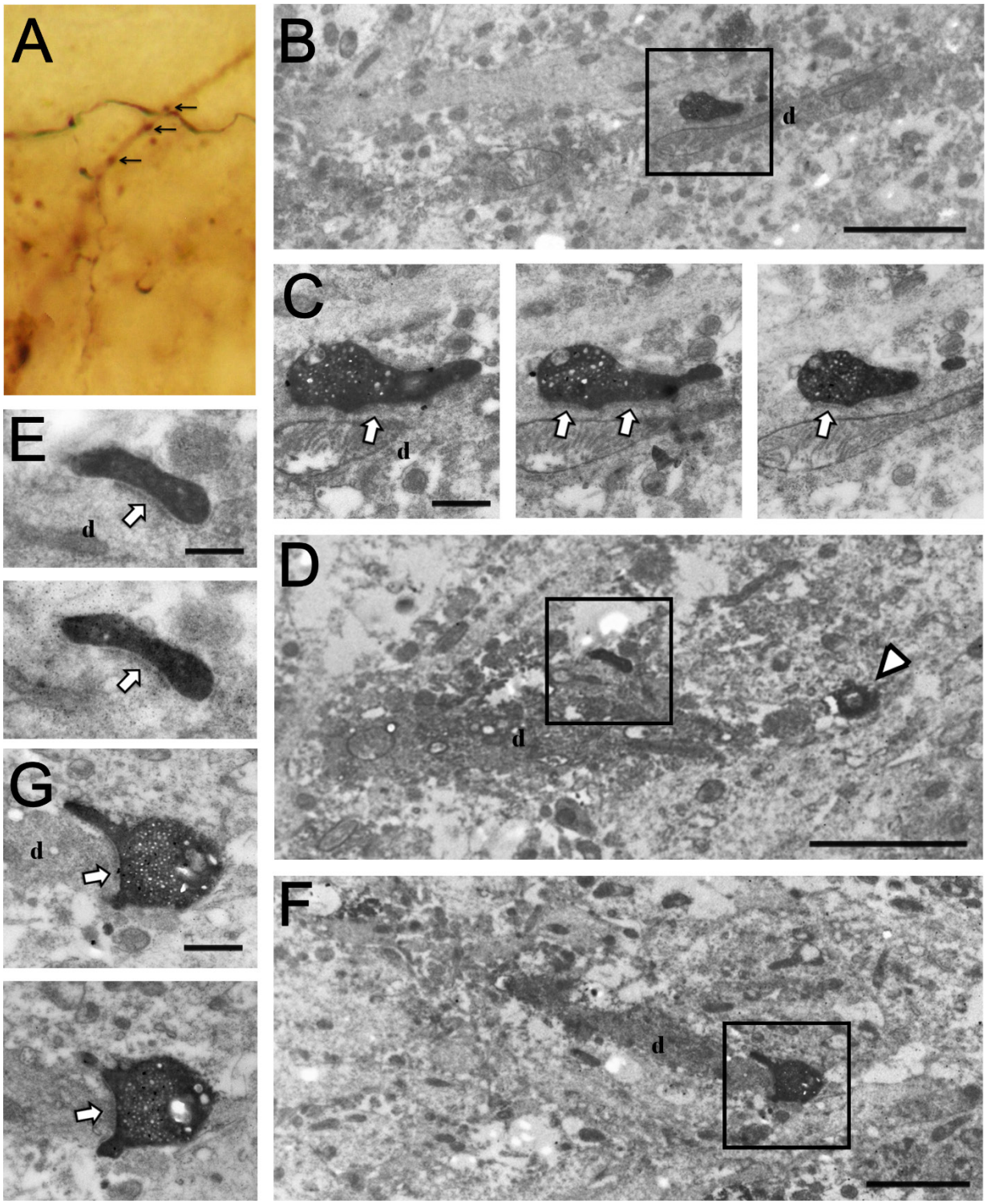
A
B
d
C
d
E
d
D
d
G
d
F
d

Figure I.13 – Axon collaterals from semilunar granule cells establish asymmetric synaptic contacts on parvalbumin dendrites in the granule cell layer and yuxtagranular hilus.
Same cells as in **Figure I.11**. The axon collateral of the semilunar granule cell is visualized with DAB-Ni, while the parvalbumin interneurons in visualized with DAB.
A) Optical-electron microscopy correlation of the apical dendritic trunk of the parvalbumin interneuron shown in **Figures I.11** and **I.12**. A synaptic bouton (boxed area) from the semilunar granule cell axon collateral is found in close apposition to the dendrite of the parvalbumin dendritic trunk (arrow). Note the presence of granule cell bodies next to the dendrites.
B) Two consecutive ultrathin sections from the bouton shown in (**A**)**.** The postsynaptic density can be observed in the dendritic profile next to a clear synaptic cleft (arrow), indicating that this bouton is establishing an asymmetric synapse.
C) Electron microscopy panoramic view of a string of labeled boutons (arrowheads) next to DAB-positive parvalbumin profiles in the hilus, in the border with the granule cell layer.
D) Higher magnification of a labeled bouton shown in a boxed area in (**C**) from a different ultrathin section. This bouton is establishing an asymmetric synapse (arrow) with parvalbumin-positive profiles in the yuxtagranular hilus, probably corresponding to basal dendrites from parvalbumin basket cells.
E) Higher magnification of a labeled bouton shown in a boxed area in (**C**). This bouton is also establishing asymmetric synapses (arrows) with a parvalbumin-positive profile in the yuxtagranular hilus.
d, parvalbumin-positive dendrite; g, granule cell; gl, granule cell layer; h, hilus.
Scale bars: A and C, 5 µm; B and D, 500 nm.

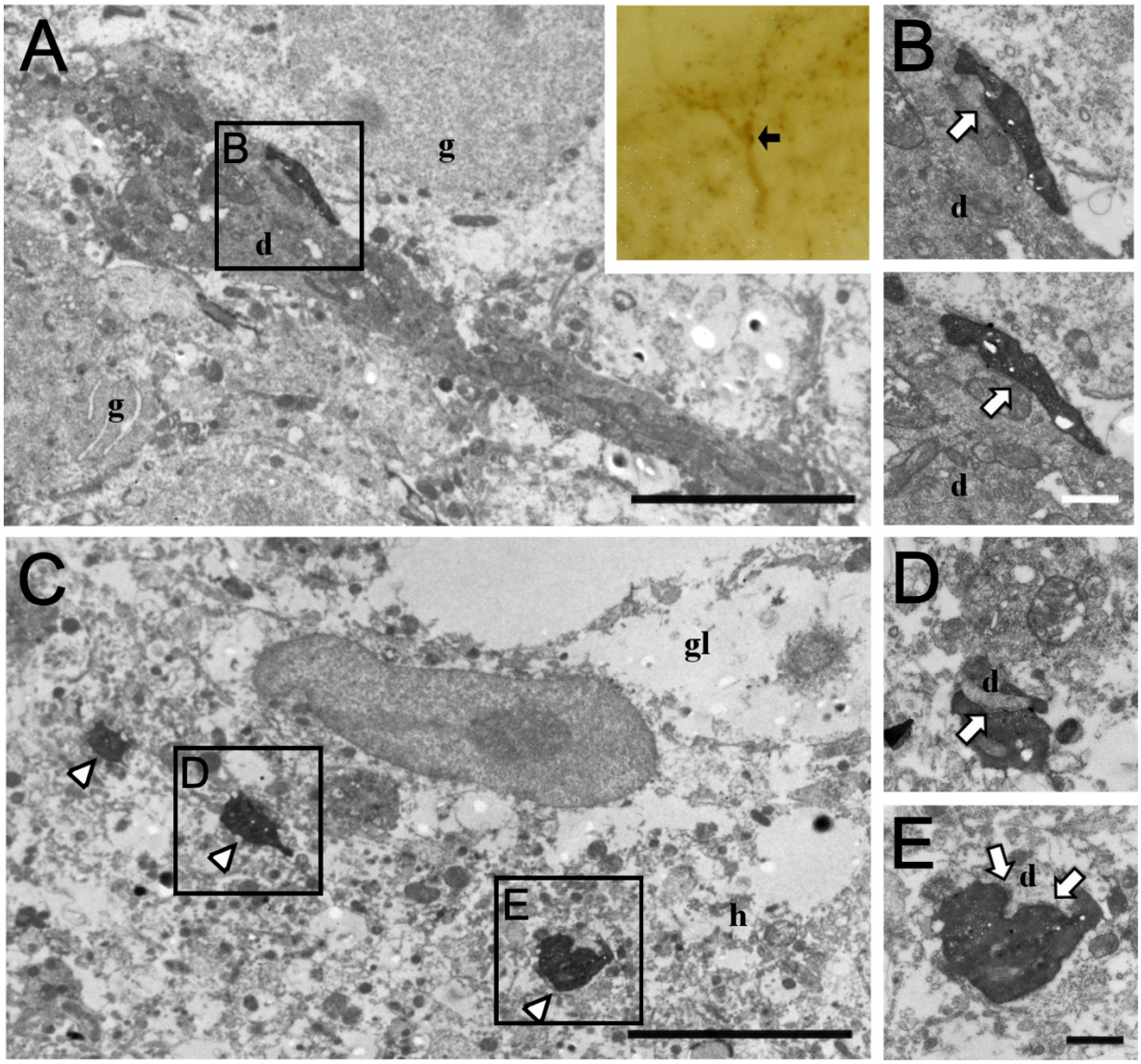
A
B
d
g
g
B
d
d
C
gl
D
E
h
D
d
E
d

RESULTS II: CHARACTERIZATION OF SEMILUNAR GRANULE CELLS

Since semilunar granule cells may play an important role in the perisomatic control of parvalbumin interneurons in the dentate gyrus, it is necessary to study what differences them from normal granule cells to gain insight in their function in the dentate circuitry.

To study the semilunar granule cells population, we used three different approaches in our laboratory: (1) intracellular injection via whole-cell patch clamp; (2) a transgenic mouse line, in which the fluorescent protein YFP is expressed under the Thy1 promoter only by a subset of the principal neurons (Feng et al., 2000; Porrero et al., 2010); (3) immunohistochemistry with Prox1, which is a specific marker for granule cells.

1. DISTRIBUTION AND ORIGIN OF SEMILUNAR GRANULE CELLS

To estimate the number of semilunar granule cells present in the mouse brain, we performed an immunohistochemistry with Prox1. This protein has been described as a specific marker for all granule cells (Oliver et al., 1993; Galeeva et al., 2007; Lavado and Oliver, 2007; Lavado et al., 2010), and allowed us to study the number and distribution of granule cells out of the granule cell layer. For that, we cut the brains in equal subseries and used one of them to count the number of Prox1-positive cells in the inner molecular layer of the dentate gyrus. We also considered as semilunar granule cells those cells located close to the border with the granule cell layer but that were separated from it, as we had previously observed that they are morphologically similar to those located more detached into the inner molecular layer. Among the similar morphological characteristics we found a more semilunar-shaped soma, wider dendritic arbor than deeper granule cells, and two or more primary dendrites emerging from the soma, generally from opposite poles.

As previously described, Prox1-positive cells in the dentate gyrus were mainly confined in the granule cell layer (Lavado and Oliver, 2007; Lavado et al., 2010; Iwano et al., 2012). Some Prox1-positive cells were found in the molecular layer and in the hilus, corresponding to semilunar granule cells (Gupta et al., 2012) or misplaced hilar granule cells. Sometimes, positive nuclei

were also found in the CA3, which have been previously identified as misplaced granule cells that are fully integrated in the circuitry (Szabadics et al., 2010). Only occasionally a Prox1-positive nuclei was found in the CA1. There were also Prox1-positive cells in the cortex, probably corresponding to interneurons (Rubin and Kessaris, 2013).

An average of 1072 ± 175 Prox1-positive cells were located in the inner molecular layer of one whole dentate gyrus from 3 young-adult mice (3 months old), from its most rostral to its most caudal level. In adult mice (12 months old), the number of semilunar granule cells in the inner molecular layer was similar (1244 ± 157 Prox1-positive cells). A summary of these results is shown in **Graph II.1**.

Generally, Prox1-positive cells considered as semilunar granule cells were more abundant at ventral levels, as well as in the apex of the dentate gyrus. They were also more common in the suprapyramidal layer than in the infrapyramidal layer of the dentate gyrus (**Figure II.1**).

Prox1-positive nuclei were also present in the outer molecular layer of all animals, though not in a homogeneous manner, corresponding to ectopic outer molecular layer granule cells. Some of these nuclei presented a more cylinder-like morphology that may correspond to a different orientation of the cell within the molecular layer (Martí-Subirana et al., 1986).

The variability of the number of these cells was also higher between animals. In young-adult mice, 260 ± 20 Prox1-positive cells were found in the outer molecular layer of the whole dentate structure. In middle-age mice the number of Prox1-positive cells in the outer molecular layer was 280 ± 96. A summary of these results is shown in **Graph II.1**.

Again, outer molecular layer Prox1-positive cells were more abundant at ventral levels of the dentate gyrus, and in the suprapyramidal layer than in the infrapyramidal layer. Interestingly, these cells generally appeared in groups, and were not evenly distributed along the whole outer molecular layer.

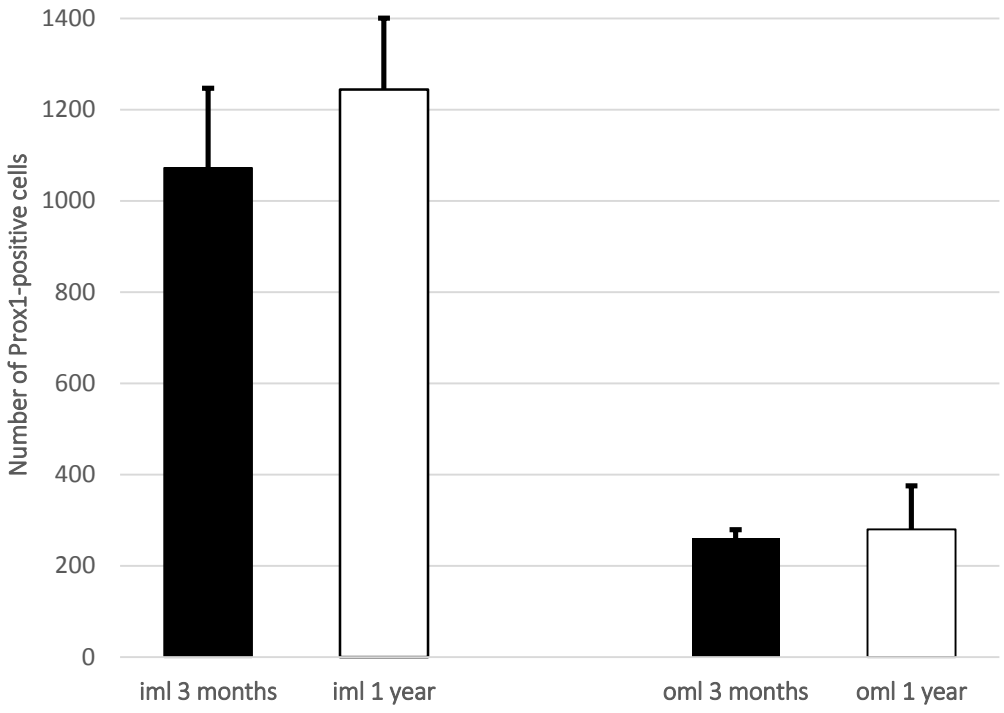

Graph II.1 - Number of total Prox1-positive nuclei per hemisphere in the inner molecular layer and outer molecular layer of three month and 1 year old mice. No significant differences could be observed between adult and aged mice regarding the number of Prox1-positive nuclei, neither in the inner molecular layer nor in the outer molecular layer. Data are shown as mean ± SEM (n=3)

An assay of studying the same population in younger animals was unsuccessfully performed. In P7, P16 and P22 animals, Prox1 staining revealed the presence of nuclei generally in the inner molecular layer but also sometimes in the outer molecular layer. However, the quality of the staining, with a high unspecific glial staining, did not allow for a quantification of the number of semilunar granule cells at this age.

To determine the appearance of the semilunar granule cells during the development of the dentate gyrus, consecutive semithin sections (1 µm-thick) of mouse dentate gyrus from postnatal ages: P1, P7, P10, P14, from previously embedded hippocampal slices available at the laboratory, were used.

On these consecutive sections, the following stainings were performed:

- Nissl staining with Toluidine Blue, used as a general histological marker to distinguish the different layers in the postnatal hippocampus.
- Calretinin, as it has been described as a good marker for immature granule cells in the mouse dentate gyrus (Liu et al., 1996). Its expression begins one day after generation and

disappears when the cell is integrated in the circuitry, between 7 and 21 days in adults (Marqués-Marí et al., 2007).

- Calbindin, which is expressed by mature granule cells that are integrated in the dentate circuitry after the loss of calretinin (Sloviter, 1989; Celio, 1990; Brandt et al., 2003).

Due to the thinness of the sections, a single cell could be followed in the three sections and co-expressions could be detected.

At P1, the dentate gyrus was still not well formed (**Figure II.2 A**). Calretinin-positive granule cells were found mainly in the deepest region of the granule cell layer (**Figure II.2 B**), but no calbindin-positive cells were found yet (**Figure II.2 C**).

At P7, the dentate gyrus already presented its typical shape (**Figure II.2 D**), and although there was still a majority of calretinin-positive cells (**Figure II.2 E**), the first calbindin-positive granule cells appeared in the upper region of the granule cell layer, and in the molecular layer (**Figure II.2 F**).

At P10, the infrapyramidal blade of the dentate gyrus presented already more calbindin granule cells, whereas the infrapyramidal did not present much yet (**Figure II.3 B**). The CA3 stratum lucidum was already labeled for calbindin, indicating that the mossy fibers were maturing and reaching their target (**Figure II.3 A**). On the other hand, we still found a majority of calretinin-positive granule cells corresponding to immature cells, and a sparsely labeled inner molecular layer, corresponding to the axons of mossy cells starting to mature (**Figure II.3 C**).

At P14, there was already a majority of calbindin cells, and calretinin immature neurons were restricted to the subgranular zone. The inner molecular layer was completely labeled for calretinin boutons, which means that mossy cells were already mature. Calbindin-positive granule cells could be seen already in the inner and outer molecular layer (**Figure II.3 E** and **F**).

Altogether, the fact that no calretinin-positive granule cells were found in the inner molecular layer, and that the first calbindin-positive granule cells appeared in this region, is indicative that semilunar granule cells are among the first to be generated and to migrate to the inner molecular layer in early postnatal development of the dentate gyrus. It is also noteworthy that the suprapyramidal cell layer, that contains higher number of semilunar granule cells, is also formed earlier than the infrapyramidal cell layer.

Figure II.1 – Prox1 expression in the mouse dentate gyrus
Immunohistochemistry for Prox1 (DAB) in different levels of the mouse dentate gyrus.
A, B) Dorsal sections of the dentate gyrus, corresponding to Bregma -1.5 mm (**A**) and -2.8 mm (**B**) approximately. Prox1-positive nuclei out of the granule cell layer abound in the apex. There is a higher incidence of semilunar granule cells in the suprapyramidal blade than in the infrapyramidal blade, as well as more Prox1-positive cells in the molecular layer at more caudal levels.
C) Ventral section of the dentate gyrus. There is an increment in the number of Prox1-positive nuclei both in the inner and outer molecular layer, in comparison with more dorsal levels.
D) Higher magnification of an area in the CA3 as delimited in the inset in panel (**C**), where a relatively high number of ectopic granule cells can be found.
E, F) Higher magnification of the insets in (**C**) of the infrapyramidal granule cell layer (**E**), and suprapyramidal granule cell layer (**F**). Semilunar granule cells are more abundant in the suprapyramidal than in the infrapyramidal layer. In the dorsal molecular layer, semilunar granule cells remain within the inner molecular layer, reaching the border but just crossing it seldom (arrows). However, in more ventral regions of the molecular layer, more ectopic granule cells can be found in the outer molecular layer (arrowheads). Note also that ectopic granule cells in the outer molecular layer are also grouped in clusters instead of being equally distributed.
gcl, granule cell layer; h, hilus; iml, inner molecular layer; infra gcl, infrapyramidal granule cell layer; oml, outer molecular layer; supra gcl, suprapyramidal granule cell layer.
Scale bar: A-C, 500 µm; D-F, 200 µm.

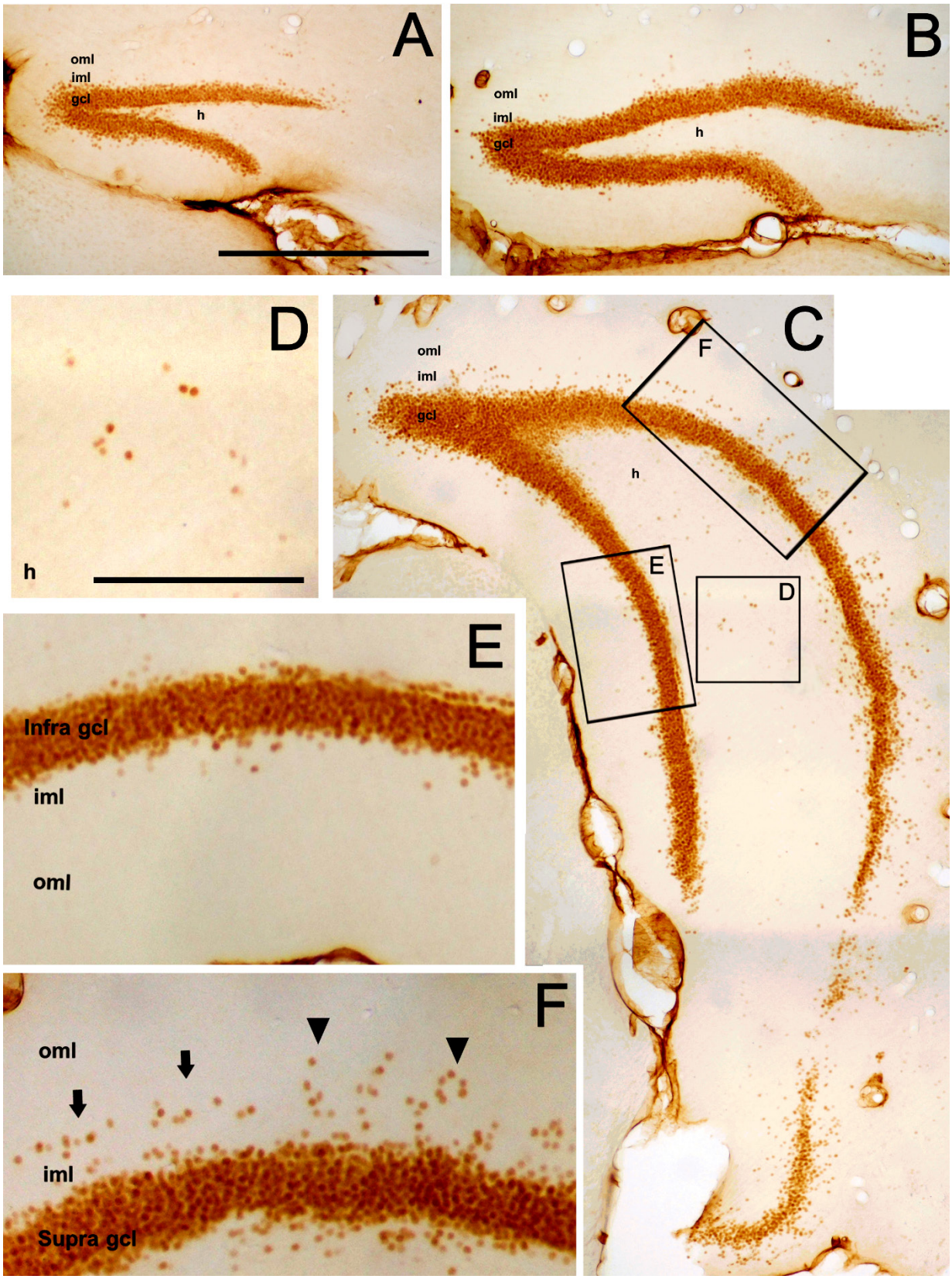
A
oml
iml
gcl
h
B
oml
iml
gcl
h
D
h
C
oml
iml
gcl
h
F
E
D
E
Infra gcl
iml
oml
F
oml
iml
Supra gcl

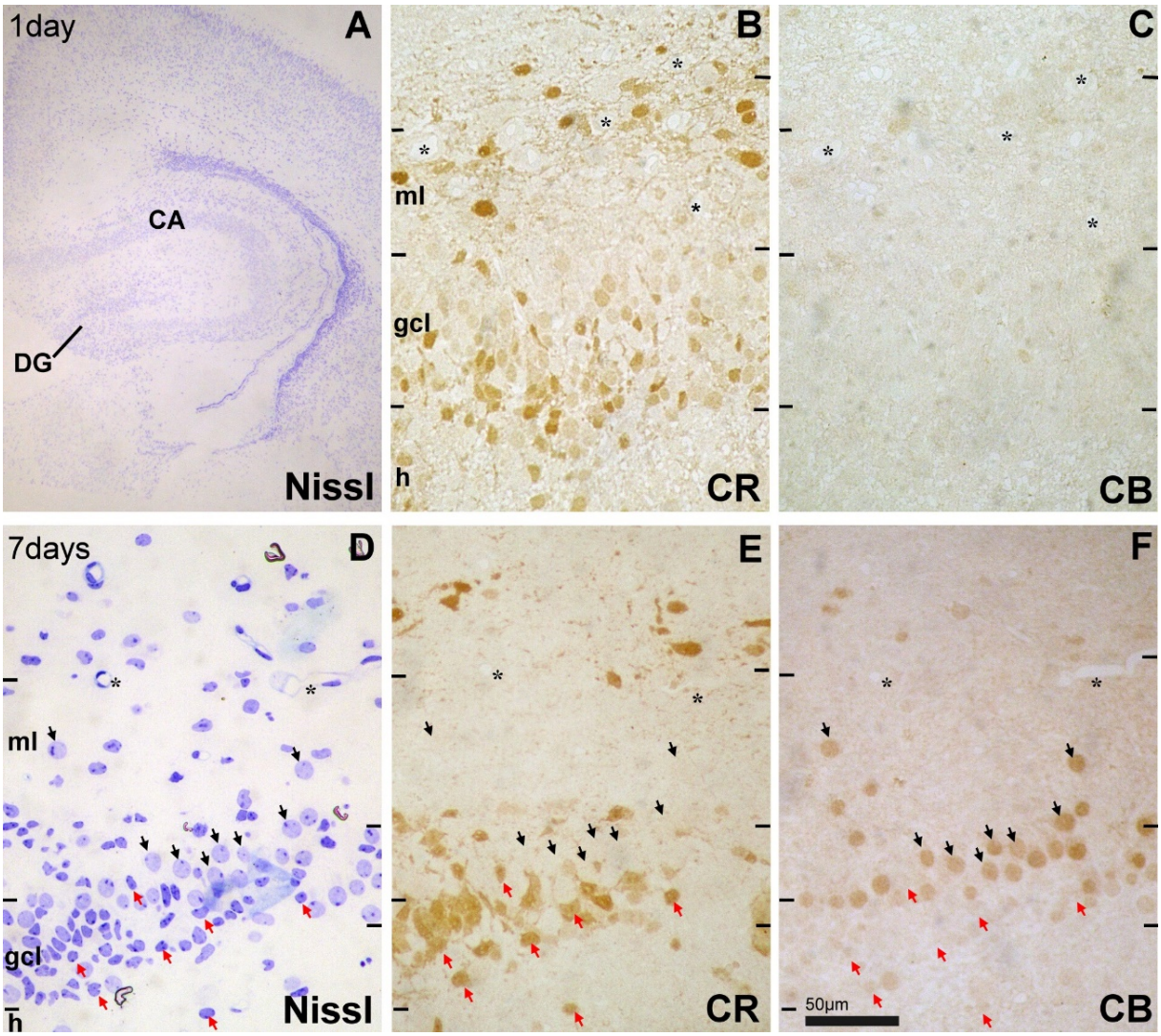

Figure II.2 - First appearance of calbindin immunoreactive granule cells.
A) At 1 day postnatal, the dentate gyrus (DG) appears as a blurred diffuse cell layer at the end of the forming Cornu Ammonis (CA).
B, C) Calretinin (**B**) and calbindin (**C**) in two consecutive semithin sections (1 µm thick). Granule cells forming the granule cell layer were small, and presented calretinin immunoreactivity. There were also numerous putative granule cells in the hilus that were also immunoreactive for calretinin. The molecular layer was narrow and some large calretinin immunoreactive cells were present there. These cells may correspond to Cajal-Retzius cells. Calbindin was still absent from cells in the dentate gyrus.
D- F) At 7days postnatal, consecutive semithin sections stained for Nissl, calretinin and calbindin respectively. The morphology of the dentate gyrus was maturing, but there were abundant immature neurons in all layers; some more mature neurons began to appear. Immature granule cells were small and immunoreactive for calretinin but not for calbindin (red arrows). Maturing cells presented larger nucleus free of chromatin lumps in which nucleoli could clearly be distinguished. They were calretinin-immunonegative granule cells that began to show calbindin immunoreactivity concentrated in the nucleus (black arrows). These calbindin cells were located in the areas in which the semilunar cells are located. Maturation began in the free border of the dorsal blade of the dentate gyrus where these pictures were taken. There is no overlapping between these granule cell populations.
CA, Cornu Ammonis; DG, dentate gyrus; h, hilus; gcl, granule cell layer; ml, molecular layer. Capillaries served as landmarks (asterisks).
Scale bar 50 µm.

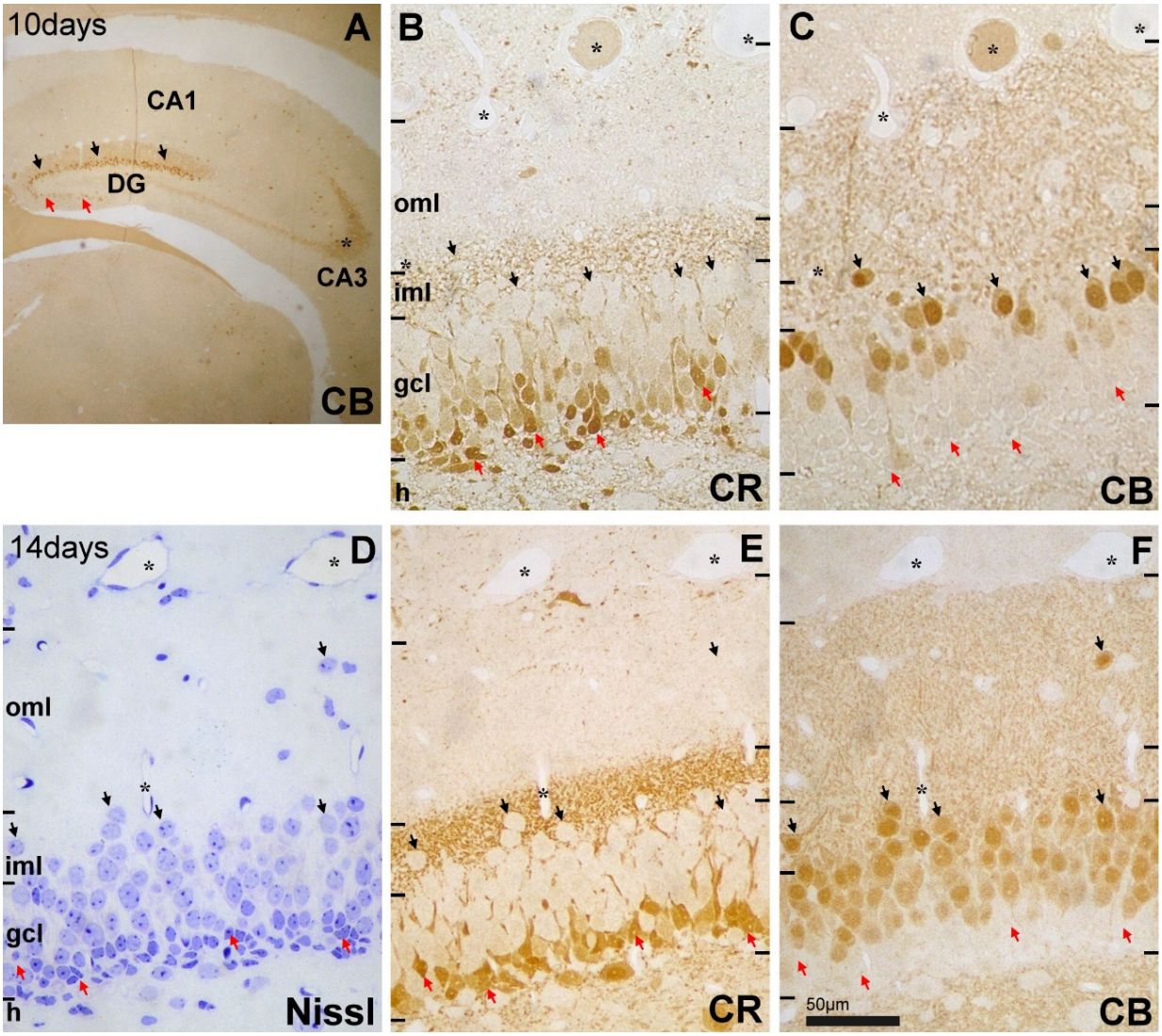

Figure II.3 - Maturation of semilunar granule cells

A) By 10 days postnatal, the dorsal blade of the dentate gyrus (black arrows) presents calbindin immunoreactivity but the ventral blade (red arrows) only has sparse calbindin cells. The stratum lucidum of CA3 (asterisk), corresponding to the projection field of granule cells, is becoming immunoreactive.

B, C) Consecutive sections from a 10 days postnatal animal stained for calretinin (**B**) and calbindin (**C**). Calretinin granule cells (red arrows) are small cells sited mainly in the subgranular area of the dentate gyrus, and they are still very numerous. The inner molecular layer can be distinguished for the first time due to the presence of calretinin boutons in it, representing the maturation of the hilar mossy cells. Calbindin cells (black arrows) are large, by this stage they present calbindin immunoreactivity in the perykaria and in their dendrites, defining the molecular layer. Only the cells with somata in the molecular layer and the border of the granule cell layer seem to strongly express calbindin.

D-F) Consecutive semithin sections from a 14 days old animal stained for Nissl (**D**), calretinin (**E**) and calbindin (**F**). The dentate gyrus is acquiring its mature configuration. Although many small nuclei, corresponding to calretinin immunoreactive cells (red arrows), are present in the subgranular zone adjacent to the hilus, the granule cell layer is formed by large nuclei with mature granule cell characteristics and expressing the mature marker calbindin (black arrows). On the other hand the inner molecular layer is now filled with calretinin boutons, arising from the hilar mossy cells. These boutons surround the calbindin cells present in the upper border of the dentate gyrus and the granule cells present in this area. Calbindin immunoreactivity corresponding to mature granule cells dendrites fills the molecular layer, whereas the calbindin immunoreactivity in the hilus corresponds to the mossy fibers.

DG, dentate gyrus; h, hilus; gcl, granule cell layer; iml, inner molecular layer; oml, outer molecular layer. Capillaries were used as landmarks (asterisks). Scale bar 50 µm.

2. MORPHOLOGICAL CHARACTERIZATION OF SEMILUNAR GRANULE CELLS

To have a better knowledge of the morphological characteristics of semilunar granule cells, we studied 60 intracellularly filled cells. These cells were chosen according to their location in the inner molecular layer of the dentate gyrus and morphology. We discarded those cells that could not be clearly identified as granule cells, and kept for the analysis only those cells that presented a similar morphology according to previous data. Due to the staining, not all reconstructed cells could be analyzed for all different features, so the data are given as a percentage of analyzed cells.

Semilunar granule cells had a wide dendritic arbor, which generally created a half-moon shape in the soma, with a long axis generally defined by the protrusion of the main dendrites (hence the “semilunar”), and a short axis defined by the scarce cytoplasm surrounding the nucleus. From the soma, two to four principal dendrites arose toward the hippocampal fissure.

Our results showed that many semilunar granule cells displayed distinct morphological features, when compared to typical granule cells (**Figure II.4**).

One characteristic was the location of the axon initial segment (**Figure II.4 F** and **G**). We observed the semilunar granule cell axon initial segment was located in a main dendrite in 31% of the analyzed reconstructed cells (8 out of 26), rising from it and forming an almost right angle. Though this feature has been previously observed in interneurons, it is not so common for principal cells. The frequency in which we observe axon-carrying dendrites in semilunar granule cells is high compared to typical granule cells, in which the axon almost always emerges from the cell body.

Another morphological feature was the presence of dendrites entering the granule cell layer and even the hilus, instead of travelling to the hippocampal fissure (**Figure II.4 I**). This phenomenon appeared with less frequency than the former one, in only 21% of the analyzed reconstructed cells (11 out of 52). In these cells, we could usually observe dendritic mature dendritic spines and a completely formed mossy fiber, which discards the possibility that they are still migrating immature granule cells.

2.1. SHOLL ANALYSIS

Sholl analysis was used to determine the dendritic arborization pattern of biocytin filled semilunar granule cells. Intersections were set at 20 µm, and different crossing points were statistically compared with typical granule cells. The aim of this analysis was to observe if the wider dendritic arborization observed for semilunar granule cells was translated into a higher neurite complexity, especially in distal dendrite branches located in the outer molecular layer, where they receive input from the entorhinal cortex.

As a normal distribution was not accomplished in all situations, a U Mann-Whitney test was performed. In closer distances to the soma, the number of crossings in the sholl analysis was statistically significant, as expected. However, in longer distances, there was no statistical significance between the numbers of crossings (**Graph II.2**).

These data indicate that the arborization complexity in both cell populations is similar, and suggest that semilunar granule cells do not present a higher chance of receiving more input from entorhinal cortex than typical granule cells.

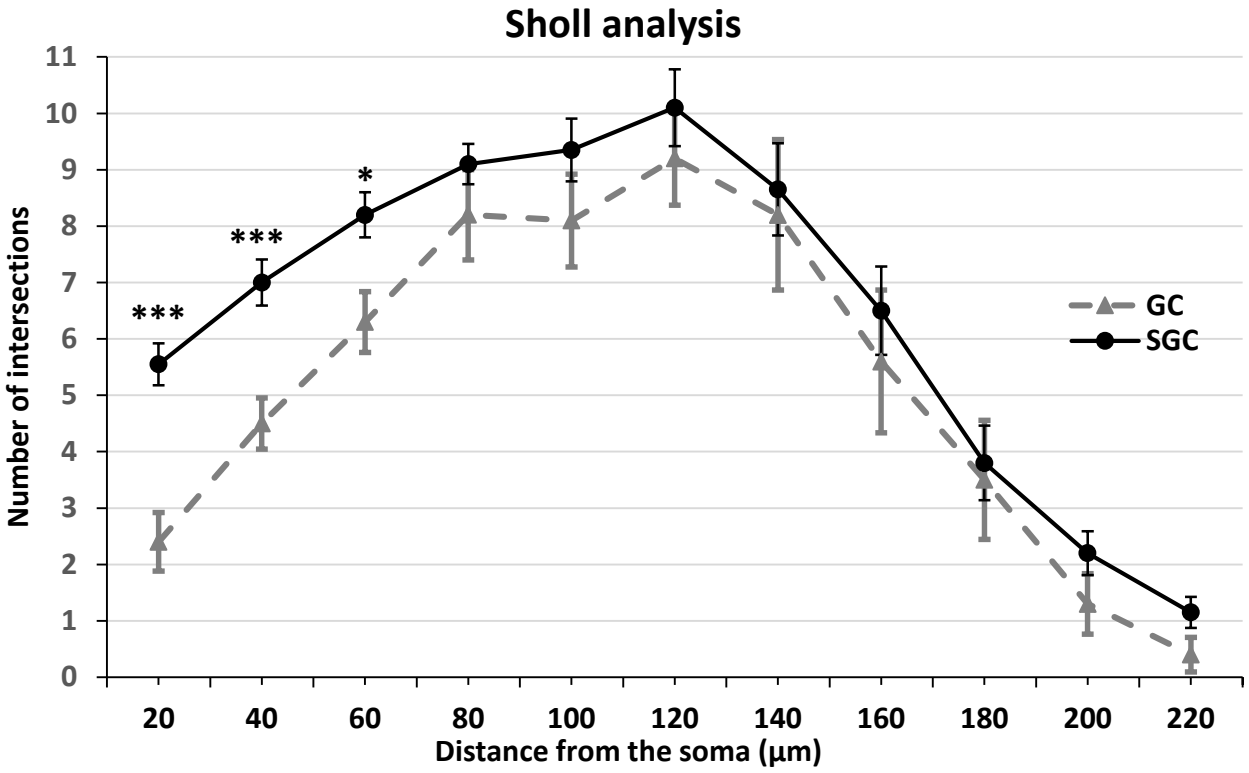

Graph II.2 - Sholl analysis of anatomically reconstructed typical granule cells and semilunar granule cells. Statistical difference is found in the proximal dendritic tree, where the number of crossings is higher for semilunar granule cells (n=20) than for typical granule cells (n=10). In the distal dendritic arbor, no differences are found. Data are shown as mean ± SEM. *($p < 0.05$) and *** ($p<0.001$) indicate statistically significant differences between groups after U-Mann Whitney test.

We measured the longest and shortest diameter of the somata of YFP-positive typical granule cells (n=28) and YFP-positive semilunar granule cells (n=32) in Thy1 transgenic mice, to assess whether there was a difference in the cell body size. Our results show that both cell populations present a similar cell body size (long diameter: 12.04 ± 1.09 μm for typical granule cells, and 11.95 ± 1.91 μm for semilunar granule cells; short diameter: 8.41 ± 0.97 μm for typical granule cells, and 8.97 ± 1.01 μm for semilunar granule cells).

2.2. ULTRASTRUCTURAL STUDY OF SEMILUNAR GRANULE CELLS IN THE INNER MOLECULAR LAYER AND ECTOPIC GRANULE CELLS IN THE OUTER MOLECULAR LAYER

Ultrastructural analysis was also conducted in semilunar granule cells in the inner molecular layer, and ectopic granule cells in the outer molecular layer. For the ultrastructural analysis, semilunar and ectopic granule cells were recognized either by their granule-like morphology, or by the nuclear marker Prox1. Several approaches were used, and all of them shared the same characteristics.

Semilunar granule cells were usually as big as typical granule cells, although apparently more cytoplasm could be observed in semilunar granule cells than in typical granule cells. The cell body sometimes presented a more triangular-shaped (or semilunar) morphology. In our preparations from 3-5 months old mice, the Golgi apparatus were quite abundant, as well as lipofuscin bodies. No other differences were found between semilunar granule cells and typical granule cells.

Their cell bodies seemed to have glial processes in apposition more frequently than typical granule cells. Satellite glial cells somata were frequently found close to ectopic granule cells located in the outer molecular layer. However, this fact may be probably due to their location in the molecular layer instead of their function.

Quite often, and more frequently in the outer molecular layer, semilunar or ectopic granule cells presented small protrusions which resembled small somatic spines (**Figure II.5**). Examples of this phenomenon have been found, with varying incidence, in most of the semilunar and outer molecular layer ectopic granule cells studied. However, only few synapse specializations have been found on them, and also generally in the outer molecular layer.

To exclude the possibility that these somatic spines may be an artifact due to fixation with acrolein or the mouse strain, rat tissue for standard electron microscopy was analyzed in search

of somatic spines (**Figure II.5 H-I**). Our results show that these cells also present spine-like protrusions on their cell body although, due to the small sample analyzed, no actual synapses were found on them.

Figure II.4 – Morphological features of semilunar granule cells
A-C) Three examples of intracellularly filled normal granule cells. From an ovoid body protrudes one apical dendrite that ramifies extensively in the molecular layer and reaches the hippocampal fissure. The axon grows from the basal part of the soma and goes directly to the hilus (arrows).
D-E) Example of two intracellularly filled semilunar granule cells in the border between the inner molecular layer and the granule cell layer. The axon in these cells (arrows) originates in the cell soma, and either enters straightly in the granule cell layer (**D**) or travels along the inner molecular layer until it enters the granule cell layer (**E**).
F-G) Example of two intracellularly filled semilunar granule cells at different levels of the inner molecular layer. In these cells, the axon (arrows) arises from the proximal part of the dendrite in (**G**), and from a relatively distant dendritic segment in (**F**). Note also the huge dendritic extension of the cell in (**F**) in the molecular layer when compared to typical granule cells.
H-I) Example of two intracellularly filled semilunar granule cells in the border between the inner molecular layer and the granule cell layer. These cells display more than two main dendrites originating in the soma. They also extend their dendritic arbor in a wider extension than typical granule cells. The axons in both cells travel a considerable distance along the inner molecular layer until they enter in the granule cell layer (arrows), presenting varicosities during its transit by the granule cell layer. The semilunar granule cell in (**I**) shows, in addition, one basal dendrite entering the granule cell layer and reaching the hilus (arrowhead).
Scale bar for all images: 50 μm.

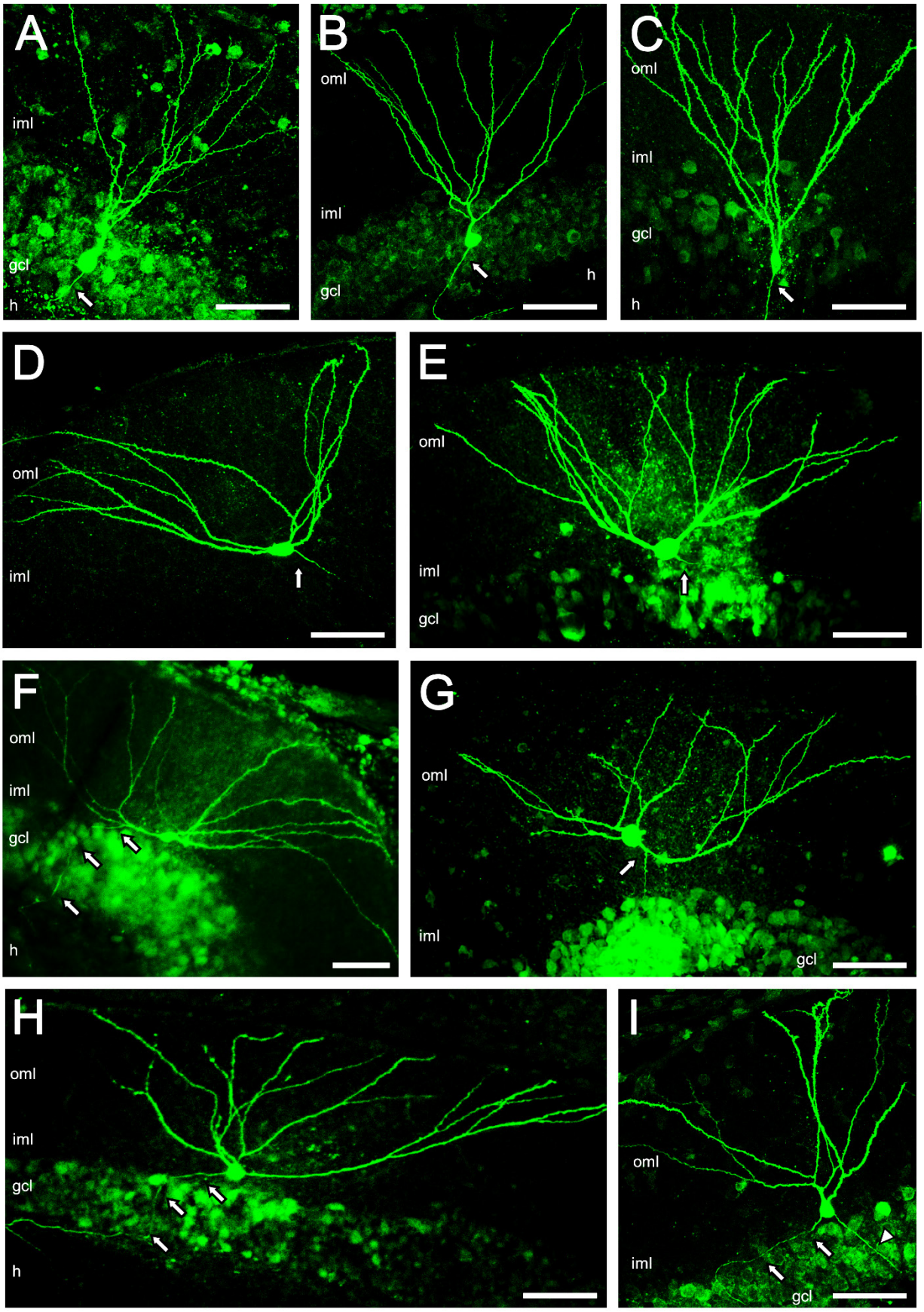
A
iml
gcl
h
B
oml
iml
gcl
h
C
oml
iml
gcl
h
D
oml
iml
E
oml
iml
gcl
F
oml
iml
gcl
h
G
oml
iml
gcl
H
oml
iml
gcl
h
I
oml
iml
gcl

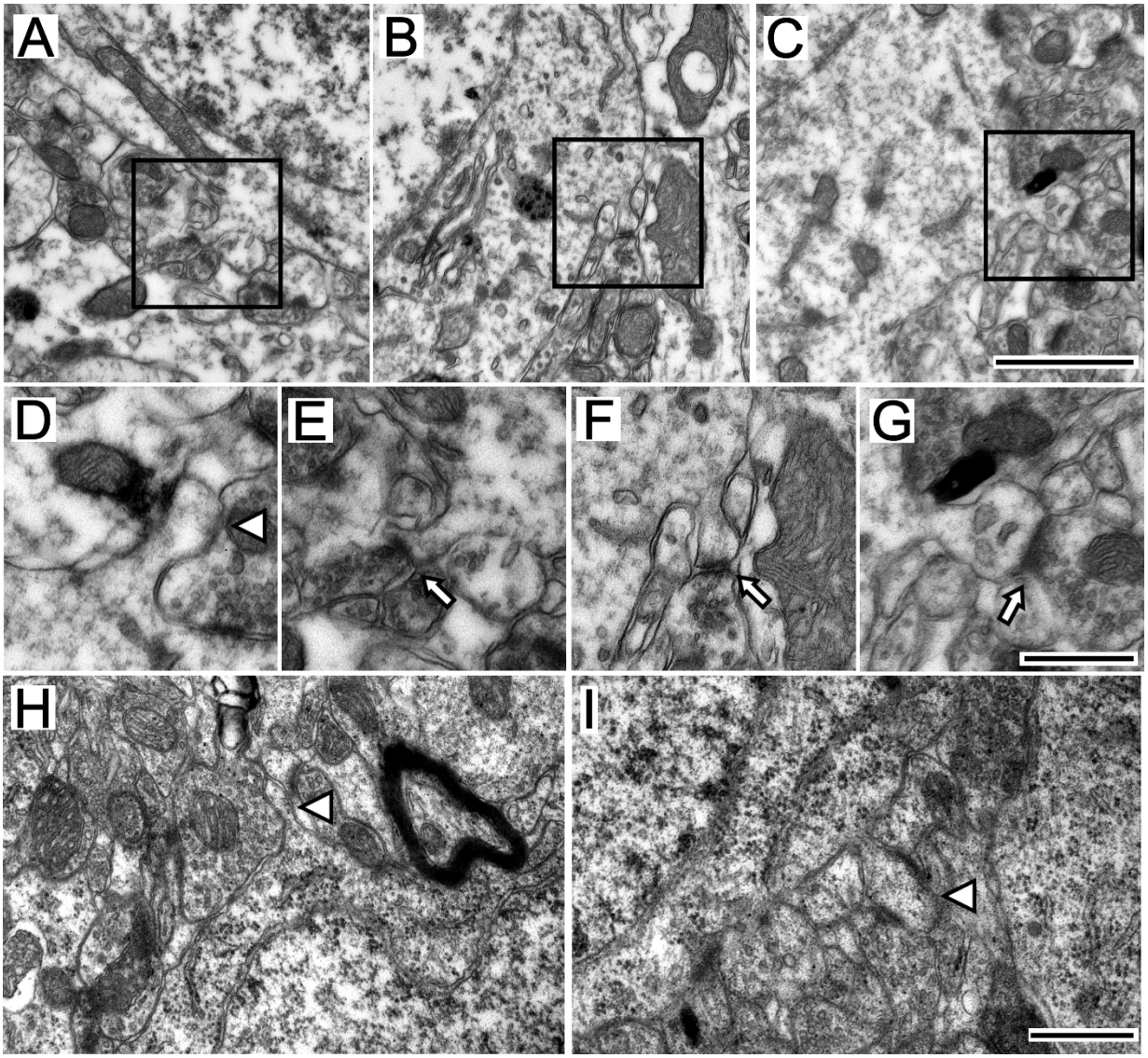

Figure II.5 – Semilunar granule cells present spine-like protrusions and spines in the cell soma
A-C) Low-magnification views of somatic spines of three different semilunar granule cells of the inner molecular layer under electron microscopy.
D) High-magnification image of a spine-like protrusion of a semilunar granule cell (arrowhead). No synaptic contact or indicative was found on the head or neck of this protrusion in consecutive sections.
E) High magnification of the spine shown in (**A**). This protrusion lacks the typical shape of spines found in the dendrites of principal cells, and no neck-head structure is found. It receives an excitatory synaptic contact in its head (white arrow).
F) High magnification of the spine shown in (**B**). This spine-like protrusion is probably receiving a synaptic contact in its head (white arrow).
G) High magnification of the spine shown in (**C**). The white arrow indicates the synaptic contact received from a probably excitatory presynaptic bouton.
H-I) Two examples of spine like protrusions (arrows) from semilunar granule cells in the inner molecular layer of the rat dentate gyrus. The fixation used here is GA 2%, in contrast to acrolein used in the previous examples. This shows that the presence of these spine-like protrusions is found both in mouse and rat, and it is not dependent of the fixation agent.
Scale bar: A-C, 1 µm; D-I, 400 nm.

3. NEUROCHEMICAL CHARACTERIZATION OF SEMILUNAR GRANULE CELLS

In order to determine the phenotypic characteristics of these neurons, and to find a marker which could be used to differentiate this population, we tried a set of different immunohistochemical stainings using several markers.

We used a transgenic mice line expressing the fluorescent protein YFP under the Thy1 promoter, resulting in a selective staining of principal cells in several regions of the brain (Feng et al., 2000; Porrero et al., 2010), including the dentate gyrus, to test the expression of the markers on the semilunar granule cells. We decided to test this methodology instead of a double immunostaining protocol with Prox1 and the selected marker for two reasons: (1) for unknown causes, it was difficult to obtain good-quality preparations with double immunohistochemistry for Prox1 and other markers for fluorescence microscopy; (2) with Thy1 transgenic mice we could see only a proportion of the principal cells among which semilunar granule cells are included, but with the advantage that we could see the cells of interest in a golgi-like manner, helping us to distinguish the semilunar granule cells based on their morphological features.

If all granule cells were Thy1-YFP-positive, the intense fluorescence from their somata and dendrites would make analysis impossible. But on the other hand, since not all the granule cells are Thy-1 positive, we present the data in this chapter referred to the number of Thy1-YFP-positive cells, and not referred to the total number of cells present in each area. It is also worth noting that those cells whose cell body was located close to the border between the granule cell layer and the inner molecular layer presented similar morphological characteristics previously described for semilunar granule cells (Ramón y Cajal, 1911; Williams et al., 2007). Therefore, they were also included among the semilunar granule cells.

3.1. CO-EXPRESSION OF GRANULE CELL MARKERS AND PRINCIPAL CELL MARKERS

3.1.1. CAMKII

YFP-positive cells (n=372) were analyzed in the inner molecular layer from three different animals, and all of them co-expressed the marker for mature excitatory neurons Ca^{2+}/calmodulin-dependent protein kinase II (CAMKII). From the 47 YFP-positive cells analyzed in the outer molecular layer, only one was not CAMKII-positive. Therefore, virtually all the YFP-

positive cells in the dentate gyrus of these animals correspond to excitatory cells. This fact makes YFP in combination with morphology a reliable marker for this subpopulation of semilunar granule cells (**Figure II.6**).

3.1.2. PROX1

We used Prox1 to determine whether the YFP-positive cells that we see in this transgenic strain corresponded with the "misplaced" granule cells located in the molecular layer, that we considered semilunar granule cells.

From 360 YFP-positive cells analyzed in the inner molecular layer in three different animals, 99.8 ± 0.4% colocalized with Prox1. In the outer molecular layer, 93.4 ± 7.2% of the 43 YFP-positive cells analyzed colocalized with Prox1 (**Figure II.7**). Therefore, the majority of the Prox1 cells in the inner molecular layer corresponded to granule cells. In the outer molecular layer there is a possibility that some of the principal cells located in this area do not correspond to granule cells, still the high colocalization suggests that all granule cells in this area express Prox1.

A summary of the colocalization between YFP and the different markers for principal cells, in Thy1 transgenic mice, can be seen in **Table II.1**.

3.2. CO-EXPRESSION OF CALCIUM BINDING PROTEINS

Semilunar granule cells are known to present different intrinsic Ca^{+2} dynamics than typical granule cells (Williams et al., 2007). To assess if this difference could be underlined by a different buffering of Ca^{+2} in these cells, we examined the colocalization of Thy1 positive neurons with the three calcium binding proteins: parvalbumin, calretinin and calbindin.

3.2.1. CALBINDIN

The calbindin D-28k immunostaining observed in Thy1 mice was as previously described (Sloviter, 1989; Celio, 1990): granule cell somata and processes were labeled with calbindin, though not all of granule cells were labeled.

YFP-positive cells were analyzed in the inner molecular layer (n=379) and outer molecular layer (n=44), in three different animals. In the inner molecular layer, 78.6% ± 10.4% of Thy1-postive cells were also positive for calbindin. In the outer molecular layer, however, 81% ± 7.8% of

Thy1-positive cells coexpressed calbindin (**Figure II.8**). Therefore calbindin is a maker for semilunar granule cells but it does not label all of them.

3.2.2. PARVALBUMIN

The immunostaining of parvalbumin in Thy1 mice also presented the expected pattern (Sloviter, 1989; Celio, 1990). The labelling corresponded to the somata of parvalbumin interneurons located in the granule cell layer, hilus and in the border of the inner molecular layer and granule cell layer. Positive dendrites were located both in the hilus and molecular layer, and we also observed axon terminals located in the granule cell layer with synaptic boutons surrounding granule cells.

As expected, no colocalization of YFP-positive neurons and parvalbumin was observed (**Figure II.9**). On the other hand, we could find basket-like boutons surrounding many YFP-positive somata in the inner and outer molecular layer. This means that semilunar granule cells are probably perisomatically controlled by parvalbumin basket cells, in a similar way as granule cells. This inhibitory innervation may come from local parvalbumin-positive basket cells, or, less probably, from projecting parvalbumin interneurons.

3.2.3. CALRETININ

The immunostaining of calretinin adjusted to the expected pattern in the mouse (Liu et al., 1996; Blasco-Ibáñez and Freund, 1997; Fujise et al., 1997). Hilar mossy cells were immunoreactive, in an increasing number as we reached more ventral sections. There were also some immature granule cells in the subgranular zone. A few calretinin interneurons were present in the hilus and granule cell layer. We could also find some calretinin-positive cells in the molecular layer that probably correspond to interneurons as well as to Cajal-Retzius cells (Liu et al., 1996). The inner molecular layer was completely filled with calretinin neuropil coming from mossy cells (Blasco-Ibáñez and Freund, 1997; Fujise et al., 1997).

Our slides showed no colocalization between YFP-positive neurons and calretinin in the inner or the outer molecular layer (**Figure II.10**). However, we could see calretinin-positive puncta resembling synaptic boutons in close apposition to some YFP-positive cell somata in both the inner molecular layer and the outer molecular layer. Due to the dense packing of the calretinin-positive fibers in the inner molecular layer, it was expected to find calretinin-positive neuropile

close to our cells, leading to a false-positive colocalization in confocal microscopy. However, the presence of calretinin-positive puncta in apposition with YFP-positive somata in the outer molecular layer, where the calretinin-positive elements are more scattered, could mean that outer molecular layer ectopic granule cells specifically receive a calretinin-positive innervation and were suggestive of calretinin perisomatic innervation on the semilunar granule cells in the inner molecular layer.

A summary of the colocalization between YFP and the different calcium binding proteins, in Thy1 transgenic mice, can be seen in **Table II.1**.

	iml	**oml**
Principal cell markers		
Prox1	99.8 ± 0.4%	93.4 ± 7.2%
CAMKII	100.0 ± 0.0%	97.0 ± 5.3%
Calcium Binding Proteins		
Parvalbumin	0%	0%
Calretinin	0%	0%
Calbindin	78.6 ± 10.4%	81.0 ± 7.8%

Table II.1 - Colocalization of YFP-positive cells in the inner molecular layer and outer molecular layer with different principal cell markers and calcium binding proteins. Data are shown as mean ± SD of three different animals

3.3. CART PEPTIDE EXPRESSION

Cocaine- and amphetamine-regulated transcript (CART) peptide has been shown to be expressed by mossy cells in the human, and by a subpopulation of granule cells in the rat (Seress et al., 2004; Abrahám et al., 2007). This subpopulation is comprised by the granule cells located in the border between the molecular layer and the granule cell layer, and could be therefore similar to the subpopulation of granule cells that we are interested in.

CART peptide has also been shown to be expressed by granule cells which are located in the border between the granule cell layer and the molecular layer in other rodent species, like the vole or the guinea pig (Hunter et al., 2005; Kolenkiewicz et al., 2009). Therefore it looked as a promising specific marker for semilunar granule cells.

As it had been previously described that this antigen is degraded rapidly, at least in post-mortem tissue (Seress et al., 2004), sections from fresh perfused animals were used for these experiments.

Expression of CART in the hypothalamus was similar to the labelling previously reported (Koylu et al., 1998). The antibody labeled, with an intense stain, the subpopulation of hypothalamic neurons that specifically express CART peptide. Thick CART peptide-positive fibers were found, though scarce, all over the telencephalon with a high degree of staining.

When we tested this antibody in the mouse and rat hippocampus, the number of labeled cells was too low, even although we were able to find CART-positive neurons that resembled semilunar granule cells (**Figure II.11**). Other cell types, with different morphological characteristics than semilunar granule cells, were found in the molecular layer and in the hilus. These CART-positive cells may correspond to mossy cells or interneurons, but no further effort was performed to characterize them. CART-positive fibers were also present in the dentate molecular layer, mainly in the outer two thirds. Sometimes, these fibers travelled from the hippocampal fissure to the hilus, were they established collaterals (**Figure II.11 B**). These CART-positive fibers were scarce, and exhibited several varicosities.

CART peptide immunostaining was combined with a Timm staining in hippocampal sections from six recently perfused mice, to check whether the apparent Timm-positive fibers present in the granule cell layer could arise from CART-positive cells. When we found a CART-positive putative semilunar granule cell, we could usually observe a Timm-positive fiber close to the cell. This suggests that Timm-positive fibers may arise from CART-positive semilunar granule cells. However, as Timm staining only labels the boutons, and the axon in semilunar granule cells not always protrudes from the cell soma, we could not be certain that these Timm fibers did arise from the CART-positive cells.

We also tested CART peptide immunostaining in tissue from recently perfused colchicine-treated animals (n=3) in order to increase the immunoreactivity at the somata. CART immunostaining showed slightly more positive cells in colchicine treated animals than in control animals. However, the amount of positive-cells was still low, and not constrained to semilunar granule cells.

Therefore, though promising, we had to discard this peptide as a marker for semilunar granule cells in our particular conditions.

3.4. SEMILUNAR GRANULE CELL ACTIVATION: EXPRESSION OF THE CELL ACTIVATION MARKER FOS

Semilunar granule cells receive a stronger glutamatergic input than typical granule cells, partially coming from mossy cells (Williams et al., 2007). This, among other facts, ensure a physiological state that allows semilunar granule cells to trigger plateau potentials (Larimer and Strowbridge, 2010). Therefore, they are expected to be constitutively more active than typical granule cells, both in control conditions and after excitation.

To verify this hypothesis, we studied the expression of the neuronal marker Fos in the dentate gyrus of adult mice, as it is extensively used as a marker for cell activity (Dragunow and Faull, 1989). The expression of the *c-fos* gene is dependent on the presence of calcium as a second messenger (Sheng et al., 1990). Therefore, the presence of the c-Fos protein can be related to a high synaptic activity, as the intracellular calcium levels increase when the cell fires action potentials.

In a first approach, we studied the colocalization of pan-fos with YFP-expressing cells in the inner and outer molecular layer of three Thy1 transgenic mice, to have and overall idea of the level of activity of this cell population. Our results show that the proportion of YFP-positive cells that colocalized with pan-Fos reached 83.9 ± 4.7% from 427 YFP-positive cells analyzed in the inner molecular layer, and 88.6 ± 10.9% from 45 YFP-positive cells in the outer molecular layer.

In contrast, from a total of 806 YFP-positive randomly selected typical granule cells from 4 different animals, only 12.9 ± 3,9% of the cells were considered also pan-Fos positive. From these data, we can assume a higher activity level for semilunar granule cells than for normal granule cells.

However, considering that pan-Fos labels several proteins of the Fos family (c-Fos, Fra1, Fra2 and FosB), the difference in this staining cannot fully correlate with cell activity, and other cellular mechanisms can be influencing our results. Therefore, the staining for c-Fos was preferred in further analysis, as it is temporally more accurate in terms of neuron activity. In this case, a big heterogeneity in the labeling pattern was observed in the different animals used, as well as in the dorso-ventral axis of each single animal. Therefore, no quantitative analysis was performed for this partial objective.

A gradation in the staining intensity was obtained, and we considered only nuclei with moderate or high c-Fos labelling. In the dentate gyrus, c-Fos-positive nuclei were generally

located all along the granule cell layer. Very frequently, intensely labeled c-Fos nuclei were observed in the border between the granule cell layer and the inner molecular layer, and sometimes (though not so often) also in the outer molecular layer. Both weak and intense labeled nuclei were found among the typical granule cells and among the semilunar granule cells.

However, considering the amount of c-Fos-positive nuclei in the inner molecular layer and in the granule cell layer, and the number of cells present in both laminae, semilunar granule cells seem to express c-Fos more frequently, and therefore they may be more active than typical granule cells.

To rule out the possibility of having c-Fos positive elements that belong to interneurons instead to semilunar granule cells, a double immunostaining against Prox1 and c-Fos was performed in three adult animals. In the outer and inner molecular layer, c-Fos expression was almost always associated with Prox1-positive nuclei, and only once a c-Fos nucleus did not coexpress Prox1.

Whenever a Prox1-positive nucleus was seen in the hilus, its c-Fos expression was also checked. In this regard, we found no colocalization between putative hilar ectopic granule cells and c-Fos. The same absence of colocalization was observed for the scarce Prox1-positive nuclei found in the CA3 region of the hippocampus.

Figure II.6 – CAMKII and YFP-positive cells in Thy-transgenic mice colocalize in the molecular layer of the mouse dentate gyrus

The YFP protein is expressed under the promoter of Thy1, and selectively labels principal cells. For clarity, YFP is visualized in red, and the term Thy1 was used instead of YFP to avoid further confusion with the color.

All YFP-positive cells were also immunopositive for CAMKII, indicating that all the cells studied are principal cells. Note the presence of CAMKII-positive cells that are not positive for YFP.

A) Colocalization of CAMKII and YFP (arrow) in the border between the granule cell layer and the inner molecular layer.

B) Colocalization of CAMKII and YFP (arrows) in the border between the inner molecular layer and the outer molecular layer.

C) Colocalization of CAMKII and YFP (arrow) in the outer molecular layer. In this region, the majority of YFP-cells present their cell body with the long axis oriented perpendicularly to the granule cell layer.

gcl, granule cell layer; iml, inner molecular layer; oml, outer molecular layer. Scale bar for all images: 50 µm.

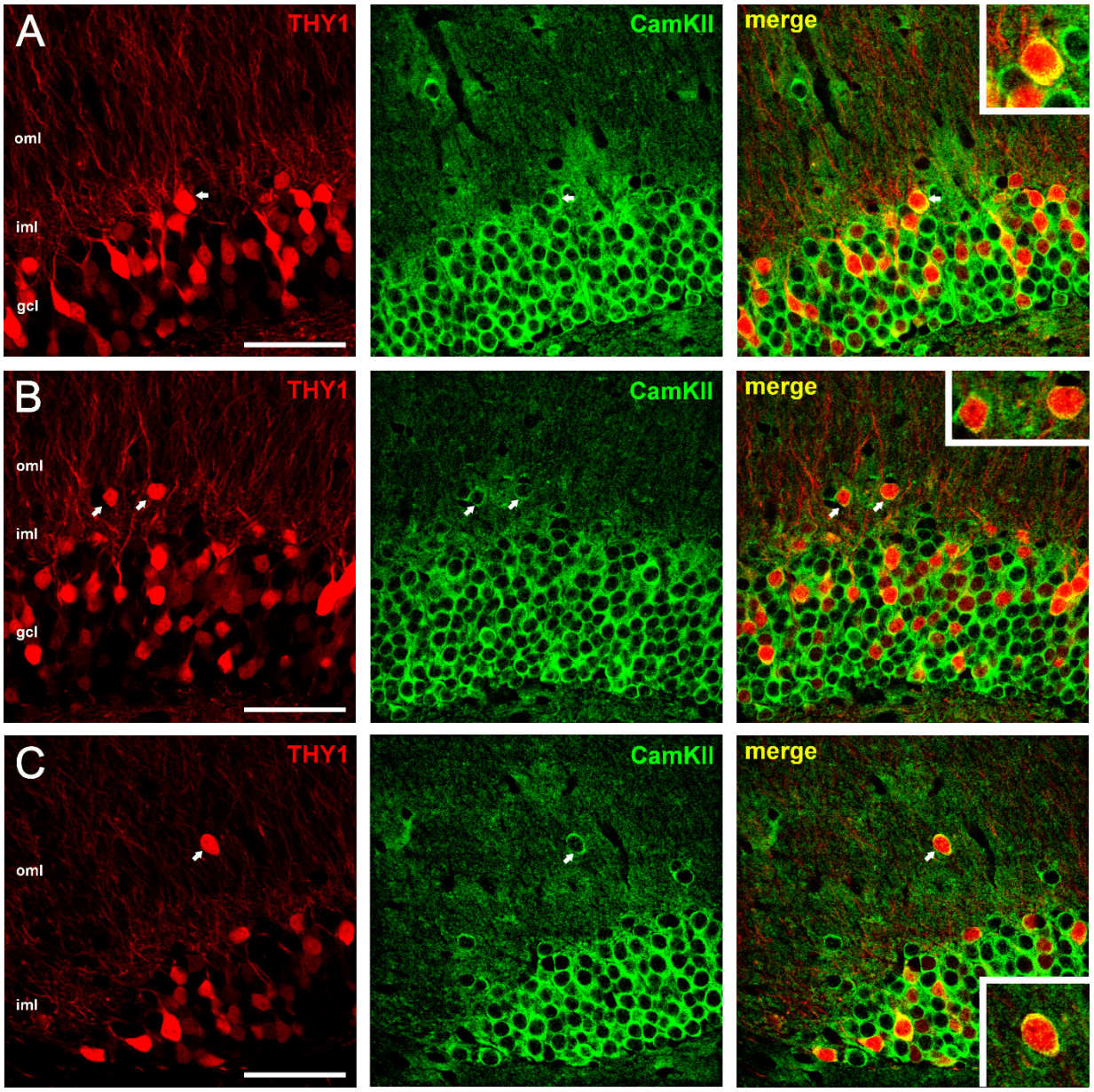
A
THY1
CamKII
merge
oml
iml
gcl
B
THY1
CamKII
merge
oml
iml
gcl
C
THY1
CamKII
merge
oml
iml

Figure II.7 – Prox1 and YFP-positive cells colocalize in the molecular layer of the Thy1 transgenic mouse dentate gyrus

The YFP protein is expressed under the promoter of Thy1, and selectively labels principal cells. For clarity, YFP is visualized in red, and the term Thy1 was used instead of YFP to avoid further confusion with the color.

Almost all YFP-positive cells present Prox1-positive nuclei. Therefore, the vast majority of the principal cells present in the molecular layer correspond to semilunar granule cells and ectopic outer molecular layer cells.

A) Colocalization of Prox1 and YFP (arrow) in the inner molecular layer, next to the border of the granule cell layer.

B) Colocalization of Prox1 and YFP (arrow) in the limit between the inner molecular layer and the outer molecular layer.

C) Colocalization of Prox1 and YFP (arrow) in the outer molecular layer.

D) An example of the scarce YFP-positive cells not colocalizing Prox1 (arrowhead). These cells represent a low proportion of the YFP population in the molecular layer. Note that the morphology of this cell does not correspond to the morphology of semilunar granule cells.

gcl, granule cell layer; iml, inner molecular layer; oml, outer molecular layer. Scale bar for all images: 50 μm.

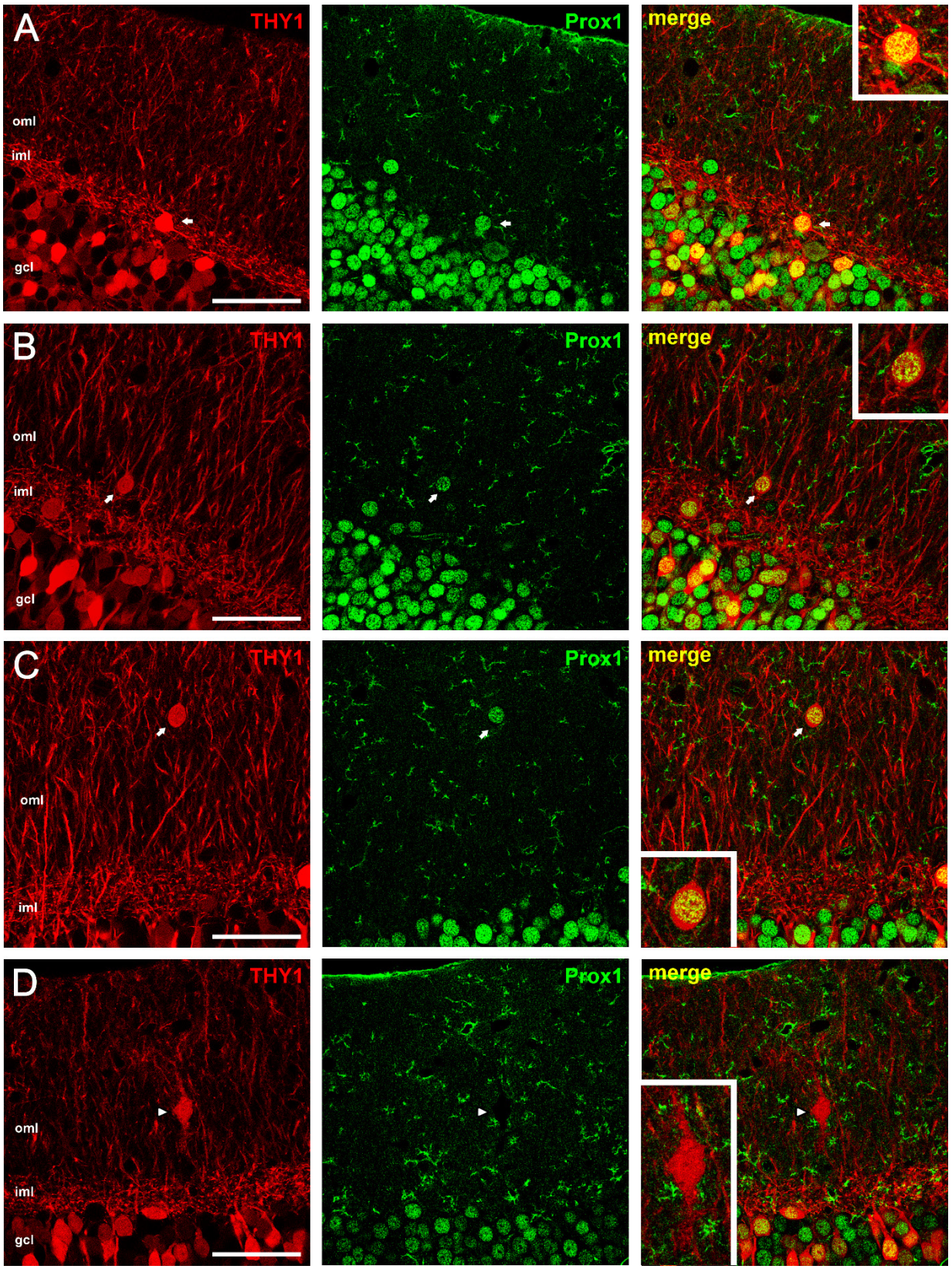
A
THY1
Prox1
merge
oml
iml
gcl
B
THY1
Prox1
merge
oml
iml
gcl
C
THY1
Prox1
merge
oml
iml
D
THY1
Prox1
merge
oml
iml
gcl

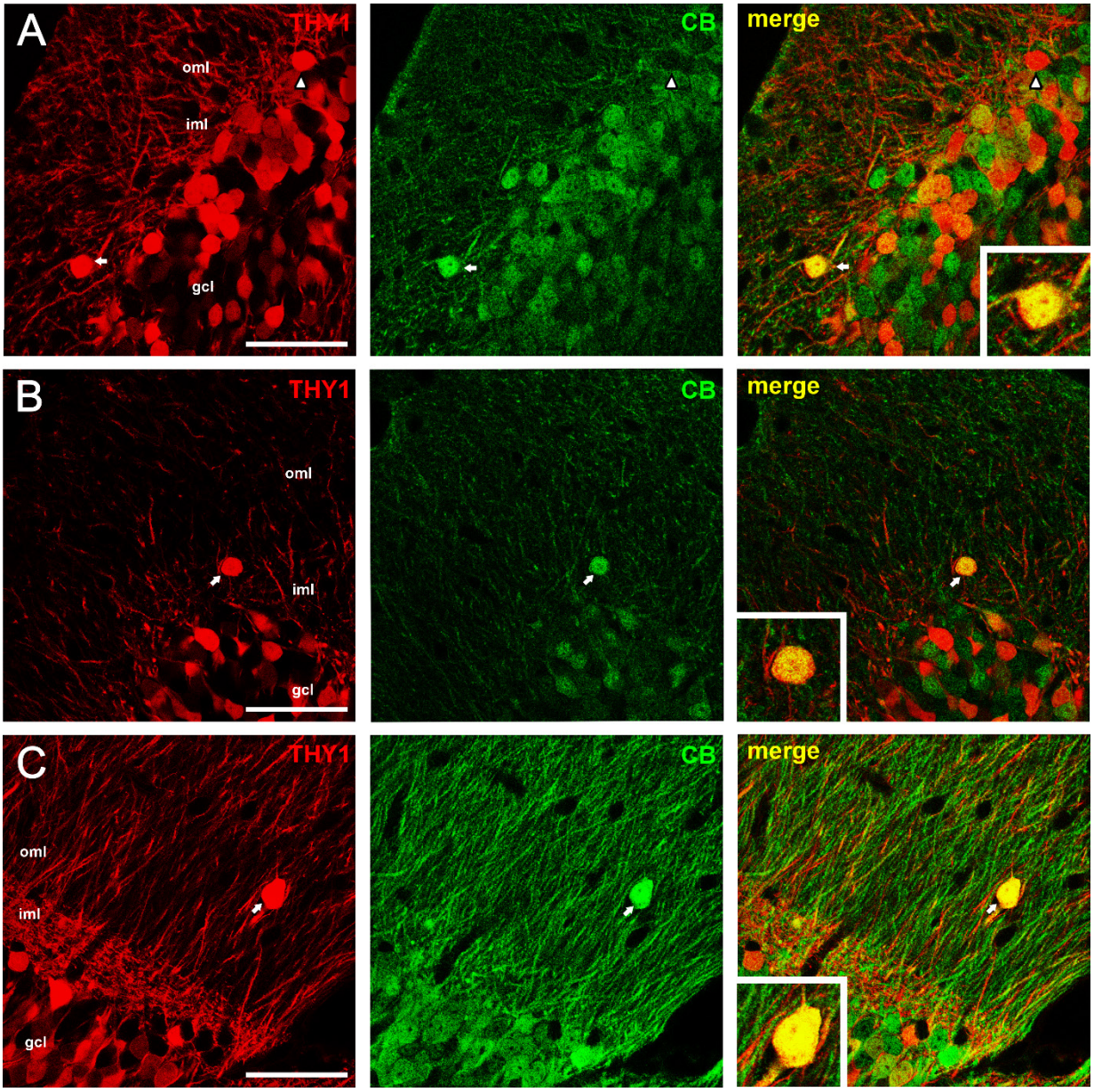

Figure II.8 – Calbindin and YFP-positive cells colocalize in the molecular layer of Thy-transgenic mice dentate gyrus.
YFP protein is expressed under the promoter of Thy1, and selectively labels principal cells. For clarity, YFP is visualized in red, and the term Thy1 was used instead of YFP to avoid further confusion with the color.
The majority of the YFP-positive cells, though not all, express the calcium binding protein calbindin.
A) White arrows show one YFP-positive colocalizing calbindin (arrow), and one YFP-positive immunonegative for calbindin (arrowhead) in the border between the inner molecular layer and the granule cell layer.
B) Colocalization of calbindin and YFP (arrow) in the inner molecular layer.
C) Colocalization of calbindin and YFP (arrow) in the outer molecular layer.
gcl, granule cell layer; iml, inner molecular layer; oml, outer molecular layer. Scale bar for all images: 50 µm.

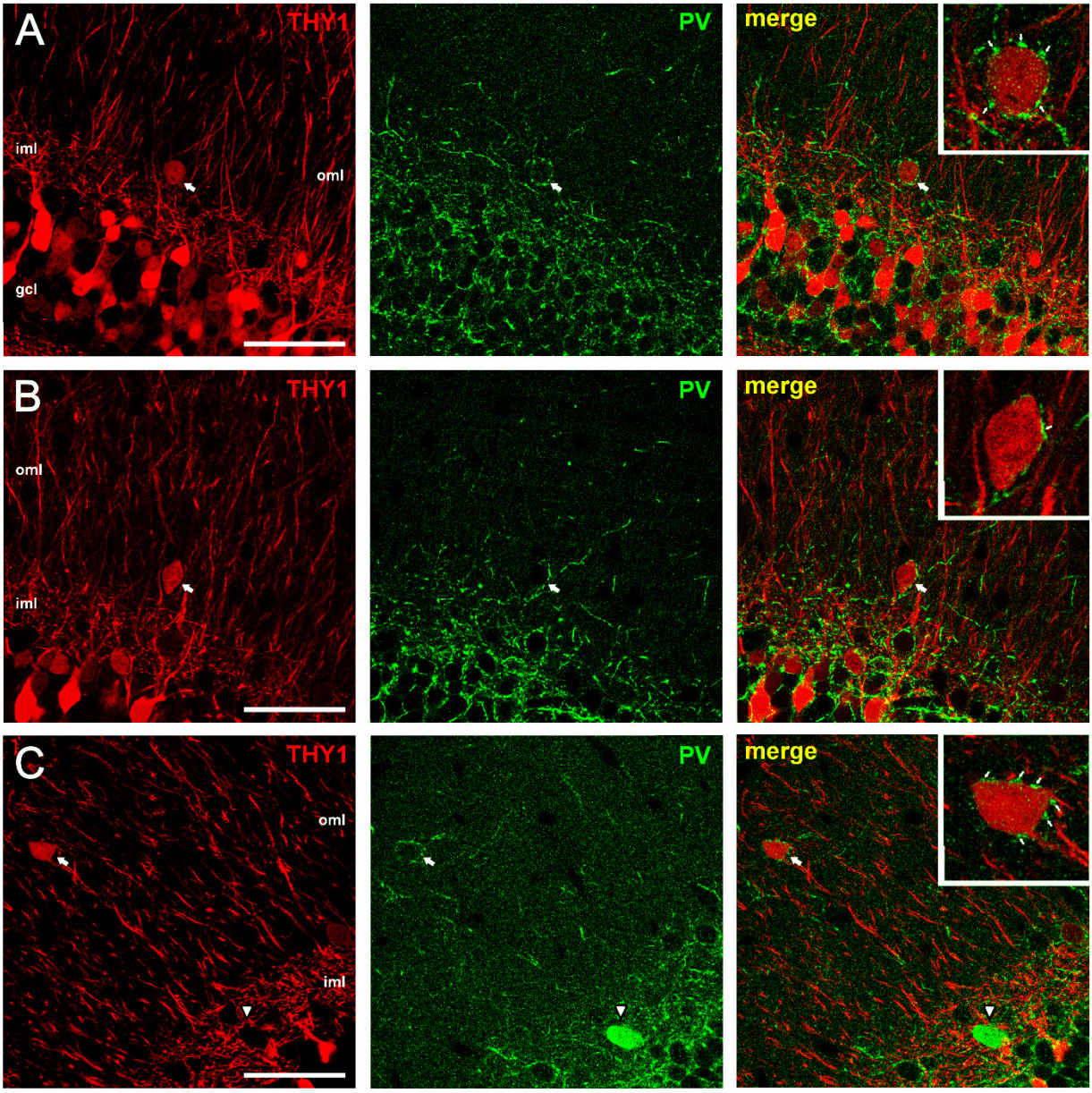

Figure II.9 – YFP-positive cells in Thy-transgenic mice are immunonegative for the calcium binding protein parvalbumin

The YFP protein is expressed under the promoter of Thy1, and selectively labels principal cells. For clarity, YFP is visualized in red, and the term Thy1 was used instead of YFP to avoid further confusion with the color.

A) No YFP-positive cells were found immunopositive for parvalbumin in the inner molecular layer. Example of an YFP-positive cell negative for parvalbumin (arrow). Parvalbumin-positive puncta was found in apposition to cell somata in the granule cell layer. YFP-positive cells in the inner molecular layer also presented parvalbumin-positive puncta (arrows inside the inset) in apposition to the cell soma, indicating a putative perisomatic inhibitory innervation from parvalbumin interneurons to semilunar granule cells.

B-C) No YFP-positive cells were found immunopositive for parvalbumin in different heights of the outer molecular layer, but generally presented parvalbumin-positive puncta in apposition to the cell soma (arrows inside the inset), indicating a putative perisomatic inhibitory innervation from parvalbumin interneurons to ectopic granule cells in the molecular layer. In (**C**), a parvalbumin-positive profile from an interneuron is observed in the granule cell layer. gcl, granule cell layer; iml, inner molecular layer; oml, outer molecular layer. Scale bar for all images: 50 µm.

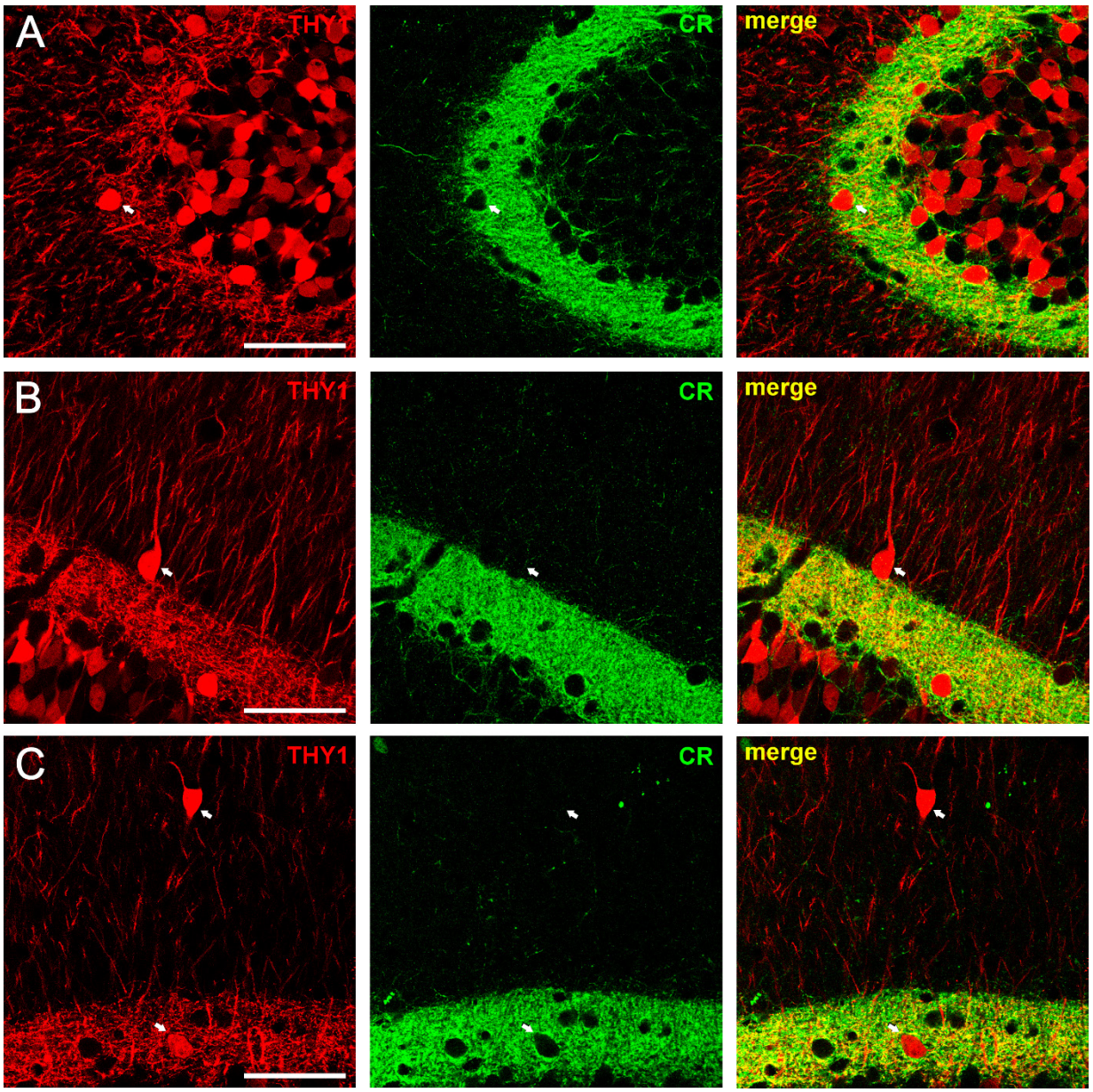

Figure II.10 – YFP-positive cells in Thy1 transgenic mice are immunonegative for the calcium binding protein calretinin

The YFP protein is expressed under the promoter of Thy1, and selectively labels principal cells. For clarity, YFP is visualized in red, and the term Thy1 was used instead of YFP to avoid further confusion with the color.

A) No YFP-positive cells were found immunopositive for calretinin in the inner molecular layer. Example of an YFP-positive calretinin-negative cell (arrows). Note the high density of calretinin-positive puncta in the inner molecular layer, due to the fibers and boutons of mossy cells.

B-C) No YFP-positive cells were found immunopositive for calretinin in different heights of the outer molecular layer, as shown in these two examples of YFP-positive calretinin-negative cells ectopic granule cells (arrows). This may also indicate that none of the semilunar granule cells and the outer molecular layer ectopic granule cells are immature cells. Another example of a calretinin-immunonegative semilunar granule cell is depicted with an arrow in (**C**).

Scale bar for all images: 50 µm.

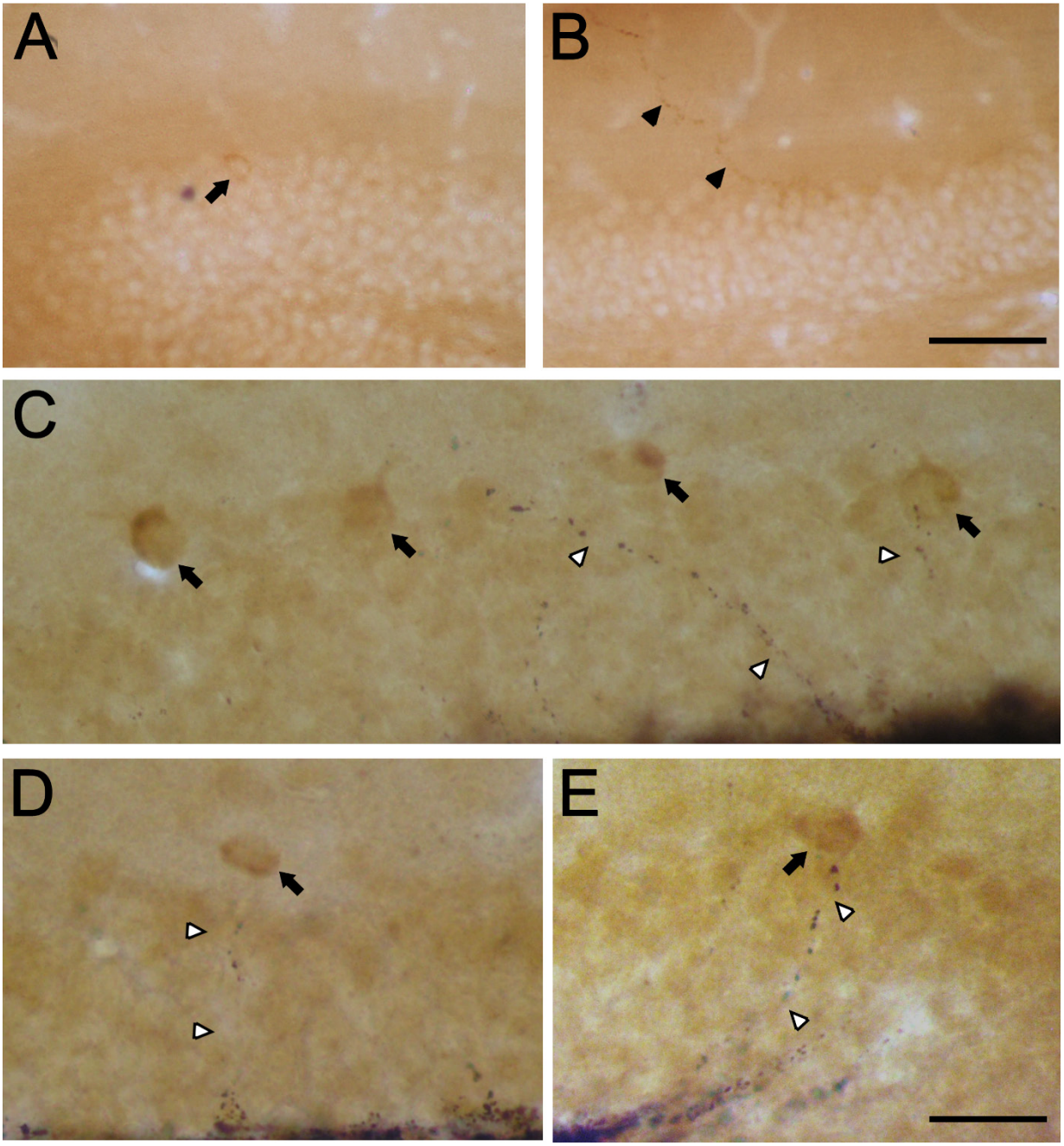

Figure II.11 – CART peptide antigenicity in semilunar granule cells.
CART peptide expression was scarce in the mouse dentate gyrus. It was not limited to semilunar granule cells, as some hilar neurons were also CART-positive (not shown).
A) A more intense labelling of CART peptide was generally found in the cells of the most superficial part of the granule cell layer, in its border with the inner molecular layer. The size and shape of the labeled cells (arrows) was similar as the one expected for semilunar granule cells, and similar to the staining obtained with CAMKII.
B) CART-positive fibers were observed rarely in the dentate gyrus, entering via the hippocampal fissure and travelling through the molecular (black arrowheads) and granule cell layer to the hilus (not shown). In their way, several varicosities were observed.
C-E) Images from a CART peptide staining performed after a Timm staining, to check if Timm-positive fibers arise from the vicinity of these cells. We could often see Timm-positive fibers (arrowheads) appearing close to the cell bodies of CART peptide-positive cells (arrows). Due to the nature of the technique, that only labels the boutons, we could not be absolutely certain that these Timm boutons did arise in every case from the labeled cell.
Scale bar: A-B, 100 µm; C-E, 50 µm.

4. SYNAPTIC INPUT TO SEMILUNAR GRANULE CELLS

The study aiming the phenotypical characterization of semilunar granule cells gave us a clue that although they shared characteristics with typical granule cells, they could receive different drive due to their different location.

To verify that the perisomatic innervation suggested by the preceding chapter was really present, and not just false-positive elements, the perisomatic innervation of semilunar granule cells was studied under the electron microscope.

4.1. PERISOMATIC INHIBITORY INNERVATION

No previous anatomical study has been made to identify the innervation that semilunar granule cells receive differently from typical granule cells. In this dissertation we have centered the study to the perisomatic innervation, using Prox1 and c-Fos as a marker for this cell population, and confirming its granule nature under the electron microscope.

In the previous section, we showed that YFP-positive neurons in the molecular layer, corresponding to semilunar granule cells, presented parvalbumin-positive puncta surrounding their somata. In another immunostaining with VGAT and Prox1 (not shown) we confirmed that this cell population receives an important perisomatic inhibition. This perisomatic innervation extended also to cells located into the outer molecular layer.

To confirm the existence of a perisomatic inhibitory drive to semilunar granule cells, two different sources were studied: (1) parvalbumin-positive boutons that correspond to perisomatic-targeting fast-spiking interneurons; and (2) CCK-positive boutons that correspond to perisomatic-targeting regular-spiking interneurons.

4.1.1. PERISOMATIC INNERVATION FROM PARVALBUMIN BASKET CELLS

First, we made a double immunostainig with DAB-Ni for parvalbumin and DAB for Prox1. We observed clear basket-like parvalbumin-positive arrangements around some Prox1-positive cells. Usually these boutons were intensely labeled, but we also found weak labeled terminals surrounding Prox1-positive nuclei, which could indicate a lower expression level of parvalbumin in those cases. Only rarely we found Prox1-positive cells that did not show any parvalbumin-positive puncta in apposition (**Figure II.12**).

To confirm that these boutons established synaptic contacts with semilunar granule cells, we checked them under the electron microscope. Parvalbumin-positive boutons were generally large, with flat vesicles and a large mitochondria almost always present. They established symmetric synaptic contacts with the targeted semilunar granule cell. Several parvalbumin-positive boutons establishing synaptic contacts were seen in the same cell, indicating a strong inhibitory drive from parvalbumin interneurons. In addition, these boutons established sometimes more than one symmetric contact (**Figure II.13**).

4.1.2. PERISOMATIC INNERVATION FROM CCK BASKET CELLS

Two approaches were used to study the perisomatic innervation on semilunar granule cells by CCK-positive interneurons.

Our first approach was to use an antibody against CCK. In the mouse, this antibody labeled the inner molecular layer quite intensely, and also the mossy fibers. Positive cell bodies could also be detected, though they were clearer in CA1, where no mossy fibers were labeled. In CA1 pyramidal layer, a clear pattern of perisomatic boutons was observed, but it was absent in the granule cell layer. Only seldom an intensely-labeled fiber crossed the granule cell layer. No evident difference between the dorsal and dentate gyrus was observed.

Only in mice where a general intense staining was observed, perisomatic boutons in the outer two thirds of the molecular layer could be seen around Prox1-positive cells, but the labelling was not optimal to continue the study under electron microscopy. Therefore, we decided to study CCK immunoreactivity in the rat. Here, no staining from mossy fibers or mossy cells' fibers was observed. The staining pattern was similar as the one expected according to the literature (Freund and Buzsáki, 1996; Hájos et al., 1996). CCK-positive cell bodies were found in the hilus and in the granule cell layer (**Figure II.14 A**), as well as in stratum radiatum and pyramidale from CA3 and CA1.

In a double immunostaining with Prox1, perisomatic CCK-positive boutons were observed both in the inner molecular layer and the outer molecular layer. The amount of perisomatic boutons was heterogeneous, and cells with two or three CCK-positive boutons could be found together with cells that exhibit only one CCK-positive if any (**Figure II.14**)**.** Although much better than in mice, this heterogeneity could be due to problems with the immunoreactivity of the antibody.

At the electron microscopy level, these boutons were confirmed to make symmetric contacts with the Prox1-positive cells they surrounded. We observed smaller boutons that made symmetric synapses, with slightly ovoid vesicles and sometimes one small mitochondria. We also analyzed larger invaginating boutons, with one big mitochondria at one side and slightly ovoid vesicles confronting the Prox1-positive postsynaptic cell (**Figure II.15**). These boutons also formed symmetric synapses and resembled the ones described as VGluT3-positive in the amygdala (Yoshida et al., 2011; Omiya et al., 2015).

Since the staining against CCK was not completely satisfactory, the cannabionid receptor type 1 (CB1R) was used to label CCK-positive fibers, as it has been previously shown that CB1R is co-expressed with CCK in fibers emerging from CCK-positive interneurons, both in rat and mouse (Katona et al., 1999; Marsicano and Lutz, 1999). The staining pattern that we observed in the dentate gyrus was homogeneous. A dense plexus of fibers covered all the granule cell layer, molecular layer and hilus (**Figure II.16**). No evident difference was observed between the dorsal and ventral dentate gyrus, as well as in the infra- or suprapyramidal layer of the granule cell layer, although the clear basket arrangement of boutons around semilunar granule cells was highly suggestive.

At the electron microscopy level, we confirmed that the CB1R-positive boutons that were in apposition with Prox1-positive cells were making synaptic contacts, both on the Prox1-positive cells in the inner molecular layer and in the outer molecular layer. CB1R-positive boutons were generally smaller compared to parvalbumin-positive boutons, and also established symmetric synapses (**Figure II.17**). If present, only one small mitochondria was observed. Their characteristics corresponded well with the CCK boutons but the labelling of the boutons was better and allowed us for a better estimation of the input relevance.

4.2. SUPRAMAMMILLARY NUCLEI AFFERENTS ON SEMILUNAR GRANULE CELLS

An important afferent system to the dentate gyrus is the supramammilary-hippocampal pathway. Calretinin has been shown to be expressed by excitatory cells in the supramammillary nuclei (Nitsch and Leranth, 1993), and supramammilary-hippocampal projection is mainly made by these cells.

To assess whether semilunar granule cells could be a preferential target for fibers arising in the supramammilary nuclei, an immunostaining against calretinin was performed in the dentate

gyrus of rat brain sections (**Figure II.18**). We decided to use rats for this experiment since the intense labelling for mossy cell terminals in the inner molecular layer would have impeded the study of the supramammilary projection in the mouse using calretinin. In rats, in addition to a subpopulation of interneurons present in the hilar area and in the molecular layer of the dentate gyrus, there were also present boutons located mainly in the border between the granule cell layer and the inner molecular layer. As it has been previously confirmed that there is no staining of mossy cells with calretinin in the rat, we assumed that these boutons were either from local calretinin-positive interneurons, or that they came from the supramammilary nuclei. Therefore, it was necessary to analyze these boutons at the electron microscopy level, so that we could observe whether they established contacts and of which types they were.

Under the electron microscope, we found calretinin-positive boutons establishing perisomatic asymmetric contacts onto granule cells located in the border between the granule cell layer and the inner molecular layer, which had the characteristics of semilunar granule cells (**Figure II.18**).

The morphological features of calretinin-positive boutons synapsing semilunar granule cells were the same as previously described by Maglóczky et al. (1994). All boutons analyzed were relatively small *en passant* boutons that made asymmetrical synapses, filled with round vesicles and one to two mitochondria.

Studies using calretinin as a marker for supramammillary afferents have all been performed in the rat dentate gyrus, and no previous studies have reported the presence of calretinin in the boutons formed by supramammillary fibers in the mouse dentate gyrus. Another reliable marker for the supramammillary projection in the dentate gyrus is VGluT2 (Fremeau et al., 2001; Soussi et al., 2010). To check whether there are differences in calretinin expression in the supramammilary afferents between both species, we performed a double immunostaining for VGluT2 and calretinin in the mouse dentate gyrus. An *a visu* study showed that, in contrast to what happens with the rat, VGluT2-positive boutons did not generally colocalize with calretinin in the mouse granule cell layer or inner molecular layer (**Figure II.19**). This suggests that neither mossy cell boutons are VGluT2-positive, nor that supramammillary afferents are calretinin-positive in the mouse dentate gyrus.

To extend the study of the supramammillary innervation on semilunar granule cells to mice, we made a double immunostaining with VGluT2 and Prox1. Virtually all semilunar granule cells analyzed presented VGluT2-positive boutons in apposition (**Figure II.20**). Though the presence

of VGluT2-positive boutons was constant, in some cases only one bouton was observed whereas in other cases a basket-like arrangement of VGluT2-positive boutons were found on semilunar granule cells. Surprisingly, outer molecular layer ectopic granule cells also presented VGluT2-positive boutons in apposition to their cell somata. It was necessary to confirm that this boutons were establishing synaptic contacts on semilunar granule cells. Therefore, we proceeded to study this innervation at the ultrastructural level.

Under the electron microscope, VGluT2-positive boutons in apposition to semilunar granule cells established asymmetric synaptic contacts on them (**Figure II.21**). They were small and filled with round vesicles. In some occasions they found to establish synaptic contacts to more than one postsynaptic profile, as observed when we used calretinin for labelling the same boutons.

Finally, to further prove this innervation, mice were injected with the anterograde tracer BDA 10 KDa in the supramammilary nuclei. The injection site was checked in all the animals, and those which had a wrong injection site or such a big injection that could affect our analysis were immediately discarded.

In the dentate gyrus, anterograde-labeled fibers were located mainly in the innermost part of the molecular layer, with some fibers entering in the granule cell layer, as previously described by Maglóczky et al. (1994). Also some axons were found in the hilar region, with a similar morphology.

To check if the semilunar granule cells were innervated by supramammilary fibers, we made a double immunostaining for the anterograde labeled fibers (DAB-Ni) and Prox1 (DAB).

Some Prox1-positive cells in the inner molecular layer were surrounded by BDA-filled fibers. We also found some Prox1-positive cells in the outer molecular layer that were innervated by anterograde-labeled axon terminals in a basket-like arrangement. We could find axon collaterals emerging from the main axonal branch and traveling a considerable distance straight to the target Prox1-positive cell. This indicates a target-specific distribution of supramammilary fibers. We also found some Prox1-positive cells in the hilus innervated in the same way (**Figure II.22**)**.**

We checked some of the cells apparently contacted by the supramammillary fibers under electron microscopy to confirm that the fibers made synaptic contact and their ultrastructural features (**Figure II.23**).

The morphology of the analyzed boutons synapsing semilunar granule cells was similar to the ones observed with VGluT2 in mouse and calretinin in rat. They were *en passant* boutons, filled with round vesicles and one small mitochondria. Though the quality of the tissue was not generally good enough to clearly identify the postsynaptic density, we observed that not only asymmetric boutons but also symmetric could be found.

In conclusion, semilunar granule cells receive a strong, mainly excitatory perisomatic input from supramammillary fibers in a target dependent manner.

Figure II.12 – Parvalbumin interneurons form baskets around semilunar granule cells in the mouse dentate gyrus
Double immunostaining for parvalbumin (DAB-Ni) and Prox1 (DAB) shows that the majority of semilunar granule cells and ectopic outer molecular layer granule cells are innervated by parvalbumin-positive boutons.
A) Panoramic view of a dentate gyrus with parvalbumin and Prox1 staining. Parvalbumin-positive boutons are found in the whole thickness of the granule cell layer, but also some fibers can be seen in the inner molecular layer.
B) Example of two semilunar granule cells found in the border between the inner molecular layer and the granule cell layer. These cells receive putative contacts of parvalbumin boutons (arrows), shown more clearly in the cell on the left (asterisk). As Prox1 is a nuclear marker, the presence of boutons surrounding the Prox1 profile are an indicative of innervation, but electron microscopy is needed to confirm the presence of synaptic contacts.
C) Example of semilunar granule cell in the inner molecular layer, also showing parvalbumin-positive boutons (arrows) in apposition (asterisk), in a basket-like arrangement.
D) Ectopic outer molecular layer granule cell (asterisk), showing several parvalbumin-positive boutons (arrows) in a basket-like manner. The image is a Z-stack reconstruction of several focal planes, to better show the basket arrangement. Note the weak staining of the nucleus with Prox1. This staining could be used to distinguish the cell nuclei at the optical level, but generally a correlation optical-electron microscope was needed when studying this connection at the ultrastructural level.
E) Example of a Prox1-positive cell that did not show any parvalbumin-positive boutons in the perisomatic region (arrowhead). The black asterisk shows a profile, surrounded by parvalbumin boutons, that does not correspond to semilunar granule cells.
gcl, granule cell layer; h, hilus; iml, inner molecular layer; oml, outer molecular layer. Scale bars: A 200 µm; B-E, 10 µm.

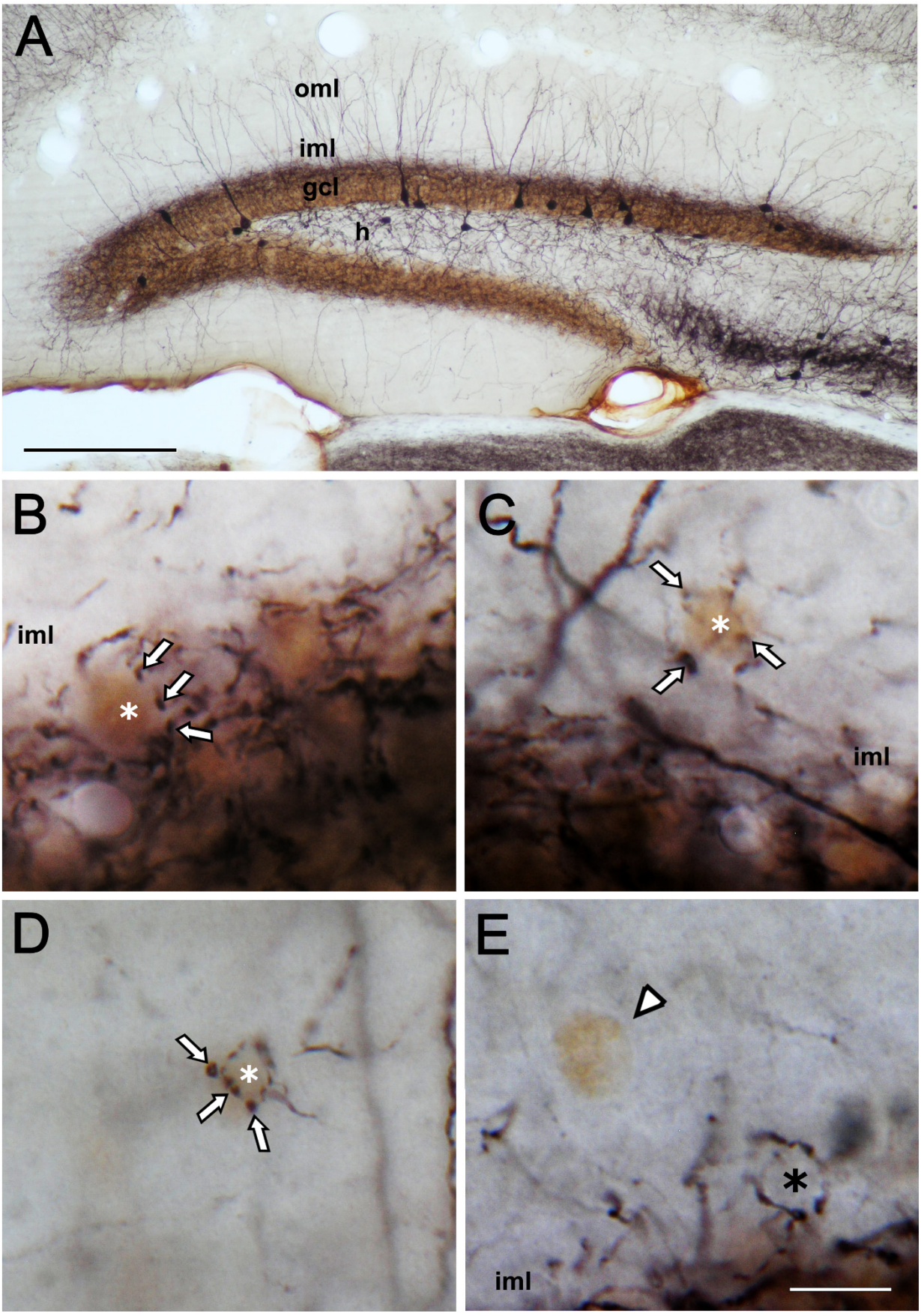
A
oml
iml
gcl
h
B
iml
C
iml
D
E
iml

Figure II.13 – Electron microscopy study showing that semilunar granule cells in the inner molecular layer are innervated by parvalbumin interneurons

In this case, to identify the postsynaptic cell under light microscopy, the nuclear marker c-Fos was used. In every case, the identity of the semilunar granule cell was confirmed by its ultrastructural features. Semilunar granule cells that were immunonegative presented similar connectivity.

A) Example of three semilunar granule cell profiles in the inner molecular layer of the mouse dentate gyrus. They were distinguished based on their morphology. Only cell **1** shows a high immunoreactivity for c-Fos.

B) Panoramic view of the cells shown in (**A**) at the electron microscopy level.

C) Parvalbumin-positive bouton in apposition to the cell **3**, establishing a symmetric contact (arrow). The bouton presents a high density of synaptic vesicles. The arrowhead shows a parvalbumin-negative bouton that, based on the shape and disposition of the synaptic vesicles and on the postsynaptic density, it is establishing an asymmetric synapse.

D) Example of a parvalbumin-positive bouton establishing a symmetric contact on the c-Fos positive semilunar granule cell **1** shown in (**A**).

E) Examples of symmetric synapsis (arrows) established by parvalbumin-positive boutons on the semilunar granule cell **3** shown in (**A**).

F) Example of a symmetric synapse by a parvalbumin-positive presynaptic bouton (arrow) in close vicinity with a parvalbumin negative bouton that is establishing an asymmetric synapse (arrowhead), both on the semilunar granule cell **3** shown in (**A**).

G) Example of a symmetric synapse (arrow) established by a parvalbumin-positive bouton on the semilunar granule cell **2** shown in (**A**).

Scale bars: A, 10 µm; B, 5 µm; C-G, 500 nm.

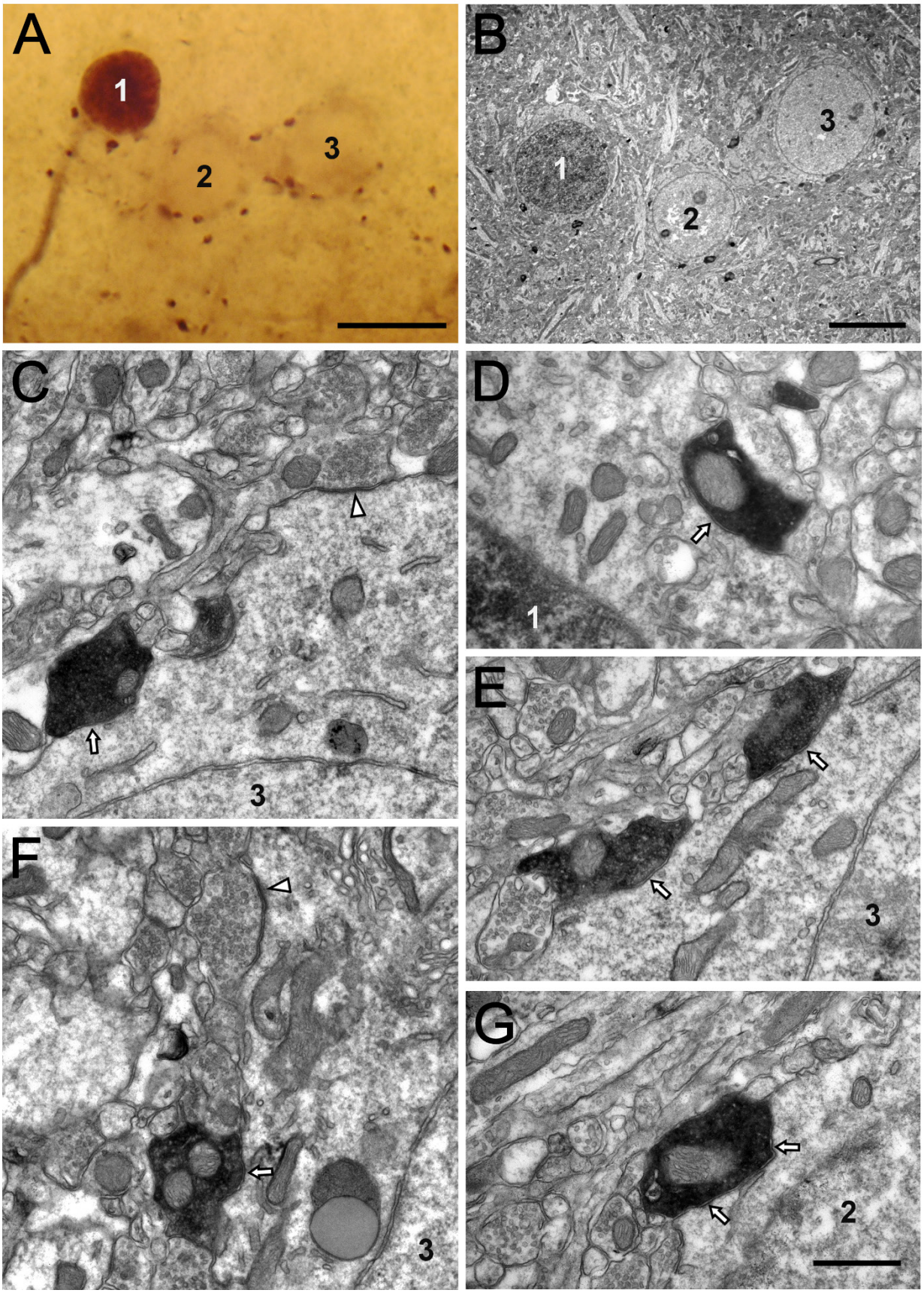
A
1
2
3
B
1
2
3
C
3
D
1
E
3
F
3
G
2

Figure II.14 – CCK boutons are found in apposition to semilunar granule cells and outer molecular layer ectopic granule cells in the rat dentate gyrus

Double immunostaining for CCK (DAB-Ni) and Prox1 (DAB) shows that semilunar granule cells and ectopic outer molecular layer granule cells are surrounded by CCK-positive boutons.

A) Panoramic view of a rat dentate gyrus with CCK staining. CCK-positive cells, corresponding to regular spiker basket interneurons, are found in the hilar border of the granule cell layer.

B and C) Example of a Prox1-positive (asterisk) cell in the outer molecular layer, shown at higher magnification in (**C**)**.** This ectopic granule cell is receiving two CCK-positive boutons on the soma (arrows), probably arising from the same fiber.

D-F) Example of semilunar granule cells (asterisks) sitting at two different depths of the inner molecular layer. In (**E**), two examples of semilunar granule cells (asterisk) sitting in the border with the granule cell layer, that present several CCK-positive boutons displayed in a basket-like arrangement (arrows). In (**F**), an example of a semilunar granule cell (asterisk) sitting in the border with the outer molecular layer also has three CCK-positive boutons in close apposition to the cell soma (arrows).

As Prox1 is a nuclear marker, a more in depth study in the electron microscopy is needed to confirm that this putative boutons establish synapses with semilunar granule cell somata.

gcl, granule cell layer; h, hilus; iml, inner molecular layer; oml, outer molecular layer. Scale bars: A 200 µm; B and D, 50 µm; C, E and F, 10 µm.

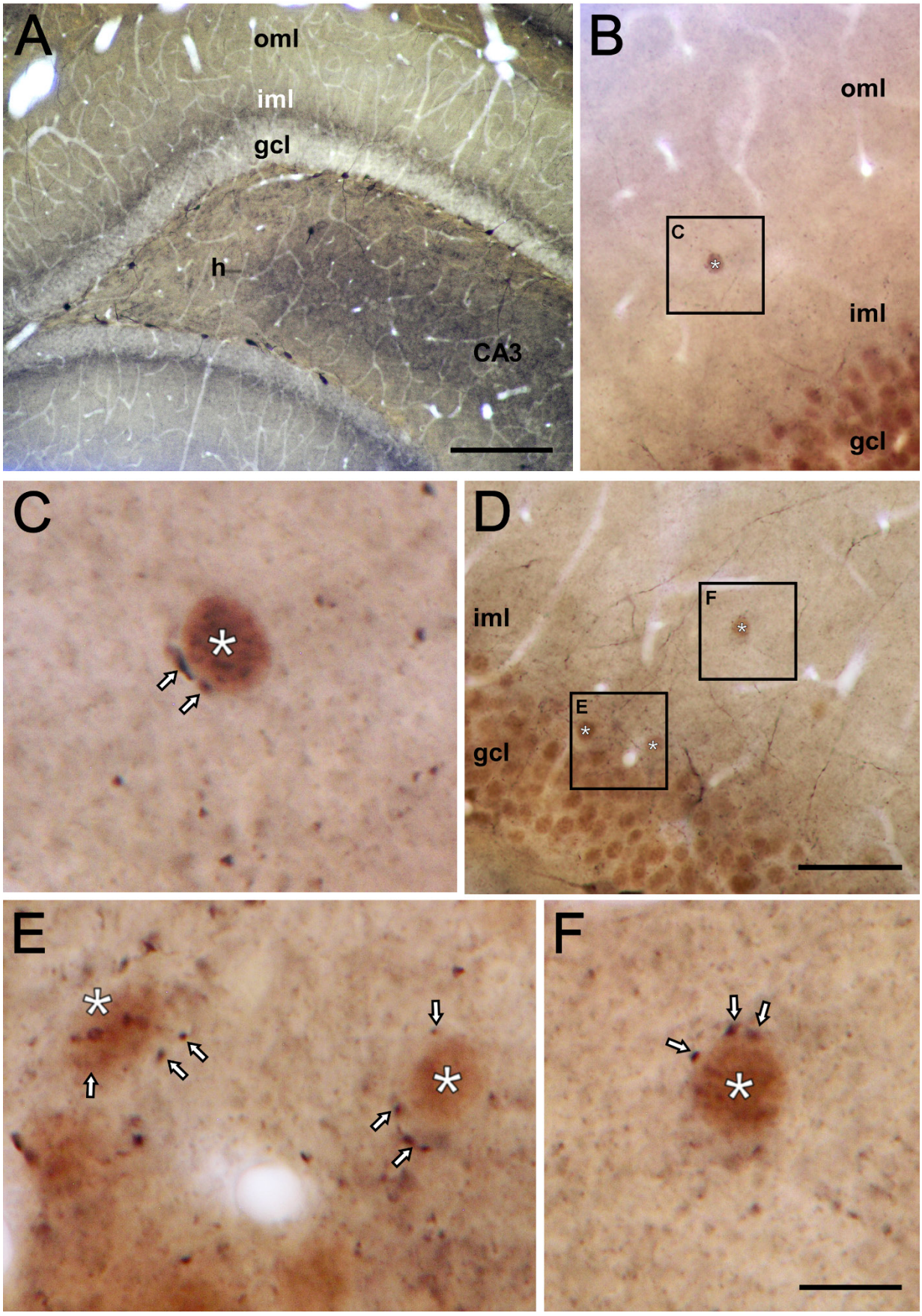
A
oml
iml
gcl
h
CA3
B
oml
C
iml
gcl
C
D
iml
F
E
gcl
E
F

Figure II.15 – Electron microscopy study showing that semilunar granule cells and outer molecular layer granule cells are perisomatically innervated by CCK interneurons

A) Optical-electron microscopy correlation of a Prox1-positive outer molecular layer granule cell innervated by CCK-positive boutons.

B and C) Synaptic boutons establishing symmetric synaptic contacts (black arrows) to the cell shown in (**A**). In (**C**), two additional synaptic boutons immunonegative for CCK are shown to establish a symmetric synaptic contact (white arrow) and an asymmetric contact (white arrowhead).

D) Panoramic view of a semilunar granule cell in the inner molecular layer.

E and F) CCK-positive synaptic boutons establishing symmetric synaptic contacts (black arrows) on the cell in (**D**).

Scale bar: A, D 2 µm; B-C, E-F, 500 nm.

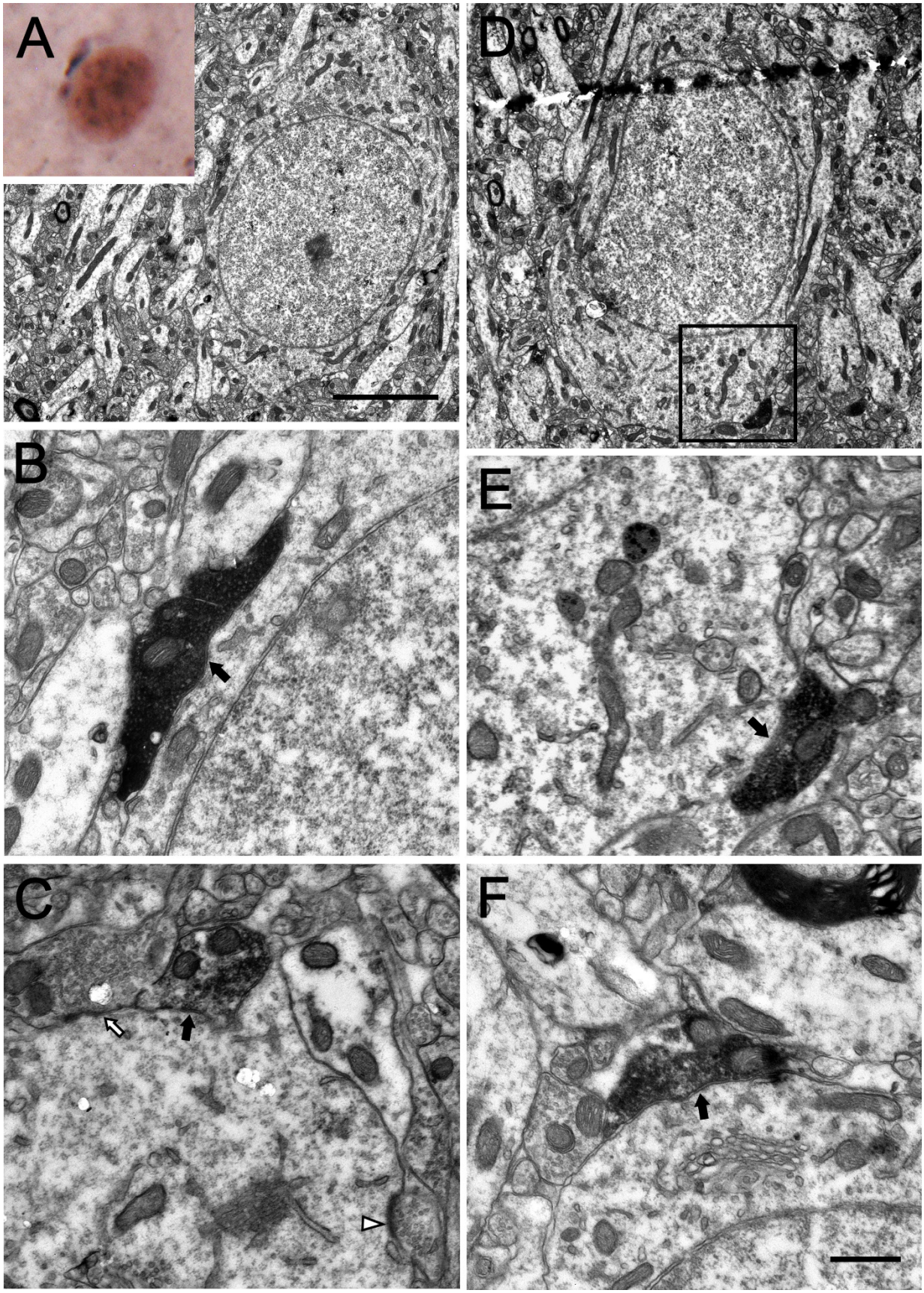
A
D
B
E
C
F

Figure II.16 – CB1R-positive boutons are found in close apposition to semilunar granule cells and outer molecular layer granule cells in the mouse dentate gyrus

Double immunostaining for CB1R (DAB-Ni) and Prox1 (DAB) shows that semilunar granule cells and ectopic outer molecular layer granule cells are innervated by boutons that contain the endocannabinoid receptor, corresponding to CCK interneurons.

A) Panoramic view of a dentate gyrus with CB1R and Prox1 staining. CB1R-positive fibers are found within the whole dentate gyrus. In the inner molecular layer the background staining of the tissue is higher.

B) Low magnification of an area in the dentate gyrus showing several examples of semilunar granule cells (black arrows) embedded in a dense plexus of CB1R fibers in the inner molecular layer.

C) Higher magnification of the box shown in (**B**)**.** This image shows two semilunar granule cells (cells **1** and **2**) sitting in the border between the inner molecular layer and the granule cell layer, that display CB1R-positive boutons in close apposition to the cell soma (arrows). Another semilunar granule cell (cell **3**) in the inner molecular layer is shown, also surrounded by CB1R-positive boutons (arrows).

D) Low magnification of an area in the dentate gyrus showing two examples of outer molecular layer ectopic granule cells surrounded by a dense plexus of CB1R fibers.

E) Higher magnification of the box shown in (**D**)**.** Outer molecular layer ectopic granule cells also present CB1R-positive boutons in apposition to their cell somata arranged in a basket-like manner (arrows).

All these cells seemed contacted by CB1R boutons. However, electron microscopy was needed to confirm these putative contacts.

gcl, granule cell layer; h, hilus; iml, inner molecular layer; oml, outer molecular layer. Scale bar: A, 200 µm; B and D, 50 µm; C and E, 20 µm.

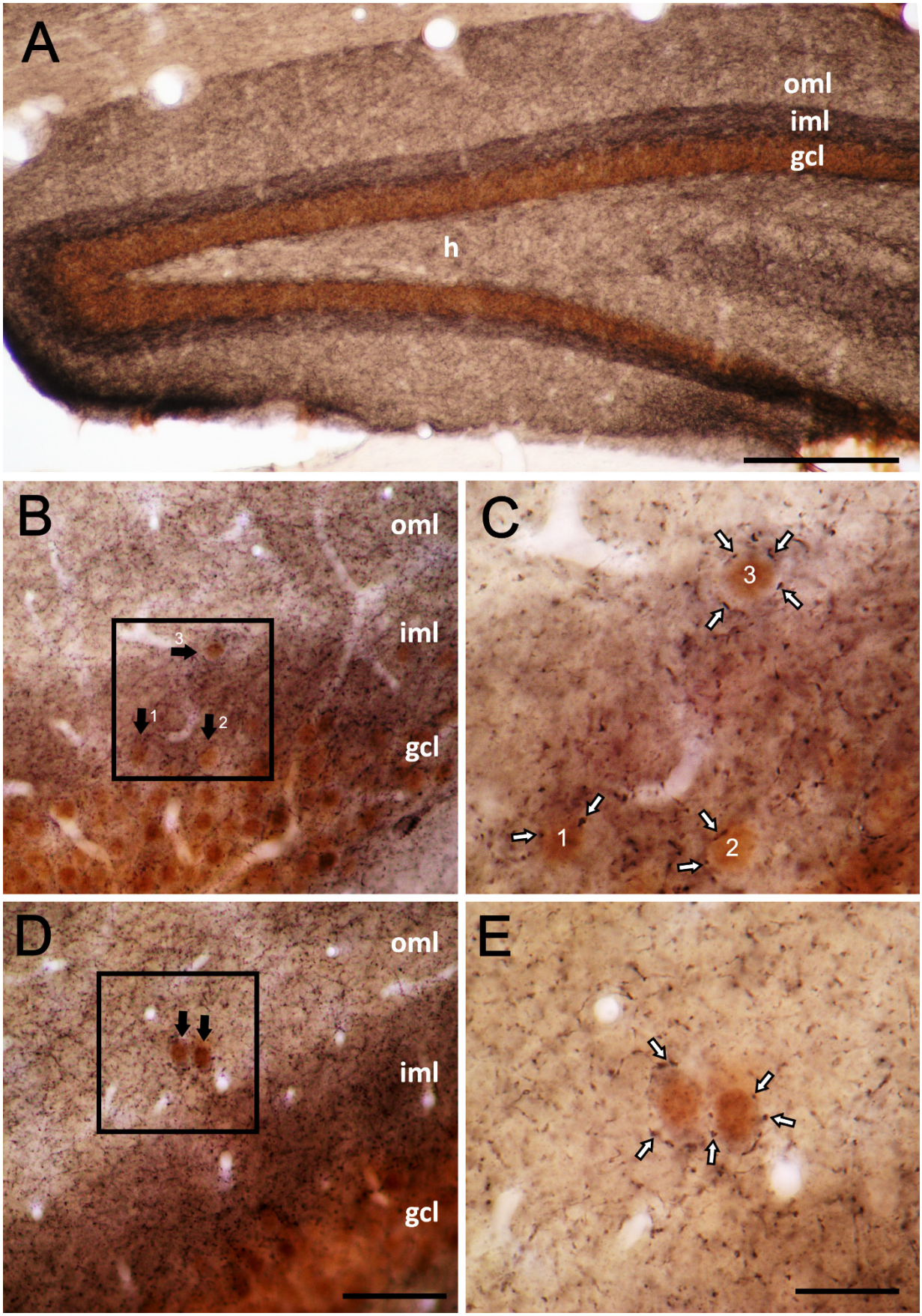
A
oml
iml
gcl
h
B
oml
iml
gcl
3
1
2
C
3
1
2
D
oml
iml
gcl
E

Figure II.17 – Semilunar granule cells in the inner molecular layer and ectopic granule cells in the outer molecular layer are innervated by CB1R positive boutons under electron microscopy.
Correlation between optical and electron microscopy from a double immunostaining of CB1R (DAB-Ni) and Prox1 (DAB). Under the electron microscope, Prox1-positive nuclei are only slightly more electrondense than the negative profiles. For this reason the correlation was necessary. The electron microscopy confirmed the granule nature of the Prox1 studied cells.
A) Optical-electron microscopy correlation of a semilunar granule cell in the inner molecular layer (asterisk). Two boutons are found in apposition to the cell body and one on the proximal dendrite of this cell.
B-D) Higher magnification of the perisomatic boutons found in consecutive sections from the cell in (**A**) (asterisk). DAB-Ni positive profiles, corresponding to CB1R-positive boutons, establish symmetric synaptic contacts (arrows) with the soma of the semilunar granule cell. Among the CB1R-positive boutons, we found both big (**C**) and small ones (**B** and **D**), in all cases filled with slightly oval vesicles. Other boutons, immunonegative for CB1R, making symmetric synaptic contacts (arrowhead) were found on the same cell, with characteristics that resembled parvalbumin boutons.
E) Optical-electron microscopy correlation of an ectopic granule cell (asterisk) in the outer molecular layer.
F-H) Higher magnification of the perisomatic boutons found in consecutive sections from the cell shown in (**E**)**.** CB1R-positive boutons established symmetric synaptic contacts (arrows) with the soma of the semilunar granule cell (asterisk). The morphology of CB1R-positive boutons contacting ectopic granule cells was the same as the ones found in apposition to semilunar granule cells.
Scale bars: A and E, 5 µm; C, 400 nm; B, D, F-H, 500 nm.

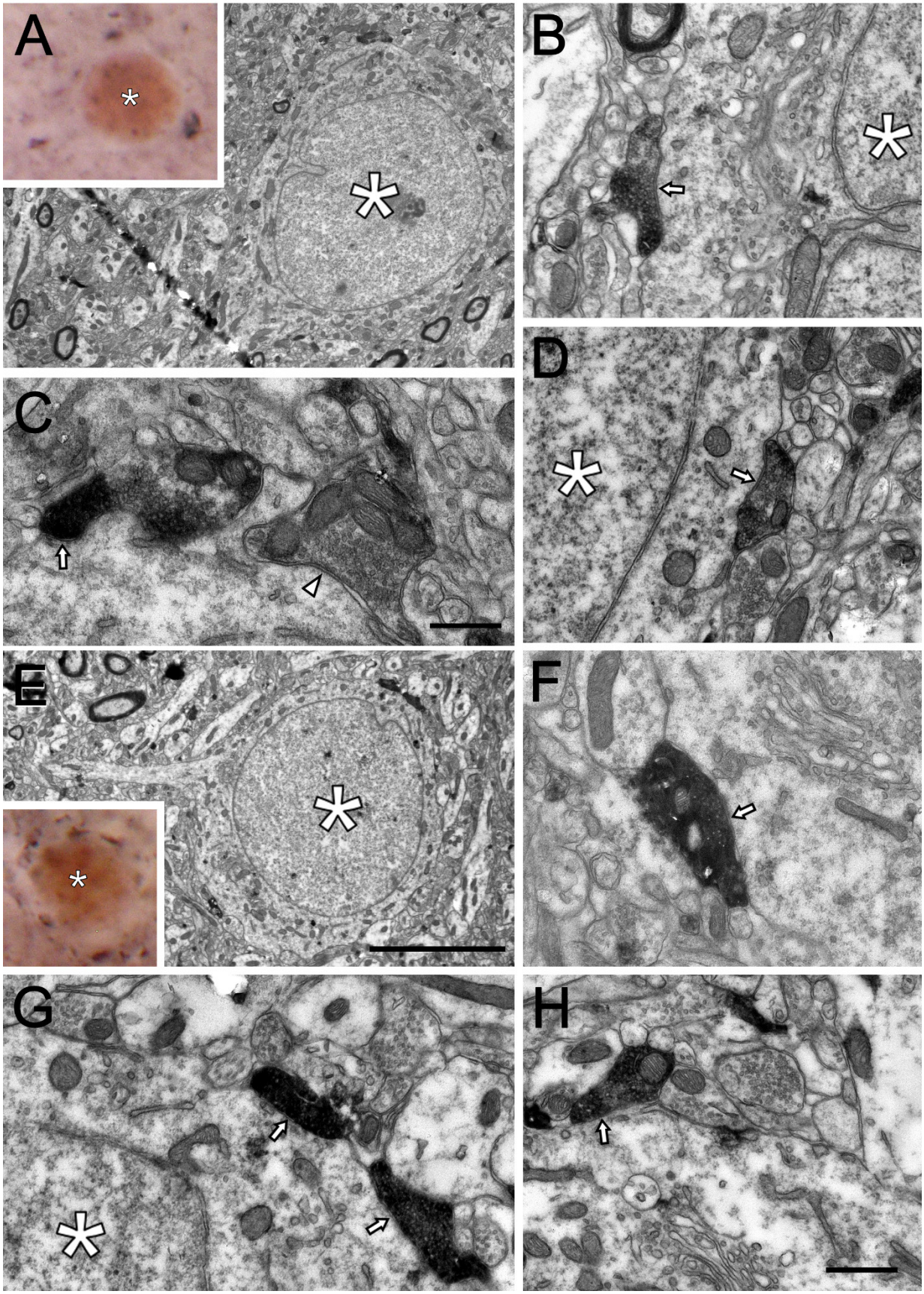
A
B
C
D
E
F
G
H

Figure II.18 – Calretinin positive fibers from supramammillary nuclei establish perisomatic excitatory contacts on semilunar granule cells in the rat dentate gyrus
Immunostaining for calretinin (DAB-Ni) in the rat dentate gyrus.
A) Panoramic view of a rat dentate gyrus with calretinin staining. The calretinin-positive boutons corresponded to the staining expected for supramammillary fibers.
B and C) Panoramic view of two semilunar granule cells (asterisks) in the inner molecular layer and in the border between the inner molecular layer and granule cell layer respectively. The cells were identified by their ultrastructural features (small cell somata with thin cytoplasm, semilunar like shape).
D) Higher magnification of the calretinin-positive synaptic bouton establishing an asymmetric synaptic contact (arrow) on the cell shown in (**B**). A clear postsynaptic cleft and postsynaptic density is observed in two non-consecutive sections of the same bouton. This bouton showed the morphological features expected for a supramammillary bouton.
E and F) Calretinin positive synaptic boutons establishing asymmetric synaptic contacts (arrows) on the cell shown in (**C**).
G and H) Additional examples found on semilunar granule cells of calretinin-positive boutons establishing asymmetric synaptic contacts (arrows).
Scale bars: A 100 µm; B and C, 2 µm; D-H, 500 nm.

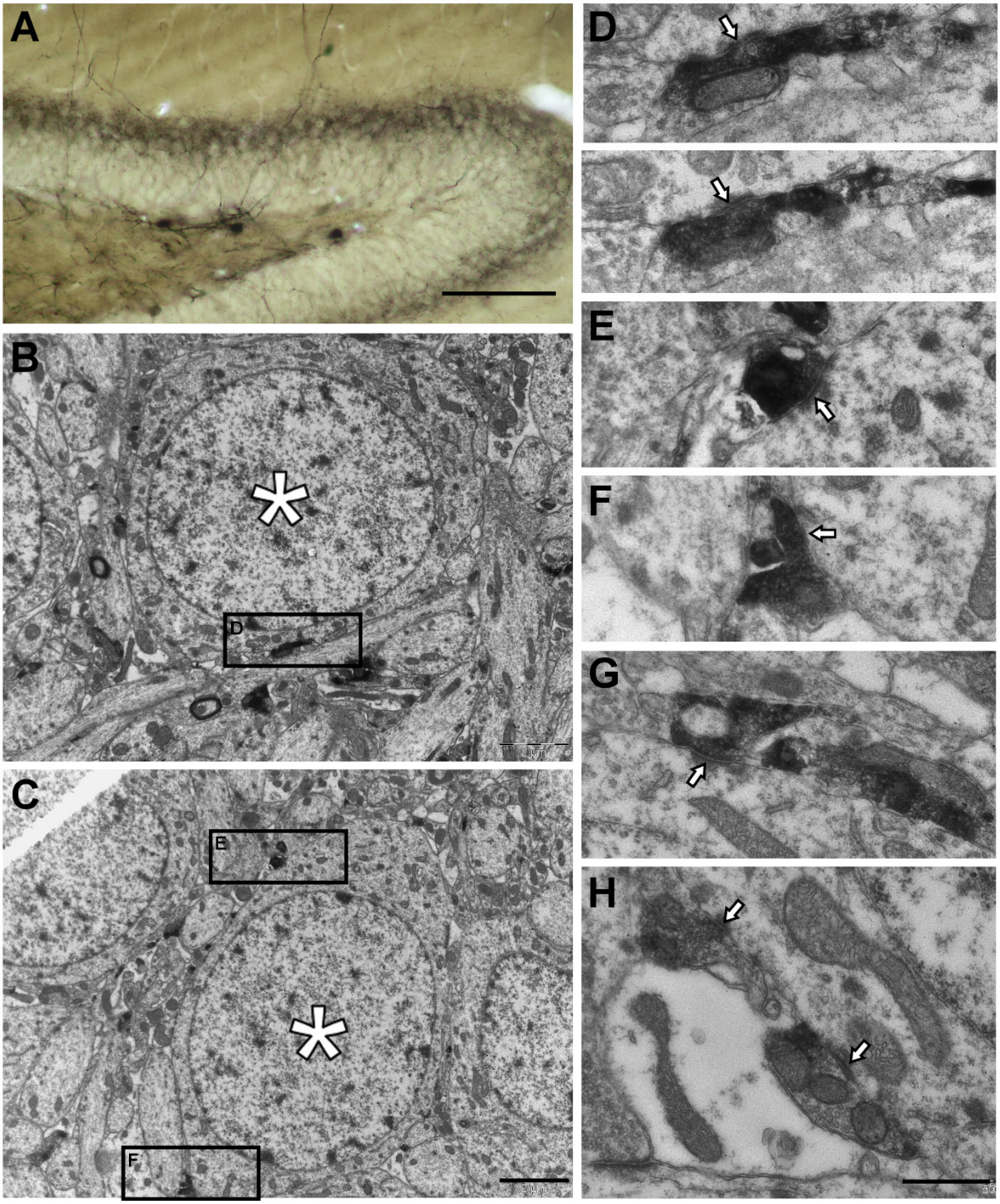
A
B
D
C
B
F
D
E
F
G
H

Figure II.19 – Different expression of calretinin by supramammillary fibers in rat and mouse
Double immunostaining showing VGluT2 (green) as a marker of supramammillary afferents to the dentate gyrus, and calretinin (red).
A) Calretinin staining in the rat shows a high density of boutons in the border of the granule cell layer with the inner molecular layer. VGluT2 staining shows the same pattern of innervation than calretinin, and both markers highly colocalize in this region. This confirms that in the rat, supramammillary afferents can be labeled reliably labeled both with VGluT2 and calretinin.
B) Calretinin staining in the mouse shows a high density of boutons in the inner molecular layer, but not in the granule cell layer. Calretinin-positive element have been previously shown to represent boutons from hilar mossy cells that highly innervate this area. VGluT2 staining shows the same pattern as in the rat, with a high density of positive boutons found in the upper half of the granule cell layer. In this case, however, there is no colocalization between calretinin-positive elements and VGluT2-positive elements, indicating that in our experimental conditions calretinin is not a marker for supramammillary afferents in the mouse.
gcl, granule cell layer; h, hilus; iml, inner molecular layer. Scale bar for all images: 50 µm.

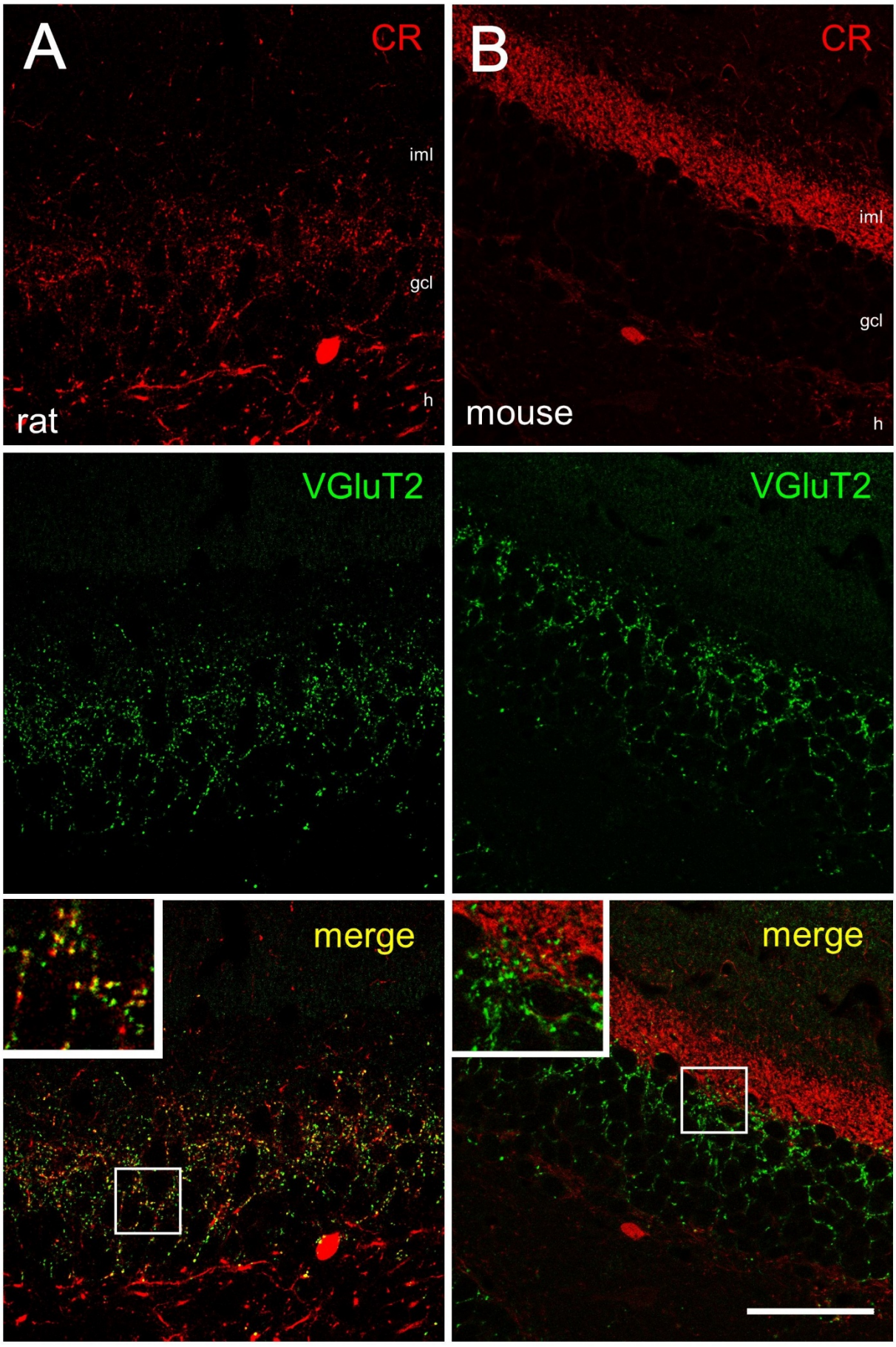
A
CR
iml
gcl
h
rat
B
CR
iml
gcl
h
mouse
VGluT2
VGluT2
merge
merge

Figure II.20 – VGluT2-positive boutons form baskets around semilunar granule cells and outer molecular layer ectopic granule cells in the mouse dentate gyrus

Double immunostaining for VGluT2 (DAB-Ni) and Prox1 (DAB) shows that semilunar granule cells and ectopic outer molecular layer granule cells are surrounded by boutons from the supramammillary nuclei.

A) Example of a semilunar granule cell in the border between the inner molecular layer and granule cell layer. The inset shows the cell of interest at higher magnification. It presents multiple VGluT2-positive boutons in apposition to its cell soma (arrowheads).

B) Example of a semilunar granule cell in the inner molecular layer which presents multiple VGluT2-positive boutons in apposition to the cell soma. The inset shows the cell of interest at higher magnification. Note that not all semilunar granule cells presented a similar amount of VGluT2-positive boutons in apposition, and a high variability was found. Next to the cell of interest in this panel, we find a semilunar granule cell (**1**) that is receiving no VGluT2-positive boutons, and also some cells with only one or two boutons (cells categorized as **2**).

C) Example of a semilunar granule cell in the border between the inner molecular layer and outer molecular layer. The inset shows the cell of interest at higher magnification, with multiple VGluT2-positive boutons in apposition to the cell soma (arrowheads). This cell was located in the dentate apex, where the amount of VGluT2 boutons seemed to be apparently higher, as well as the presence of semilunar granule cells.

D) Example of an outer molecular layer ectopic granule cell. The inset shows the cell of interest at higher magnification. Here, a VGluT2-positive fiber is clearly distinguish, and several VGluT2-positive boutons are found in apposition to the soma (arrowheads) in a basket-like arrangement. This suggests that the innervation from supramammillary afferents is not only lamina dependent but also shows a target dependence, as we only found rarely VGluT2-positive boutons in the outer molecular layer.

gcl, granule cell layer; iml, inner molecular layer; oml, outer molecular layer. Scale bar for all images: 25 µm.

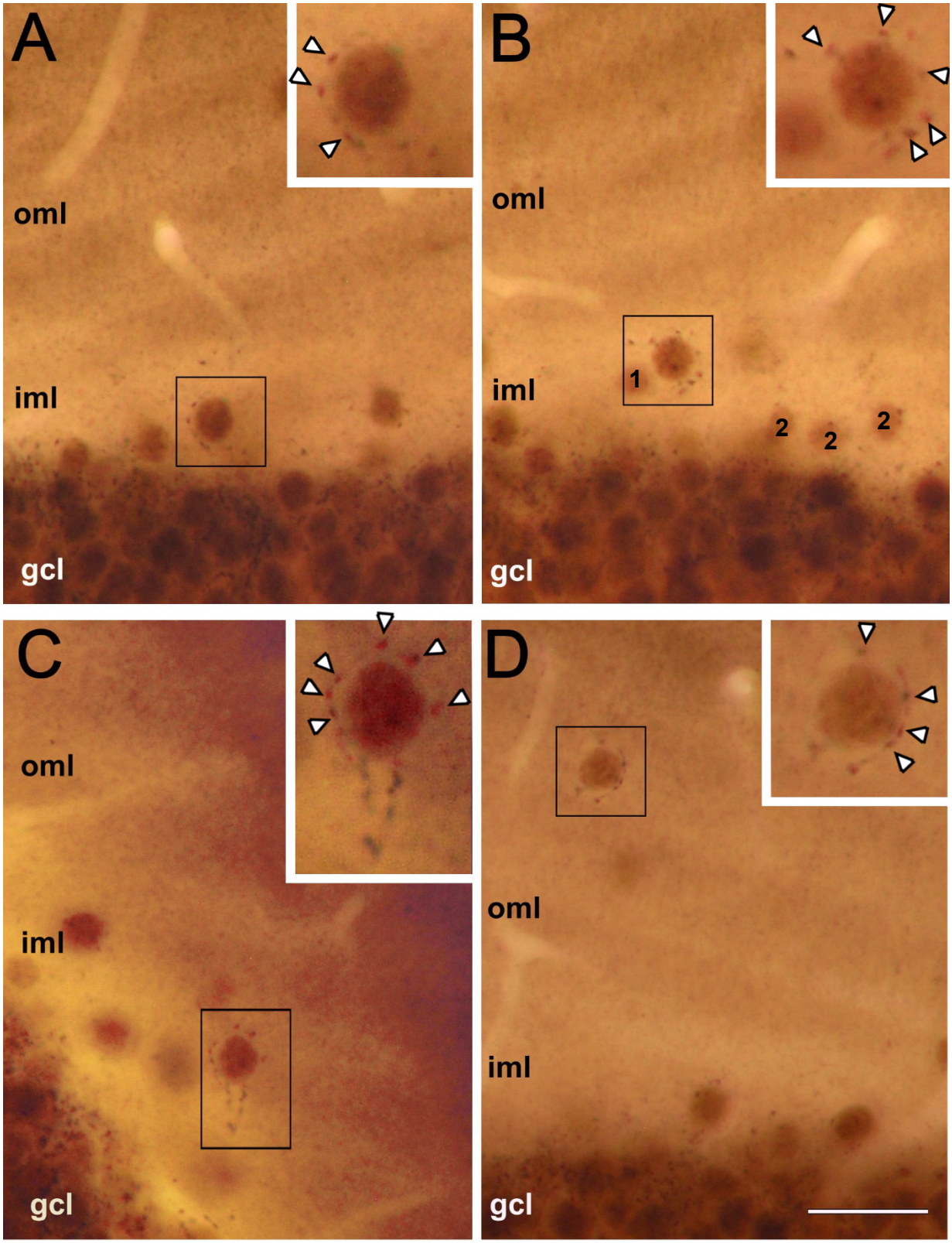
A
oml
iml
gcl
B
oml
iml
1
2
2
2
gcl
C
oml
iml
gcl
D
oml
iml
gcl

Figure II.21 – VGluT2-positive boutons establish synaptic contacts with the perisomatic region of semilunar granule cells in the mouse dentate gyrus

Double immunostaining for VGluT2 (DAB-Ni) and Prox1 (DAB), as shown in **Figure II.20.** The cells studied were chosen by its Prox1 positivity when resectioned for electron microscopy, and were confirmed as semilunar granule cells by its granular morphology.

A) Electron microscopy panoramic view of a semilunar granule cell in the inner molecular layer (sgc), in the border with the granule cell layer as shown by the presence of two typical granule cells (gc). In the boxed area, two VGluT2-positive boutons (arrowheads) are found in apposition to the proximal dendrite of the semilunar granule cell.

B-C) Higher magnification of the boutons in apposition to the proximal dendrite (d) shown in (**A**). These boutons establish asymmetric synaptic contacts (arrows).

D-G) Examples of VGluT2-positive boutons from the cell shown in (**A**) and other semilunar granule cells in the same area. VGluT2-positive boutons were generally small, and established asymmetric synaptic contacts with the perisomatic region of semilunar granule cells (arrows). They were sometimes observed to establish synaptic contacts to more than one postsynaptic target, as also shown in (**E,** black arrow).

d, dendrite; gc, granule cell; n, nucleus; sgc, semilunar granule cell. Scale bars: A, 5 µm; B-G, 500 nm.

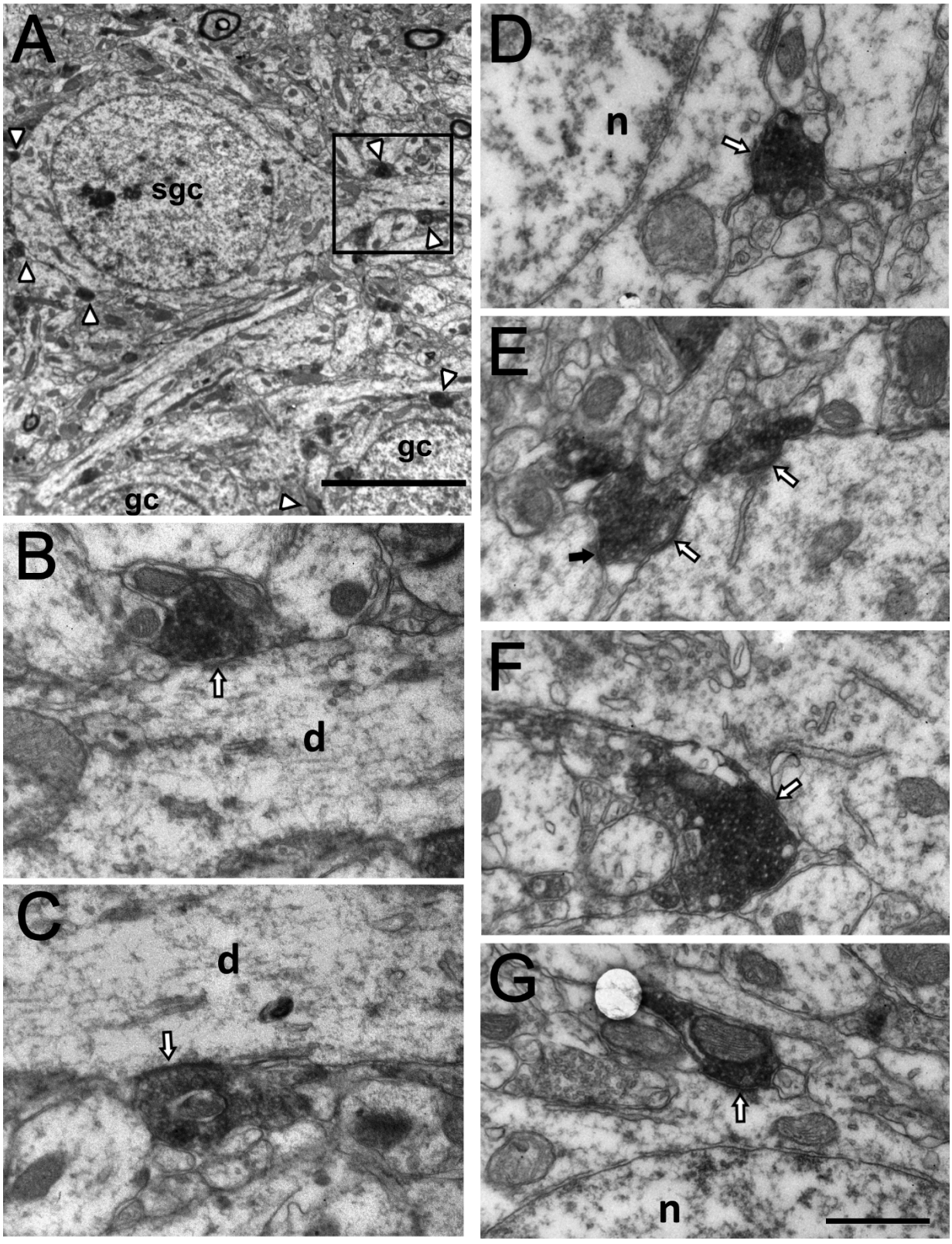
A
sgc
gc
gc
B
d
C
d
D
n
E
F
G
n

Figure II.22 – Fibers arising from the supramammillary nuclei establish putative baskets with semilunar granule cells in the inner molecular layer and with ectopic granule cells in the outer molecular layer

A) The anterograde tracer BDA-10 KDa was injected in the medial supramammilary nucleus at bregma -2.80 mm. **B)** Panoramic view of one of the injection sites that targeted the supramammillary nuclei. Big injections, centered in the supramammillary nuclei, were needed to have enough labeled fibers in the dentate gyrus.

C-D) Innervation pattern of the fibers arising from the supramammillary nuclei. BDA-positive fibers are shown in DAB-Ni. Sections were stained with toluidine blue to better delimit the injection site and fiber distribution. A high density of fibers were found in the border between the granule cell layer and inner molecular layer, in both supra- and infrapyramidal granule cell layer (**C**). Almost no fibers were found in the hilus, and only some fibers appeared in the outer molecular layer. As previously described, the CA2 region of the hippocampus presented also a high density of labeled fibers (**D**).

E-H) Double immunostaining for BDA-positive fibers (DAB-Ni) and Prox1 (DAB). BDA-positive boutons were frequently found in close apposition to Prox1-positive cells (arrows), in the inner molecular layer of dorsal (**E**) and ventral (**F**) dentate gyrus, in the border between the granule cell layer and inner molecular layer (**G**), and in the outer molecular layer (**H**). Insets show the cells marked with arrows at higher magnification. Usually two or more boutons were found surrounding the cell body of the semilunar granule cells. However, as Prox1 is a nuclear marker, the presence of synapses had to be further studied at the electron microscopy level. Note in (**H**) that the BDA-positive fiber, that establish a basket arrangement of boutons around the outer molecular layer ectopic granule cell, travels from the inner molecular layer straight to its target. This suggests a target specific innervation of granule cells by these fibers, rather than a layer specific innervation. (**E-G**) are focal planes, while (**H**) is a reconstruction of three focal planes to be able to properly show the basket distribution of boutons on this cell.

DG, dentate gyrus; gcl, granule cell layer; iml, inner molecular layer; oml, outer molecular layer. Scale bars: B, 1 mm; C-D, 400 μm; E-H, 40 μm.

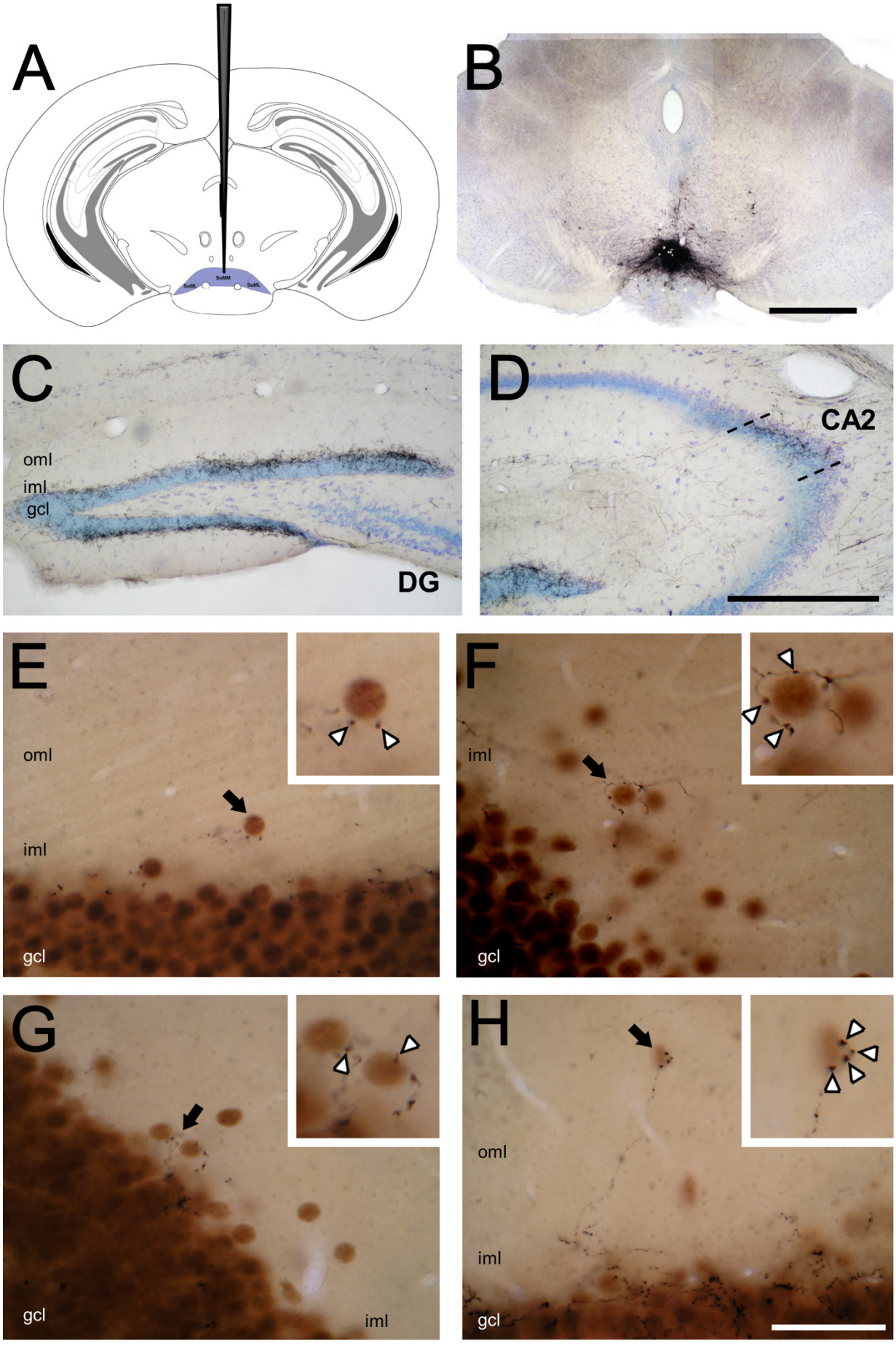
A
B
C
oml
iml
gcl
DG
D
CA2
E
oml
iml
gcl
F
iml
gcl
G
gcl
iml
H
oml
iml
gcl

Figure II.23 – Anterogradely labeled fibers from supramammillary nucleus establish perisomatic contacts on semilunar granule cells and outer molecular layer ectopic granule cells in the mouse dentate gyrus
Double immunostaining for anterogradely labeled fibers from the supramammillary nucleus (DAB-Ni) and Prox1 (DAB), as shown in figure II.22.
A) Electron microscopy panoramic view of the yuxtagranular inner molecular layer. In the boxed area, a BDA-positive bouton is found in apposition to two different granule cells and one semilunar granule cell (asterisk).
B) Higher magnification of the bouton shown in (**A**). This bouton presents the morphological characteristics expected for a supramammillary bouton: it is filled with slightly flat vesicles and a small mitochondria, and establishes synaptic contacts with multiple granule cell layer somata (arrows), either in this section or in consecutive ones.
C) Example of a BDA-positive bouton in the border between the inner molecular layer and granule cell layer, establishing an apparently symmetric synaptic contact with a granule cell soma (arrow) and an asymmetric synaptic contact with a dendrite (arrowhead). However, the quality of the postsynaptic density staining does not allow for an accurate description for the excitatory or inhibitory nature of the bouton.
D) BDA-positive bouton in the yuxtagranular inner molecular layer, establishing a synaptic contact with the soma of a granule cell layer (arrow). Interestingly, this bouton is embracing a somatic spine.
E) Optical-electron microscopy correlation of the outer molecular layer ectopic granule cell shown in **Figure II.22**. Adjacent to it, the cell body of a satellite glial cell (asterisk). The neuron is surrounded by BDA-positive boutons.
F-H) Higher magnification of BDA-positive boutons located in apposition to the cell soma of the outer molecular layer ectopic granule cell shown in (**E**)**.** They establish synaptic contacts (arrows) with the postsynaptic granule cell. In (**H**), the synaptic bouton is also establishing a synaptic excitatory contact (arrowhead) with a spine profile.
Scale bars: A and E, 5 µm; B-D, F-G, 500 nm.

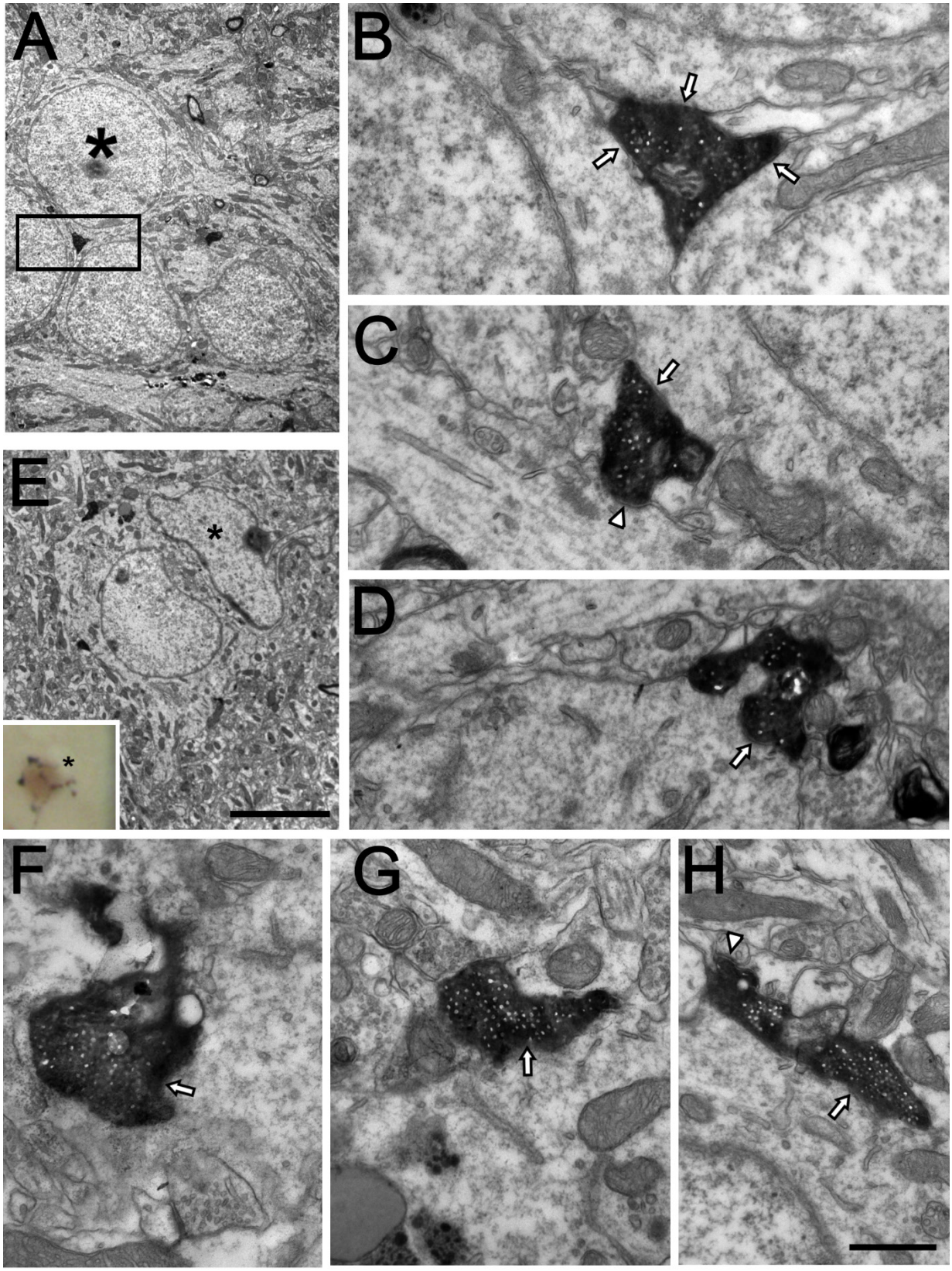
A
B
C
D
E
F
G
H

RESULTS III:
ROLE OF SEMILUNAR GRANULE CELLS AND PARVALBUMIN INTERNEURONS IN ANIMAL MODELS OF EPILEPSY

The dentate gyrus is arguably the most common focus of seizures in temporal lobe epilepsy (Dudek and Sutula, 2007). Therefore it has been extensively studied regarding this epileptic activity and several hypothesis have been postulated about the role of their different cell populations in the generation of epileptic activity, like the "Dormant basket cell" or the "Irritable mossy cells" hypotheses (Sloviter, 1992; Bernard et al., 1998; Santhakumar et al., 2000, 2005; Ratzliff et al., 2002, 2004; Sloviter et al., 2003; Zhang and Buckmaster, 2009; Jinde et al., 2012, 2013). Since parvalbumin basket cells, mossy cells and semilunar granule cells seem to be in a key position to control the activity of the dentate gyrus, we decided to study how they are affected in different models of epilepsy.

For this task we used previous material generated in our laboratory, and generated new animals using a softer induction by chemical kindling using pentylenetetrazole. We studied the survival of these cells as well as their possible activation during the process.

1. PENTYLENETETRAZOLE-INDUCED KINDLING MODEL OF EPILEPSY

Experimental animals were considered kindled when they reached stage 5 in Racine scale for four consecutive pentylenetetrazole injections at an initially subconvulsive dose. However, the nature of the seizures observed corresponded better to the stage 6 of an adaptation for pentylenetetrazole-induced seizures of the Racine scale, consisting of tonic-clonic convulsions while lying on the side (Racine, 1972; Lüttjohann et al., 2009).

The subconvulsive dose of pentylenetetrazole used, 40 mg/Kg, caused the first stage 4-5 seizure after an average of 7 ± 2 injections. Only in one case this dose initially caused a stage 4-5 seizure, and this animal was discarded and not further processed.

1.1. CHANGES IN CELL POPULATIONS AFTER KINDLING INDUCTION WITH PENTYLENETETRAZOLE

1.1.1. PROX1 AND TIMM STAINING

Prox1 immunostaining was performed to check if the amount of semilunar granule cells and ectopic granule cells had changed with the treatment. However, for technical reasons, the quality of the staining did not allow for a reliable quantification of the total number of Prox1-positive cells, due to unspecific glia staining generally in the dorsal dentate gyrus.

Although no quantification was made, it was evident that the semilunar granule cell population was not especially affected by the pentylenetetrazole-induced kindling procedure. The Prox1-positive cells in the inner molecular layer and in the outer molecular layer remained after kindling. In both experimental cases and their controls, the amount of Prox1-positive nuclei seemed similar.

In order to detect sprouting from the mossy fibers in the inner molecular layer and granule cell layer after pentylenetetrazole, Timm staining was performed in 3 treated and 1 control animal one month after being fully kindled. This long time was necessary since mossy fiber sprouting needs time to develop and be detected. No mossy fiber sprouting was observed in the inner molecular layer from treated animals, and no differences were observed with the control one, which in turn displayed the Timm-staining pattern previously observed in animals in which no experimental procedure was performed.

1.1.2. CALRETININ

Since hilar mossy cells are the most sensitive cell type in murine models of epilepsy, an estimation of the number of calretinin-positive mossy cells was performed in the hilar region of kindled animals, to check whether we could see cell death in this model of epilepsy.

We analyzed the number of mossy cells in the dorsal dentate gyrus (around bregma -2.6 mm). The expression of calretinin is less abundant in more dorsal levels (Blasco-Ibáñez and Freund, 1997), and changes are more easily detected at these levels that have shown to be specially sensitive to hilar cell death in other models (Nadler et al., 1980; Cavazos and Sutula, 1990; Cavazos et al., 1991; Longo et al., 2003). Calretinin-positive interneurons in the hilus, and immature granule cells were not taken into account, since they could be differentiated from mossy cells easily due to their morphology.

We found no statistical difference in the density of mossy cells between control (666.92 ± 93.55 calretinin cells/mm^2, n=5) and fully kindled animals (653.99 ± 63.02 calretinin cells/mm^2, n=8; p=0.907). However, we found a statistically significant decrease in the density of mossy cells one month after kindling, between control (665.24 ± 66.93 calretinin cells/mm^2, n=6) and fully kindled animals (488.22 ± 30.29 calretinin cells/mm^2, n=5; p=0.031). These data is summarized in **Graph III.1**.

These results suggest that there is a progressive loss of mossy cells in the dorsal hilus of fully kindled animals. This fact was confirmed by the presence of refractive shrunken cells in the hilus under bright illumination. By the time the animal was recently kindled, this loss had not begun, or was too low to be detected. Therefore, it seems to be a slow phenomenon that needs time to be observed.

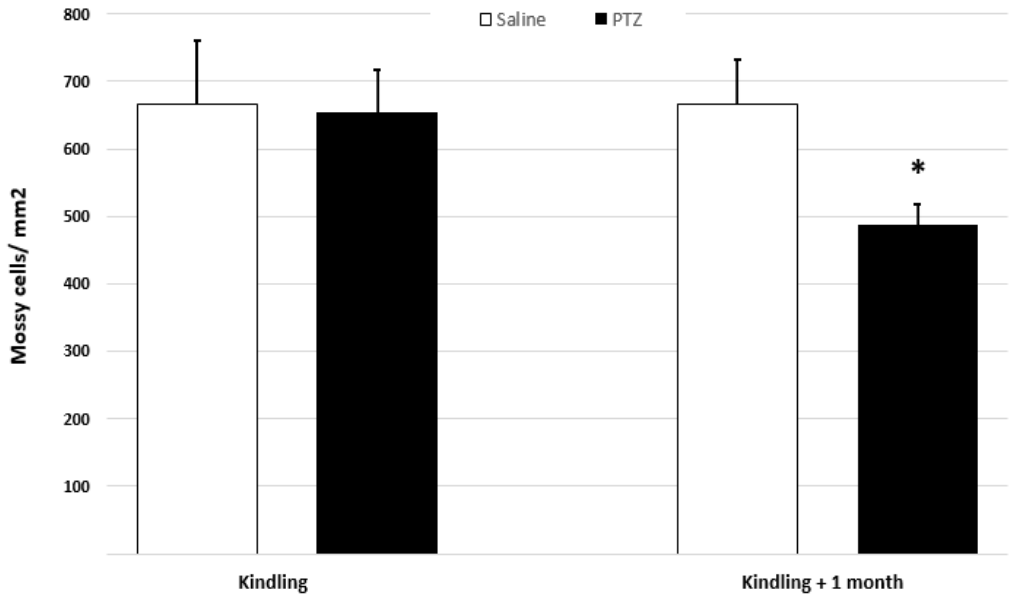

Graph III.1 - Density of mossy cells in dorsal dentate gyrus after kindling and one month after kindling. The density of mossy cells is not changed when the kindled status is reached, but there is a statistically significant decrease in the mossy cell density one month after kindling. * indicates statistically significant ($p < 0.05$) differences between groups after t-student test.

1.1.3. PARVALBUMIN

The total number of parvalbumin interneurons was counted in the whole dentate gyrus, from the most rostral to the most caudal section (including those sitting in the hilus), as no differences in their intensity expression have been reported.

After the kindled status had been reached, we found no statistical difference between the control group (1318 ± 109 parvalbumin cells, n=5) and pentylenetetrazole treated animals (1342 ± 60 parvalbumin cells, n=12; p=0.839). Unexpectedly, we observed a statistically significant increase in the number of parvalbumin-positive interneurons one month after the animals were fully kindled (1620 ± 67 parvalbumin cells, n=6) in comparison to control animals (1413 ± 21 parvalbumin cells, n=6; p=0.025). These data is summarized in **Graph III.2.**

These data show an apparent increase in the expression of parvalbumin one month after the treatment. This increment is unlikely to come from generation of new cells and could be attributed to an increase of parvalbumin immunoreactivity or of the number of fast-spiking basket cells that express it.

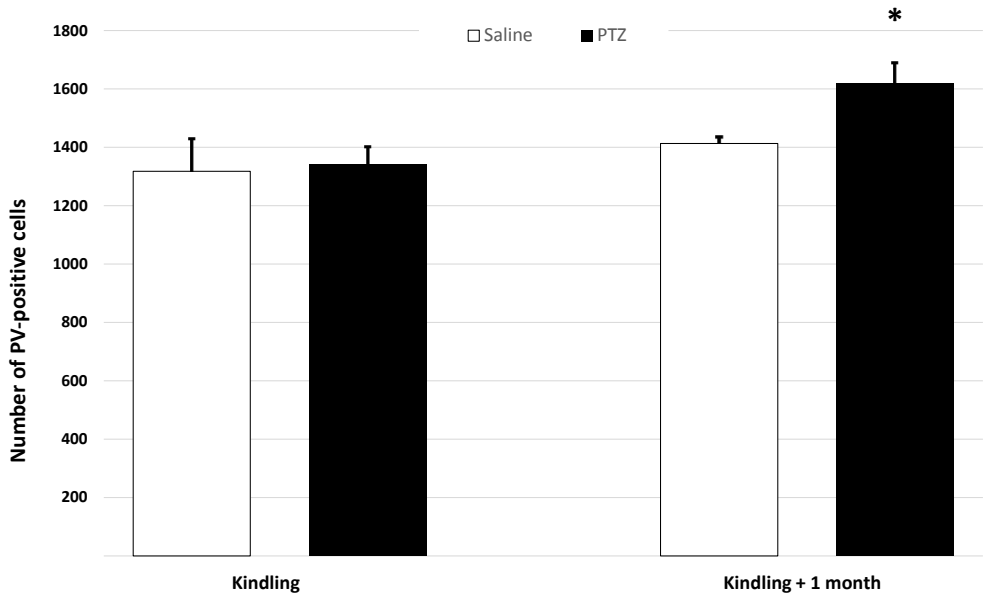

Graph III.2 - Changes in the total number of parvalbumin interneurons after kindling and one month after kindling. The total number of parvalbumin (PV) interneurons does not change when the kindled status is reached, but there is a statistically significant increase one month after kindling. * indicates statistically significant ($p < 0.05$) differences between groups after t-student test.

1.1.4. SOMATOSTATIN

Although it is not directly related to the circuitry that we are analyzing in this work, somatostatin-positive cell loss in the hilus has been reported in several models of epilepsy (Sloviter, 1987; Houser and Esclapez, 1996; Sun et al., 2007; Zhang et al., 2009), but not in all of them (Cardoso et al., 2010). To assess whether there is a change in the hilar somatostatin-positive interneuron population in the pentylenetetrazole-induced kindling model of epilepsy, we decided to count the total number of somatostatin-positive interneurons in the whole dentate gyrus, also taking into account from the most rostral to the most caudal section.

We found no statistical difference after the kindling status between the control group (2078 ± 167 somatostatin cells, n=6) and pentylenetetrazole treated animals (2044 ± 160 somatostatin cells, n=13; p=0.849), neither one month after kindling between the control (2094 ± 193 somatostatin cells, n=5) and pentylenetetrazole treated animals (1935 ± 96 somatostatin cells, n=6; p=0.456). These data is summarized in **Graph III.3.**

Therefore, under this experimental paradigm, somatostatin-positive interneurons are not affected in the pentylenetetrazole kindling model of epilepsy.

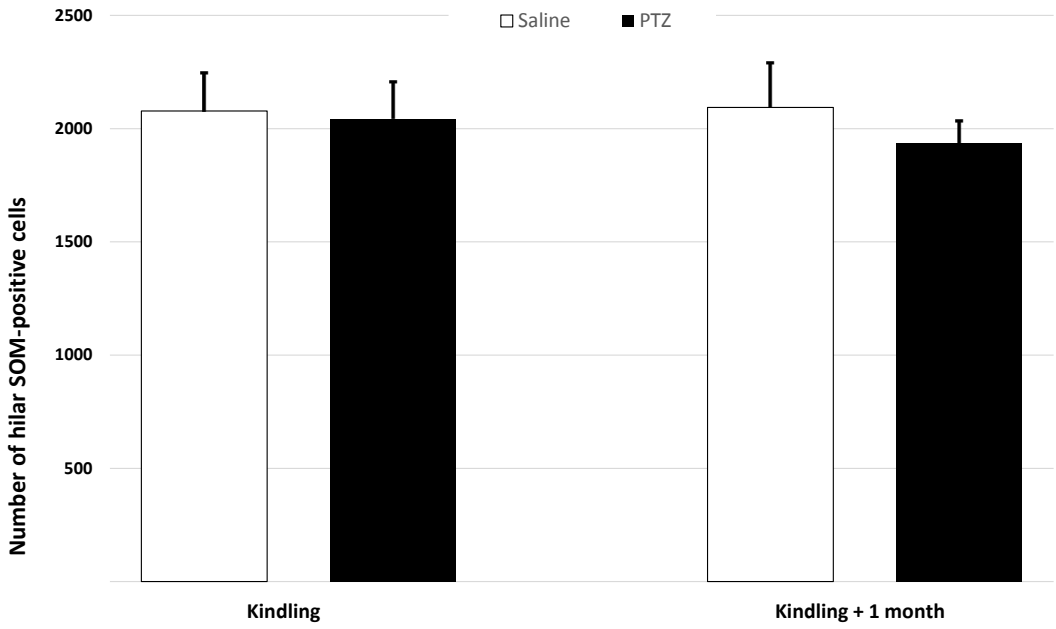

Graph III-3 - The total number of hilar somatostatin interneurons is kept constant after kindling and one month after kindling. There is no statistical difference between pentylenetetrazole-treated and control groups either when the kindled status is reached or one month after kindling.

In summary, by the time that the animal is kindled we could find no changes in the cell populations studied. However, after the animal is kindled there is a progressive loss of the number of mossy cells at dorsal levels, likely due to cell death. Simultaneously, there is an increase in the number of parvalbumin basket cells that probably represents an increment in the expression of this marker rather than a real increment in the number of cells.

1.2. EXPRESSION OF C-FOS AFTER MILD EXCITATION WITH PENTYLENETETRAZOLE

The previous data show that in this model the cell changes are subtle, although they seem to begin by the weakest link in the chain that is the mossy cells. The nature of the study did not allow us to infer if the semilunar granule cells had any impact on it.

We decided to check the activation of the dentate gyrus at short times after the administration of a unique dose of pentylenetetrazole at the subconvulsive dose used for kindling. The animals were injected one single injection of 40 mg/Kg and sacrificed at 2h, 4h and 8h respectively. 2 hours after pentylenetetrazole injection, the whole brain showed an overall increment of c-Fos expression. In the dentate gyrus this increment included numerous nuclei in the molecular layer and in the juxtamolecular granule cell layer (**Figure III.1 B**). The activation of the dentate gyrus increased at 4 hours. The juxtamolecular half of the granule cell layer presented a high proportion of c-Fos nuclei, but most of the granule cell layer remained immunonegative with the exception of granule cells in the hilar border (**Figure III.1 C**). Finally, at 8 hours, c-Fos expression had almost reached the basal level again. In the dentate gyrus, the number of immunoreactive nuclei was clearly inferior to controls, though some regions like the CA3 seemed slightly more active than controls (**Figure III.1 D**).

Therefore, the subconvulsive dose used in this experiment was enough to produce an overall overexcitation in the treated animals that also affected the dentate gyrus. In this structure the overexcitation acted mainly on granule cells in the juxtamolecular granule cell layer. These results show that under these conditions granule cells in the juxtamolecular granule cell layer are more sensitive to overexcitation than typical granule cells.

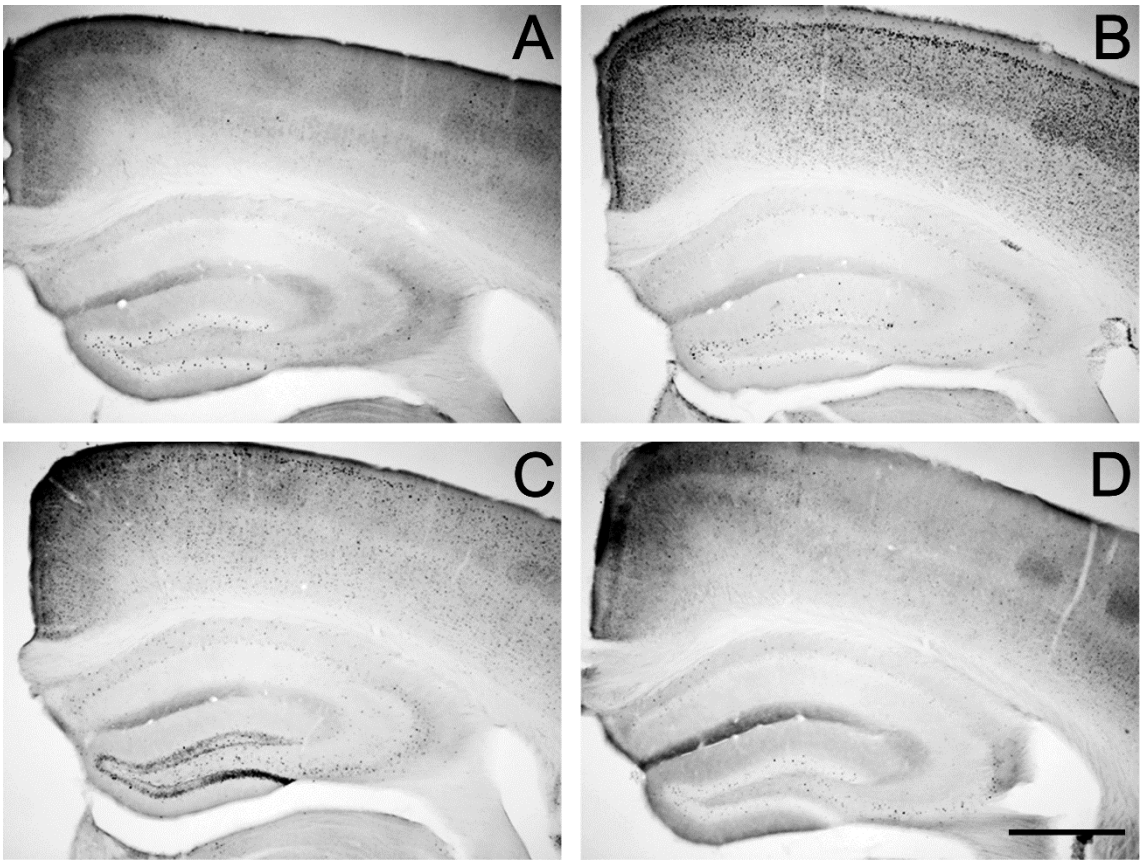

Figure III.1 - General increase in c-Fos expression after pentylenetetrazole administration at a subconvulsive dose.
A) Basal expression of c-Fos in the mouse hippocampus and cerebral cortex.
B) 2 hours after the injection of pentylenetetrazole, the cerebral cortex showed an overall increase in the number of c-Fos labeled nuclei, which implied high cell activation at short term due to the injection. In the dentate gyrus and hippocampus, the expression of c-Fos was increased.
C) 4 hours after the injection of pentylenetetrazole, c-Fos expression reaches its maximum in the dentate gyrus, with a high number of juxtamolecular granule cells and typical granule cells in the hilar border positive for this marker. The expression level in the cortex was still high compared to the control conditions, but the number of c-Fos positive nuclei was starting to decrease.
D) c-Fos expression returned to a lower level at 8 hours after the pentylenetetrazole injection, both in the cortex and in the dentate gyrus.
Scale bar 500 µm.

2. KAINIC ACID AND DEDTC-INDUCED MODEL OF EPILEPSY

2.1. FATE OF SEMILUNAR GRANULE CELLS IN THE KAININC ACID AND DEDTC MODEL OF EPILEPSY

In the model of kainic acid and DEDTC used previously in our laboratory we did not find loss of granule cells or parvalbumin basket cells, although there was a fast and almost complete loss of mossy cells (Domínguez et al., 2006). Briefly, the administration of kainic acid and DEDTC led to a fast activation of mossy cells, shown by their expression of the Heat shock protein HSP72 (**Figure III.2 A**), as a response to a situation of stress and injury after the seizure (Gass et al., 1995; Planas et al., 1997). This was followed by a loss of mossy cells, as seen with a decreased number of calretinin-positive cells in the hilus and reduced calretinin immunoreactivity in the inner molecular layer (**Figure III.2 B**).

A re-analysis of this material looking for loss of semilunar granule cells was performed, using the granule cell marker calbindin and the cell activation marker pan-Fos (**Figure III.2 C** and **D**)**.** We observed that there was no apparent loss of semilunar granule cells at the times studied (up to 14 days).

2.2. EXPRESSION OF C-FOS AFTER MILD EXCITATION WITH KAINIC ACID

Since the model was studied for cell activation, we studied the timing of the hilar activation after kainic acid and DEDTC administration, joined and separately Kainic acid 10mg/Kgbw by itself produced overexcitation without cell loss.

As previously shown in the second chapter of this thesis, in basal levels of c-Fos expression we found c-Fos positive nuclei preferentially in the upper half of the granule cell layer, and in the border between the granule cell layer and the inner molecular layer (**Figure III.3A**). After the injection of kainic acid, virtually all granule cells were immunopositive for c-Fos, but this expression returned to basal levels 6 to 8 hours after the injection (**Figure III.3B-D**). As expected, the expression of c-Fos by granule cells was accompanied by the expression of c-Fos in hilar cells, probably mossy cells. After 8 hours, the expression of c-Fos by granule cells and semilunar granule cells was low, although some granule cells in the inner molecular layer and in the juxtamolecular granule cell layer still expressed c-Fos. C-Fos expression remained depressed for several days reaching again the basal level 14 days after the injection (**Figure III.3E-H**).

Kainic acid administration at subconvulsive levels produces a general overexcitation in all cell types and it is difficult to find a pattern in the c-Fos expression. But in the subsequent depression of c-Fos expression produced after 6 hours, putative semilunar cells in the dentate gyrus are among the most actively c-Fos expressing cells.

2.3. EXPRESSION OF C-FOS AFTER MILD EXCITATION WITH DEDTC

Administration of the zinc chelator DEDTC by itself has been proven to produce enough overexcitation to induce HSP72 in the mossy cells of the rat, at a dose of 500 mg/Kgbw (Blasco-Ibáñez et al., 2004). Although in the analyzed material DEDTC was used at a dose of 150mg/Kg, the overexcitation was enough to induce the expression of c-Fos in the hilus that lasted for several hours.

In control animals, the expected pattern for c-Fos staining was observed. Briefly, c-Fos positive nuclei appeared more frequently in the border between the granule cell layer and the inner molecular layer (**Figure III.4 A**). Four to six hours after the administration of DEDTC, the number of c-Fos positive nuclei in the border between the granule cell layer and the inner molecular layer border seemed to increase. Interestingly, bigger nuclei in the granule cell layer were also positive for c-Fos, possibly corresponding to parvalbumin interneurons according to their location. A large number of positive nuclei were also found in the hilus, likely from mossy cells and interneurons. Faint astroglial cells were also present at Timm-positive areas as the hilus and the stratum lucidum (**Figure III.4 B** and **C**). From 8 to 12 hours, the expression of c-Fos decreased even below control levels for all cell types, but it began to recover 1 day after the DEDTC administration, and reached the basal levels four days (**Figure III.4 D-H**).

In conclusion, the mild excitation produced by DEDTC induced first c-Fos expression mainly in semilunar granule cells located close to the border between the granule cell layer and the inner molecular layer, likely activating both mossy cells and interneurons. It is interesting to note that a general activation of typical granule cells was not induced. After overexcitation, a transient silent period for c-Fos expression was observed in the hilus for all cell types, followed by a slow recovery. This could be possibly generated by an inhibitory compensation to previous overexcitation.

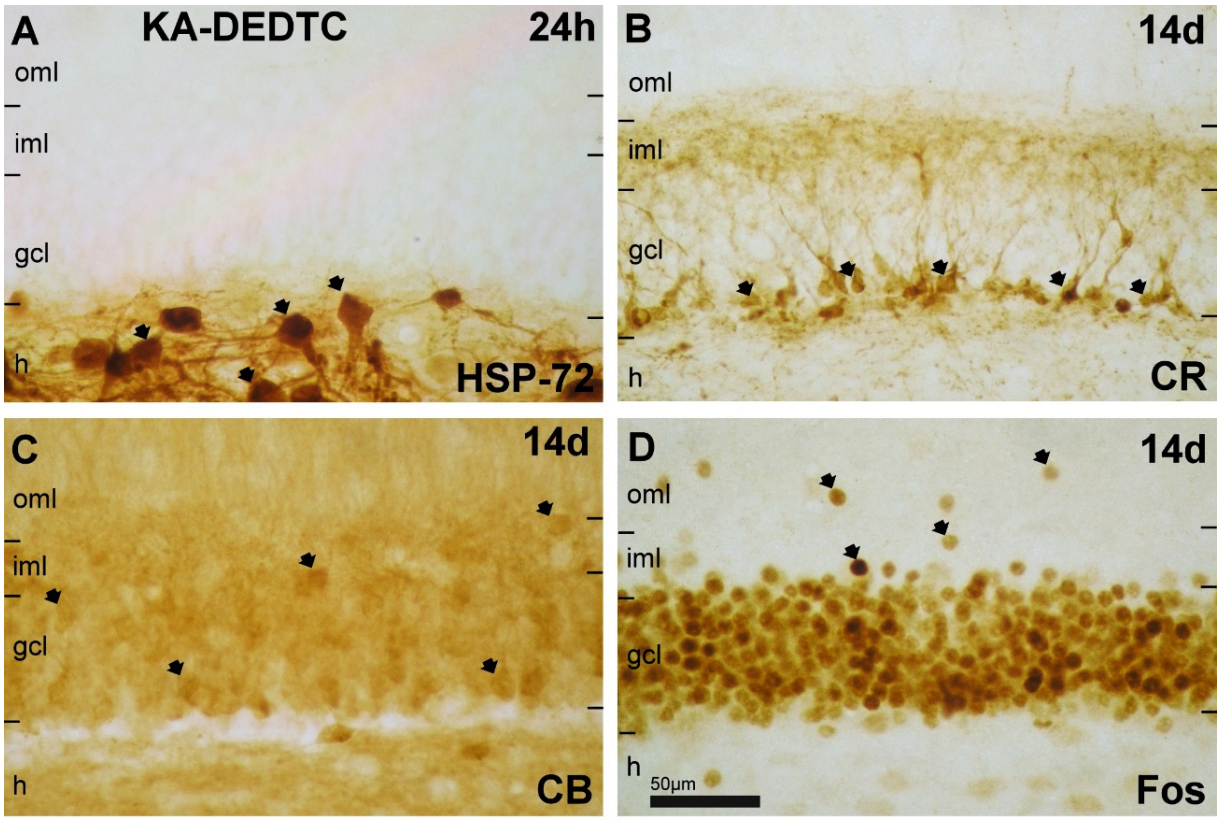

Figure III.2 - Semilunar granule cells are preserved in the kainic acid-DEDTC model of epilepsy.
A) Twenty four hours after kainic acid administration the only dentate gyrus cells expressing HSP72 are the hilar neurons (arrows). Neither semilunar cells nor granule cell layer interneurons express HSP72 at any time.
B) Fourteen days after kainic acid administration, immunoreactivity for calretinin shows the complete disappearance of mossy cells in this animal and the presence of abundant calretinin immunoreactive immature granule cells (arrows) in the base of the granule cell layer.
C) Most granule cells, including those in the molecular layer, are weakly calbindin immunoreactive (arrows).
D) c-Fos immunoreactivity is present in almost all mature granule cells including those in the molecular layer (arrows).
B-D images belonged to the same animal. gcl, granule cell layer; h, hilus; iml, inner molecular layer; oml, outer molecular layer. Scale bar 50 µm.

Figure III.3 - c-Fos detected cell activation in the dentate gyrus after Kainic Acid administration at a subconvulsive dose

A) In control animals, c-Fos labelled a scattered population of granule cells. Intensely labeled granule cells appeared more frequently in upper layers of the granule cell layer, including cells in the inner molecular layer border (arrows).

B) Four hours after Kainic Acid administration, all granule cells seemed to express c-Fos. In the hilus, mossy cells (arrowheads) as well as hilar interneurons also expressed c-Fos.

C) C-Fos immunoreactivity in the granule cells proved to be transitory, and after 6 hours it remitted. Mossy cells in the hilus were still immunoreactive, although fainter than at 4 hours. The number of hilar immunoreactive cells was highly reduced.

D) After 8 hours, c-Fos immunoreactivity was limited to some granule cells, including those sited in the inner molecular border.

E) At 12 hours, the low number of immunoreactive granule cells remained. On the other hand, there was a weak expression of c-Fos by glial cells in all layers of the dentate gyrus.

F and **G)** From day 1 to day 4, the number of labeled granule cells remained low.

H) Only by day 14, the pattern and number of immunoreactive granule cells was similar to controls.

gcl, granule cell layer; h, hilus; ml, molecular layer. Scale bar 50 μm.

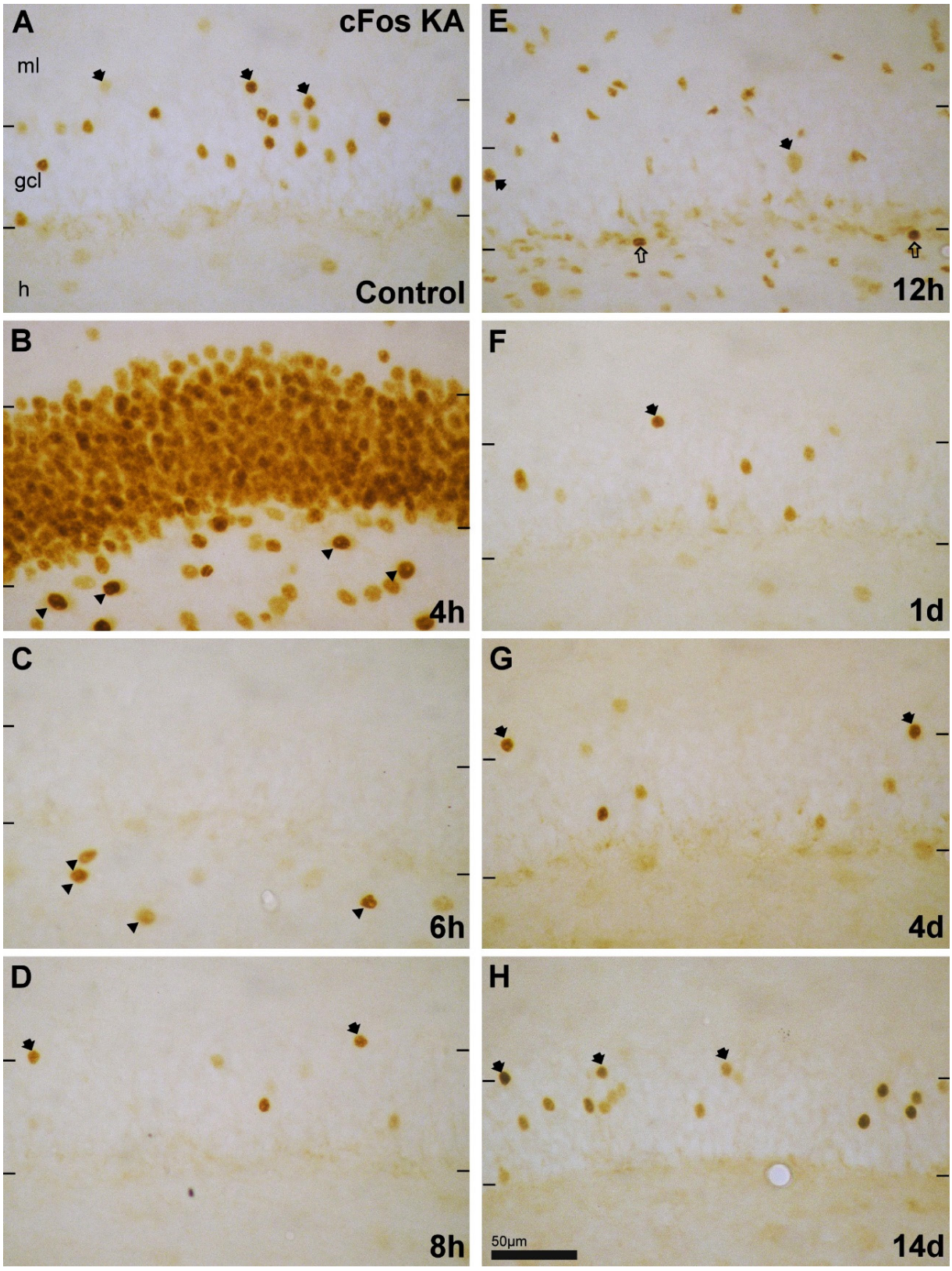
A
cFos KA
ml
gcl
h
Control
E
12h
B
4h
F
1d
C
6h
G
4d
D
8h
H
50µm
14d

Figure III.4 – c-Fos detected cell activation in the dentate gyrus after DEDTC injection
A) In control animals c-Fos labeled a scattered population of granule cells. Intensely immunoreactive granule cells seemed to be more abundant in upper layers of the granule cell layer, including cells in the inner molecular layer border (arrows).
B) Four hours after DEDTC administration, the number of c-Fos positive granule cells in the inner molecular border increased (arrows). On the contrary, granule cells inside the granule cell layer were scarce and faintly stained. In the hilar border of the granule cell layer we found large nuclei corresponding to putative pyramidal basket interneurons (open arrows). In the hilus a high level of immunoreactivity was induced. Among them, by their nuclear size and location inside the hilus, we recognized hilar mossy cells (arrowhead) and numerous faint glial cells.
C) After 6 hours, c-Fos immunoreactivity in granule cells was limited to the border with the inner molecular layer. Interneurons in the infragranular area and mossy cells in the hilus were becoming faint. Additionally, there was an increment of immunoreactivity in the hilar glial cells.
D) After 8 hours there was an attenuation of c-Fos immunoreactivity in all cells.
E) At 12 hours the loss of c-Fos immunoreactivity was almost complete in the dentate gyrus, including granule cells, mossy cells, interneurons and glia.
F) Immunoreactivity began to recover 1 day after DEDTC administration. There were only few immunoreactive granule cells located at any level, including the inner molecular layer.
G, H) By day 4 the dentate gyrus recovered the usual pattern of c-Fos immunoreactivity, including cells in the inner molecular border. By day 14 the pattern of immunoreactivity still kept similar to controls, but the increment of granule cells present by day 4 persisted.
gcl, granule cell layer; h, hilus; ml, molecular layer. Scale bar 50 μm.

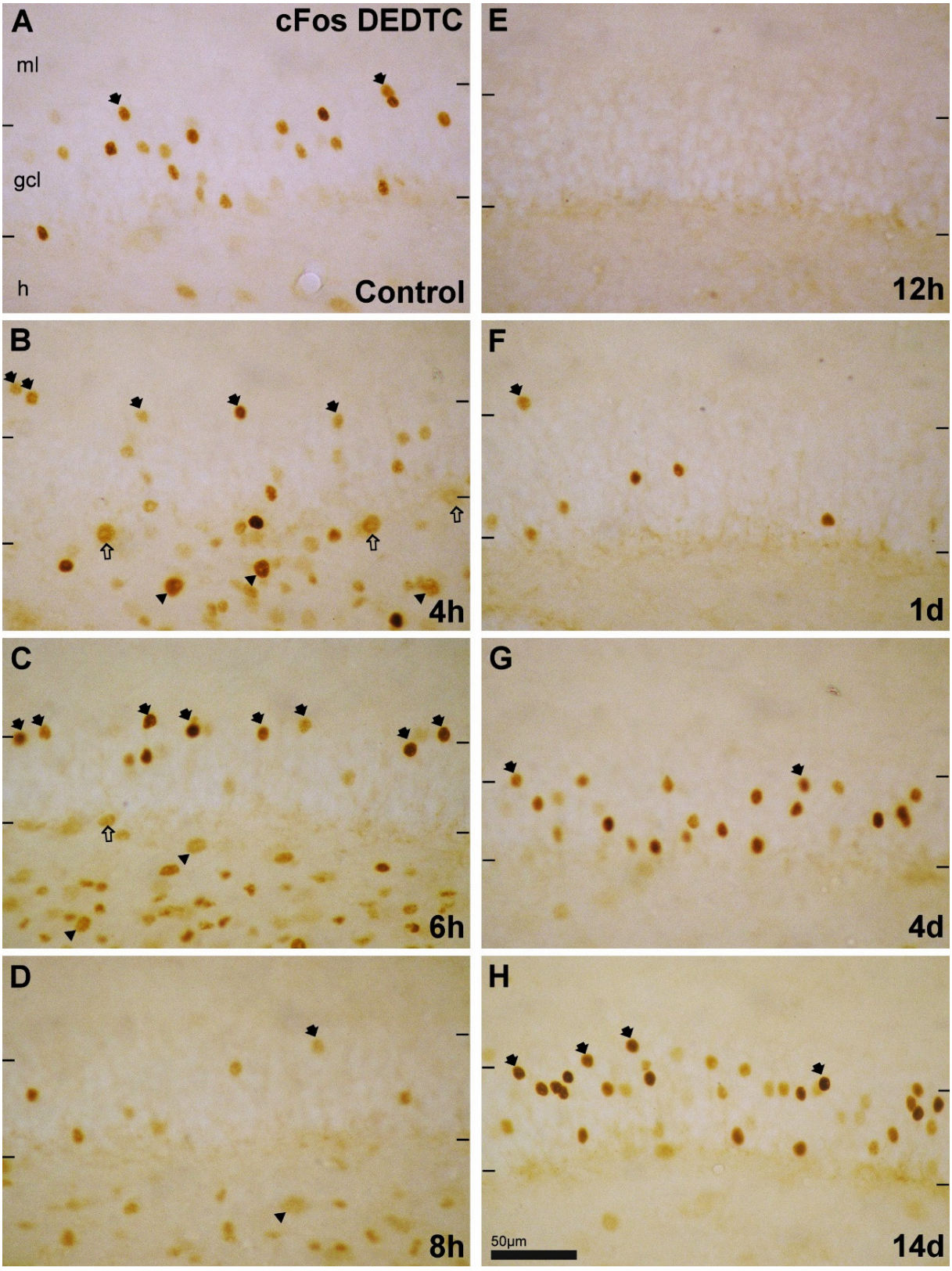
A
cFos DEDTC
ml
gcl
h
Control
E
12h
B
4h
F
1d
C
6h
G
4d
D
8h
H
50µm
14d

3. SURVIVAL OF SEMILUNAR GRANULE CELLS IN THE PILOCARPINE MODEL OF EPILEPSY

We also studied the survival of semilunar granule cells in a pilocarpine model of epilepsy in the mouse. For further details of the experimental procedure, see (Marqués-Marí et al., 2007). Briefly, adult mice were injected intraperitoneally with pilocarpine at a convulsive dose of 300 mg/Kgbw, and perfused at different times after the administration of pilocarpine. This dose was enough to produce lesion in the treated animals. The control group was injected with saline solution instead. The nature of the study did not allow us to analyze cell activation but we could study cell survival since survival times up to 5 months after pilocarpine were used.

We checked the animal for different stainings that allowed us to determine the possible fate of semilunar granule cells: (1) toluidine blue was used to analyze the lesion and the presence of granule-like cells in the molecular layer; (2) calretinin staining, to evaluate the quality of the lesion obtained, as a correlation with the loss of mossy cells; (3) calbindin, used as a granule cell marker; and (4) Timm staining, to evaluate the extent of the mossy fiber sprouting.

No apparent loss of semilunar granule cells was observed in the pilocarpine model after lesion, neither with toluidine blue nor with calbindin, as calbindin-positive cells were still present in the inner molecular layer (**Figure III.5 A**). The loss of mossy cells, instead, was severe as seen with calretinin (**Figure III.5 B**). Timm staining was well developed in the inner molecular layer 60 days after pilocarpine administration. Still Timm stained fibers could be observed in the granule cell layer following putative dendrites of basket cells (**Figure III.5 C**).

Therefore, there is no loss of granule cells that could correspond to semilunar granule cells at long times in this model of epilepsy, neither there is any indication that this loss is produced in the other models analyzed. We should conclude that semilunar granule cells as well as parvalbumin basket cells are resilient to damage in this models whereas mossy cells are greatly affected by cell death.

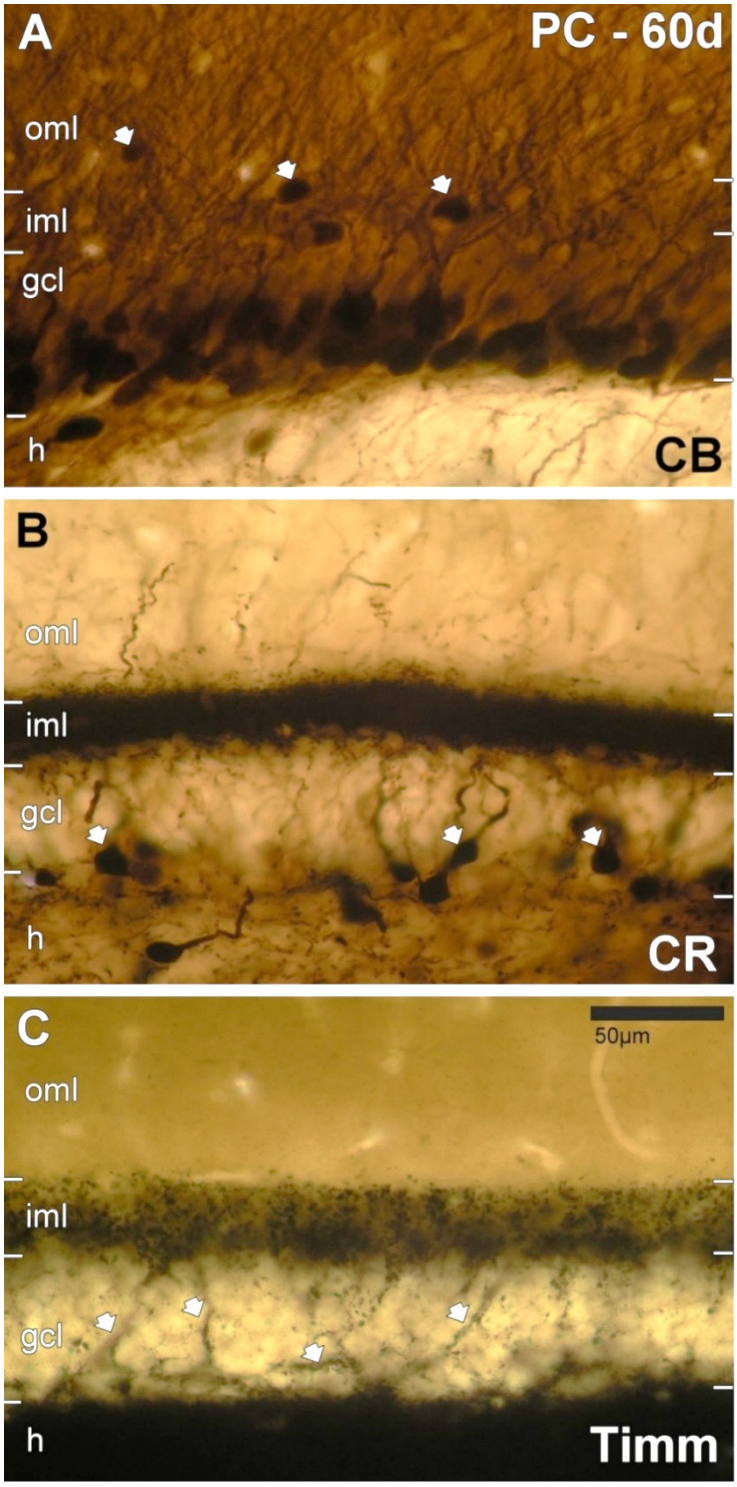

Figure III.5- Semilunar granule cells are preserved in the pilocarpine model of epilepsy.
All images are taken from the same animal.
A) 60 days after pilocarpine administration the expression of calbindin in the dentate gyrus remained altered. Calbindin was expressed mainly by granule cells in the lower half of the granule cell layer, whereas in the upper half granule cells were not immunoreactive. Nevertheless, granule cells inside or in the border of the molecular layer were calbindin immunoreactive (arrows).
B) Calretinin immunoreactivity in these animals showed a disappearance of calretinin immunoreactive mossy cells in the hilus and a strong expression by immature granule cells (arrows).
C) Timm staining for vesicular zinc showed a strong sprouting from the mossy fibers, filling the inner molecular layer. Presumptive interneurons and somata of granule cell layer interneurons were densely covered by Timm-positive boutons (arrows).
gcl, granule cell layer; h, hilus; iml, inner molecular layer; oml, outer molecular layer. Scale bar 50 µm.

DISCUSSION

In this work we have studied the connectivity of parvalbumin basket cells and semilunar granule cells, to try to understand how this connection could influence the dentate gyrus in normal and pathologic conditions.

1. PERISOMATIC INNERVATION ON PARVALBUMIN BASKET CELLS IN THE MOUSE DENTATE GYRUS

Parvalbumin-positive cells in the granule cell layer represent two different types of fast-spiking perisomatic-innervating interneurons: the most abundant are basket cells, whereas the rest correspond to axo-axonic cells (Kosaka et al., 1987; Soriano and Frotscher, 1989; Nitsch et al., 1990; Soriano et al., 1990; Howard et al., 2005; Freund and Katona, 2007). Previous data show that axo-axonic interneurons mainly sit in the border between the granule cell layer and the inner molecular layer (Soriano and Frotscher, 1989; Soriano et al., 1990), and no further effort has been made in this thesis to distinguish one subpopulation from the other. Although we are aware that an identification of the target profiles is needed to define the basket or axo-axonic nature of parvalbumin interneurons, we will use the term “parvalbumin basket cells” in the discussion, as the study was centered in those parvalbumin cells sitting in the granule cell layer, unless indicated otherwise.

In the first part of the results we studied the origin of the excitatory perisomatic innervation on parvalbumin basket cells. The concept of “perisomatic region” has been generally applied in the literature to principal cells, in which a clearer different synaptic input and physiological function of this region can be observed if compared to spiny dendrites (Megías et al., 2001; Papp et al., 2001). However, there is a lack of information regarding the description of a “perisomatic region” in interneurons, focusing on their physiological function. In this work, we considered that the term “perisomatic region” should include both soma and the most proximal part of the dendritic trunk of the parvalbumin basket cells, up to the point where it branches; i.e. while it is still inside the granule cell layer. This is a common opinion, since there is generally a gradual transition between the cell body and the principal dendrite, and in this case the dendrite caliber is large enough to share common features with the soma.

Our first approach to understand the importance of this excitatory innervation was made by comparing it with the inhibitory one, using Gephyrin and PSD95 as postsynaptic markers (Lin et al., 2004; Fritschy et al., 2008; Jackson and Nicoll, 2011). Our data reported that both

excitatory and inhibitory perisomatic input on basket cells are at least equally important. This is in agreement with previous results obtained from parvalbumin interneurons in the CA1 region of the hippocampus, in which the density of somatic excitatory input was higher than the inhibitory (Gulyás et al., 1999). On the other hand, we found no differences among parvalbumin basket cells located differently in the dentate gyrus. Therefore, the excitatory drive on the somata is a common characteristic shared by them.

Although Gephyrin and PSD95 only label the postsynaptic density and do not allow us to visualize the boutons, the use of generalist presynaptic markers, such as VGAT or VGluT1, would have not been adequate by themselves. Since the parvalbumin basket cells under study are located in the granule cell layer, where cell bodies and dendrites of granule cells are tightly packed, a presynaptic marker could have introduced many false-positives if not coupled in a determinant manner with a postsynaptic density element, which would be the decisive element to consider it a putative contact.

Disregarding technical considerations, it is clear that there is an important excitatory input to parvalbumin interneurons which cannot be obviated when exploring the dentate gyrus function.

Previous knowledge related to the excitatory innervation that dentate parvalbumin cells receive can be summarized as follows: they receive excitatory contacts from the entorhinal cortex via the perforant path in the outer two thirds of the molecular layer (Zipp et al., 1989), as well as from fibers from mossy cells in the inner molecular layer (Seress and Ribak, 1984). The latter described a frequent perisomatic innervation from degenerated commissural fibers (likely from mossy cells) on one type of parvalbumin interneuron: the molecular layer type. However, in the particular case of perisomatic interneurons, they state neither the symmetric nor the asymmetric nature of such innervation. These degenerated axons could originate from hilar interneurons. On the other hand, the molecular layer type parvalbumin-containing interneuron has been generally considered as axo-axonic (Soriano and Frotscher, 1989; Soriano et al., 1990), and only one synaptic contact was observed by the authors in the other types of parvalbumin interneurons. Therefore, although it has been suggested that commissural boutons could synapse on the somata of parvalbumin basket cells, it has not been undoubtedly proved.

Other excitatory input to consider is the subcortical drive to parvalbumin interneurons coming from supramammillary fibers (Leranth and Nitsch, 1994; Nitsch and Leranth, 1994). However,

these authors showed in the monkey that not all parvalbumin interneurons are targeted by substance P-positive supramammillary boutons, but only a small fraction of them that are located in the upper half of the granule cell layer. Therefore, this innervation cannot explain by itself the perisomatic excitatory input that all parvalbumin interneurons in the dentate gyrus receive, as it skips the parvalbumin basket cells sitting in the hilar border with the granule cell layer.

On the other hand, it has been shown that parvalbumin basket cell somata receive a high number of Timm-positive boutons that make asymmetric contacts on them (Blasco-Ibáñez et al., 2000; Seress et al., 2001; Frotscher et al., 2006). Timm-positive boutons concentrate in the hilus and stratum lucidum, where they correspond to mossy fibers. In the granule cell layer, only a few collaterals can be detected. These collaterals have been described to originate from granule cells, however, no definitive proof has been provided. Other glutamatergic sources of boutons that contain zinc have been described in this area, such as the mossy cells and the entorhinal cortex pyramidal cells (Pérez-Clausell and Danscher, 1985; Valente et al., 2002; Paoletti et al., 2009), and although their level of Timm staining is considerably lower, they cannot be discarded.

Since the different excitatory inputs onto parvalbumin basket cells are not randomly distributed, the location of these inputs would play an important role in the modulation and triggering of action potentials. Innervation located in distal dendrites is usually considered to modulate the firing response, whereas innervation in proximal dendrites, or even better at the cell body, is more important to actually control the capability of the cell to fire somatic action potentials (Cobb et al., 1995; Miles et al., 1996).

Excitatory perisomatic drive of parvalbumin basket cells by local principal cells has been previously studied in different brain areas such as the visual cortex (Buhl et al., 1997), the hippocampus and the amygdala (Sik et al., 1993; McDonald et al., 2005). In the dentate gyrus, perisomatic excitatory input has been also studied in both control and epileptic animals (Ribak and Peterson, 1991; Kotti et al., 1997; Blasco-Ibáñez et al., 2000). The presence of this regulatory system in other cortical structures suggests a general control mechanism in all brain areas.

To better understand the function of the excitatory perisomatic input on the parvalbumin basket cells of the dentate gyrus, we aimed to analyze the origins of this input.

1.1. PERISOMATIC EXCITATORY INNERVATION FROM MOSSY CELLS ON PARVALBUMIN BASKET CELLS IN THE GRANULE CELL LAYER

Our data at the confocal microscopy level show that there may be a few perisomatic synaptic contacts from mossy cells in parvalbumin-containing basket cells, both on the soma and on the apical dendritic trunk. However, puncta in close apposition at the confocal level is no guarantee that there is an actual synaptic contact, and no previous studies have shown these contacts at the electron microscopy level.

In our correlated optical-electron microscopy study, no clear synaptic contacts from mossy cells could be found in the perisomatic region of parvalbumin basket cells with somata located in the granule cell layer. We found instead some questionable ones, and many calretinin-positive elements that passed close to parvalbumin interneurons but did not make synaptic contacts.

These calretinin-elements could come from different sources: (1) they could be axons from the mossy cells, that pass close to parvalbumin-positive interneurons through the granule cell layer, and present varicosities that can be observed as puncta, but make no contacts on their way; (2) boutons coming from the supramammilary nuclei (Maglóczky et al., 1994); (3) boutons from IS-1 calretinin-positive interneurons that pass nearby (Freund and Buzsáki, 1996).

We cannot completely rule out the possibility that some of the scarce and testimonial calretinin-positive elements that we see are not coming from supramammilary fibers, since they present a similar morphology and also establish asymmetric synapses. The possibility of having calretinin-positive elements that establish symmetric contacts is also low, as IS-1 calretinin fibers generally avoid parvalbumin basket cells (Gulyás et al., 1996; Blasco-Ibáñez et al., 1998).

In summary, our results show that the main, and almost exclusive, source of perisomatic excitatory innervation onto parvalbumin-positive basket cells are the Timm-positive boutons, as only rare questionable examples of calretinin-positive synapses have been found. However, excitatory synapses that shared the characteristics of *en passant* boutons from mossy fibers were relatively easily found. These results indicate that the general idea that mossy cells exert an important excitatory drive to parvalbumin basket cells on the soma is mistaken, and its influence is restricted to parvalbumin-positive dendrites in the inner molecular layer.

1.2. PERISOMATIC EXCITATORY INNERVATION FROM GRANULE CELLS AND SEMILUNAR GRANULE CELLS ON PARVALBUMIN BASKET CELLS IN THE GRANULE CELL LAYER

Previous studies have shown that parvalbumin-positive interneurons are innervated by Timm-positive fibers, which contain high levels of Zn^{+2} (Ribak and Peterson, 1991; Blasco-Ibáñez et al., 2000; Seress et al., 2001; Frotscher et al., 2006). These Timm-positive fibers have been presumed to arise from granule cells, and to be therefore mossy fibers. Ultrastructural features of these boutons are similar to those of mossy fiber contacting hilar interneurons, with small round and a few dense-core vesicles (Claiborne et al., 1986; Acsády et al., 1998). Still no definitive proof has been provided that granule cells are the origin of the Timm-positive fibers on the parvalbumin basket cells. In fact, the number of fibers is quite low in relation with the total number of cells. Therefore, even if they come from granule cells, this population of granule cells must be quite a restricted one (Blasco-Ibáñez et al., 2000). On the other hand, another origin cannot be discarded.

Although difficult to evaluate, if we admit a number of parvalbumin-positive interneurons about 1000 per dentate gyrus (data from the control group in the pentylenetetrazole-induced kindling experiment, shown in chapter **Results III**, **Section 1** in this thesis) and we admit a media of 4 Timm-positive fibers on one of them, even if each collateral arises from a different cell, the cell population that would generate this innervation should be limited to 4000 cells, and that number is likely an overestimation. As the number of granule cells in the mouse dentate gyrus has been estimated to approximately 500.000 cells (Amrein et al., 2004), if these fibers arose from granule cells, less than 1% of granule cells would be in charge of this innervation.

The entorhinal cortex afferents also present synaptic zinc in their terminals, as do many other glutamatergic cells (Pérez-Clausell and Danscher, 1985; Valente et al., 2002; Paoletti et al., 2009), but the Timm staining for these fibers is low, and the perisomatic puncta obtained do not correspond to their innervation pattern. Therefore, it is unlikely that entorhinal fibers are the source of this innervation on the perisomatic region of parvalbumin basket cells. However, there is evidence in the literature of entorhinal fibers entering in the hilus through the granule cell layer (Deller et al., 1996), and we cannot rule out the possibility that a small, specialized population of entorhinal cells could participate in it.

It is also very unlikely that supramammillary afferents are zincergic, as previous studies regarding the staining of thalamic and hypothalamic subnuclei with the Timm method do not show any evidence of it (Mengual et al., 2001; Hamani et al., 2005). In addition, the Timm-

positive fibers observed in the dentate gyrus do not follow the pattern that would be expected if they arouse from these systems.

In any case, although mossy fibers are the most probable source of the Timm-positive innervation of the perisomatic region of parvalbumin interneurons in the dentate gyrus, it was necessary to prove it, and to isolate that subpopulation.

To determine the origin of the Timm-positive fibers that innervate parvalbumin basket cells in the dentate gyrus unmistakably it is necessary to visualize the axons of identified cells. Although granule cells in rodents have been analyzed as a homogeneous population, in recent years semilunar granule cells have been proven to have special characteristics (Williams et al., 2007; Larimer and Strowbridge, 2010; Gupta et al., 2012). The location of these cells in the dentate gyrus makes them a suitable source for the perisomatic excitatory innervation on parvalbumin basket cells.

To study the innervation from typical and semilunar granule cells to parvalbumin interneurons, completely filled (axon included) cells were needed. For this purpose, as there are no markers available and the granule cells are densely packed, the best tool that we could use was the intracellular injection via whole-cell patch clamp. This technique allowed us to fill almost all the dendritic tree of typical and semilunar granule cells, and even more important, the main axon and axon collaterals.

Golgi staining could have allowed us to fill cell bodies and their axons as well. However, with this technique cells are randomly filled, good examples are hard to find, and further anatomical studies are not possible or become very difficult in this type of material. Nevertheless, we were provided with some suggestive examples by Professor Carlos López García, showing the presence of collaterals in the granule cell layer that could correspond to the boutons making asymmetric contacts on parvalbumin basket cells.

The study of intracellularly filled typical granule cells did not provide any indication that the Timm-positive collaterals may arise from them. The granule cell axon always raised from the basal pole of the cell and traveled directly through the granule cell layer to the hilus, where it ramified. In addition, no varicosities were observed in their way through the granule cell layer.

Although intracellular injection only allows us to fill the part of the axonic arbor present in the slice, it is unlikely that typical granule cells contribute to this innervation. Otherwise, mossy fibers collaterals in the granule cell layer should originate from the hilus and make their way

up through the granule cell layer. However, this phenomenon has only been described in pathological situations such as epilepsy (Kotti et al., 1997; Kobayashi and Buckmaster, 2003), but not in control conditions.

According to our material, the presence of axon collaterals from typical granule cells is unlikely to explain the innervation of parvalbumin basket cells. Still, since only a small proportion of granule cells would be necessary to produce this innervation according to our calculation above, we cannot completely rule out that some of them may contribute to it.

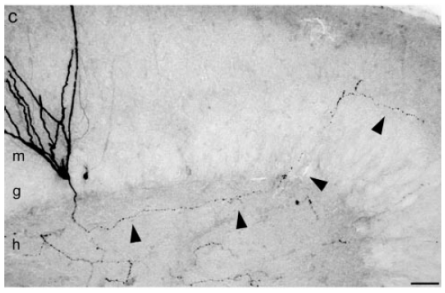

Granule cell collateral entering the granule cell layer in epilepsy
Modified from Kobayashi et al, 2003

On the other hand, our results indicate that semilunar granule cells could be the origin of this innervation, at least of most of it. Semilunar granule cell axons emerge in the inner molecular layer where they often run parallel to the lamination before entering the granule cell layer, and generate collaterals that also enter the granule cell layer (Williams et al., 2007). These collaterals are in an ideal location to contact parvalbumin-positive cell bodies and dendrites from the parvalbumin interneurons in their way to the hilus. Moreover, while their axons travel through the granule cell layer, they present varicosities that could perfectly be synaptic boutons.

Combining the intracellular tracer with an immunostaining for parvalbumin we found clear examples that semilunar granule cells do innervate perisomatically parvalbumin basket cells. Although often we could not find contacts of these cells on parvalbumin cells, it should be taken into account several technical considerations that could have influenced these results: (1) an incomplete filling of the axon; (2) dead or degenerating target parvalbumin cells in the slice that lose the antigenicity for the antibody. In fact, even in slices with a large number of surviving cells, many cells including parvalbumin interneurons are dead. Parvalbumin dead cells in acute slices seem to lose immunoreactivity quickly. Possibly the use of other markers for parvalbumin basket cells such as $Kv_{3.1}$ (Chow et al., 1999) could have help to improve the results.

It was necessary to check under the electron microscope if the axons of semilunar granule cells make synaptic contact on parvalbumin basket cells. The electron microscopy confirmed this hypothesis. In fact, the ultrastructure of the boutons corresponded to the descriptions for the Timm-positive boutons already published (Blasco-Ibáñez et al., 2000), confirming that the Timm-positive innervation on parvalbumin cells comes from semilunar granule cells. Interestingly, boutons from the same fiber continued on the parvalbumin dendrites present in hilus, also presumably from the parvalbumin basket cells.

Innervation of Timm-positive boutons on hilar parvalbumin cells has been described previously (Seress et al., 2001). Further studies will be necessary to understand the relevance of typical and semilunar granule cells in the innervation of hilar parvalbumin interneurons.

Nevertheless, even if we make allowances for the limitation of the technique, it is likely that semilunar granule cells are not a homogeneous population, and that not all but only a subpopulation of semilunar granule cells are responsible for the innervation onto parvalbumin basket cells, (i.e. parvalbumin interneuron selective semilunar granule cells) that should be better described. This fact could possibly be extended to the cells involved in the hilar up states described by Larimer and Strowbridge (2010). Based on their original paper, there is no evidence that only a subset of semilunar granule cells are responsible for the generation of hilar up-states. However, a sampling bias can be the underlying reason for this, and additional studies should be performed to answer the question whether semilunar granule cells that contact parvalbumin basket cells also participate in the hilar up-states generation.

1.3. DIFFERENCES IN THE INNERVATION OF THE MORPHOLOGICALLY DIFFERENT PARVALBUMIN BASKET CELL TYPES

Parvalbumin cells in the granule cell layer of the dentate gyrus have been differentiated into different types considering their morphology (Ribak and Seress, 1983). There are some clues suggesting that this could be reflected in different function, although all of them are fast-spiking and, with the exception of the axo-axonic cells, they innervate the somata of granule cells. In fact, the location of the cell body and dendrites is crucial to determine the inputs parvalbumin interneurons are going to receive, and to understand the strength of these inputs and the signal integration that would determine the interneuron firing.

In our study we only had access to morphological considerations, but we realized that there are differences between the different types. Unfortunately, we could not find many differences at the level of perisomatic input using the generalist markers studied in this thesis, but we found clear differences in the intensity of the Timm-positive staining on the different cell types. While some subtypes are massively surrounded by Timm-positive boutons (horizontal and pyramidal types), others are weakly innervated (molecular type, inverted fusiform type). For example, molecular layer parvalbumin-positive cells are thought to be axoaxonic cells (Soriano and Frotscher, 1989; Soriano et al., 1990), and they are weakly innervated by Timm-positive boutons in the soma. Further studies are needed to clarify whether this differential innervation may be translated in a different physiological function.

If this phenomenon turned to be true also at a physiological level, basket cells and axoaxonic cells would receive different perisomatic input, which could determine different functions under physiological and pathological conditions. Further research will be necessary to test the differences among the different types of parvalbumin cells respective to their innervation by semilunar granule cells.

On the other hand, although this work is centered on parvalbumin cells of the granule cell layer, we have to take into consideration the presence of parvalbumin-positive cells in the hilus, especially at ventral levels. These cells have been shown to be somatically and dendritically innervated by mossy fibers (Acsády et al., 1998). We confirmed that they also receive input from semilunar granule cells, but we cannot weight it against innervation from normal granule cells.

Although the firing of the semilunar granule cells is likely to facilitate the firing of the parvalbumin interneurons in the hilus and granule cell layer, its influence is probably higher in those cells that are highly innervated at a perisomatic level than in those that are weakly innervated or are only innervated at a dendritic level.

2. CHARACTERIZATION OF SEMILUNAR GRANULE CELLS

2.1. ON THE TERM “SEMILUNAR GRANULE CELL” IN THIS THESIS

An important decision that we had to face when working in this thesis was to select a name for the subpopulation of granule cells that we were to study. Different names have been given to these cells along time, according to different criteria. Ramón y Cajal was the first to describe

this cell population, and termed them “semilunar granule cells” due to their semilunar morphology (Ramón y Cajal, 1911). The term “semilunar” is a morphological concept also used for non-granule cells in other brain areas (Gómez-Climent et al., 2008).

The other term used habitually to define non-standard granule cells is “ectopic granule cell”. Ectopic granule cell includes all granule cells located outside the granule cell layer disregarding any morphological or functional criteria. However, the term “ectopic granule cell” is generally associated to the appearance of misplaced granule cells in the molecular layer, hilus or even the CA3 after seizures (Scharfman et al., 2000; Shapiro and Ribak, 2005; Muramatsu et al., 2008; Scharfman and Pierce, 2012). Our study, on the contrary, tries to focus on granule cells present in control conditions and that are a feature of the dentate gyrus circuitry.

Although both terms partially overlap, they are not synonymous. It is not known whether all the ectopic cells are semilunar granule cells, nor if all the semilunar granule cells can be considered ectopic. “Ectopic cells” is a less compromising term since it makes no preconception about morphology or function. On the other hand in recent years important literature on the granule cells in the inner molecular layer has been published characterizing this population and using the term “semilunar granule cell” to define them.

In this thesis, we chose the term semilunar granule cell since these studies have used the term to name a population of granule cells located in the inner molecular layer with special characteristics. The location of these cells and their differential characteristics in axon localization or physiology suggested that they could in addition be suitable candidates to innervate parvalbumin basket cell somata. On the other hand, we wanted a term that did not involve hilar ectopic granule cells, or ectopic granule cells that could appear in a pathological situation.

A detailed systematic description of semilunar granule cell’s morphology is missing in the literature. The lack of a specific marker for semilunar granule cells made their characterization difficult. Martí-Subirana and colleagues already showed that the population of molecular layer ectopic granule cells in young control rats is heterogeneous (Martí-Subirana et al., 1986). The different morphologies and location of the semilunar granule cells of the inner molecular layer suggest that they can fulfill different functions, since their synaptic input will be different. However, no functional examination has been previously performed.

Based on the previous literature we chose to include in the definition of semilunar granule cells those granule cells located in the border between the granule cell layer and inner molecular

layer and that could not be aptly named ectopic cells. Three important facts support this decision:

- From the morphological point of view, these cells can also be considered as “semilunar”, as they present a wider dendritic arbor in comparison with their lower neighbors. This dendritic orientation, in which two primary dendrites arise from opposite poles of the cell, shapes the cell body in a more triangular or semilunar way instead of ovoid.
- From the phenotypical point of view, these cells express some markers in a different extent than middle layer-granule cells. For example, these cells show a distinct expression of markers such as CART peptide (Seress et al., 2004; Hunter et al., 2005; Abrahám et al., 2007; Kolenkiewicz et al., 2009), and in an excited brain state, c-Fos.
- They receive similar input than the cells in the inner molecular layer. These cells are innervated by fibers coming from the supramammilary nucleus in a higher extent than rest of the cells in the granule cell layer. In addition, they may receive a stronger excitatory input from mossy cells, as their proximal dendrites are already in the molecular layer (in opposition to the lower granule cells, which present an apical dendrite that must travel some microns to reach the inner molecular layer, therefore receiving less excitatory input).

However, the election of a name is a tool, and should be reconsidered on the light of further data that could redefine the population. To delimit this population clearly it will be necessary to find a cell marker that could actually discriminate semilunar granule cells from typical granule cells or ectopic granule cells.

2.2. TECHNICAL CONSIDERATIONS

Due to the lack of specific markers for this subpopulation, the remaining techniques available for this study were three: (1) intracellular injection via whole-cell patch clamp; (2) transgenic Thy1 mice; (3) immunohistochemistry for Prox1.

We discarded the Golgi technique, although there are previous studies that have used it to study the cell population of the molecular layer in the rat brain (Martí-Subirana et al., 1986) and in the rabbit brain (Sancho-Bielsa et al., 2012), where a morphological description is carried out. In addition, this technique is whimsical and makes difficult further analysis, since immunohistochemistry for putative targets is not easily combined.

On the other hand, intracellular injection via whole-cell patch clamp allowed us to target the cells that we thought were better candidates for innervating parvalbumin basket cells. Their dendritic arbor could be filled and compared, as well as their main axonal branch and collaterals. One of the problems associated with this technique is that it is labor intensive, and therefore cannot produce a very large number of samples. Therefore we had to select the most promising neurons introducing a subjective criterion. Additionally, when making the acute slices, some of the granule cells and parvalbumin basket cells degenerate. To reduce cell degeneration these studies are usually performed in young mice. These problems can interfere with the study, since the susceptibility of the different cell types can be different and the cell types can also be not fully mature. As an additional disadvantage, the acute slices can only be fixed by immersion after several hours of study, and the quality of the tissue for optical and ultrastructural analysis is affected.

Thy1 transgenic mice allowed us to focus on excitatory cells located in the molecular layer and the border with the granule cell layer. Its use allowed us to study their general morphology, cell body shape and proximal dendrites. Therefore we could identify semilunar granule cells clearly. It had the advantage that only principal cells expressed the fluorescent protein YFP, and in a Golgi-like manner, but not all of them expressed it. Therefore we could single out semilunar granule cells, but we could not see all of them in a given section. There is a chance that all the different types are not labeled randomly. In addition, although the quality of the genetically encoded fluorescence was optimal, the number of cells labeled simultaneously did not allow for complete reconstruction of the dendritic arbor. However, it allowed us to make a phenotypic study in which the possible differences could be associated with the semilunar morphology.

Finally, Prox1 has been widely accepted as a granule cell marker (Lavado and Oliver, 2007; Lavado et al., 2010; Iwano et al., 2012), and even used to confirm that semilunar granule cells are a subpopulation of granule cells (Gupta et al., 2012). It has the advantage of staining all of the granule cells, but only the nuclei. This gave us a tool for studying the incoming innervation on granule cells that by their size and position we considered semilunar granule cells. However, due to its nuclear nature, we could only focus the study in the perisomatic region. The antibody for Prox1 also presented several difficulties, mainly related to the fixation. First, it was very sensitive to the quality of the fixation, and microglia appeared as background staining when the fixation was not optimal. Second, the staining that we got was in all cases weak, enough to

be distinguished at the optical level, but hard to see its nuclear staining in the electron microscope, which forced us to work with correlated optical-electron microscopy. In addition, GA based fixatives decreased the intensity of the staining, already weak *per se*, and acrolein-based fixatives had to be used instead.

2.3. DISTRIBUTION AND NUMBER OF SEMILUNAR GRANULE CELLS

Due to the small number of semilunar granule cells, or ectopic granule cells located in the outer molecular layer of the dentate gyrus, no quantitative studies have been performed previously.

We used Prox1 to label the granule cells. Although it only labels the nucleus of the granule cells, it labels all of them and allowed us to calculate the size of the population of granule cells in the molecular layer. Our estimation showed that the studied animals present a relatively similar number of Prox1-positive cells in this area, and that they are more abundant in the inner molecular layer than in the outer molecular layer. In addition, we found Prox1-positive cells in the molecular layer are present in two different strains (C57BL/6J and CD-1), and in Wistar rats. Therefore, this cell population cannot be considered either as a curiosity or due to a pathological condition.

There are studies that report an increase in the number of ectopic granule cells after seizure (Scharfman et al., 2000; McCloskey et al., 2006; Pierce et al., 2007). In fact many of the morphological features previously described for ectopic granule cells correspond to these seizure-induced newly-formed ectopic granule cells, or for granule cell dispersion and migration to the molecular layer (Murphy and Danzer, 2011). These cells should not be confused with normal ectopic granule cells and their features characteristics cannot be translated to them.

Prox1 has also been described as a marker for a subpopulation of interneurons that originate in the lateral/caudal ganglionic eminence and preoptic area during development (Rubin and Kessaris, 2013). In that paper they skip the study of the presence of Prox1 interneurons in the dentate gyrus. On the other hand, it is unlikely that the interneuron population that originates in the lateral/caudal ganglionic eminence (VIP- or Reelin-positive, but not parvalbumin- or somatostatin-positive) could affect much our study (for review, see Wonders and Anderson, 2005; Hernández-Miranda et al., 2010), considering the low frequency at which they are found in the molecular layer. In addition, semilunar and ectopic granule cells present in Thy1 animals

have Prox1 nuclei with shape and size similar to all of the Prox1 nuclei in the molecular layer, and that are smaller than interneuron nuclei. We also found that Thy1-positive cells in this region have the same distribution and are Prox1-positive. Finally, our analysis at the electron microscope showed granule-like features for Prox1-positive cells in the molecular layer.

Therefore, although we cannot absolutely discard the presence of a few Prox1-positive interneurons in the molecular layer of the dentate gyrus, on the whole, we can consider Prox1 as a selective marker for granule cells for the present study.

The number of Prox1 nuclei in the inner molecular layer is not high (around 1200 cells per hemisphere), corresponding to less than 1% of the granule cells, and therefore similar to the number of parvalbumin basket cells or mossy cells. The distribution of these cells is more abundant in the suprapyramidal layer than in the infrapyramidal layer. This fact is in agreement with the density of Timm-positive fibers on parvalbumin basket cells.

We cannot compare the amount of Prox1 nuclei in the molecular layer with other studies in normal animals, but Golgi studies have reported the presence of ectopic granule cells in the whole molecular layer, with more cells being stained in the suprapyramidal than in the infrapyramidal blade (Martí-Subirana et al., 1986), which is in accordance with our results.

2.4. ORIGIN OF SEMILUNAR GRANULE CELLS

We decided to study the postnatal development of the dentate gyrus to understand if semilunar granule cells are an intrinsically different type of granule cells or if they are different because of their time of origin and location. Since during young adult age and even adulthood, newly formed granule cells are being generated (for a review see Kempermann et al., 2004; Mongiat and Schinder, 2011), and they incorporate in the subgranular zone next to the hilus, it has been assumed that the cells close to the molecular layer are older. We used semithin sections with calretinin as a marker for immature granule cells in mice (Liu et al., 1996; Brandt et al., 2003), and calbindin as a marker for more mature and integrated granule cells (Sloviter, 1989).

Our study confirm that the first granule cells to mature (expressing calbindin by day 7) are those cells that correspond by localization to semilunar granule cells. By day 10 the circuitry is beginning to mature, as seen by calretinin expression in the mossy cell axons in the inner molecular layer. By day 14, the dentate gyrus is reaching normality.

In rats, dentate gyrus formation and granule cell differentiation follow a gradient from the external dentate limb to the internal dentate limb (Altman and Bayer, 1990). This is also observed in the calbindin staining by day 10 in our preparations. It is interesting that the first areas of the dentate gyrus to form and mature are those where more abundant are semilunar granule cells during adulthood.

Dentate GABAergic neurons originate in the subventricular zone of the medial and lateral ganglionic eminences (Bayer, 1980a; b; Pleasure et al., 2000), and are generated earlier than granule cells (Lübbers et al., 1985). However, maturation of the dendritic and axonal arbor may take place in the postnatal life, probably influenced by interactions with their synaptic partners (Seress et al., 1989; Seress and Ribak, 1990).

We hypothesize that semilunar granule cells are originated from the first population of hippocampal granule precursors described by Altman and Bayer (1990). This area, designed as the secondary dentate matrix, dissolves by day P5 in rat and becomes the outer shell of the granule cell layer. Therefore, this early generated granule cells are in a privileged position to establish synaptic contacts with parvalbumin basket cells and mossy cells. Their expression of calbindin is an indicative of their integration in the circuitry (Sloviter, 1989). Once the perisomatic synaptic places in the parvalbumin interneuron are no longer available for the new generated granule cells, the next generations of granule cells, originating from the tertiary dentate matrix, will have no opportunity to contact the parvalbumin cells in the granule cell layer.

Since axon collaterals from semilunar granule cells also contact parvalbumin cells in the hilus, there is a possibility that this preponderance of contacts on parvalbumin cells extends to the hilus, although probably in a less absolute manner.

In addition, the fact that we found more Prox1-positive nuclei in the inner molecular layer in ventral levels than in dorsal levels of the dentate gyrus is in agreement with the fact that more Timm-positive fibers are found there, more parvalbumin interneurons and more mossy cells.

2.5. MORPHOLOGICAL CHARACTERIZATION OF SEMILUNAR GRANULE CELLS

Although granule cells in rodents are usually considered as a homogeneous population (Lindsay and Scheibel, 1981; Seress and Pokorny, 1981; Desmond and Levy, 1982; Claiborne et al., 1990), some works have found differences in granule cell morphology and size in rat (Yan et al., 2001),

and in other species. In the red fox, large granule cells represent 17% approximately of the total number of granule cells, and are characterized by a bigger cell body and nucleus, different orientation of the axon hillock and stronger expression of NeuN (Amrein and Slomianka, 2010), which can be due to a different physiological state as hypothesized by Mullen et al (1992). Seress and Ribak compared granule cells from rat and primates, and they found that in primates axo-somatic synapses, somatic spines and infolded nuclei were common, although these characteristics were rare in the rat (Seress and Ribak, 1992). They attribute these differences to lower GABAergic inhibition since the soma is a preferred location for GABAergic synapses and therefore they propose that primate granule cells are physiologically more active than rat granule cells. These features are in accordance with our results for semilunar granule cells in mouse and rat.

Axon originating from a dendrite

We found that a frequent feature of semilunar granule cells is that the axon arises from the dendrite. This is not a characteristic unique to semilunar granule cells. Several interneuron populations, such as dentate basket cells, present the axon in a main order dendrite (Ribak and Seress, 1983). Glutamatergic pyramidal cells from CA1, CA3 and subiculum have also been shown to present axon-carrying dendrites (Kaifosh and Losonczy, 2014; Thome et al., 2014). However, it is widely accepted that typical dentate granule cells present an axon originating in the basal pole of their cell body, and only some reports of its emergence from a dendrite are found in the literature, and were generally considered as an anomaly (Seress and Pokorny, 1981).

The fact that the axon may arise from a primary order dendrite, which in many physiological cases could be considered within the perisomatic region, could have important implications in the function of these cells, related to the action potential generation. Some studies have shown that the location of the axon initial segment respective to the soma may help the neurons to modify their excitability (Grubb et al., 2011; Baranauskas et al., 2013).

Interestingly, it has been shown that in dissociated hippocampal cultures, chronic depolarization leads the axon initial segment to move further away from the soma in a reversible way to reduce their excitability (Grubb and Burrone, 2010). Therefore, this characteristic could be indicative of a functional difference with normal granule cells and points towards a higher level of activity.

Basal dendrites entering the hilus

We found that 21% of the biocytin-filled analyzed cells presented an axonal branch traveling through the granule cell layer and entering the hilus. Hilar basal dendrites are common during postnatal development, but they eventually disappear (Lübbers and Frotscher, 1988; Jones et al., 2003; Shapiro and Ribak, 2005). An unlikely hypothesis will be that they represent a stage in which the granule cell was still migrating in a radial way. However, nothing in the cells from our preparations indicated that the cells were immature. In fact, their fully developed dendritic tree with mature spines, and axon already in the CA3, suggested that they were not immature granule cells.

The presence of hilar basal dendrites in the rodent has been reported mainly in pathological conditions, such as ischemia or epilepsy (Spigelman et al., 1998; Ribak et al., 2000; Díaz-Cintra et al., 2009). These hilar basal dendrites were postsynaptic to mossy fibers, probably participating in an excitatory recurrent circuit. It has been previously shown that hilar basal dendrites that appear normally during development are maintained under hyperactivity conditions (Hara et al., 2006).

On the other hand, the presence of these "hilar dendrites" may be due to technical issues. The acute slices for this studies had to be obtained from intracellularly filled cells in postnatal P15-P23 mice. Although the general dentate gyrus structure at this age is similar to adults, many newly generated granule cells are still being generated and maturing, a process that takes between 7 and 21 days (Marqués-Marí et al., 2007).

Somatic spines

Our data show a relatively high incidence in somatic spines in semilunar granule cells, and even higher in outer molecular layer ectopic granule cells when compared to normal granule cells, in which are practically absent.

The presence of somatic spines has been previously reported in granule cell somata *in vivo* in the adult rat (Kosaka et al., 1984; Deller et al., 1996a) and primate dentate gyrus (Seress and Ribak, 1992), though with a very low frequency in adult rats. However, somatic spines in granule cells somata have been described in neurodevelopment, in dentate slices prepared *in vitro,* and in pathological conditions such as the reeler mice or seizure-induced mice (Stirling

and Bliss, 1978; Martí-Subirana et al., 1986; Bundman and Gall, 1994; Bundman et al., 1994; Wenzel et al., 1994). It is important to remark that previous anatomical studies have focused on granule cells located in the granule cell layer and not in the molecular layer.

No somatic spines have been described in other principal cell populations within the hippocampus, even in the pathological or experimental situations described above. This fact may reflect that the formation of somatic spines is an intrinsic property of granule cells in response to external stimuli.

Therefore, considering the morphological and physiological different features between typical granule cells and semilunar granule cells, the high incidence of somatic spines in semilunar granule cells, and even higher in the outer molecular layer ectopic granule cells, could be explained by the following reasons:

- A higher activity of this cell subpopulation could imply a higher calcium inward current (such as that observed in seizure-induced situations in granule cells). A high intracellular Ca^{+2} level had been previously hypothesized as a possible cause for the formation of somatic spines (Wenzel et al., 1994). This is also possibly the case with semilunar granule cells during the plateau potentials. This influx of calcium could also relate with a higher expression of cell activity markers as we will comment below.
- The location of semilunar granule cells in the molecular layer, with a higher probability of receiving asymmetric perisomatic synaptic contacts from supramammillary fibers or mossy cells, could explain the increase in the intracellular somatic calcium levels, and therefore the higher incidence of somatic spines. Still in the inner molecular layer we could not observe that mossy cells boutons contacted usually the somata of semilunar cells. Even when surrounded by them, the somata received perisomatic symmetric and asymmetric synapses from other sources.

The presence of somatic spines in semilunar granule cells may be triggered by the same mechanisms of structural plasticity than dendritic spines, i.e. an increase in the cell activity for a review, see (Nikonenko et al., 2002; Sala and Segal, 2014). In addition, our observations are in agreement with Wenzel et al. work (1994), who described that only 20% of the new-formed somatic spines *in vitro* found a postsynaptic partner. Under electron microscopy from our fixed *in vivo* preparations, we observed that these somatic spines from semilunar granule cells usually lacked a presynaptic element, and could be considered only as protrusions from the cell

soma. However, we also found some somatic spines that presented an associated presynaptic element with a postsynaptic density characteristic of active excitatory synapses.

Dendritic arborization

We performed a Sholl analysis on the injected cells to test for differences in dendritic innervation that could explain the difference between the different types of granule cells. The sholl analysis showed that there is no difference in the arborization of semilunar granule cells and typical granule cells, except in proximal dendrites. This suggests that only the innervation pattern that they receive in the inner molecular layer is affected. Mossy cells innervate densely the inner molecular layer (Blasco-Ibáñez and Freund, 1997), and semilunar granule cells extend the most proximal dendrites in this region, which may be translated in a more important drive from mossy cells than in typical granule cells. In addition, for semilunar granule cells the synaptic contacts from mossy cells are located closer to the cell body and would be comparatively more important for the generation of action potentials.

Our results showed that semilunar granule cells followed the same dendritic pattern as granule cells. There were differences due to their position above the granule cell layer. The dendritic cone was wider the higher the granule cells were in the cell layer, in agreement with former descriptions of these cells morphology (Claiborne et al., 1990), and this was also true for semilunar granule cells.

Ours and other studies on semilunar cell morphology suffer from the bias introduced by the decision on what to consider a semilunar granule cell. Those cells that did not resemble semilunar granule cells, or that were damaged during the experimentation, were discarded. This problem will persist until a specific marker for these cells is found.

2.6. NEUROCHEMICAL CHARACTERIZATION OF SEMILUNAR GRANULE CELLS

Since semilunar granule cells had special characteristics regarding origin, connectivity and physiology, we tried to find a neurochemical marker that allowed us to study them without resorting to morphology. We used the transgenic mouse line Thy1-YFP, to be able to correlate markers with morphology, as principal cells in these animals strongly expresses YFP in a Golgi-like manner that allows further anatomical studies.

Principal cell and granule cell marker expression

All YFP-positive semilunar granule cells were CAMKII-positive, and the vast majority of them were also Prox1-positive, and therefore granule cells. These results were as expected, and confirmed that the cells that we considered semilunar granule cells based on their morpholy, were in fact principal cells and granule cells. No interneurons in this area interfere with our results, and the vast majority of the principal cells present in the molecular layer are semilunar granule cells.

However, there are a small number of principal cells located in the molecular layer, which could not be semilunar granule cells. This may be probably due to lack of staining for Prox1, although neighbor cells were well labeled in the same level of the sections. As a possible explanation, they could represent a second glutamatergic cell type, that have been previously described in the rabbit molecular layer and that was called "*Sarmentous*" (Sancho-Bielsa et al., 2012). But considering the similarities in shape and size, and the morphological diversity of semilunar granule cells, could also be semilunar granule cells presenting a low level of Prox1 immunoreactivity masked by the strong YFP-fluorescence.

YFP-positive cells also expressed calbindin in a high proportion. This result corresponds to the one expected for typical granule cells. This fact indicates that semilunar granule cells express the same principal and granule cell markers than the ones used for typical granule cells.

Calcium binding proteins expression

Calcium binding proteins are in charge of chelating the excess of intracellular calcium that can come in the cell after continuous spike discharges. In the mouse and other animals calretinin is a good marker for mossy cells possibly due to higher activity, and changes in calcium binding proteins are observed in the dentate gyrus and other areas in response to a physiological alteration, such as epilepsy (Maglóczky et al., 1997; Carter et al., 2008). It has been reported that semilunar granule cells present different functional properties in comparison with typical granule cells, like a difference in the spike frequency adaptation in long duration current steps, which have been attributed to distinct calcium dynamics (Williams et al., 2007).

In any case, semilunar granule cells acted similarly to normal granule cells. They expressed calbindin consistently, but they expressed neither calretinin nor parvalbumin.

c-Fos expression

Since semilunar granule cells seem to be more active than typical granule cells, we used the early gene c-Fos protein family to analyze the activity of this cell population. Intense labeled c-Fos nuclei were more common in the inner molecular layer and in the juxtamolecular granule cell layer, than in the granule cell layer. When combined with Thy1 immunostaining, many of the pan-Fos nuclei corresponded to semilunar granule cells. On the other hand, c-Fos expression is rare in interneurons during normal conditions.

Larimer and Strowbridge (2010) showed that semilunar granule cells participate in hilar up-states. After perforant path stimulation, a plateau potential could be evoked in semilunar granule cells in a NMDA, L-type and T-type voltage gated calcium channel dependent manner. As a result, semilunar granule cells could discharge for prolonged periods of time and activate cell assemblies of both mossy cells and hilar interneurons, creating the so-called hilar up-states (Larimer and Strowbridge, 2010). This fact, together with the higher innervation that they receive from mossy cells (Williams et al., 2007), made us assume that these cells were constitutively more activated than typical granule cells, and should express the c-Fos marker more frequently.

Unfortunately although the expression of c-Fos is rarer in normal granule cells than in semilunar granule cells, the high number of granule cells makes c-Fos an unselective maker for labelling semilunar granule cells by itself, although it is useful in combination with location and other labels.

CART peptide expression

CART peptide labels a subpopulation of granule cells in the rat that largely overlaps in number and location with the semilunar granule cell population (Seress et al., 2004; Abrahám et al., 2007). However, our test with this antibody did not provide the expected results, as we only found a few scattered CART immunoreactive cells in the dentate gyrus. Although some of them could correspond to semilunar granule cells because of their location, CART peptide was not a good marker for these cells in our experiments, either in mouse or in rat. We tried different fixatives and protocols with no better success. On the other hand, CART cells and fibers were well marked in the hypothalamus and other areas in which are more abundant. Also, the few cells present in the dentate gyrus were well labeled.

One possible explanation is that the antibody used by Seress et al. (2004). was noncommercial and directed towards the peptide fragment 41-89, whereas the available commercial antibodies against CART were generally directed towards the fragment 61-102. However, this last antibody was shown to be also expressed in the granule cells of the border between the inner molecular layer and the granule cell layer in other rodents such as voles (Hunter et al., 2005) and guinea pigs (Kolenkiewicz et al., 2009). A difference in the post-translational processing of the CART peptide, or species-variations may be the reason for our different results. Therefore CART seems a promising candidate as specific marker for semilunar granule cells in other species, but was not useful in our conditions.

CART peptide gene transcription is dependent on the intracellular calcium levels and phosphorylated CREB via cAMP (Barrett et al., 2002; Jones et al., 2009). More specifically, an increase in the intracellular Ca^{+2} led to an increase in the CART peptide mRNA, which was attenuated by the inhibition of CAM or CAMKII, both implicated in the Ca^{+2}-dependent phosphorylation of CREB. Therefore, an increase in the intracellular Ca^{+2} in semilunar granule cells, due to a higher activity rate, could lead to the increase in the CART transcript levels.

3. SYNAPTIC INNERVATION ON SEMILUNAR GRANULE CELLS

We decided to study the innervation on semilunar granule cells to check whether they are innervated differently from normal granule cells in a way that could be relevant for their function. Unfortunately, technical limitation prohibited us to study the innervation on dendrites, so we had to center on perisomatic innervation. In fact, supramammillary innervation has been described to focus in this area (Segal and Landis, 1974; Segal, 1979; Maglóczky et al., 1994). It has also been suggested that they could be void of perisomatic inhibition from basket cells, since they are out of the granule cell layer (Gupta et al., 2012).

We analyzed different subcortical monoamine afferences on this area combining tracing or immunocytochemistry with granule cell markers. We found no evidences of basket arrangement of serotonergic fibers (in a double immunostaining with 5-HT and Prox1 in both rat and mouse, not shown), dopaminergic fibers (in a double immunostaining with TH and Prox1 in both rat and mouse, not shown) or the noradrenergic fibers (in a double immunostaining with DβH and Prox1 in both rat and mouse, not shown).

The septal GABAergic and cholinergic innervation was also studied (not shown in results). Though cholinergic fibers were everywhere in the molecular layer and could have potentially innervated semilunar granule cells perisomatically, at the electron microscopy level we found no synaptic contacts from VAChT-positive boutons onto the somata of semilunar granule cells. In addition, the GABAergic innervation was also studied by an anterograde tracer injection in the medial septum, and rare examples of basket-like arrangement of fibers resembling GABAergic due to their morphology were found on Prox1-positive cells (not shown in the results). Though some putative contacts were checked at the electron microscopy level and recognized as inhibitory synapses, the number of such septal basket-like arrangements, and the fact that they were only found in ventral levels lead us to the conclusion that this innervation was not extended enough to play a main role in the function of semilunar granule cells.

It must be taken into account, however, that the previous studies were focused on the innervation in the somata of semilunar granule cells. Therefore, we cannot discard that the aforementioned monoaminergic and septal systems exert an important role in the function of semilunar granule cells by the innervation of their dendrites.

However, we had evidence of GABAergic perisomatic puncta on semilunar granule cells, and we decided to study if this inhibition came from fast-spiking or regular-spiking interneurons. We had previously observed in Thy1 transgenic mice that YFP-positive somata were surrounded by parvalbumin-positive boutons. To validate this observation, double stainings for parvalbumin and Prox1 showed that almost all Prox1 cells were surrounded by strongly labeled parvalbumin boutons. The staining intensity of the fibers was not homogeneous, and we also observed some cells that presented weak labeled fibers in apposition. Though we also found some nuclei that were not surrounded by parvalbumin boutons. This happened very rarely and may be probably due to false negatives. We confirmed this innervation under electron microscopy. All boutons labeled for parvalbumin were those typical of fast spiking basket cells, presenting large boutons with large mitochondria, ovoid clear vesicles and symmetric synaptic contacts (Ribak and Seress, 1983; Halasy and Somogyi, 1993). About half of the boutons making symmetrical contact on semilunar cells were labeled for parvalbumin.

The fact that semilunar granule cells are innervated by parvalbumin basket cells was discussed and discarded by Gupta et al. (2012), as their cell somata are located away from the granule cell layer and the basket interneuron axonal plexus would not reach that far. However, it had

been previously shown that it exists a high variability in the pyramidal-shaped basket cells of the granule cell layer, and that some of their axons even reach the outer molecular layer (Scharfman, 1995).

As stated above, the innervation of medial septum on semilunar granule cells was negligible. For this reason, we discard a subcortical origin for the vast majority of parvalbumin boutons innervating semilunar granule cells. Therefore, we propose a local origin for the boutons, which are likely the same basket cells contacting granule cells in the granule cell layer.

Since we observed parvalbumin-negative boutons that established symmetric synapses on semilunar granule cell somata, we decided to check whether the latter were also controlled by the other basket interneuron in the dentate gyrus: CCK interneurons.

We first attempted to detect CCK boutons on semilunar granule cells in the mouse dentate gyrus. Using a CCK antibody we obtained a labeling pattern in the CA1 that was consistent with previous descriptions (Freund and Buzsáki, 1996; Hájos et al., 1996. For a review, see Freund and Buzsáki, 1996). However, in the dentate gyrus we only detected occasional strongly labeled CCK fibers, and we could even observe some putative baskets on Prox1-positive cells in the outer molecular layer. Unfortunately, this antibody also labeled mossy cell fibers, resulting in a densely stained inner molecular layer. This fact complicated the study of the CCK innervation on semilunar granule cell somata, since it made the optical-electron microscopy correlation technically challenging. Therefore, we decided to use a different strategy. With the same CCK antibody, we obtained in rat a labeling pattern that suited better our purposes. The staining pattern was also in agreement with previous descriptions, but we avoided the labelling of mossy cell fibers in the inner molecular layer.

Double immunostaining for CCK and Prox1 allowed us to observe baskets on granule-like cells in the inner and outer molecular layer. Some of the Prox1-positive cells were abundantly contacted by CCK boutons whereas others were only occasionally contacted by one or two boutons. Although the quality of the immunostaining was good for CCK standards, we could not discard that not all the boutons from regular-spiking basket cells were labeled.

Next, we confirmed under the electron microscope that these boutons made symmetric contacts with the Prox1-positive cells they surrounded. We found two types of boutons, both making symmetric synapses: one type was comprised of boutons with slightly ovoid vesicles and sometimes one small mitochondria, as we expected from CCK interneurons present in the

dentate gyrus (Leranth and Frotscher, 1986); the second type was formed by larger, more boutons making symmetric synapses that were suggestive of a VGluT3-positive bouton (Somogyi et at, 2004; Omiya et al, 2015).

Although the data were enough to confirm that semilunar granule cells received contacts from CCK regular-spiking basket cells, it was not satisfactory enough to reveal the relevance of this projection. Therefore, we decided to use antibodies against CB1R, since it is coexpressed with CCK in fibers emerging from CCK-positive interneurons, both in the rat and in the mouse (Katona et al., 1999; Marsicano and Lutz, 1999). The antibody labeled intensely fibers and boutons that seemed to fill the dentate gyrus. Under higher magnification, clear baskets of CB1R-positive boutons could be found around semilunar granule cells.

When we studied some of these cells under electron microscopy, we confirmed that the CB1R-positive boutons in apposition with Prox1-positive cells were making symmetric synaptic contacts, both in the inner molecular layer and in the outer molecular layer. Their characteristics were similar to the ones that we described in the rats stained for CCK, but their frequency was higher. That confirmed our belief that we were not observing all CCK boutons. These CCK boutons would account for the other half of the boutons making symmetrical perisomatic contact on semilunar granule cells.

On the whole, the study of the perisomatic inhibition on semilunar granule cells showed that they were innervated by basket interneurons, similarly to normal granule cells. Therefore, both types of granule cells would be subjected to similar control mechanisms and would be synchronized by their activity. On the other hand, the perisomatic innervation is higher on semilunar basket cells than on normal granule cells. This higher inhibition would be in accordance with the higher excitability that they would have due to their dendritic disposition and short distance from the excitatory input to the axon hillock.

In addition to the inhibitory perisomatic innervation, we have also shown that semilunar granule cells and outer molecular layer ectopic granule cells are innervated by supramammillary fibers. This has been demonstrated by three different experiments: (1) using calretinin as a marker for supramammillary afferents in rat (Nitsch and Leranth, 1993); (2) using VGluT2 as a marker for supramammillary boutons in mice (Fremeau et al., 2001; Boulland et al., 2009; Soussi et al., 2010); (3), by stereotaxic injection of the anterograde tracer BDA 10 KDa

in mice. Our results in all cases point to an important, mainly excitatory innervation on semilunar granule cells and ectopic outer molecular layer granule cells. This observation is in agreement with the asymmetric nature of the innervation described in the literature (Nitsch and Leranth, 1993; Maglóczky et al., 1994). However, our results point to a target-selective innervation of these cell populations, as the main axonal plexus of supramammillary fibers are located just in the juxtamolecular granule cell layer (Segal and Landis, 1974; Segal, 1979; Nitsch and Leranth, 1993; Maglóczky et al., 1994), and both semilunar granule cells and outer molecular layer ectopic granule cells are frequently separated from the juxtamolecular granule cell layer.

Although some authors have proposed that the supramammilary-hippocampal projection is inhibitory in nature (Segal, 1979), supramammillary innervation is likely excitatory since the boutons establish asymmetrical synaptic contacts (Nitsch and Leranth, 1993; Maglóczky et al., 1994). This hypothesis is supported by the fact that supramammilary innervation enhances perforant-path elicited population spikes (Mizumori et al., 1989). That observation is consistent with the excitation of semilunar granule cells by this projection and the facilitation of hilar up states. Perisomatic excitatory innervation on principal cells is an uncommon event. It would represent a subcortical control of cortical activity via principal cell amplification, rather than the disinhibition mechanism described for the basal forebrain on interneurons (Freund and Antal, 1988; Tóth et al., 1993).

An important issue, which is generally obviated in both electrophysiological and anatomical studies, is the huge variations between dorsal and ventral dentate gyrus. While most anatomical studies center in coronal sections of the dorsal dentate gyrus, most electrophysiological studies use ventral horizontal dentate slices. Projections from supramammillary nuclei also differ in the dorso-ventral axis (Soussi et al., 2010), as septal projections do (Amaral and Kurz, 1985; Nyakas et al., 1987; Gaykema et al., 1990). Different subcortical drive should lead to different function of semilunar granule cells located in the dorsal dentate gyrus and semilunar granule cells located in the ventral dentate gyrus. In fact, we show that the number of these cells varies also along the dorso-ventral axis, being more abundant at ventral levels.

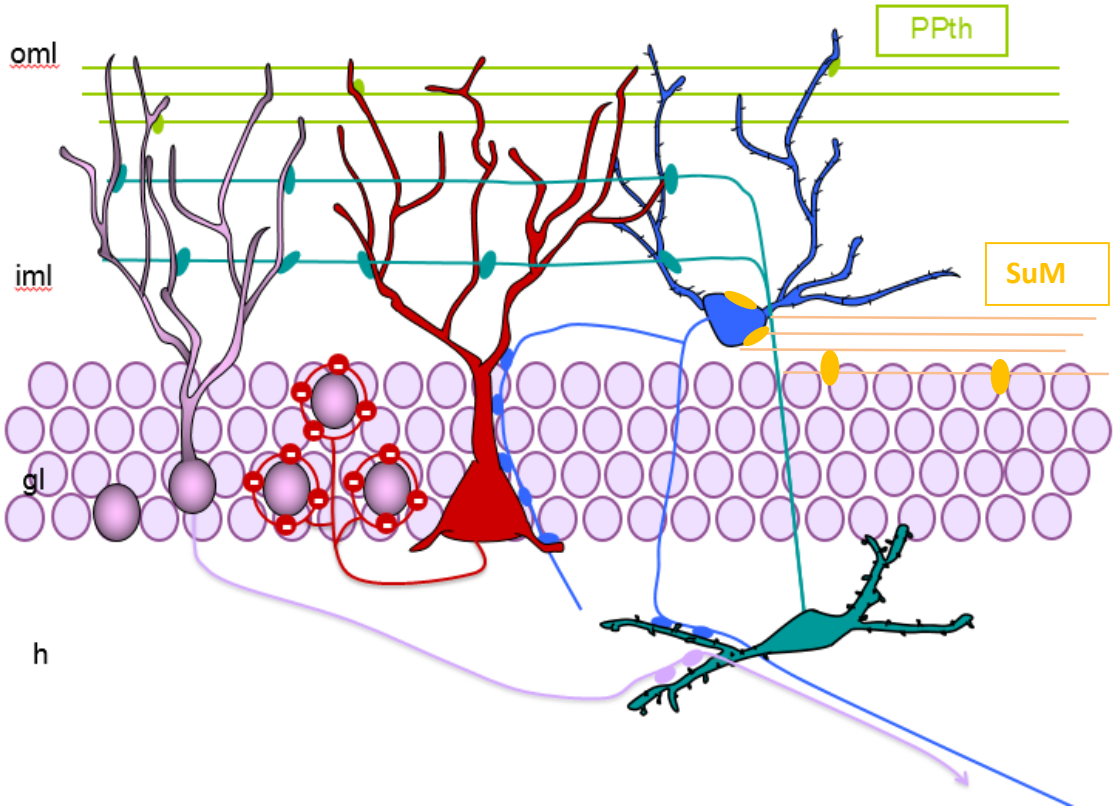

Figure 1. Semilunar granule cells in the dentate gyrus circuitry
Parvalbumin basket cells (red) receive excitatory input from the perforant pathway (PPth) in distal dendrites, from mossy cells in dendrites located in the inner molecular layer, and from semilunar granule cells in the perisomatic region. Parvalbumin basket cells innervate the perisomatic region of granule cell. Mossy cells receive excitatory innervation from semilunar granule cells, as well as from typical granule cells. Semilunar granule cells receive perisomatic excitatory afferents from supramammillary (SuM) fibers. Both semilunar granule cells and typical granule cells receive input from entorhinal fibers in the distal dendrites. In this figure, the perisomatic inhibitory innervation on semilunar granule cells is not shown. Supramammillary fibers are in an ideal position to influence the activity of the dentate gyrus. Gcl, granule cell layer; h, hilus; iml, inner molecular layer; oml, outer molecular layer; PPth, perforant pathway; SuM, supramammillary nuclei.

4. SEMILUNAR GRANULE CELLS AND EPILEPSY MODELS

The dentate gyrus is a common focus of epileptic activity in the nervous system. Therefore, it has been extensively studied and several hypotheses have been postulated about the role of its different cell population in the generation of epileptic activity. For a review, see (Sloviter et al., 2012). Since parvalbumin basket cells, mossy cells and semilunar granule cells seem to be in a key position to control the activity of the dentate gyrus, we decided to study how they were affected in different models of epilepsy.

Loss of granule cells has been only very rarely reported in animal models of epilepsy, and only for newly generated granule cells (Walter et al., 2007). Although semilunar granule cells

represent a small proportion of granule cells, their distinct location in the molecular layer would make their loss detectable.

To check how these cells were affected in epilepsy we decided to test three different models. For two of the models we used previous material generated in our laboratory: DEDTC-kainic acid model and pilocarpine epilepsy model in mouse.

In the DEDTC-kainic acid model of kainic acid and DEDTC used previously in our laboratory we did not find loss of granule cells or parvalbumin basket cells, although there was a fast and almost complete loss of mossy cells (Domínguez et al., 2006). We reanalyzed this material to check whether there is a loss of semilunar granule cells. The labeling for the granule cell marker calbindin and the cell activation marker c-Fos suggested that these cells were resistant to cell death in this model.

The Pilocarpine epilepsy model in mouse, when combined with scopolamine and finalized 90 min after onset by diazepam injection, usually produced animals with loss of hilar mossy cells. Otherwise, the other cell populations in the dentate gyrus and *Cornu Ammonis* remained generally undamaged (Marqués-Marí et al., 2007). The analysis of the dentate gyrus from pilocarpine-induced epileptic animals suggested that semilunar granule cells were not lost in those animals, though the expression of calbindin changed in those animals and sometimes affected semilunar granule cells. When analyzing sections stained for neo-Timm, axons delineating the shape of parvalbumin basket cells could be detected, also suggesting the persistence of the semilunar granule cells. Therefore, there is no loss of granule cells that could correspond to semilunar granule cells at long times in this model of epilepsy, neither there is any indication that this loss is produced in the other models analyzed.

We should conclude that semilunar granule cells as well as parvalbumin basket cells are resilient to damage in these models, whereas mossy cells are greatly affected by cell death. Further studies should address the question whether semilunar granule cells present axonal sprouting as typical granule cells (which probably do), and if the increase in Timm-positive innervation on parvalbumin cells (Kotti et al., 1997; Frotscher et al., 2006; Sloviter et al., 2006) is due to the sprouting of semilunar granule cells and/or the sprouting of typical granule cells.

We also questioned the role that semilunar granule cells may play in the process leading to cell damage. The two models that we had analyzed were too drastic for it, although in the DEDTC-kainic acid model, control animals for kainic acid and DEDTC could be analyzed in terms of cell

activation. Therefore, we decided to generate epileptic animals using a softer induction of overexcitation leading to epilepsy using chemical kindling with subconvulsive doses of pentylenetetrazole.

4.1. EXPERIMENTAL CONSIDERATIONS IN PENTYLENETETRAZOLE-INDUCED KINDLING MODEL OF EPILEPSY

In the experimental design of the kindling status, and considering the interindividual variability, there were two different options. First, we could use the same number of subconvulsive injections, independently of the number of seizures that the animal presented (as not all animals reacted in the same way to the drug). Alternatively, we could use behavioral criteria as the end point of the experiment for the kindling status achievement, based in the evolution of the nature of the seizures throughout the Racine scale.

Both possibilities have their own complications: in the first case, we could end up comparing animals with changes due to the addition effect of more seizures once reached the kindling status, instead of the kindling evolution per se. In the second case, we could end up comparing animals with different ages and final cumulative doses of pentylenetetrazole. Considering the goal of this study - to dilucidate the neurochemical evolution of the dentate gyrus due to a mild model of epilepsy such as pentylenetetrazole-induced kindling– and the implications of both possibilities, we decided that the best choice was using the behavioral achievement of the kindling status.

The slight difference in the age in which animals were sacrificed constitutes a minor objection to this choice, as no more than one month passed between the first animals and the last animal that reached the kindled status. There have been reported differences in the kindling achievement (Grecksch et al., 1997) throughout age, but not in this time window of 3-4 month old animals.

However, the different amount of pentylenetetrazole used in each animal introduces an uncontrolled variable to the study. However, this error is not of different nature to the one introduced when, in classical experiments regarding epilepsy, the same dose of any convulsant drug is used to produce seizures in different animals, as not all of them respond in the same way or suffer the induced seizures with the same severity.

In our particular paradigm, previous studies have solved this problem by using a rather high (50-100 mg/Kg) dose of pentylenetetrazole (Przewłocki et al., 1995; Stringer, 1995; Park et al., 2006), ensuring that all animals would reach the kindling status in the same number of injections. Those doses can be useful when the aim of the study is to analyze the effects of pentylenetetrazole fast-induced kindling, but not to study the evolution of the kindling achievement.

4.2. DENTATE CIRCUITRY IN THE PENTYLENETETRAZOLE-MODEL OF EPILEPSY

Our results in the experimental paradigm chosen for pentylenetetrazole-induced kindling model of epilepsy indicate that the dentate circuitry cell population change, but only on long term. Right after the animals were kindled, we observed no changes in the populations of mossy cells, parvalbumin interneurons or somatostatin interneurons.

Although at the end of the kindling process we observed no quantifiable alterations in the number of cells, one month after the animals had reached the kindled status, we observed a decrease in the density of the hilar mossy cells, and an increase in the number of parvalbumin cells. We performed Timm-staining in some animals to check if an increment of sprouting was responsible for the progression of the kindling overexcitation, and we found no differences with controls. This suggest that the sprouting of the mossy fibers is due to the loss of mossy cells, as other studies have suggested (Cavazos and Sutula, 1990; Houser et al., 1990; Cavazos et al., 1991). Our results are in agreement with previous studies with pentylenetetrazole-induced kindling, in which it has not been observed cell death or mossy fiber sprouting in the inner molecular layer during and right after the kindling procedure (Tian et al., 2009).

As interneurons are not newly generated in the adult dentate gyrus, the increase in the number of parvalbumin-positive interneurons may be correlated with an increase in the expression of this protein, which could make that more parvalbumin interneurons reach the detection threshold. Donato et al. (2013) described different parvalbumin network configurations in the hippocampus. These network configurations changed from low to high expression of parvalbumin in fear conditioning, when high excitatory/inhibitory ratios were observed on parvalbumin interneurons. In our case, we may be observing an increase in the excitation on parvalbumin interneurons, which would increase their activity and increase inhibition on the population of granule cells.

The number of mossy cells decreased one month after pentylenetetrazole-induced kindling. Since we used calretinin to detect mossy cells in mouse, there is a possibility that we are observing a decrease in calretinin expression instead of cell loss. On the other hand, the presence of refractive shrunken somata on the hilus under bright illumination confirmed that cell loss is present in the hilus. Although a loss of somatostatin interneurons is frequently observed in animal models of epilepsy (Sloviter, 1987; Houser and Esclapez, 1996; Sun et al., 2007), we did not observe loss of somatostatin cells either at kindled state or one month afterwards, which confirms that refractive cells correspond to mossy cells. These results suggest that mossy cells loss, in this model, is a progressive slow phenomenon that needs time to be detected.

Mossy cells are known to be more sensitive to overexcitation than granule cells. Although they are innervated by parvalbumin interneurons, this innervation is weaker than in granule cells (Acsády et al., 2000). In addition, mossy cells would be recruited in hilar up-states by active semilunar granule cells. This suggests that the dentate gyrus circuitry is altered during the kindling and the process continues inducing the loss of mossy cells.

Unfortunately we could not make a quantification of the number of semilunar granule cells. We tried using Prox1 as maker, but under this condition unspecific glial staining was too intense. In any case, there were Prox1 nuclei in the inner and outer molecular layer, therefore it seems that semilunar granule cells are not lost.

The previous data show that in this model the cell changes are subtle. Semilunar granule cells are in an optimal position to overexcite mossy cells and the parvalbumin basket cells simultaneously. Mossy cells seem to be the weakest link in this circuitry. Unfortunately the nature of the study did not allow us to infer if the semilunar granule cells had any impact on it.

4.3. EXPRESSION OF C-FOS AFTER MILD EXCITATION WITH KAINIC ACID

Since it seemed that a subconvulsive dose of pentylenetetrazole was able to preferentially activate semilunar granule cells, we decided to check this hypothesis by studying c-Fos expression in the animals injected with a subconvulsive dose of DEDTC combined with Kainic acid that by itself produced overexcitation without cell loss (10 mg/Kgbw).

In control saline animals, semilunar granule cells were easily found in an activated state, since the expression of c-Fos in these cells was relatively higher than in granule cells if we consider the cell numbers for both types.

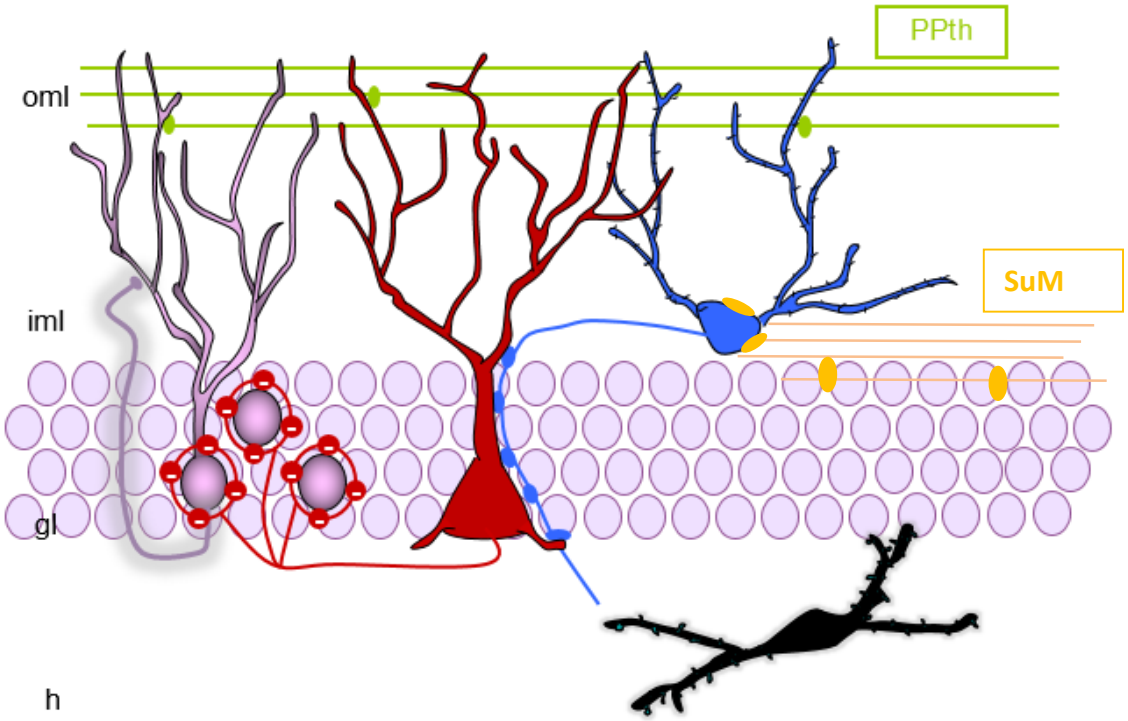

Figure 2. Dentate gyrus circuitry after status epilepticus.
Mossy cells die but semilunar granule cells and parvalbumin cells are preserved. The loss of the mossy cells greatly reduces the activation of the granule cells via semilunar granule cell activation, whereas recurrent inhibition is preserved. Granule cells compensate for the loss of recurrent excitatory activation by sprouting of the mossy fibers. This monosynaptic recurrent excitation is not coupled to recurrent inhibition, leading to a progressive over-excitation of the granule cells. Gcl, granule cell layer; h, hilus; iml, inner molecular layer; oml, outer molecular layer; PPth, perforant pathway; SuM, supramammillary nuclei.

At short times there was a general activation of the granule cells and hilar cells. Hilar mossy cells presented a high level of immunoreactivity that outlasted c-Fos expression in the granule cells. These results suggest a sequence of activation from granule cells to hilar mossy cells. These may reflect the hilar up-states described by Larimer, in which semilunar granule cells and hilar cells would recruit themselves and remain active (Larimer and Strowbridge, 2010) while the rest of the dentate is silent. It also proved that after a brief activation of the granule cells, the dentate gyrus activity remained under basal level for several days until recovering normality. During that low activity period semilunar granule cells are among the most active. Although this alteration caused by the overexcitation is not permanent, it persists for days.

4.4. EXPRESSION OF C-FOS AFTER MILD EXCITATION WITH DEDTC

The use of the zinc chelator DEDTC by itself would seem an inefficient source of dentate gyrus activation, but it has been proven to produce enough overexcitation to induce HSP72 in the mossy cells of the rat (Domínguez et al., 2003b, 2006; Blasco-Ibáñez et al., 2004).

In this model, DEDTC induced expression of c-Fos in the hilus that lasted for several hours. This was probably a very mild overexcitation, since the dose was low and it was not able to induce a general c-Fos expression in the normal granule cells. It was, however, able to induce expression of c-Fos in large nuclei in the hilus, most likely corresponding to mossy cells, and in large nuclei in the subgranular zone consistent with parvalbumin basket cells. This expression was transitory but linked the activation of semilunar granule cells, parvalbumin basket cells and mossy cells, suggesting that they interrelate as a recurrent circuit subjacent to the dentate gyrus structure.

There was also some expression of c-Fos in glia, but that can be easily expected since they are responsible for cleaning the zinc chelate. In fact, this transitory glial expression is generally limited to the hilus were vesicular zinc rich mossy fibers are present, being absent in other areas.

The overactivation of the dentate gyrus went under basal level after 6 hours of DEDTC administration, and needed 4 days to recover normality. This seems to be a common feature of dentate gyrus after overactivation, and probably underlines a compensatory increment of inhibition.

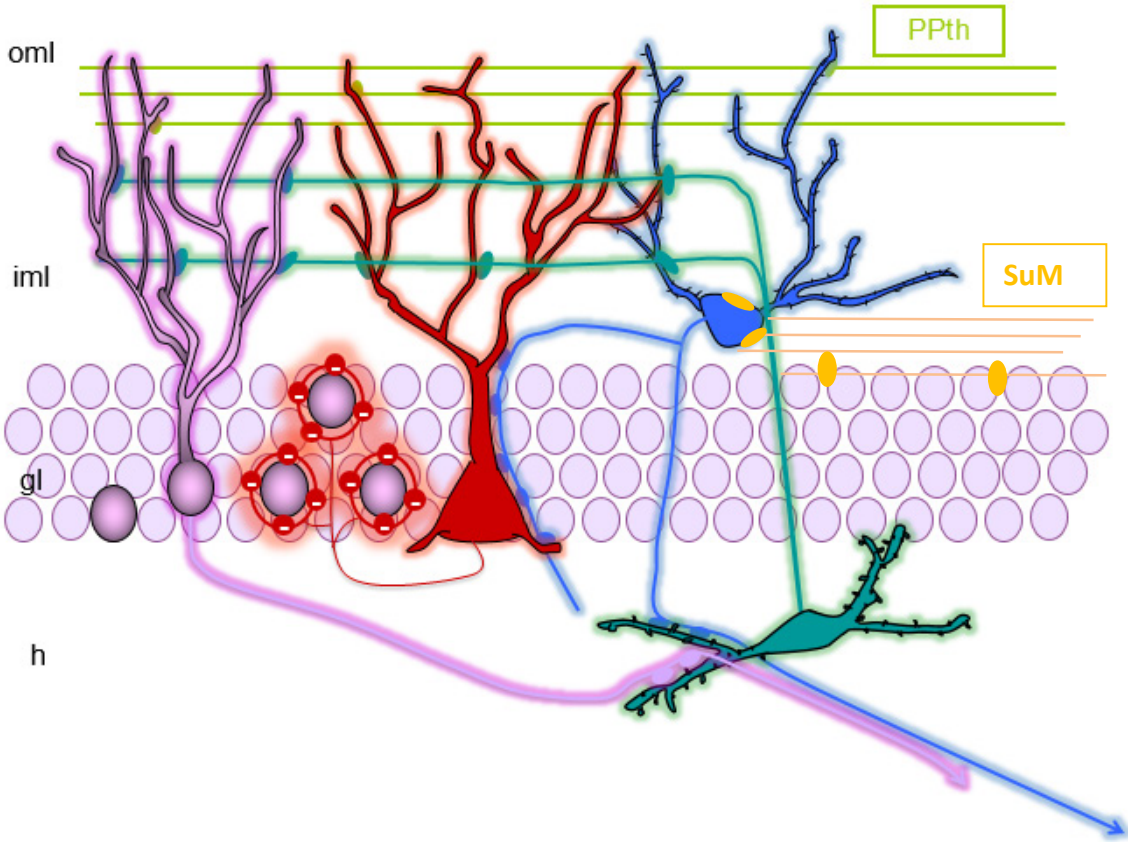

Figure 3. Mild transient overexcitation preferentially activates semilunar granule cells, mossy cells and parvalbumin basket cells.
Hilar mossy cells and semilunar granule cells are recurrently connected and have a tendency to fire together during hilar up-states. The recurrent activation of semilunar granule cells would activate parvalbumin basket cells. During this period of high activity granule cells will be simultaneously activated by excitatory input from the mossy fibers in the inner molecular layer and somatic inhibition via parvalbumin cells. Gcl, granule cell layer; h, hilus; iml, inner molecular layer; oml, outer molecular layer; PPth, perforant pathway; SuM, supramammillary nuclei.

The next goal was to check the cell activation in the dentate gyrus at short times after the administration of a unique dose of pentylenetetrazole at the subconvulsive dose used for kindling. At shorter times the effect of pentylenetetrazole in the dentate gyrus was first present on nuclei in the molecular and juxtamolecular layers. By 4 hours c-Fos immunoreactivity extended to other granule cells. This expression reverted to basal by 8 hours. The subconvulsive dose used in this experiment was enough to produce a transitory overexcitation that also affected the dentate gyrus, in agreement with previous literature (Szyndler et al., 2009). Semilunar granule cells in the border between the inner molecular layer and granule cell layer seem to be more sensitive to overexcitation than typical granule cells. Their continuous activation may affect their circuit with the mossy cells.

4.5. RELEVANCE OF THE SEMILUNAR GRANULE CELLS IN THE DENTATE GYRUS CIRCUITRY AND FUNCTION

The fact that not all the granule cells are equivalent has consequences in our understanding of the circuitry of the dentate gyrus. We began our study searching for the source of the perisomatic asymmetric boutons on parvalbumin basket cells in the granule cell layer, and concluded that the overwhelming majority came from granule cells, whereas other possible sources of asymmetric innervation were negligible. We then succeeded in finding that those granule cells located in the inner molecular layer and juxtamolecular border of the granule cell layer were the main source of this innervation. We used the term “semilunar granule cell” through this thesis to denominate them, since this classic morphological name has been used in recent works for a population of granule cells that largely overlaps with our cells.

Semilunar granule cells share many characteristics with common granule cells but they probably originate earlier from a separate migration of precursors (Altman and Bayer, 1990) and have special physiological properties (Williams et al., 2007; Larimer and Strowbridge, 2010) that enhance their ability to fire longer than normal granule cells. Parvalbumin basket cells are contacted by semilunar granule cells mossy fibers in their way to the hilus. These fibers usually made several contacts on the somata and proximal dendrites of basket cells, and they probably continue on basal dendrites in the hilus.

Parvalbumin basket cells can sustain a high frequency train of action potentials under stimulation. We hypothesize that, during hilar up-states, repeated firing of semilunar granule cells and mossy cells would reliably recruit parvalbumin basket cells. Whereas hilar up-states may contribute to recruit more granule cells in their progression. The activation of the parvalbumin basket cells would contribute to synchronize the whole population of granule cells.

Semilunar granule cells are in an ideal position to be excited by mossy cells axons, since their input is closer to the soma. In fact, excitatory input from mossy cells has been shown to be stronger in semilunar granule cells than in typical granule cells (Williams et al., 2007).

Our results indicate that subcortical innervation from supramammilary nuclei has a preference for semilunar granule cells. It could be argued that this preference is due to the layer distribution of supramammillary fibers. However, our results suggest an additional target

component of this innervation, since we found collaterals from the supramammillary nuclei purposely target also semilunar granule cells that were out from this area.

In summary, semilunar granule cells receive a stronger excitatory input from mossy cells, and a preferential excitatory input from supramammillary fibers than typical granule cells. This fact could be translated in a higher excitability in semilunar granule cells than in typical granule cells, which could also explain the apparently higher amount of perisomatic inhibitory terminals found on them.

Subcortical control of cortical areas has been described for many brain regions, including the hippocampus. The most common mechanism for subcortical control is via disinhibition: inhibitory afferents targeting interneurons, e.g. the GABAergic septo-hippocampal projection (Freund and Antal, 1988; Gulyás et al., 1990; Miettinen and Freund, 1992a; b; Acsády et al., 1993). This is an interesting amplification mechanism that allows a comparatively scarce inhibitory projection to exert its effect on a large population of principal cells. Other subcortical connections that are not clearly inhibitory can target synaptically some neurons but their action is mainly through metabotropic receptors. Although the projection from the supramammillary nuclei on granule cells is well known (Maglóczky et al., 1994), the fact that concentrates on a special type of granule cells can offer an explanation of the results described by Mizumori et al. (1989), indicating that supramammilary innervation enhances perforant-path elicited population spikes in the dentate gyrus and therefore facilitate information flow in the rat dentate gyrus. The reality is more complex, since at the same time the activation of the semilunar granule cells will produce the firing of parvalbumin basket cells causing inhibition, but this inhibition will induce synchronization and should coordinate with perisomatic inhibition on dentate interneurons coming from the septum that will silent them. The subcortical innervation coming from the septum can be coordinated with the supramammillary nucleus since there is a projection from supramammillary to septum (Borhegyi and Freund, 1998; Kiss et al., 2000).

Exciting a few granule cells that are located in a prevalent position in the dentate gyrus circuitry can be an efficient way of amplification. The same number of boutons from the supramammillary nucleus distributed uniformly all over the population of granule cells would have a comparatively small effect on the dentate gyrus circuitry when compared with the formation of excitatory baskets concentrated on semilunar granule cells that are situated in a privileged position in the dentate gyrus. The fact that semilunar granule cells contact

parvalbumin basket cells and hilar mossy cells in their way to CA3 helps in this purpose. These two latter cell types have large axonic arbors containing thousands of boutons that extend widely in the dentate gyrus. They are also highly excitable, mossy cells presenting comparatively poor perisomatic inhibition (Livsey and Vicini, 1992; Scharfman, 1992, 1993). Therefore, although both typical and semilunar granule cells have very restricted axonic arbors contacting rather few cells, the innervation of a few mossy cells and a few parvalbumin basket cells by a semilunar granule cell can control the activity of large numbers of typical granule cells, and produce as a result a widespread effect in the dentate gyrus. Considering that the firing ratio of granule cells under physiological conditions is low but effective (Staley et al., 1992; Penttonen et al., 1997; Henze et al., 2002), this mechanism could control the firing of certain granule cells and filter the information that reaches the CA3. On the whole, these data suggest that the supramammillary can control dentate gyrus activity in a feedforward manner via semilunar granule cells.

Functional differences among the principal cells of an hippocampal area has been proved recently in the CA1 (Lee et al., 2014). These authors demonstrate the presence of distinct pyramidal cell populations that show different interactions with local parvalbumin-positive basket cells. Interestingly, they found that pyramidal cells located in the superficial layer of stratum pyramidale established excitatory inputs to parvalbumin-positive basket cells more frequently than pyramidal cells located in deeper layers of stratum pyramidale.

The control of the dentate gyrus activity can have relevance in the development of epilepsy. Semilunar granule cells, as common granule cells and parvalbumin basket cells, are resilient to damage, whereas mossy cells are highly sensitive to cell death. Overexcitation of the dentate gyrus will often produce loss of mossy cells with little or no loss of the other cell types. Under these conditions the activation of semilunar granule cells will not induce recurrent activation of the circuitry via mossy cells but will still induce inhibition via parvalbumin basket cells. This could be the underlying circuitry under the silent period observed after the loss of mossy cells and previous to the development of substantial mossy fiber sprouting on granule cells.

Although it has been postulated that after dentate gyrus overexcitation the parvalbumin basket cells become silent causing an overexcitation leading to epilepsy (Sloviter, 1991; Sloviter et al., 2003), there are proof that in fact the parvalbumin basket cells become more active (for a review see Bernard et al., 1998). The dormant basket cells hypothesis does not fit well with the silent period that has been described after induction of status epilepticus.

The excess of inhibition may activate compensatory mechanisms, leading granule cells into the acquisition of new routes of activation via sprouting. Some authors have tried to block the generation of sprouting as a demonstration of its relevance in the induction of epileptic crisis, and as a possible way to avoid the generation of epilepsy after dentate damage (Buckmaster, 2004; Toyoda and Buckmaster, 2005). The blocking of the supramammillary-hippocampus pathway offers a vehicle to try to suppress the generation of sprouting by avoiding the overactivation of parvalbumin basket cells.

CONCLUSIONS

1. Parvalbumin basket cells receive an important perisomatic excitatory input, similar to the inhibitory input, as shown by the expression of post-synaptic markers PSD95 and Gephyrin.
2. Perisomatic innervation on parvalbumin basket cells by mossy cells is negligible.
3. The main excitatory perisomatic input onto parvalbumin basket cells in the dentate gyrus is made by Timm-positive fibers.
4. Parvalbumin basket cells with somata located in the border between the granule cell layer and hilus receive more Timm-positive perisomatic input than parvalbumin interneurons with their somata sitting in the upper half of the granule cell layer, or in the inner molecular layer.
5. Semilunar granule cells are the origin of the Timm-positive innervation of parvalbumin interneurons in the dentate gyrus.
6. Semilunar granule cells present morphological characteristics that differentiates them from typical granule cells: their somata is located in the inner molecular layer and spread their dendrites in a wider region of the molecular layer. Some of them present dendrites entering the hilus, axons originating from dendrites and somatic spines. Their axon travel through the inner molecular layer and sends collaterals into the granule cell layer.
7. Semilunar granule cells represent less than 1% of the total granule cells in the dentate gyrus and are located in the inner molecular layer and juxtamolecular border with the granule cell layer. They are more frequent in ventral levels, and in the apex of the dentate gyrus.
8. Semilunar granule cells express cell markers for principal cells (CAMKII) and adult granule cells (calbindin, Prox1). They do not express calretinin or parvalbumin, and only rarely the CART peptide.
9. Semilunar granule cells in the border between the inner molecular layer and granule cell layer express more often cell activity markers c-Fos and pan-Fos than typical granule cells.
10. Semilunar granule cells receive abundant inhibitory perisomatic innervation from parvalbumin and cholecystokinin-positive interneurons.
11. Fibers arising from the supramammillary nuclei innervate semilunar granule cells and outer molecular layer granule cells on the perisomatic region. This excitatory innervation on semilunar granule cells is target-specific.
12. Low transient overexcitation of the dentate gyrus using Zn^{2+} quelator DEDTC induces c-Fos expression in semilunar granule cells without general induction of the granule cells. This induction is coupled with c-Fos expression in mossy cells and dentate interneurons.

13. Semilunar granule cells and parvalbumin basket cells are resilient to cell damage in the kainic acid, pilocarpine and pentylenetetrazole models of epilepsy.
14. Changes in the dentate gyrus cell populations is a slow process in the pentylenetetrazole-induced kindling model of epilepsy. Loss of mossy cells and an increase in the expression of parvalbumin by the basket cells is observed one month after kindling. Somatostatin cell population is not changed in this epilepsy model.

RESUMEN

INTRODUCCIÓN

El giro dentado es una estructura cortical que cumple una importante función en la consolidación de la memoria espacial y el aprendizaje. Ha sido objeto de numerosos estudios, debido a su especial susceptibilidad de ser dañado en procesos como epilepsia de lóbulo temporal o isquemia (para una revisión: Amaral et al., 2007). Ampliar el conocimiento de su circuitería local, así como de su modulación, es esencial para poder entender con más claridad por qué es una región tan susceptible de convertirse en foco de crisis epilépticas, así como de las consecuencias de este fenómeno.

Se sabe que las interneuronas basket parvalbúmina tienen un papel esencial en la regulación del correcto funcionamiento del giro dentado. Al inervar de forma perisomática a las células granulares y presentar un umbral de disparo bastante bajo, son capaces de mantener inhibidas a una población amplia de células granulares y sincronizar su disparo.

Las células granulares, células principales del giro dentado, juegan un papel muy importante en la patogénesis de la epilepsia del lóbulo temporal (Houser, 1992). Aunque en la mayoría de modelos experimentales de epilepsia estas células no sufren daño celular, sí participan en la remodelación de la circuitería local derivada de una crisis epiléptica. Los axones de las células granulares – las llamadas fibras musgosas – generan colaterales axónicas que proyectan de forma aberrante a la capa molecular interna del giro dentado, fenómeno conocido como “sprouting”. En condiciones normales, las células granulares reciben contactos sinápticos por parte de otra población de células glutamatérgicas presentes en el hilus, las células musgosas. Una de las hipótesis más aceptada para explicar la remodelación de la circuitería local del giro dentado sugeriría que la pérdida de las células musgosas (muy susceptibles de sufrir daño celular tras crisis epiléptica) y la consecuente pérdida de su inervación excitadora sobre las células granulares en la región de la capa molecular interna, favorecería el establecimiento de nuevas conexiones sinápticas entre las colaterales aberrantes de las fibras musgosas y las dendritas de las propias células granulares. De este modo, se generaría un circuito excitador recurrente difícil de controlar por el sistema inhibidor local.

Por otra parte, otra de las hipótesis comúnmente aceptadas para explicar el hecho de que el giro dentado se convierta con tanta facilidad en foco de nuevas crisis epilépticas es la conocida como “hipótesis de las dormant basket cells” (Sloviter, 1991). En ella se postula que aunque en la mayoría de los modelos de epilepsia experimental no parece haber una reducción del

número de interneuronas basket parvalbúmina, sí se produce una pérdida de su capacidad inhibidora debido a la pérdida del input excitador recibido de las células musgosas. Este hecho daría lugar a un fallo en la inhibición del circuito excitador recurrente de las células granulares, y por tanto facilitaría que el giro dentado se convirtiese en foco epiléptico. Sin embargo, este fenómeno no se cumple en todos los modelos de epilepsia experimental (Buckmaster et al., 2000).

Se ha demostrado que esta población de interneuronas basket parvalbúmina está inervada en animales control por fibras Timm-positivas pertenecientes posiblemente a las células granulares (Blasco-Ibáñez et al., 2000), y que esta inervación aumenta en situación de epilepsia experimental (Kotti et al., 1997), por lo que no habría motivo a priori para que disminuya su función inhibidora. Una mejor comprensión de la importancia relativa de cada uno de los dos inputs excitadores que reciben las interneuronas basket parvalbúmina (de las células musgosas y de las células granulares) sería esencial para poder interpretar el funcionamiento del giro dentado en situación normal y tras las alteraciones producidas tras status epilepticus.

Recientemente ha sido caracterizado con mayor detalle un tipo de célula granular que ya fue descrito originalmente por Ramón y Cajal (1911). Estas células granulares, denominadas semilunares (Williams et al., 2007; Larimer and Strowbridge, 2010), se sitúan en el borde entre el estrato molecular interno y externo, y presentan colaterales en la capa granular, como las granulares que inervan a las células parvalbúmina. Sus dendritas en la capa molecular externa son más extensas que las de las células granulares típicas. Aunque son también glutamatérgicas y excitan monosinápticamente a interneuronas del hilus y a las células musgosas, sus características electrofisiológicas son diferentes de las células granulares típicas. El número y localización de estas células las convertirían en un candidato plausible a ser el tipo de célula granular que inerva las células parvalbúmina.

OBJETIVOS

De acuerdo a lo expuesto anteriormente, establecemos como hipótesis de trabajo que las células granulares semilunares son las encargadas del control perisomático de las interneuronas parvalbúmina del giro dentado. Por tanto, nuestro objetivo principal es estudiar los diferentes inputs excitadores perisomáticos sobre interneuronas parvalbúmina en el giro

dentado, y confirmar el origen de esta inervación por parte de las células granulares semilunares. En segundo lugar, nos propusimos integrar a las células granulares semilunares en la circuitería local desde un punto de vista anatómico. Finalmente, estudiamos las posibles implicaciones de esta inervación en diferentes modelos de epilepsia animal.

Los objetivos parciales de esta tesis son:

- Estudio del input excitador sobre las interneuronas parvalbúmina del giro dentado. Análisis cuantitativo mediante microscopía confocal del número de especializaciones postsinápticas excitadoras e inhibidoras en la región perisomática de las interneuronas parvalbúmina del giro dentado.
- Estudio del input perisomático por parte de las células musgosas sobre las interneuronas parvalbúmina en el giro dentado a nivel de microscopía confocal y electrónica.
- Estudio del input perisomático excitador por parte de las células granulares típicas y semilunares a nivel de microscopía óptica y electrónica.
- Estudio del número de células granulares ectópicas y semilunares, y estudio de su presencia durante el desarrollo postnatal.
- Caracterización morfológica de las células granulares semilunares del giro dentado.
- Caracterización neuroquímica de las células granulares semilunares y las células granulares ectópicas mediante estudios de colocalización de diferentes marcadores en animales transgénicos con expresión de la proteína YFP por parte de células excitadoras.
- Estudio del input excitador e inhibidor que reciben las células granulares semilunares, a nivel de microscopía óptica y electrónica.
- Estudio de la supervivencia y actividad de las células granulares semilunares, células musgosas e interneuronas parvalbúmina en tres modelos diferentes de epilepsia experimental: kindling inducido con pentylenetetrazole, status epilepticus inducido con ácido kaínico y DEDTC, y status epilepticus inducido con pilocarpina.

DESARROLLO EXPERIMENTAL Y RESULTADOS

En primer lugar se estudió la inervación perisomática excitadora sobre las interneuronas parvalbúmina, primero en comparación con la inhibidora, y seguidamente por parte de dos posibles candidatos expuestos anteriormente: las células musgosas del hilus y las células granulares localizadas en la capa molecular interna del giro dentado y que por su morfología se han denominado "células granulares semilunares". Para cumplir este objetivo parcial, se llevó a cabo un estudio del input sináptico que reciben las interneuronas basket parvalbúmina a nivel de microscopía confocal y, para evitar posibles confusiones debidas a falsos positivos, a nivel de microscopía electrónica. Nuestros resultados indican que las interneuronas parvalbúmina-positivas reciben contactos sinápticos en la capa molecular interna por parte de las células musgosas, pero no en la región perisomática. Sin embargo, sí encontramos que una misma célula granular semilunar establecía múltiples contactos sinápticos en las dendritas de la capa molecular interna y tronco dendrítico de las interneuronas parvalbúmina-positivas, lo que parece corroborar que el principal control excitador perisomático sobre esta población de interneuronas es establecido por células granulares, y más concretamente, por una subpoblación de éstas: las células granulares semilunares.

Una vez hallada esta inervación, nuestro siguiente objetivo fue caracterizar a esta población de células granulares semilunares, utilizando para ello diferentes aproximaciones. En primer lugar, llevamos a cabo un estudio de sus características morfológicas. Nuestros resultados indican que las células granulares semilunares forman una población heterogénea a pesar de que comparten un patrón de arborización dendrítica mucho más extenso que las granulares típicas. Las características morfológicas más llamativas son: (1) del cuerpo celular salen varias dendritas principales, en lugar de una sola dendrita apical como es el caso de las granulares típicas; (2) las dendritas se extienden en paralelo a la capa de células granulares hasta que empiezan a dirigirse hacia la fisura hipocámpica; (3) algunas dendritas atraviesan el estrato granular; y (4) el segmento inicial del axón sale en ocasiones de una de las dendritas en lugar del soma (hecho muy poco frecuente en las granulares típicas). Sin embargo, ninguna de estas características parecía ser identificativa de las células granulares semilunares encargadas de la inervación de las interneuronas basket parvalbúmina.

Un análisis de Sholl de células semilunares llenadas intracelularmente muestra un patrón de arborización muy diferente al de las células granulares típicas, como era de esperar. Sin

embargo, no hemos encontrado mediante esta técnica ningún patrón que permita diferenciar inequívocamente diferentes subpoblaciones dentro de las células granulares semilunares.

El estudio de estas células a nivel de microscopía electrónica no reveló ninguna diferencia significativa a nivel cualitativo respecto a los orgánulos intracelulares, si bien una mayor presencia de aparato de Golgi. Sin embargo, sí observamos la presencia puntual de pequeñas protrusiones somáticas similares a espinas, pero que sólo en un muy bajo porcentaje reciben sinapsis excitadoras. La presencia de protrusiones somáticas similares a espinas también se observó en células llenadas intracelularmente.

La siguiente aproximación, dado que el análisis morfológico no había sido concluyente para distinguir la subpoblación de células semilunares de nuestro interés, fue un estudio fenotípico de estas células. Para ello, utilizamos un animal transgénico en el que la proteína YFP se expresa bajo el promotor Thy1, resultando en un marcaje específico de neuronas principales, incluidas las semilunares. El análisis de colocalización a nivel de microscopía confocal de las células semilunares YFP-positivas con marcadores de células principales (CAMKII), células granulares (Prox1), y dada su diferente dinámica del calcio respecto a las granulares típicas, con proteínas ligantes de calcio (PV, CB y CR) tampoco nos permitió una distinción inequívoca de esta población de células. El péptido CART tampoco nos permitió definir la población de células granulares semilunares.

A continuación, dado que se ha descrito que las células granulares semilunares reciben mayor inervación por parte de las células musgosas, comprobamos si este hecho se traduce en una mayor expresión del marcador de actividad celular pan-Fos en condiciones normales. Nuestros resultados indican que hay una mayor proporción de células semilunares c-Fos-positivas respecto al total de semilunares, que células granulares típicas c-Fos positivas respecto al total de células granulares.

La presencia de botones perisomáticos parvalbúmina-positivos sobre las células granulares semilunares nos hicieron establecer como nuevo objetivo el estudio de la inervación perisomática que éstas reciben. Para ello, combinamos estudios a nivel de microscopía óptica, confocal y electrónica, así como trazado de conexiones mediante la inyección intracraneal del trazador anterógrado BDA10KDa. Nuestros resultados indican que hay una inervación perisomática inhibidora sobre las células granulares semilunares por parte de las interneuronas

parvalbúmina y CCK, así como una inervación perisomática excitadora por fibras procedentes principalmente de los núcleos supramamilares.

Dada la elevada expresión de c-Fos por parte de las células granulares semilunares, y la inervación perisomática excitadora que reciben, planteamos si después de una sobreexcitación moderada se produce una activación selectiva de la población de células granulares semilunares. Para ello, analizamos de forma separada la acción de diferentes fármacos pro-convulsivos a dosis subconvulsivas: pentylenetetrazole, DEDTC y ácido kaínico. Nuestros resultados indican que hay una inducción de la expresión de c-Fos en las células semilunares en condiciones de excitación moderada.

Otro de los objetivos parciales planteados inicialmente en el proyecto de tesis era estudiar el comportamiento de las interneuronas parvalbúmina, células musgosas y células granulares semilunares en modelo de epilepsia experimental. Para ello, estudiamos la supervivencia de estas poblaciones celulares mediante los siguientes modelos de epilepsia experimental: *status epilepticus* inducido por ácido kaínico, *status epilepticus* inducido por pilocarpina, y modelo de kindling inducido por pentylenetetrazole. Los resultados obtenidos indican que hay una pérdida de células musgosas (pequeña y progresiva en el caso de kindling mediante pentylenetetrazole), pero no de células granulares semilunares ni de interneuronas parvalbúmina.

DISCUSIÓN

El presente trabajo intenta profundizar en los conocimientos existentes de la circuitería local del giro dentado. Ya existían datos previos de la existencia de una inervación sobre las interneuronas basket parvalbúmina por parte de fibras zincérgicas (Blasco-Ibáñez et al., 2000). Sin embargo, en el presente estudio se ha caracterizado por primera vez la fuente de esta inervación, que corresponde a las células granulares semilunares.

Dado su escaso número y su localización ectópica, las células granulares semilunares han sido obviadas en la mayor parte de estudios anatómicos y funcionales del giro dentado. Recientemente han aparecido estudios centrados en sus propiedades fisiológicas (Williams et al., 2007; Larimer and Strowbridge, 2010). Estos trabajos permiten entender la implicación de las células semilunares en la circuitería local del giro dentado, resaltando que son capaces de mantener su frecuencia de disparo durante largos periodos de tiempo, induciendo estados

activados del hilus y aumentando la excitación de las células musgosas (Larimer and Strowbridge, 2010). Además se ha comprobado que durante estos estados también ocurre una inhibición persistente en las células granulares, pero no hay datos relativos a la posible circuitería responsable de este hecho.

Nuestros resultados evidencian a nivel anatómico que las células granulares semilunares controlan perisomáticamente a la población de interneuronas basket parvalbúmina del estrato granular. Esta inervación podría ser la responsable de la inhibición persistente encontrada en las células granulares. Además, el control de las interneuronas basket parvalbúmina del giro dentado también tendría como consecuencia la regulación del disparo de las células granulares y por tanto del primer paso en la vía trisináptica del hipocampo.

La supervivencia de las células semilunares en modelo de epilepsia, junto con la muerte de las células musgosas, implicaría que las células granulares perderían el circuito excitador establecido con las células musgosas, pero no el circuito inhibitorio debido a las células basket parvalbúmina (mediada por las células semilunares). De este modo, en estadíos iniciales tras *status epilepticus*, el giro dentado permanecería silente. Solo cuando aparece el fenómeno de sprouting, el circuito inhibidor local perdería su capacidad de controlar el loop excitador recurrente y el giro dentado acabaría convirtiéndose en foco epiléptico.

De forma paralela, nuestros datos indican que las células granulares semilunares reciben una inervación perisomática diferente a las células granulares típicas. La inervación aferente de otras estructuras corticales, como es el caso de los núcleos supramamilares, de forma selectiva sobre subpoblaciones de células semilunares, parece estar relacionada con una función diferente de las células semilunares respecto a las granulares. Las células semilunares se encuentran, por tanto, en una ubicación única para regular el correcto funcionamiento del giro dentado, modulando los circuitos feed-back y feed-forward que se establecen.

Nuestro intento por dilucidar si todas las células semilunares participan en el control excitador de las interneuronas parvalbúmina, o bien si solo una pequeña subpoblación de células semilunares es la encargada de establecer esta inervación, ha resultado infructuoso. Las técnicas de que disponemos no nos han permitido distinguir inequívocamente diferente subpoblaciones dentro de las células semilunares. La inexistencia de un marcador característico conocido para esta subpoblación de células dificulta su estudio, así como las conclusiones que podemos extraer de los resultados obtenidos. Sin embargo, sí hemos logrado obtener una

caracterización morfológica y fenotípica general, así como una primera piedra en su integración en la circuitería del giro dentado.

CONCLUSIONES

Las conclusiones derivadas de la tesis se resumen en:

1. Las interneuronas parvalbúmina reciben un input perisomático excitador importante a nivel cuantitativo.
2. La inervación perisomática excitadora sobre las interneuronas parvalbúmina por parte de las células musgosas es despreciable en comparación con el input perisomático excitador total que reciben.
3. El input excitador mayoritario sobre interneuronas parvalbúmina en el giro dentado proviene de fibras Timm-positivas.
4. Las células parvalbúmina situadas en el estrato granular reciben mayor inervación Timm positiva que las situadas en el estrato molecular.
5. Las células granulares semilunares son la fuente de la inervación Timm-positiva sobre las interneuronas parvalbúmina del giro dentado.
6. Las células granulares semilunares presentes en la capa molecular interna y en el borde con la capa granular representan aproximadamente un 2% de la población total de células granulares del giro dentado. Son más frecuentes en el ápex del giro dentado, así como a medida que avanzamos a niveles más ventrales. Además, dentro de un mismo nivel, son más abundantes en la capa suprapiramidal respecto a la infrapiramidal.
7. Las células granulares semilunares presentan características morfológicas que las diferencian de las células granulares típicas: su cuerpo celular se encuentra en la capa molecular interna, y extienden sus dendritas ocupando una región más amplia en la capa molecular. Sus axones viajan a través de la capa molecular interna, en paralelo al estrato de somas hasta que lo atraviesan hasta llegar al hilus, donde establecen varias colaterales axónicas en su camino al estrato lucido de CA3. Presentan además colaterales axónicas en la capa granular. Una subpoblación de células granulares presentan dendritas que atraviesan el hilus, en otras ocasiones el axón parte de una dendrita principal, y en general presentan espinas somáticas con mayor frecuencia que las granulares típicas.

8. Las células granulares semilunares expresan marcadores de células principales (CAMKII) y de células granulares maduras (calbindina y Prox1). No expresan selectivamente CART o proteínas ligantes de calcio como parvalbúmina o calretinina.
9. Las células granulares semilunares están más activas en general, según muestran marcadores de actividad celular c-Fos y pan-Fos.
10. Las células granulares semilunares reciben inervación inhibidora de las dos poblaciones de interneuronas cuya diana es la región perisomática: parvalbúmina y CCK.
11. Las fibras procedentes de los núcleos supramamilares, inervan a las células granulares semilunares de forma selectiva, independientemente de su situación en la capa molecular.
12. La inducción de sobreexcitación moderada en el giro dentado mediante el quelante de Zn^{+2} DEDTC induce la expresión de c-Fos por parte de las células granulares semilunares sin inducir de modo generalizado la activación de las células granulares.
13. Las células granulares semilunares y las interneuronas parvalbúmina son resistentes al daño celular en modelos de epilepsia inducidos por pilocarpina, ácido kaínico o pentylenetetrazole.
14. Los cambios observados en el modelo de kindling inducido con pentylenetetrazole son lentos y progresivos. Se produce una pérdida de células musgosas, y un aumento de la expresión de parvalbúmina por parte de las interneuronas de los cestos. La población de interneuronas somatostatina no se ve afectada en estas condiciones.

REFERENCES

Abrahám H, Orsi G, Seress L. 2007. Ontogeny of cocaine- and amphetamine-regulated transcript (CART) peptide and calbindin immunoreactivity in granule cells of the dentate gyrus in the rat. Int J Dev Neurosci 25:265–74.

Acsády L, Halasy K, Freund TF. 1993. Calretinin is present in non-pyramidal cells of the rat hippocampus--III. Their inputs from the median raphe and medial septal nuclei. Neuroscience 52:829–41.

Acsády L, Kamondi a, Sík a, Freund TF, Buzsáki G. 1998. GABAergic cells are the major postsynaptic targets of mossy fibers in the rat hippocampus. J Neurosci 18:3386–3403.

Acsády L, Katona I, Martínez-Guijarro F-J, Buzsáki G, Freund TF. 2000. Unusual target selectivity of perisomatic inhibitory cells in the hilar region of the rat hippocampus. J Neurosci 20:6907–6919.

Altman J, Bayer SA. 1990. Migration and distribution of two populations of hippocampal granule cell precursors during the perinatal and postnatal periods. J Comp Neurol 301:365–81.

Amaral DG, Cowan WM. 1980. Subcortical afferents to the hippocampal formation in the monkey. J Comp Neurol 189:573–91.

Amaral DG, Kurz J. 1985. An analysis of the origins of the cholinergic and noncholinergic septal projections to the hippocampal formation of the rat. J Comp Neurol 240:37–59.

Amaral DG, Scharfman HE, Lavenex P. 2007. The dentate gyrus: fundamental neuroanatomical organization (dentate gyrus for dummies). Prog Brain Res 163.

Amaral DG. 1978. A golgi study of cell types in the hilar region of the hippocampus in the rat. J Comp Neurol 182:851–914.

Amrein I, Slomianka L, Lipp H-P. 2004. Granule cell number, cell death and cell proliferation in the dentate gyrus of wild-living rodents. Eur J Neurosci 20:3342–50.

Amrein I, Slomianka L. 2010. A morphologically distinct granule cell type in the dentate gyrus of the red fox correlates with adult hippocampal neurogenesis. Brain Res 1328:12–24.

Anderson P, Morris R, Amaral DG, Bliss T, O'Keefe J. 2007. The Hippocampus Book.

Babb TL, Brown WJ, Pretorius J, Davenport C, Lieb JP, Crandall PH. 1984. Temporal lobe volumetric cell densities in temporal lobe epilepsy. Epilepsia 25:729–40.

Bakst I, Avendano C, Morrison JH, Amaral DG. 1986. An experimental analysis of the origins of somatostatin-like immunoreactivity in the dentate gyrus of the rat. J Neurosci 6:1452–62.

Baranauskas G, David Y, Fleidervish IA. 2013. Spatial mismatch between the Na+ flux and spike initiation in axon initial segment. Proc Natl Acad Sci U S A 110:4051–6.

Barrett P, Davidson J, Morgan P. 2002. CART gene promoter transcription is regulated by a cyclic adenosine monophosphate response element. Obes Res 10:1291–8.

Bauer J. 2001. Interactions between hormones and epilepsy in female patients. Epilepsia 42 Suppl 3:20–2.

Bayer SA. 1980a. Development of the hippocampal region in the rat. I. Neurogenesis examined with 3H-thymidine autoradiography. J Comp Neurol 190:87–114.

Bayer SA. 1980b. Development of the hippocampal region in the rat. II. Morphogenesis during embryonic and early postnatal life. J Comp Neurol 190:115–34.

Ben-Ari Y, Tremblay E, Ottersen OP, Meldrum BS. 1980. The role of epileptic activity in hippocampal and “remote” cerebral lesions induced by kainic acid. Brain Res 191:79–97.

Ben-Ari Y. 1985. Limbic seizure and brain damage produced by kainic acid: mechanisms and relevance to human temporal lobe epilepsy. Neuroscience 14:375–403.

Bernard C, Esclapez M, Hirsch JC, Ben-ari Y. 1998. Interneurones are not so dormant in temporal lobe epilepsy: a critical reappraisal of the dormant basket cell hypothesis. Epilepsy Res 32:93–103.

Blasco-Ibáñez JM, Freund TF. 1997. Distribution, ultrastructure, and connectivity of calretinin-immunoreactive mossy cells of the mouse dentate gyrus. Hippocampus 7:307–320.

Blasco-Ibáñez JM, Martinez-Guijarro FJ, Freund TF. 1998. Enkephalin-containing interneurons are specialized to innervate other interneurons in the hippocampal CA1 region of the rat and guinea-pig. Eur J Neurosci 10:1784–1795.

Blasco-Ibáñez JM, Martínez-Guijarro F-J, Freund TF. 2000. Recurrent mossy fibers preferentially innervate parvalbumin-immunoreactive interneurons in the granule cell layer of the rat dentate gyrus. Neuroreport 11:3219–3225.

Blasco-Ibáñez JM, Poza-Aznar J, Crespo C, Marqués-Marí A-I, Gracia-Llanes FJ, Martínez-Guijarro F-J. 2004. Chelation of synaptic zinc induces overexcitation in the hilar mossy cells of the rat hippocampus. Neurosci Lett 355:101–104.

Bliss T V, Goddard G V, Riives M. 1983. Reduction of long-term potentiation in the dentate gyrus of the rat following selective depletion of monoamines. J Physiol 334:475–91.

Borhegyi Z, Freund TF. 1998. Dual projection from the medial septum to the supramammillary nucleus in the rat. Brain Res Bull 46:453–459.

Boulland J-L, Jenstad M, Boekel AJ, Wouterlood FG, Edwards RH, Storm-Mathisen J, Chaudhry F a. 2009. Vesicular glutamate and GABA transporters sort to distinct sets of vesicles in a population of presynaptic terminals. Cereb Cortex 19:241–248.

Brandt MD, Jessberger S, Steiner B, Kronenberg G, Reuter K, Bick-Sander A, Behrens W von der, Kempermann G. 2003. Transient calretinin expression defines early postmitotic step of neuronal differentiation in adult hippocampal neurogenesis of mice. Mol Cell Neurosci 24:603–613.

Buckmaster PS, Dudek FE. 1997. Neuron loss, granule cell axon reorganization, and functional changes in the dentate gyrus of epileptic kainate-treated rats. J Comp Neurol 385:385–404.

Buckmaster PS, Jongen-Rêlo a L, Davari SB, Wong EH. 2000. Testing the disinhibition hypothesis of epileptogenesis in vivo and during spontaneous seizures. J Neurosci 20:6232–6240.

Buckmaster PS, Strowbridge BW, Kunkel DD, Schmiege DL, Schwartzkroin PA. 1992. Mossy cell axonal projections to the dentate gyrus molecular layer in the rat hippocampal slice. Hippocampus 2:349–62.

Buckmaster PS, Wenzel HJ, Kunkel DD, Schwartzkroin P a. 1996. Axon arbors and synaptic connections of hippocampal mossy cells in the rat in vivo. J Comp Neurol 366:271–292.

Buckmaster PS. 2004. Prolonged infusion of tetrodotoxin does not block mossy fiber sprouting in pilocarpine-treated rats. Epilepsia 45:452–8.

Buhl EH, Szilagyi T, Somogyi P. 1997. Effect, number and location of synapses made by single pyramidal cells onto aspiny interneurones of cat visual cortex. J Physiol 500:689–713.

Bundman MC, Gall CM. 1994. Ultrastructural plasticity of the dentate gyrus granule cells following recurrent limbic seizures: II. Alterations in somatic synapses. Hippocampus 4:611–22.

Bundman MC, Pico RM, Gall CM. 1994. Ultrastructural plasticity of the dentate gyrus granule cells following recurrent limbic seizures: I. Increase in somatic spines. Hippocampus 4:601–10.

Cardoso A, Freitas-da-Costa P, Carvalho LS, Lukoyanov N V. 2010. Seizure-induced changes in neuropeptide Y-containing cortical neurons: Potential role for seizure threshold and epileptogenesis. Epilepsy Behav 19:559–67.

Carre GP, Harley CW. 1991. Population spike facilitation in the dentate gyrus following glutamate to the lateral supramammillary nucleus. Brain Res 568:307–310.

Carter DS, Harrison AJ, Falenski KW, Blair RE, DeLorenzo RJ. 2008. Long-term decrease in calbindin-D28K expression in the hippocampus of epileptic rats following pilocarpine-induced status epilepticus. Epilepsy Res 79:213–23.

Cavalheiro EA, Leite JP, Bortolotto ZA, Turski WA, Ikonomidou C, Turski L. 1991. Long-term effects of pilocarpine in rats: structural damage of the brain triggers kindling and spontaneous recurrent seizures. Epilepsia 32:778–82.

Cavazos JE, Golarai G, Sutula TP. 1991. Mossy fiber synaptic reorganization induced by kindling: time course of development, progression, and permanence. J Neurosci 11:2795–803.

Cavazos JE, Sutula TP. 1990. Progressive neuronal loss induced by kindling: a possible mechanism for mossy fiber synaptic reorganization and hippocampal sclerosis. Brain Res 527:1–6.

Celio MR. 1990. Calbindin D-28k and parvalbumin in the rat nervous system. Neuroscience 35:375–475.

Chow A, Erisir A, Farb C, Nadal MS, Ozaita A, Lau D, Welker E, Rudy B. 1999. K+ Channel Expression Distinguishes Subpopulations of Parvalbumin- and Somatostatin-Containing Neocortical Interneurons. J Neurosci 19:9332–9345.

Claiborne BJ, Amaral DG, Cowan WM. 1986. A light and electron microscopic analysis of the mossy fibers of the rat dentate gyrus. J Comp Neurol 246:435–58.

Claiborne BJ, Amaral DG, Cowan WM. 1990. Quantitative, three-dimensional analysis of granule cell dendrites in the rat dentate gyrus. J Comp Neurol 302:206–19.

Cobb SR, Buhl EH, Halasy K, Paulsen O, Somogyi P. 1995. Synchronization of neuronal activity in hippocampus by individual GABAergic interneurons. Nature 378:75–8.

Conner-Kerr TA, Simmons DR, Peterson GM, Terrian DM. 1993. Evidence for the corelease of dynorphin and glutamate from rat hippocampal mossy fiber terminals. J Neurochem 61:627–36.

Corda MG, Orlandi M, Lecca D, Carboni G, Frau V, Giorgi O. 1991. Pentylenetetrazol-induced kindling in rats: effect of GABA function inhibitors. Pharmacol Biochem Behav 40:329–33.

Deller T, Martinez a, Nitsch R, Frotscher M. 1996a. A novel entorhinal projection to the rat dentate gyrus: direct innervation of proximal dendrites and cell bodies of granule cells and GABAergic neurons. J Neurosci 16:3322–33.

Deller T, Nitsch R, Frotscher M. 1996b. Heterogeneity of the commissural projection to the rat dentate gyrus: a Phaseolus vulgaris leucoagglutinin tracing study. Neuroscience 75:111–121.

Desmond NL, Levy WB. 1982. A quantitative anatomical study of the granule cell dendritic fields of the rat dentate gyrus using a novel probabilistic method. J Comp Neurol 212:131–45.

Desmond NL, Levy WB. 1985. Granule cell dendritic spine density in the rat hippocampus varies with spine shape and location. Neurosci Lett 54:219–224.

Díaz-Cintra S, Xue B, Spigelman I, Van K, Wong AM, Obenaus A, Ribak CE. 2009. Dentate granule cells form hilar basal dendrites in a rat model of hypoxia-ischemia. Brain Res 1285:182–7.

Domínguez M-I, Blasco-Ibáñez JM, Crespo C, Marqués-Marí A-I, Martínez-Guijarro F-J. 2003a. Calretinin/PSA-NCAM immunoreactive granule cells after hippocampal damage produced by kainic acid and DEDTC treatment in mouse. Brain Res 966:206–217.

Domínguez M-I, Blasco-Ibáñez JM, Crespo C, Marqués-Marí A-I, Martnez-Guijarro FJ. 2003b. Zinc chelation during non-lesioning overexcitation results in neuronal death in the mouse hippocampus. Neuroscience 116:791–806.

Domínguez M-I, Blasco-Ibáñez JM, Crespo C, Nacher J, Marqués-Marí A-I, Martínez-Guijarro F-J. 2006. Neural overexcitation and implication of NMDA and AMPA receptors in a mouse model of temporal lobe epilepsy implying zinc chelation. Epilepsia 47:887–899.

Donato F, Rompani SB, Caroni P. 2013. Parvalbumin-expressing basket-cell network plasticity induced by experience regulates adult learning. Nature 504:272–6.

Dragunow M, Faull R. 1989. The use of c-fos as a metabolic marker in neuronal pathway tracing. J Neurosci Methods 29:261–265.

Dudek FE, Sutula TP. 2007. Epileptogenesis in the dentate gyrus: a critical perspective. Prog Brain Res 163:755–73.

Eichenbaum H. 2004. Hippocampus: cognitive processes and neural representations that underlie declarative memory. Neuron 44:109–20.

Feng G, Mellor RH, Bernstein M, Keller-Peck C, Nguyen QT, Wallace M, Nerbonne JM, Lichtman JW, Sanes JR. 2000. Imaging neuronal subsets in transgenic mice expressing multiple spectral variants of GFP. Neuron 28:41–51.

Fremeau RT, Troyer MD, Pahner I, Nygaard GO, Tran CH, Reimer RJ, Bellocchio EE, Fortin D, Storm-Mathisen J, Edwards RH. 2001. The expression of vesicular glutamate transporters defines two classes of excitatory synapse. Neuron 31:247–260.

Freund TF, Antal M. 1988. GABA-containing neurons in the septum control inhibitory interneurons in the hippocampus. Nature 336:170–3.

Freund TF, Buzsáki G. 1996. Interneurons of the hippocampus. Hippocampus 6:347–470.

Freund TF, Gulyás AI, Acsády L, Görcs T, Tóth K. 1990. Serotonergic control of the hippocampus via local inhibitory interneurons. Proc Natl Acad Sci U S A 87:8501–8505.

Freund TF, Hájos N, Acsády L, Górcs TJ, Katona I. 1997. Mossy Cells of the Rat Dentate Gyrus are lmmunoreactive for Calcitonin Gene-related Peptide (CGRP). Eur J Neurosci 9:1815–1830.

Freund TF, Katona I. 2007. Perisomatic inhibition. Neuron 56:33–42.

Fritschy J-M, Harvey RJ, Schwarz G. 2008. Gephyrin: where do we stand, where do we go? Trends Neurosci 31:257–64.

Frotscher M, Jonas P, Sloviter RS. 2006. Synapses formed by normal and abnormal hippocampal mossy fibers. Cell Tissue Res 326:361–367.

Frotscher M, Leranth C. 1988. Catecholaminergic innervation of pyramidal and GABAergic nonpyramidal neurons in the rat hippocampus. Double label immunostaining with antibodies against tyrosine hydroxylase and glutamate decarboxylase. Histochemistry 88:313–9.

Frotscher M, Léránth C. 1985. Cholinergic innervation of the rat hippocampus as revealed by choline acetyltransferase immunocytochemistry: a combined light and electron microscopic study. J Comp Neurol 239:237–46.

Frotscher M, Léránth C. 1986. The cholinergic innervation of the rat fascia dentata: identification of target structures on granule cells by combining choline acetyltransferase immunocytochemistry and Golgi impregnation. J Comp Neurol 243:58–70.

Frotscher M, Seress L, Schwerdtfeger WK, Buhl E. 1991. The mossy cells of the fascia dentata: a comparative study of their fine structure and synaptic connections in rodents and primates. J Comp Neurol 312:145–63.

Fujise N, Liu Y, Hori N, Kosaka T. 1997. Distribution of calretinin immunoreactivity in the mouse dentate gyrus: II. Mossy cells, with special reference to their dorsoventral difference in calretinin immunoreactivity. Neuroscience 82:181–200.

Gaarskjaer FB. 1978. Organization of the mossy fiber system of the rat studied in extended hippocampi. I. Terminal area related to number of granule and pyramidal cells. J Comp Neurol 178:49–72.

Galeeva A, Treuter E, Tomarev S, Pelto-Huikko M. 2007. A prospero-related homeobox gene Prox-1 is expressed during postnatal brain development as well as in the adult rodent brain. Neuroscience 146:604–16.

Gall C, Brecha N, Karten HJ, Chang KJ. 1981. Localization of enkephalin-like immunoreactivity to identified axonal and neuronal populations of the rat hippocampus. J Comp Neurol 198:335–50.

Gass P, Prior P, Kiessling M. 1995. Correlation between seizure intensity and stress protein expression after limbic epilepsy in the rat brain. Neuroscience 65:27–36.

Gaykema RP, Luiten PG, Nyakas C, Traber J. 1990. Cortical projection patterns of the medial septum-diagonal band complex. J Comp Neurol 293:103–24.

Givens B, Sarter M. 1997. Modulation of cognitive processes by transsynaptic activation of the basal forebrain. Behav Brain Res 84:1–22.

Gómez-Climent MA, Castillo-Gómez E, Varea E, Guirado R, Blasco-Ibáñez JM, Crespo C, Martínez-Guijarro F-J, Nácher J. 2008. A population of prenatally generated cells in the rat paleocortex maintains an immature neuronal phenotype into adulthood. Cereb Cortex 18:2229–2240.

Gray WP, Sundstrom LE. 1998. Kainic acid increases the proliferation of granule cell progenitors in the dentate gyrus of the adult rat. Brain Res 790:52–9.

Grecksch G, Becker A, Rauca C. 1997. Effect of age on pentylenetetrazol-kindling and kindling-induced impairments of learning performance. Pharmacol Biochem Behav 56:595–601.

Van Groen T, Miettinen P, Kadish I. 2003. The entorhinal cortex of the mouse: organization of the projection to the hippocampal formation. Hippocampus 13:133–49.

Grubb MS, Burrone J. 2010. Activity-dependent relocation of the axon initial segment fine-tunes neuronal excitability. Nature 465:1070–4.

Grubb MS, Shu Y, Kuba H, Rasband MN, Wimmer VC, Bender KJ. 2011. Short- and long-term plasticity at the axon initial segment. J Neurosci 31:16049–55.

Gulyás AI, Görcs TJ, Freund TF. 1990. Innervation of different peptide-containing neurons in the hippocampus by GABAergic septal afferents. Neuroscience 37:31–44.

Gulyás AI, Hájos N, Freund TF. 1996. Interneurons containing calretinin are specialized to control other interneurons in the rat hippocampus. J Neurosci 16:3397–411.

Gulyás AI, Megías M, Emri Z, Freund TF. 1999. Total number and ratio of excitatory and inhibitory synapses converging onto single interneurons of different types in the CA1 area of the rat hippocampus. J Neurosci 19:10082–97.

Gupta a., Elgammal FS, Proddutur a., Shah S, Santhakumar V. 2012. Decrease in Tonic Inhibition Contributes to Increase in Dentate Semilunar Granule Cell Excitability after Brain Injury. J Neurosci 32:2523–2537.

Hájos N, Acsady L, Freund TF. 1996. Target selectivity and neurochemical characteristics of VIP-immunoreactive interneurons in the rat dentate gyrus. Eur J Neurosci 8:1415–31.

Halasy K, Somogyi P. 1993. Distribution of GABAergic synapses and their targets in the dentate gyrus of rat: a quantitative immunoelectron microscopic analysis. J Hirnforsch 34:299–308.

Hamani C, Paulo I de, Mello LEAM. 2005. Neo-Timm staining in the thalamus of chronically epileptic rats. Brazilian J Med Biol Res 38:1677–1682.

Han ZS, Buhl EH, Lörinczi Z, Somogyi P. 1993. A high degree of spatial selectivity in the axonal and dendritic domains of physiologically identified local-circuit neurons in the dentate gyrus of the rat hippocampus. Eur J Neurosci 5:395–410.

Hara T, Nakamura K, Matsui M, Yamamoto A, Nakahara Y, Suzuki-Migishima R, Yokoyama M, Mishima K, Saito I, Okano H, Mizushima N. 2006. Suppression of basal autophagy in neural cells causes neurodegenerative disease in mice. Nature 441:885–889.

Henze DA, Wittner L, Buzsáki G. 2002. Single granule cells reliably discharge targets in the hippocampal CA3 network in vivo. Nat Neurosci 5:790–5.

Hernández-Miranda LR, Parnavelas JG, Chiara F. 2010. Molecules and mechanisms involved in the generation and migration of cortical interneurons. ASN Neuro 2:e00031.

Houser CR, Esclapez M. 1996. Vulnerability and plasticity of the GABA system in the pilocarpine model of spontaneous recurrent seizures. Epilepsy Res 26:207–18.

Houser CR, Miyashiro JE, Swartz BE, Walsh GO, Rich JR, Delgado-Escueta a V. 1990. Altered patterns of dynorphin immunoreactivity suggest mossy fiber reorganization in human hippocampal epilepsy. J Neurosci 10:267–282.

Houser CR. 1992. Morphological changes in the dentate gyrus in human temporal lobe epilepsy. Epilepsy Res Suppl 7:223–34.

Houser CR. 2007. Interneurons of the dentate gyrus: an overview of cell types, terminal fields and neurochemical identity. Prog Brain Res 163:217–232.

Howard AL, Tamas G, Soltesz I. 2005. Lighting the chandelier: new vistas for axo-axonic cells. Trends Neurosci 28:310–6.

Hunter RG, Lim MM, Philpot KB, Young LJ, Kuhar MJ. 2005. Species differences in brain distribution of CART mRNA and CART peptide between prairie and meadow voles. Brain Res 1048:12–23.

Iwano T, Masuda A, Kiyonari H, Enomoto H, Matsuzaki F. 2012. Prox1 postmitotically defines dentate gyrus cells by specifying granule cell identity over CA3 pyramidal cell fate in the hippocampus. Development 139:3051–62.

Jackson AC, Nicoll RA. 2011. The expanding social network of ionotropic glutamate receptors: TARPs and other transmembrane auxiliary subunits. Neuron 70:178–99.

Jinde S, Zsiros V, Jiang Z, Nakao K, Pickel J, Kohno K, Belforte JE, Nakazawa K. 2012. Hilar mossy cell degeneration causes transient dentate granule cell hyperexcitability and impaired pattern separation. Neuron 76:1189–200.

Jinde S, Zsiros V, Nakazawa K. 2013. Hilar mossy cell circuitry controlling dentate granule cell excitability. Front Neural Circuits 7:14.

Jones DC, Lakatos A, Rogge GA, Kuhar MJ. 2009. Regulation of cocaine- and amphetamine-regulated transcript mRNA expression by calcium-mediated signaling in GH3 cells. Neuroscience 160:339–47.

Jones SP, Rahimi O, O'Boyle MP, Diaz DL, Claiborne BJ. 2003. Maturation of granule cell dendrites after mossy fiber arrival in hippocampal field CA3. Hippocampus 13:413–27.

Kaifosh P, Losonczy A. 2014. The Inside Track: Privileged Neural Communication through Axon-Carrying Dendrites. Neuron 83:1231–1234.

Katona I, Sperlagh B, Sik A, Kafalvi A, Vizi ES, Mackie K, Freund TF. 1999. Presynaptically Located CB1 Cannabinoid Receptors Regulate GABA Release from Axon Terminals of Specific Hippocampal Interneurons. J Neurosci 19:4544–4558.

Kempermann G, Jessberger S, Steiner B, Kronenberg G. 2004. Milestones of neuronal development in the adult hippocampus. Trends Neurosci 27:447–52.

Khachaturian H, Watson SJ, Lewis ME, Coy D, Goldstein A, Akil H. 1982. Dynorphin immunocytochemistry in the rat central nervous system. Peptides 3:941–54.

Kiss J, Csáki A, Bokor H, Shanabrough M, Leranth C. 2000. The supramammillo-hippocampal and supramammillo-septal glutamatergic/aspartatergic projections in the rat: a combined

[3H]D-aspartate autoradiographic and immunohistochemical study. Neuroscience 97:657–69.

Kneisler TB, Dingledine R. 1995. Spontaneous and synaptic input from granule cells and the perforant path to dentate basket cells in the rat hippocampus. Hippocampus 5:151–64.

Kobayashi M, Buckmaster PS. 2003. Reduced inhibition of dentate granule cells in a model of temporal lobe epilepsy. J Neurosci 23:2440–52.

Kolenkiewicz M, Robak a, Równiak M, Bogus-Nowakowska K, Całka J, Majewski M. 2009. Distribution of cocaine- and amphetamine-regulated transcript in the hippocampal formation of the guinea pig and domestic pig. Folia Morphol (Warsz) 68:23–31.

Kosaka T, Hama K, Wu J. 1984. GABAergic synaptic boutons in the granule cell layer of rat dentate gyrus. 293:353–359.

Kosaka T, Katsumaru H, Hama K, Wu JY, Heizmann CW. 1987. GABAergic neurons containing the Ca2+-binding protein parvalbumin in the rat hippocampus and dentate gyrus. Brain Res 419:119–30.

Kotti T, Riekkinen PJ, Miettinen R. 1997. Characterization of target cells for aberrant mossy fiber collaterals in the dentate gyrus of epileptic rat. Exp Neurol 146:323–330.

Koylu EO, Couceyro PR, Lambert PD, Kuhar MJ. 1998. Cocaine- and amphetamine-regulated transcript peptide immunohistochemical localization in the rat brain. J Comp Neurol 391:115–32.

Larimer P, Strowbridge BW. 2010. Representing information in cell assemblies: persistent activity mediated by semilunar granule cells. Nat Neurosci 13:213–222.

Laurberg S, Sørensen KE. 1981. Associational and commissural collaterals of neurons in the hippocampal formation (hilus fasciae dentatae and subfield CA3). Brain Res 212:287–300.

Lavado A, Lagutin O V, Chow LML, Baker SJ, Oliver G. 2010. Prox1 is required for granule cell maturation and intermediate progenitor maintenance during brain neurogenesis. PLoS Biol 8.

Lavado A, Oliver G. 2007. Prox1 expression patterns in the developing and adult murine brain. Dev Dyn 236:518–524.

Lee S-H, Marchionni I, Bezaire M, Varga C, Danielson N, Lovett-Barron M, Losonczy A, Soltesz I. 2014. Parvalbumin-Positive Basket Cells Differentiate among Hippocampal Pyramidal Cells. Neuron 82:1129–44.

Leite JP, Bortolotto ZA, Cavalheiro EA. 1990. Spontaneous recurrent seizures in rats: an experimental model of partial epilepsy. Neurosci Biobehav Rev 14:511–7.

Leranth C, Frotscher M. 1986. Synaptic connections of cholecystokinin-immunoreactive neurons and terminals in the rat fascia dentata: a combined light and electron microscopic study. J Comp Neurol 254:51–64.

Leranth C, Hajszan T. 2007. Extrinsic afferent systems to the dentate gyrus. Prog Brain Res 163:63–84.

Leranth C, Nitsch R. 1994. Morphological evidence that hypothalamic substance P-containing afferents are capable of filtering the signal flow in the monkey hippocampal formation. J Neurosci 14:4079–4094.

Lin Y, Skeberdis VA, Francesconi A, Bennett MVL, Zukin RS. 2004. Postsynaptic density protein-95 regulates NMDA channel gating and surface expression. J Neurosci 24:10138–48.

Lindsay RD, Scheibel AB. 1981. Quantitative analysis of the dendritic branching pattern of granule cells from adult rat dentate gyrus. Exp Neurol 73:286–97.

Liu Y, Fujise N, Kosaka T. 1996. Distribution of calretinin immunoreactivity in the mouse dentate gyrus. I. General description. Exp Brain Res 108:389–403.

Livsey CT, Vicini S. 1992. Slower spontaneous excitatory postsynaptic currents in spiny versus aspiny hilar neurons. Neuron 8:745–755.

Longair MH, Baker DA, Armstrong JD. 2011. Simple Neurite Tracer: open source software for reconstruction, visualization and analysis of neuronal processes. Bioinformatics 27:2453–4.

Longo B, Covolan L, Chadi G, Mello LE a M. 2003. Sprouting of mossy fibers and the vacating of postsynaptic targets in the inner molecular layer of the dentate gyrus. Exp Neurol 181:57–67.

Lorente De Nó R. 1934. Studies on the structure of the cerebral cortex. II. Continuation of the study of the ammonic system. J Psychol Neurol 46:113–177.

Löscher W. 2002. Animal models of epilepsy for the development of antiepileptogenic and disease-modifying drugs. A comparison of the pharmacology of kindling and post-status epilepticus models of temporal lobe epilepsy. Epilepsy Res 50:105–123.

Löscher W. 2011. Critical review of current animal models of seizures and epilepsy used in the discovery and development of new antiepileptic drugs. Seizure 20:359–368.

Lothman EW, Stringer JL, Bertram EH. 1992. The dentate gyrus as a control point for seizures in the hippocampus and beyond. Epilepsy Res Suppl 7:301–13.

Lübbers K, Frotscher M. 1988. Differentiation of granule cells in relation to GABAergic neurons in the rat fascia dentata. Combined Golgi/EM and immunocytochemical studies. Anat Embryol (Berl) 178:119–27.

Lübbers K, Wolff JR, Frotscher M. 1985. Neurogenesis of GABAergic neurons in the rat dentate gyrus: A combined autoradiographic and immunocytochemical study. Neurosci Lett 62:317–322.

Lübke J, Deller T, Frotscher M. 1997. Septal innervation of mossy cells in the hilus of the rat dentate gyrus: an anterograde tracing and intracellular labeling study. Exp Brain Res 114:423–432.

Lüttjohann A, Fabene PF, van Luijtelaar G. 2009. A revised Racine's scale for PTZ-induced seizures in rats. Physiol Behav 98:579–86.

Maglóczky Z, Acsády L, Freund TF. 1994. Principal cells are the postsynaptic targets of supramammillary afferents in the hippocampus of the rat. Hippocampus 4:322–34.

Maglóczky Z, Halász P, Vajda J, Czirják S, Freund TF. 1997. Loss of Calbindin-D28K immunoreactivity from dentate granule cells in human temporal lobe epilepsy. Neuroscience 76:377–85.

Manahan-Vaughan D. 2003. Regulation of Depotentiation and Long-term Potentiation in the Dentate Gyrus of Freely Moving Rats by Dopamine D2-like Receptors. Cereb Cortex 13:123–135.

Marqués-Marí A-I, Nacher J, Crespo C, Gutièrrez-Mecinas M, Martínez-Guijarro F-J, Blasco-Ibáñez JM. 2007. Loss of input from the mossy cells blocks maturation of newly generated granule cells. Hippocampus 17:510–524.

Marsicano G, Lutz B. 1999. Expression of the cannabinoid receptor CB1 in distinct neuronal subpopulations in the adult mouse forebrain. Eur J Neurosci 11:4213–4225.

Martí-Subirana A, Soriano E, García-Verdugo JM. 1986. Morphological aspects of the ectopic granule-like cellular populations in the albino rat hippocampal formation: a Golgi study. J Anat 144:31–47.

McCloskey DP, Hintz TM, Pierce JP, Scharfman HE. 2006. Stereological methods reveal the robust size and stability of ectopic hilar granule cells after pilocarpine-induced status epilepticus in the adult rat. Eur J Neurosci 24:2203–10.

McDonald AJ, Mascagni F, Mania I, Rainnie DG. 2005. Evidence for a perisomatic innervation of parvalbumin-containing interneurons by individual pyramidal cells in the basolateral amygdala. Brain Res 1035:32–40.

McIntyre DC, Poulter MO, Gilby K. 2002. Kindling: some old and some new. Epilepsy Res 50:79–92.

Megías M, Emri Z, Freund TF, Gulyás AI. 2001. Total number and distribution of inhibitory and excitatory synapses on hippocampal CA1 pyramidal cells. Neuroscience 102:527–540.

Mengual E, Casanovas-Aguilar C, Pérez-Clausell J, Giménez-Amaya J-M. 2001. Thalamic distribution of zinc-rich terminal fields and neurons of origin in the rat. Neuroscience 102:863–884.

Miettinen R, Freund TF. 1992a. Neuropeptide Y-containing interneurons in the hippocampus receive synaptic input from median raphe and GABAergic septal afferents. Neuropeptides 22:185–93.

Miettinen R, Freund TF. 1992b. Convergence and segregation of septal and median raphe inputs onto different subsets of hippocampal inhibitory interneurons. Brain Res 594:263–72.

Miles R, Tóth K, Gulyás AI, Hájos N, Freund TF. 1996. Differences between Somatic and Dendritic Inhibition in the Hippocampus. Neuron 16:815–823.

Mizumori SJ, McNaughton BL, Barnes CA. 1989. A comparison of supramammillary and medial septal influences on hippocampal field potentials and single-unit activity. J Neurophysiol 61:15–31.

Mongiat LA, Schinder AF. 2011. Adult neurogenesis and the plasticity of the dentate gyrus network. Eur J Neurosci 33:1055–61.

Moore RY, Halaris AE. 1975. Hippocampal innervation by serotonin neurons of the midbrain raphe in the rat. J Comp Neurol 164:171–83.

Morimoto K, Fahnestock M, Racine RJ. 2004. Kindling and status epilepticus models of epilepsy: rewiring the brain. Prog Neurobiol 73:1–60.

Morris RG, Garrud P, Rawlins JN, O'Keefe J. 1982. Place navigation impaired in rats with hippocampal lesions. Nature 297:681–3.

Morrison JH, Benoit R, Magistretti PJ, Ling N, Bloom FE. 1982. Immunohistochemical distribution of pro-somatostatin-related peptides in hippocampus. Neurosci Lett 34:137–42.

Moudy AM, Kunkel DD, Schwartzkroin PA. 1993. Development of dopamine-beta-hydroxylase-positive fiber innervation of the rat hippocampus. Synapse 15:307–18.

Mullen RJ, Buck CR, Smith AM. 1992. NeuN, a neuronal specific nuclear protein in vertebrates. Development 116:201–11.

Muramatsu R, Ikegaya Y, Matsuki N, Koyama R. 2008. Early-life status epilepticus induces ectopic granule cells in adult mice dentate gyrus. Exp Neurol 211:503–510.

Murphy BL, Danzer SC. 2011. Somatic translocation: a novel mechanism of granule cell dendritic dysmorphogenesis and dispersion. J Neurosci 31:2959–64.

Nadler J V, Perry BW, Cotman CW. 1980. Selective reinnervation of hippocampal area CA1 and the fascia dentata after destruction of CA3-CA4 afferents with kainic acid. Brain Res 182:1–9.

Nadler JV, Evenson DA, Smith EM. 1981. Evidence from lesion studies for epileptogenic and non-epileptogenic neurotoxic interactions between kainic acid and excitatory innervation. Brain Res 205:405–10.

Nakagawa E, Aimi Y, Yasuhara O, Tooyama I, Shimada M, McGeer PL, Kimura H. 2000. Enhancement of progenitor cell division in the dentate gyrus triggered by initial limbic seizures in rat models of epilepsy. Epilepsia 41:10–8.

Nikonenko I, Jourdain P, Alberi S, Toni N, Muller D. 2002. Activity-induced changes of spine morphology. Hippocampus 12:585–91.

Nitsch R, Leranth C. 1993. Calretinin immunoreactivity in the monkey hippocampal formation—II. Intrinsic gabaergic and hypothalamic non-gabaergic systems: An experimental tracing and co-existence study. Neuroscience 55:797–812.

Nitsch R, Leranth C. 1994. Substance P-containing hypothalamic afferents to the monkey hippocampus: an immunocytochemical, tracing, and coexistence study. Exp Brain Res 101:231–240.

Nitsch R, Soriano E, Frotscher M. 1990. The parvalbumin-containing nonpyramidal neurons in the rat hippocampus. Anat Embryol (Berl) 181:413–25.

Nunzi MG, Gorio A, Milan F, Freund TF, Somogyi P, Smith AD. 1985. Cholecystokinin-immunoreactive cells form symmetrical synaptic contacts with pyramidal and nonpyramidal neurons in the hippocampus. J Comp Neurol 237:485–505.

Nyakas C, Luiten PG, Spencer DG, Traber J. 1987. Detailed projection patterns of septal and diagonal band efferents to the hippocampus in the rat with emphasis on innervation of CA1 and dentate gyrus. Brain Res Bull 18:533–45.

Oliver G, Sosa-Pineda B, Geisendorf S, Spana EP, Doe CQ, Gruss P. 1993. Prox 1, a prospero-related homeobox gene expressed during mouse development. Mech Dev 44:3–16.

Omiya Y, Uchigashima M, Konno K, Yamasaki M, Miyazaki T, Yoshida T, Kusumi I, Watanabe M. 2015. VGluT3-expressing CCK-positive basket cells construct invaginating synapses enriched with endocannabinoid signaling proteins in particular cortical and cortex-like amygdaloid regions of mouse brains. J Neurosci 35:4215–28.

Paoletti P, Vergnano AM, Barbour B, Casado M. 2009. Zinc at glutamatergic synapses. Neuroscience 158:126–36.

Papp E, Leinekugel X, Henze DA, Lee J, Buzsáki G. 2001. The apical shaft of CA1 pyramidal cells is under GABAergic interneuronal control. Neuroscience 102:715–721.

Parent JM, Yu TW, Leibowitz RT, Geschwind DH, Sloviter RS, Lowenstein DH. 1997. Dentate granule cell neurogenesis is increased by seizures and contributes to aberrant network reorganization in the adult rat hippocampus. J Neurosci 17:3727–38.

Park J-H, Cho H, Kim H, Kim K. 2006. Repeated brief epileptic seizures by pentylenetetrazole cause neurodegeneration and promote neurogenesis in discrete brain regions of freely moving adult rats. Neuroscience 140:673–684.

Paxinos G, Franklin KBJ. 2001. The Mouse Brain in Stereotaxic Coordinates. (Paxinos G, Franklin KBJ, editors.).

Penttonen M, Kamondi a, Sik A, Acsády L, Buzsáki G. 1997. Feed-forward and feed-back activation of the dentate gyrus in vivo during dentate spikes and sharp wave bursts. Hippocampus 7:437–50.

Pérez-Clausell J, Danscher G. 1985. Intravesicular localization of zinc in rat telencephalic boutons. A histochemical study. Brain Res 337:91–98.

Pierce JP, Punsoni M, McCloskey DP, Scharfman HE. 2007. Mossy cell axon synaptic contacts on ectopic granule cells that are born following pilocarpine-induced seizures. Neurosci Lett 422:136–140.

Planas AM, Soriano MA, Estrada A, Sanz O, Martin F, Ferrer I. 1997. The heat shock stress response after brain lesions: induction of 72 kDa heat shock protein (cell types involved, axonal transport, transcriptional regulation) and protein synthesis inhibition. Prog Neurobiol 51:607–36.

Pleasure SJ, Anderson S, Hevner R, Bagri A, Marin O, Lowenstein DH, Rubenstein JL. 2000. Cell migration from the ganglionic eminences is required for the development of hippocampal GABAergic interneurons. Neuron 28:727–40.

Porrero C, Rubio-Garrido P, Avendaño C, Clascá F. 2010. Mapping of fluorescent protein-expressing neurons and axon pathways in adult and developing Thy1-eYFP-H transgenic mice. Brain Res 1345:59–72.

Preibisch S, Saalfeld S, Tomancak P. 2009. Globally optimal stitching of tiled 3D microscopic image acquisitions. Bioinformatics 25:1463–5.

Przewłocki R, Kamińska B, Lukasiuk K, Nowicka DZ, Przewłocka B, Kaczmarek L, Lasoń W. 1995. Seizure related changes in the regulation of opioid genes and transcription factors in the dentate gyrus of rat hippocampus. Neuroscience 68:73–81.

Racine RJ. 1972. Modification of seizure activity by electrical stimulation: II. Motor seizure. Electroencephalogr Clin Neurophysiol 32:281–294.

Ramón y Cajal S. 1893. Estructura del asta de Ammon y fascia dentata. Sociedad Española de Historia Natural.

Ramón y Cajal S. 1911. Histologie du système nerveux de l'homme & des vertébrés. Madrid: Instituto Ramón y Cajal.

Ratzliff ADH, Howard AL, Santhakumar V, Osapay I, Soltesz I. 2004. Rapid deletion of mossy cells does not result in a hyperexcitable dentate gyrus: implications for epileptogenesis. J Neurosci 24:2259–2269.

Ratzliff ADH, Santhakumar V, Howard AL, Soltesz I. 2002. Mossy cells in epilepsy: rigor mortis or vigor mortis? Trends Neurosci 25:140–4.

Ribak CE, Peterson GM. 1991. Intragranular mossy fibers in rats and gerbils form synapses with the somata and proximal dendrites of basket cells in the dentate gyrus. Hippocampus 1:355–64.

Ribak CE, Seress L, Amaral DG. 1985. The development, ultrastructure and synaptic connections of the mossy cells of the dentate gyrus. J Neurocytol 14:835–857.

Ribak CE, Seress L. 1983. Five types of basket cell in the hippocampal dentate gyrus: a combined Golgi and electron microscopic study. J Neurocytol 12:577–597.

Ribak CE, Tran PH, Spigelman I, Okazaki MM, Nadler JV. 2000. Status epilepticus-induced hilar basal dendrites on rodent granule cells contribute to recurrent excitatory circuitry. J Comp Neurol 428:240–53.

Rose G, Schubert P. 1977. Release and transfer of [3H]adenosine derivatives in the cholinergic septal system. Brain Res 121:353–357.

Rubin AN, Kessaris N. 2013. PROX1: a lineage tracer for cortical interneurons originating in the lateral/caudal ganglionic eminence and preoptic area. PLoS One 8:e77339.

Sala C, Segal M. 2014. Dendritic spines: the locus of structural and functional plasticity. Physiol Rev 94:141–88.

Sancho-Bielsa FJ, Navarro-López JD, Alonso-Llosa G, Molowny A, Ponsoda X, Yajeya J, López-García C. 2012. Neurons of the dentate molecular layer in the rabbit hippocampus. PLoS One 7:e48470.

Santhakumar V, Aradi I, Soltesz I. 2005. Role of mossy fiber sprouting and mossy cell loss in hyperexcitability: a network model of the dentate gyrus incorporating cell types and axonal topography. J Neurophysiol 93:437–453.

Santhakumar V, Bender R, Frotscher M, Ross ST, Hollrigel GS, Toth Z, Soltesz I. 2000. Granule cell hyperexcitability in the early post-traumatic rat dentate gyrus: the “irritable mossy cell” hypothesis. J Physiol 524 Pt 1:117–134.

Scharfman HE, Goodman JH, Sollas a L. 2000. Granule-like neurons at the hilar/CA3 border after status epilepticus and their synchrony with area CA3 pyramidal cells: functional implications of seizure-induced neurogenesis. J Neurosci 20:6144–6158.

Scharfman HE, Pierce JP. 2012. New insights into the role of hilar ectopic granule cells in the dentate gyrus based on quantitative anatomic analysis and three-dimensional reconstruction. Epilepsia 53 Suppl 1:109–115.

Scharfman HE. 1992. Blockade of excitation reveals inhibition of dentate spiny hilar neurons recorded in rat hippocampal slices. J Neurophysiol 68:978–84.

Scharfman HE. 1993. Characteristics of spontaneous and evoked EPSPs recorded from dentate spiny hilar cells in rat hippocampal slices. J Neurophysiol 70:742–57.

Scharfman HE. 1994. Evidence from simultaneous intracellular recordings in rat hippocampal slices that area CA3 pyramidal cells innervate dentate hilar mossy cells. J Neurophysiol 72:2167–2180.

Scharfman HE. 1995. Electrophysiological diversity of pyramidal-shaped neurons at the granule cell layer/hilus border of the rat dentate gyrus recorded in vitro. Hippocampus 5:287–305.

Scharfman HE. 2007. The CA3 “backprojection” to the dentate gyrus. Prog Brain Res 163:627–37.

Schmidt-Kastner R, Freund TF. 1991. Selective vulnerability of the hippocampus in brain ischemia. Neuroscience 40:599–636.

Scott BW, Wang S, Burnham WM, De Boni U, Wojtowicz JM. 1998. Kindling-induced neurogenesis in the dentate gyrus of the rat. Neurosci Lett 248:73–6.

Segal M, Landis SC. 1974. Afferents to the septal area of the rat studied with the method of retrograde axonal transport of horseradish peroxidase. Brain Res 82:263–268.

Segal M. 1979. A potent inhibitory monosynaptic hypothalamo-hippocampal connection. Brain Res 162:137–141.

Seress L, Abrahám H, Dóczi T, Lázár G, Kozicz T. 2004. Cocaine- and amphetamine-regulated transcript peptide (CART) is a selective marker of rat granule cells and of human mossy cells in the hippocampal dentate gyrus. Neuroscience 125:13–24.

Seress L, Abrahám H, Paleszter M, Gallyas F. 2001. Granule cells are the main source of excitatory input to a subpopulation of GABAergic hippocampal neurons as revealed by electron microscopic double staining for zinc histochemistry and parvalbumin immunocytochemistry. Exp brain Res 136:456–62.

Seress L, Frotscher M, Ribak CE. 1989. Local circuit neurons in both the dentate gyrus and Ammon’s horn establish synaptic connections with principal neurons in five day old rats: a morphological basis for inhibition in early development. Exp brain Res 78:1–9.

Seress L, Pokorny J. 1981. Structure of the granular layer of the rat dentate gyrus. A light microscopic and Golgi study. J Anat 133:181–95.

Seress L, Ribak CE. 1984. Direct commissural connections to the basket cells of the hippocampal dentate gyrus: anatomical evidence for feed-forward inhibition. J Neurocytol 13:215–225.

Seress L, Ribak CE. 1990. The synaptic connections of basket cell axons in the developing rat hippocampal formation. Exp brain Res:500–508.

Seress L, Ribak CE. 1992. Ultrastructural features of primate granule cell bodies show important differences from those of rats: axosomatic synapses, somatic spines and infolded nuclei. Brain Res 569:353–357.

Shapiro L a, Ribak CE. 2005. Integration of newly born dentate granule cells into adult brains: hypotheses based on normal and epileptic rodents. Brain Res Brain Res Rev 48:43–56.

Sheng M, McFadden G, Greenberg ME. 1990. Membrane depolarization and calcium induce c-fos transcription via phosphorylation of transcription factor CREB. Neuron 4:571–582.

Sik A, Penttonen M, Buzsáki G. 1997. Interneurons in the hippocampal dentate gyrus: an in vivo intracellular study. Eur J Neurosci 9:573–588.

Sik A, Tamamaki N, Freund TF. 1993. Complete axon arborization of a single CA3 pyramidal cell in the rat hippocampus, and its relationship with postsynaptic parvalbumin-containing interneurons. Eur J Neurosci 5:1719–28.

Sloviter RS, Bumanglag A V., Schwarcz R, Frotscher M. 2012. Abnormal dentate gyrus network circuitry in temporal lobe epilepsy. In: Noebels JL, Avoli M, Rogawski MA et al., editor. Jasper's Basic Mechanisms of the Epilepsies. 4th ed. National Center for Biotechnology Information (US).

Sloviter RS, Nilaver G. 1987. Immunocytochemical localization of GABA-, cholecystokinin-, vasoactive intestinal polypeptide-, and somatostatin-like immunoreactivity in the area dentata and hippocampus of the rat. J Comp Neurol 256:42–60.

Sloviter RS, Zappone C a, Harvey BD, Bumanglag A V, Bender R a, Frotscher M. 2003. "Dormant basket cell" hypothesis revisited: relative vulnerabilities of dentate gyrus mossy cells and inhibitory interneurons after hippocampal status epilepticus in the rat. J Comp Neurol 459:44–76.

Sloviter RS, Zappone CA, Harvey BD, Frotscher M. 2006. Kainic acid-induced recurrent mossy fiber innervation of dentate gyrus inhibitory interneurons: possible anatomical substrate of granule cell hyper-inhibition in chronically epileptic rats. J Comp Neurol 494:944–60.

Sloviter RS. 1987. Decreased hippocampal inhibition and a selective loss of interneurons in experimental epilepsy. Science 235:73–6.

Sloviter RS. 1989. Calcium-binding protein (calbindin-D28k) and parvalbumin immunocytochemistry: localization in the rat hippocampus with specific reference to the selective vulnerability of hippocampal neurons to seizure activity. J Comp Neurol 280:183–96.

Sloviter RS. 1991. Permanently altered hippocampal structure, excitability, and inhibition after experimental status epilepticus in the rat: the "dormant basket cell" hypothesis and its possible relevance to temporal lobe epilepsy. Hippocampus 1:41–66.

Sloviter RS. 1992. Possible functional consequences of synaptic reorganization in the dentate gyrus of kainate-treated rats. Neurosci Lett 137:91–6.

Soriano E, Frotscher M. 1989. A GABAergic axo-axonic cell in the fascia dentata controls the main excitatory hippocampal pathway. Brain Res 503:170–174.

Soriano E, Frotscher M. 1994. Mossy cells of the rat fascia dentata are glutamate-immunoreactive. Hippocampus 4:65–9.

Soriano E, Nitsch R, Frotscher M. 1990. Axo-axonic chandelier cells in the rat fascia dentata: Golgi-electron microscopy and immunocytochemical studies. J Comp Neurol 293:1–25.

Soussi R, Zhang N, Tahtakran S, Houser CR, Esclapez M. 2010. Heterogeneity of the supramammillary-hippocampal pathways: evidence for a unique GABAergic neurotransmitter phenotype and regional differences. Eur J Neurosci 32:771–85.

Spigelman I, Yan XX, Obenaus a, Lee EY, Wasterlain CG, Ribak CE. 1998. Dentate granule cells form novel basal dendrites in a rat model of temporal lobe epilepsy. Neuroscience 86:109–20.

Spruston N, Johnston D. 1992. Perforated patch-clamp analysis of the passive membrane properties of three classes of hippocampal neurons. J Neurophysiol 67:508–529.

Staley KJ, Otis TS, Mody I. 1992. Membrane properties of dentate gyrus granule cells: comparison of sharp microelectrode and whole-cell recordings. J Neurophysiol 67:1346–1358.

Steckler T, Sahgal a. 1995. The role of serotonergic-cholinergic interactions in the mediation of cognitive behaviour. Behav Brain Res 67:165–199.

Stirling R V, Bliss T V. 1978. Observations on the commissural projection to the dentate gyrus in the Reeler mutant mouse. Brain Res 150:447–65.

Stringer JL. 1995. Pentylenetetrazol causes polysynaptic responses to appear in the dentate gyrus. Neuroscience 68:407–413.

Struble RG, Desmond NL, Levy WB. 1978. Anatomical evidence for interlamellar inhibition in the fascia dentata. Brain Res 152:580–585.

Sun C, Mtchedlishvili Z, Bertram EH, Erisir A, Kapur J. 2007. Selective loss of dentate hilar interneurons contributes to reduced synaptic inhibition of granule cells in an electrical stimulation-based animal model of temporal lobe epilepsy. J Comp Neurol 500:876–893.

Swanson LW. 1982. The projections of the ventral tegmental area and adjacent regions: A combined fluorescent retrograde tracer and immunofluorescence study in the rat. Brain Res Bull 9:321–353.

Szabadics J, Varga C, Brunner J, Chen K, Soltesz I. 2010. Granule cells in the CA3 area. J Neurosci 30:8296–8307.

Szyndler J, Maciejak P, Turzyńska D, Sobolewska A, Taracha E, Skórzewska A, Lehner M, Bidziński A, Hamed A, Wisłowska-Stanek A, Krzaścik P, Płaźnik A. 2009. Mapping of c-Fos expression in the rat brain during the evolution of pentylenetetrazol-kindled seizures. Epilepsy Behav 16:216–224.

Tauck DL, Nadler J V. 1985. Evidence of functional mossy fiber sprouting in hippocampal formation of kainic acid-treated rats. J Neurosci 5:1016–22.

Thome C, Kelly T, Yanez A, Schultz C, Engelhardt M, Cambridge SB, Both M, Draguhn A, Beck H, Egorov AV. 2014. Axon-Carrying Dendrites Convey Privileged Synaptic Input in Hippocampal Neurons. Neuron 83:1418–1430.

Tian F-F, Zeng C, Guo T-H, Chen Y, Chen J-M, Ma Y-F, Fang J, Cai X-F, Li F-R, Wang X-H, Huang W-J, Fu J-J, Dang J. 2009. Mossy fiber sprouting, hippocampal damage and spontaneous recurrent seizures in pentylenetetrazole kindling rat model. Acta Neurol Belg 109:298–304.

Tóth K, Borhegyi Z, Freund TF. 1993. Postsynaptic targets of GABAergic hippocampal neurons in the medial septum-diagonal band of broca complex. J Neurosci 13:3712–3724.

Toyoda I, Buckmaster PS. 2005. Prolonged infusion of cycloheximide does not block mossy fiber sprouting in a model of temporal lobe epilepsy. Epilepsia 46:1017–20.

Turski L, Ikonomidou C, Turski WA, Bortolotto ZA, Cavalheiro EA. 1989. Review: cholinergic mechanisms and epileptogenesis. The seizures induced by pilocarpine: a novel experimental model of intractable epilepsy. Synapse 3:154–71.

Turski WA, Cavalheiro EA, Bortolotto ZA, Mello LM, Schwarz M, Turski L. 1984. Seizures produced by pilocarpine in mice: a behavioral, electroencephalographic and morphological analysis. Brain Res 321:237–53.

Turski WA, Cavalheiro EA, Schwarz M, Czuczwar SJ, Kleinrok Z, Turski L. 1983. Limbic seizures produced by pilocarpine in rats: behavioural, electroencephalographic and neuropathological study. Behav Brain Res 9:315–35.

Valente T, Auladell C, Pérez-Clausell J. 2002. Postnatal development of zinc-rich terminal fields in the brain of the rat. Exp Neurol 174:215–29.

Vertes RP, Fortin WJ, Crane AM, Systems C, Raton B. 1999. Projections of the Median Raphe Nucleus. 582:555–582.

Vertes RP. 1981. An analysis of ascending brain stem systems involved in hippocampal synchronization and desynchronization. J Neurophysiol 46:1140–1159.

Walter C, Murphy BL, Pun RYK, Spieles-Engemann AL, Danzer SC. 2007. Pilocarpine-induced seizures cause selective time-dependent changes to adult-generated hippocampal dentate granule cells. J Neurosci 27:7541–52.

Wenzel HJ, Buckmaster PS, Anderson NL, Wenzel ME, Schwartzkroin P a. 1997. Ultrastructural localization of neurotransmitter immunoreactivity in mossy cell axons and their synaptic targets in the rat dentate gyrus. Hippocampus 7:559–570.

Wenzel J, Otani S, Desmond NL, Levy WB. 1994. Rapid development of somatic spines in stratum granulosum of the adult hippocampus in vitro. Brain Res 656:127–34.

Williams P a, Larimer P, Gao Y, Strowbridge BW. 2007. Semilunar granule cells: glutamatergic neurons in the rat dentate gyrus with axon collaterals in the inner molecular layer. J Neurosci 27:13756–13761.

Witter MP, Amaral DG. 2004. Hippocampal Formation. In: Paxinos G, editor. The Rat Nervous System.

Witter MP. 2007. The perforant path: projections from the entorhinal cortex to the dentate gyrus. Prog Brain Res 163:43–61.

Wonders C, Anderson SA. 2005. Cortical interneurons and their origins. Neuroscientist 11:199–205.

Yan XX, Spigelman I, Tran PH, Ribak CE. 2001. Atypical features of rat dentate granule cells: recurrent basal dendrites and apical axons. Anat Embryol (Berl) 203:203–209.

Yoshida T, Uchigashima M, Yamasaki M, Katona I, Yamazaki M, Sakimura K, Kano M, Yoshioka M, Watanabe M. 2011. Unique inhibitory synapse with particularly rich endocannabinoid signaling machinery on pyramidal neurons in basal amygdaloid nucleus. Proc Natl Acad Sci U S A 108:3059–64.

Zhang W, Buckmaster PS. 2009. Dysfunction of the dentate basket cell circuit in a rat model of temporal lobe epilepsy. J Neurosci 29:7846–7856.

Zhang W, Yamawaki R, Wen X, Uhl J, Diaz J, Prince DA, Buckmaster PS. 2009. Surviving hilar somatostatin interneurons enlarge, sprout axons, and form new synapses with granule cells in a mouse model of temporal lobe epilepsy. J Neurosci 29:14247–56.

Zipp F, Nitsch R, Soriano E, Frotscher M. 1989. Entorhinal fibers form synaptic contacts on parvalbumin-immunoreactive neurons in the rat fascia dentata. Brain Res 495:161–166.

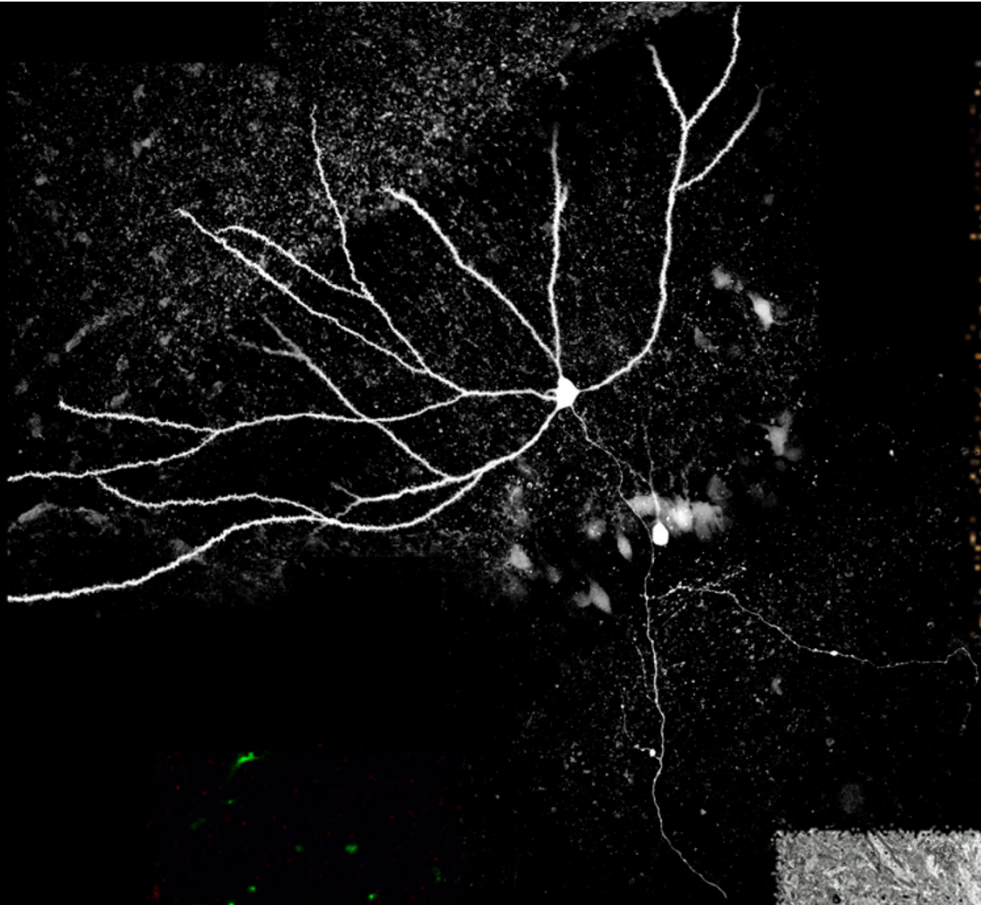

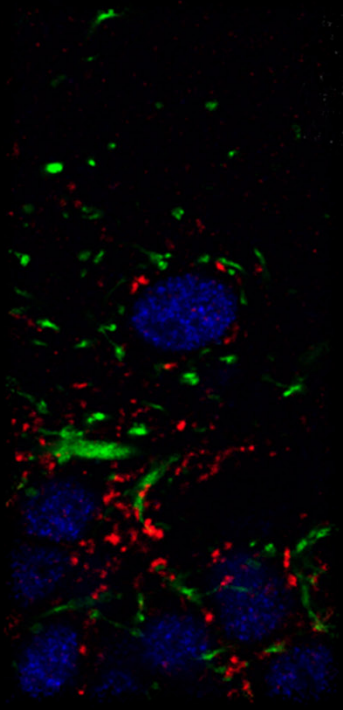

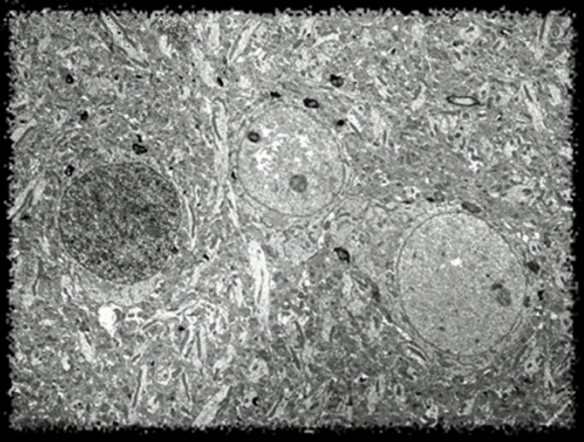

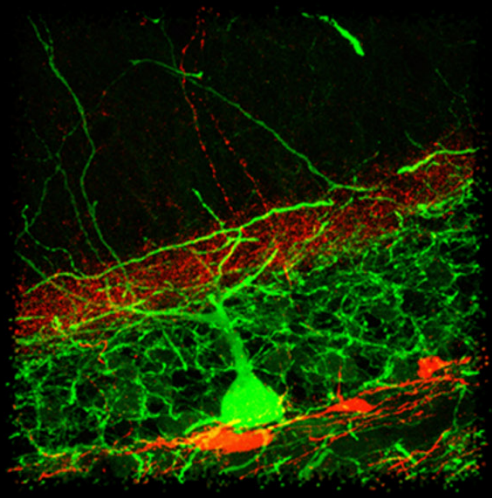

VNIVERSITAT DE VALÈNCIA

Facultad de Ciencias Biológicas

Departamento de Biología Celular y Parasitología